Localization in open quantum systems

Saptarshi Majumdar

THESE DE DOCTORAT

NNT : 2023UPASP157

université PARIS-SACLAY

Localization in Open Quantum Systems

Localisation dans les systèmes quantiques ouverts

Thèse de doctorat de l'université Paris-Saclay

École doctorale n° 564, Physique en Île-de-France (PIF)
Spécialité de doctorat: Physique
Graduate school: Physique, Référent : Faculté de Sciences d'Orsay

Thèse préparée dans l'unité de recherche **LPTMS** (Université Paris-Saclay, CNRS), sous la direction d'**Alberto ROSSO**, Directeur de Recherche CNRS, et le co-encadrement de **Laura FOINI**, Chargée de Recherche CNRS

Thèse soutenue à Paris-Saclay, le 16 Novembre 2023, par

Saptarshi MAJUMDAR

Composition du jury

Membres du jury avec voix délibérative

Gregory SCHEHR Directeur de Recherche, Sorbonne Université	Président
Edmond ORIGNAC Directeur de Recherche, Ecole Normale Supérieure de Lyon	Rapporteur & Examinateur
Rosario FAZIO Professeur, ICTP, Trieste	Rapporteur & Examinateur
Inès SAFI Chargée de Recherche HC, Université Paris-Saclay	Examinatrice

université PARIS-SACLAY | ÉCOLE DOCTORALE Physique en Île-de-France (PIF)

Titre: Localisation dans les systèmes quantiques ouverts
Mots clés: Localisation, Bosonisation, Systèmes Quantiques ouverts, Liquide de Luttinger, Dynamique de Langevin

Résumé: Nous étudions le diagramme de phase à température nulle d'une chaîne de spin unidimensionnelle couplée localement à des bains dissipatifs, chaque bain étant composé d'une multitude d'oscillateurs harmoniques. Dans le cas d'une magnétisation totale finie, ce problème quantique peut être bosonisé et ainsi réécrit via une action effective bidimensionnelle. L'étude de cette théorie des champs classique montre une transition de phase de type BKT entre la phase préexistante au bain (liquide de Luttinger) et une nouvelle phase dissipative à température nulle. Cette nouvelle phase est une onde de densité de spin sans gap qui présente une susceptibilité égale à celle du liquide luttinger et une densité superfluide nulle. Des simulations numériques de l'équation de Langevin associée à l'action effective confirment ces prédictions analytiques. Nous montrons également que ces bains locaux peuvent s'interpréter comme un désordre dynamique affectant les propriétés de transport du système quantique. En particulier, pour des bains subohmiques, la conductivité statique s'annule, signalant un effet de localisation induit par la présence du désordre dynamique. Par ailleurs, l'analyse de ce modèle pour une magnétisation totale nulle révèle que, dans ce cas, la nouvelle phase dissipative sans gap est remplacée par une phase antiferromagnétique avec un gap.

Title: Localization in Open Quantum Systems
Keywords: Localization, Bosonization, Open quantum systems, Luttinger liquid, Langevin dynamics

Abstract: We investigate the zero-temperature phase diagram of a one-dimensional XXZ spin chain coupled with local dissipative baths composed of simple harmonic oscillators. In a finite magnetization sector, we map this system onto a two-dimensional classical action using bosonization. From this classical field theory, we find the existence of a BKT phase transition between the pre-existing Luttinger liquid phase and a new dissipative phase at zero temperature. This new phase is a gapless spin density wave with unaltered susceptibility and vanishing spin stiffness. These analytical predictions are verified against numerical Langevin dynamics simulations of the action. The local baths in the spin chain can also be interpreted as annealed disorder and they affect the transport properties. Particularly for subohmic baths, the static conductivity vanishes, which can be interpreted as a localization effect induced by the presence of dynamical disorder. We also solve the model at zero magnetization and show that in that case, the gapless spin density wave is replaced by a gapped antiferromagnetic phase.

Contents

Acknowledgement

As I start writing this acknowledgment section and reflect upon my journey of three years, my mind is filled with bliss and gratitude. Firstly, I would like to thank both of my advisors, Alberto Rosso (DR CNRS, LPTMS) and Laura Foini (CR CNRS, IPhT). I have worked with both of them in close proximity for these three years; and I have had the opportunity of learning a plethora of things from them both in personal and professional capacity, which has helped me grow as a person and a researcher. I would like to thank them for not giving up on me, and for motivating me whenever it was required. I would also like to thank my collaborators and co-authors of my publications Thierry Giamarchi (Professor, DQMP, University of Geneva), Oscar Bouverot-Dupuis (intern, LPTMS), and Thibaud Maimbourg (ex Post-doctoral student, IPhT). I have had plenty of fruitful and interesting discussions with them, and they have made important contributions to solving the puzzle we were interested in. Next, I would like to thank the rapporteurs Edmond Orignac (DR CNRS, ENS Lyon) and Rozario Fazio (Professor, ICTP Trieste), and the examinateurs Inès Safi (Chercheuse CNRS, LPS) and Grégory Schehr (DR CNRS, LPTHE), who took out their precious time and gave me invaluable suggestions based on my thesis and defense presentation. I also thank Satya Majumdar for giving me important advices.

I have been immensely fortunate to be able to do my doctoral studies in LPTMS, and I would like to take this opportunity to thank the people in the administration who supported us in maintaining a friendly environment in the laboratory. First and foremost, I thank the two directors Emmanuel Trizac and Alberto Rosso for encouraging us to engage in scientific activities. I would also like to thank Claudine Le Vaou and Delphine Hannoy, to whom I could go at any point in time to ask for help regarding personal and professional bureaucratic advice. I also especially thank Karolina Kolodziej, who has been nothing short of extremely helpful, caring, and patient with me; and I am fortunate to have her as a friend.

Now comes the most important part: My colleagues and friends. It feels bizarre and at the same time extremely lucky that all of us were at the same place at the same time, and I would

like to thank all of them for helping me get through these three years. I thank Marco B., Mauro, Fabian, Francesco M., Lorenzo R., Lorenzo G., Maya, Guido, Alessandro S., Andrea T., Andrea P., Lenart, Kemal, Vanja, Ivan, Alessandro P., Giovanni, Sharon, and Zeynep for being good friends and mentors. A special shout out to Charbel, Jules, and Benoît, who shared the same office with me and made it the most comfortable professional space I have ever experienced. I thank, from the deepest part of my heart, the Ph.D. students who started their journey with me: Li Gan, who first introduced the concept of calling everyone together for lunch; Saverio, from whom I learned patience and levelheadedness; Lara, who taught me unconditional kindness and how to be hosting and accommodating; Benjamin, who was funny yet always logical; Federico, who taught me perseverance and hard work; and Flavio, whose wisdom mixed with sense of humor inspired me a lot. I would like to provide a special mention to two other people from the lab - Vincenzo, who I wish were my own brother and with whom I share the pleasure of organizing multiple fun events; and Ana, who has seen me during the worst moments of my life and yet chose to stick with me while providing mental support. I truly thank both of them for being there.

I also had the good luck of having close friends outside my laboratory. My first and foremost thanks go out to my neighbors who shared the same floor and kitchen with me: Lata, Sundar, Divya R., Ram, Divya, Urvi, Shweta, Jiya, Harshini, Shubho, David, Uttiya, Silvia, and Anita. I would also like to especially thank Jael and Elisa, whose comfortable companies I have always enjoyed. Apart from my floormates, I express my gratitude to two other friends from my Maison: Riddhi, whose kindness, intelligence, logical thinking, and political ideologies have inspired me; And Sakshi, with whom I shared countless studying sessions and who has provided me mental comfort during my tough times. Last but not least, I also would like to thank Martina R., Hélène, Miha, Lucija, Maite, Elena, Gautham, Giulia, Alexa, Ella, Francesco C., and Denise. I came across them at different periods of my life and I appreciate their contributions to my experience and growth. I thank also my friends from India: Satyaki, Moitreyi, Mayurika, Alakta, Adwitia, Arani, Bikram, Jahnvi, Angana, and Soumyadeep, thank you for keeping me in touch with my roots.

Finally, I would like to thank my parents for being supportive of my career-related decisions. They have provided me with the necessary mental and economic support, and I thank them for being brave and strong enough to let their only child go away from home to a far-away country in pursuit of higher education.

Introduction

The discovery of localization in quantum and classical systems has remained a pivotal instance to date. Originally, it was introduced by P.W.Anderson in his seminal paper in 1958 [1], where it was argued that the wave function of a single quantum degree of freedom (such as a particle or a spin) stops spatially diffusing in a lattice in the presence of impurities, which was modeled through random local potential. Instead, the wave function ψ exponentially decays over a finite length as $\sim e^{-x/\xi}$, where ξ is known as the localization length as it quantifies the extension of localization of the system. This work was further extended in the famous 'Gang of Four' letter [2], where it was shown, via a system size scaling argument of the conductance, that a localization-delocalization phase transition as a function of temperature via the existence of a mobility edge in a non-interacting system is only possible for a spatial dimension $d \geq 3$. This initially brought an impression that localization phase transitions are absent in one-dimensional quantum systems; however in the renowned Aubry-André-Harper model [3–5], it was shown that mobility edge can exist even in a one-dimensional system in the presence of a quasiperiodic potential, i.e., a periodic potential incommensurate with the periodicity of the lattice. Furthermore, localization-delocalization phase transition at zero temperature was proved to exist in disordered systems in lower dimensions in the presence of interaction. Important examples of such phenomena have been found in one dimension in the superfluid-bose glass transition in interacting bosonic systems analytically [6, 7] and numerically [8]. In fermionic systems, coupled chains of spinless and spinful fermions have been shown to have a superconductor-localized phase transition [9], specifically when the interaction is attractive in nature.

One of the many interesting aspects of this phenomenon is that the system becomes insulating in nature as transport is rendered impossible due to the lack of diffusion in the localized phase. Until now, localization has been observed in different systems in the presence of static (quenched) disorder as discussed above. But can localization be induced in a one-dimensional

many-body system via a dissipative environment at zero temperature? Intuitively, one can understand that the environment can be imagined as a source of phonons (or classically, simple harmonic oscillators). If these phonons are coupled to the system in such a way that each degree of freedom of the system has its own, independent reservoir of phonons that are uncorrelated to each other, then they act as a source of dynamic (annealed) but random local potential for the system. Particularly, if the phonons are dynamically slow, in a strong coupling limit they can inhibit the transport properties in the system, inducing a phase transition in the system. We address this scenario in this thesis.

Another motivation behind our work comes from the point of view of Open Quantum systems. Previously, it has been shown that at zero dimension, certain types of dissipative environment can induce localization at zero temperature on a single quantum degree of freedom (particle or spin) via freezing it in its initial state. This motivated us to extend this work to one-dimensional many-body systems. In the absence of a bath, a one-dimensional interacting system can stay in a perfectly conducting phase. Another set of questions that we wanted to address is: Can these dissipative baths induce phase transition on this conducting phase at zero temperature? If yes, is it possible to have a good effective low-energy description of the phase? And finally, what are the thermodynamic and dynamic properties of this new dissipative phase? We answer these questions here and corroborate them with the previously described localization scenario.

Here, we present an overview of the work, which will act as a guide to navigate the readers through the chapters of this thesis. In chapter 1, we describe in detail the current state-of-the-art in the field of 'Open Quantum Systems', which deals with characterizing the behavior of quantum models and materials in the presence of an external environment. This environment can be in the form of measurements, or in the form of external phonons coupling with the system (as motivated in the previous paragraph), and we will discuss these approaches in detail while making our formulation of the environment more mathematically compact.

Chapter 2 introduces the quantum model that we investigate, namely, a 1D XXZ spin chain coupled with local dissipative baths. These baths act on the system as an annealed or dynamical disorder. We introduce an important technique called bosonization and apply it to the spin chain to arrive at a two-dimensional classical field theory. In this scenario, the effect of the local baths is captured by a long-range cosine potential acting along only imaginary time direction, and we argue that it's able to induce a phase transition on the already existing Luttinger liquid

phase by spontaneously breaking symmetry at zero temperature due to its long-range nature. We also show that two limits of this model should be clearly differentiated: The field theoretical actions for the spin chain at zero magnetization and at a finite magnetization should be investigated separately.

To describe the phase transition and the new dissipative phase, we use certain analytical and numerical techniques which we describe in detail in Chapter 3. In particular, we describe the procedure of the perturbative renormalization group and the variational approximation method. As an example, we show the use of these methods on the renowned Sine-Gordon model, which can be obtained as a non-dissipative limit of the system that we investigate. In the final section, we describe the theory of Langevin dynamics, which is the main principle behind the numerical technique that we use, and show that this method can be used as a Monte-Carlo technique for our system and it can help us traverse the configurational phase space of the action.

We focus on the investigation of the system at finite magnetization in the next two chapters (Chapter 4 and 5). Using perturbative RG, we locate a Berezinski-Kosterlitz-Thouless type critical point. This tells us that in the parametric phase space of dissipation coupling strength and Luttinger parameter, either the system stays in the original Luttinger liquid phase with renormalized values of the parameter, or in a new dissipative phase where the cosine potential becomes relevant. In the Luttinger liquid phase, the renormalization procedure indicates that the value of the Luttinger parameter is reduced. Similar kinds of effects were investigated in [10], where it was shown that the Luttinger parameter K of a Luttinger liquid gets diminished to K' when the system is coupled with an external dissipative environment with finite resistance R as $1/K' = 1/K + (e^2R)/h$. On the other hand, to understand the dissipative phase we employ a variational analysis of the action, which tells us that the low energy excitations of this phase can be described via a Gaussian action which is gapless and fractional in bosonic Matsubara frequency modes. To characterize the dissipative phase, we analyze its thermodynamic and dynamic properties such as susceptibility, spin-spin correlation, conductivity, charge stiffness, etc. We define an order parameter for the phase transition, which we relate to the amplitude of a spin density wave via bosonization. As this quantity remains finite at zero temperature and thermodynamic limit in the dissipative phase, we argue that this phase is a gapless spin density wave with unaltered susceptibility and vanishing superfluid density. Specifically for subohmic baths, the DC conductivity of the dissipative phase vanishes, which is the signature of a conductor-insulator phase transition. Additionally, we simulate the action

with the cosine potential to generate equilibrated configurations. We support our analytical predictions by calculating the above-mentioned correlation functions from these numerically generated configurations. These works have led to a publication [11] and a pre-print [12].

The 6th chapter focuses on another limit of this model, where we take the XXZ spin chain to be in zero magnetization. This work is currently ongoing; however, we are able to predict that in this scenario, the zero-temperature physics of the system turns out to be quite different than the previously described picture. In particular, the gapless spin density wave is replaced with a gapped phase, which we suspect to be an antiferromagnetic (Mott insulator) phase. We also provide supporting preliminary numerical evidence. All the important results throughout the thesis have been highlighted with boxes.

Chapter 1

Open Quantum Systems

The quantum mechanical description of a system has been proven many times to be extremely useful in understanding different physically observable properties of the system. One of the basic assumptions that have been made for a long time while solving these models is that they are isolated from the surrounding environment and the physics of the degrees of freedom in the system is solely governed by the hamiltonian of the system itself. But in reality, this is not true: During experimental realization, it is often possible that external electromagnetic waves or phonons get coupled with the system. If left uncontrolled, these environmental factors can affect the system significantly. Thus the field of open quantum systems was born, which specializes in understanding the effect of various types of environments on a quantum mechanical system.

One of the earliest works in this regard was done in measurement theory. In the late '70s, it was hypothesized that the decay of a particle from a prepared state is stopped by a continuous measurement procedure performed on the particle to observe its decay. Closely related works were being done for some time, including Sir Alan Turing's paradox. However, a proper formulation was first done by B. Misra and E.C.G Sudarshan in their pioneering work [13], where they named it 'Quantum Zeno paradox' (named after the famous 'Arrow paradox' of Greek philosopher Zeno). Subsequent works, such as experiments with short light pulses on Beryllium atoms [14], solidified the ground of this field; and it was confirmed that in the Zeno localized phase, the particle retains memory of the initially prepared state due to the rapidly collapsing wavefunction. Note that this localization is fundamentally different from Anderson localization; as a matter of fact, a transition between Anderson and Zeno localized phases was found in a single-particle system in the presence of disorder and strongly coupled with a

measurement-inducing bath [15]. Another important effect of measurement-induced localization is that it affects the entanglement entropy of the system. Indeed, it was shown using toy models known as quantum circuits, where the hamiltonian of the system and the measurement are encoded as local unitary gate and projective measurement respectively, that there exists a phase transition in terms of entanglement entropy between an area law (high measurement phase) and a volume law (low measurement phase). Signatures of this transition have been reported in Bell pairs [16], in one dimension [17], and in two dimensions [18] (Recently, a low measurement phase with logarithmic entanglement law has been reported in absence of interaction using exact diagonalization [19]). Another popular approach for investigating phase transition with respect to entanglement entropy is solving the Lindblad equation [20], where one treats the measurement as a perturbation to the system. Using this formalism, the presence of Zeno localization has been shown in one-dimensional non-interacting [21] and many-body systems [22].

However, until now all the approaches described above have the inherent assumption that the environment acts in a markovian manner on the system, i.e., the action of the environment (measurements, in this case) is instantaneously fast in this case. The formalism that we follow in this thesis takes account of the environment in a non-markovian, non-perturbative manner. This was first introduced by A.O. Caldeira and A.J. Leggett in their work on quantum brownian motion [23], where they showed that the Langevin equation corresponding to the quantum version of a brownian motion of a particle $m\frac{d^2x}{dt^2} + \alpha\frac{dx}{dt} + V'(x) = F(t)$ (where m is the mass of the particle, α is a damping constant, V is a generic potential and F is the random force) with the correlation $\langle F(t)F(t')\rangle = \frac{1}{2\pi}\int e^{-i\omega(t-t')}\alpha\hbar\omega\coth\left(\frac{\hbar\omega}{2KT}\right)d\omega$ can be mapped onto a system in contact with a reservoir via the Feynman-Vernon path integral formalism [24]. More specifically, the dissipative system is described by a particle in a potential $V(x)$ coupled to a bath of simple harmonic oscillators, given by the hamiltonian:

$$\begin{aligned} H_{\text{sys}} &= \frac{p^2}{2m} + V(x) \\ H_{\text{bath}} &= \frac{1}{2}\sum_k \left[\frac{P_k^2}{M_k} + M_k\Omega_k^2 R_k^2\right] \\ H_{\text{SB}} &= x\sum_k C_k R_k \end{aligned}$$

Where R_k, Ω_k, and P_k are the displacement, frequency, and momenta of the kth oscillator in the reservoir respectively. C_k denotes the coupling energy of the particle to the kth oscillator. Caldeira and Leggett showed that these two systems are equivalent when the low-energy spec-

tral density of the harmonic oscillators, defined as $\boldsymbol{J(\omega) = \frac{\pi}{2} \sum_k \frac{C_k^2}{m_k \Omega_k} \delta(\omega - \Omega_k)}$, is linearly proportional to the frequency as $\boldsymbol{\alpha\omega}$. In this case, the effect of the bath is equivalent to that of a resistor in an LRC circuit, thus this kind of environment was named the '*Ohmic bath*'. This work was followed by a plethora of interesting developments [25–27], including a study of dissipative two-state systems [28]. This model is currently known as the '*Spin-Boson model*', where the two-state system is described by a single quantum spin-1/2 particle in a constant magnetic field along z and x direction: $H_{\text{sys}} = \frac{1}{2}(\epsilon\sigma^z - \hbar\Delta_0\sigma^x)$. The dissipation for this model is the same as the quantum brownian motion (described by H_{bath}), and the coupling between the bath and the system was given by $\boldsymbol{H_{\text{SB}} = \frac{1}{2}\sigma^z \sum_k C_k R_k}$, i.e. the position co-ordinate of the brownian particle is replaced by the z-component of the spin. This system in certain limits can be mapped onto a system with a particle in a double well potential. In the absence of dissipation and in the limit $\hbar\Delta_0/\epsilon >> 1$, the spin is known to constantly oscillate between spin up and down state (equivalently, the particle jumping between the left and the right well of the potential in the classical picture). More precisely, if $P(t)$ denotes the difference between the probability of finding the spin (particle) in the spin up (left well) and in the spin down (right well) states, then $P(t) = \cos\Delta_0 t$ given that $P(0) = 1$. However, this behavior changes drastically when coupled with a dissipative bath having a more generalized spectral function $\boldsymbol{J(\omega) \sim \alpha\omega^s}$. The dynamics of the bath can be controlled in this formalism with the exponent s; a smaller value of s denotes a bath with slower dynamics. This type of environment is in contrast to the previously explained random measurement picture, where the dissipation is instantaneous and corresponds to $J(\omega) = \text{const}$. Compared with [23], the case corresponding to $\boldsymbol{s = 1}$ is called the *ohmic bath*, $\boldsymbol{1 < s < 2}$ is called the *superohmic bath* and $\boldsymbol{0 < s < 1}$ is called the *subohmic bath*. One of the interesting results of the spin-boson model is that at zero temperature for a subohmic bath, the spin retains memory of the initial state instead of oscillating between the two states (equivalently, the particle stays localized in the well it was initially situated in). This can be interpreted as a signature of localization induced by dissipation in a zero-dimensional quantum system. This was in contrast to the popular belief at that time as it was previously shown that delocalized acoustic phonons can induce conductivity in a localized system via a mechanism known as variable range hopping [29–31].

In our thesis, we treat the dissipation in the system à la Caldeira-Leggett. In Chapter 2, we describe our quantum model in detail, which is a one-dimensional XXZ spin chain locally coupled with Caldeira-Leggett-type baths. In chapter 3 and 4, we investigate the possibility of a quantum phase transition induced on the spin chain by dissipation. Then, we analyze various

thermodynamic and dynamic quantities of the dissipative phase in chapter 5, which tells us about signatures of localization in the new dissipative phase.

Chapter 2

Model

In this chapter, we describe the model in detail that we study to understand the effect of dissipation in one-dimensional many body systems. In the first section, we first discuss the microscopic model, namely, a one-dimensional XXZ spin chain coupled with local phonon baths. In the next section, we use bosonization formalism to convert this model to a two-dimensional classical field theory, which will be essential in understanding the zero-temperature phase diagram of the spin chain. In particular, in the finite magnetization sector, this action is described by:

$$\begin{aligned} S_{\text{tot}} &= S_{\text{LL}} + S_{\text{int}} \\ S_{\text{LL}} &= \frac{1}{2\pi K}\int dx d\tau \left[u(\nabla\phi(x,\tau))^2 + \frac{1}{u}(\partial_\tau\phi(x,\tau))^2\right] \\ S_{\text{int}} &= -\frac{\alpha}{4\pi^2}\int dx d\tau d\tau' \frac{\cos\left[2\left\{(\phi(x,\tau)-\phi(x,\tau'))\right\}\right]}{|\tau-\tau'|^{1+s}} \end{aligned} \tag{2.1}$$

Where $\phi(x,\tau)$ is a real field in the two-dimensional space of x, the spatial dimension of the spin chain, and τ, the imaginary time coordinate. α is the coupling strength to the bath and s is the bath exponent. For the majority of this thesis, we limit our discussion to the spin chain at finite magnetization. We also show that at zero magnetization there are extra terms present in this action that change the physical properties of the system:

$$\begin{aligned} S_{\text{tot,C}} &= S_{\text{SG}} + S_{\text{int}} + S_{int,C} \\ S_{\text{SG}} &= S_{\text{LL}} - \frac{g}{2\pi^2}\int dx d\tau \cos\left(4\phi(x,\tau)\right) \\ S_{\text{int,C}} &= -\frac{\alpha}{4\pi^2}\int dx d\tau d\tau' \frac{\cos\left[2\left\{(\phi(x,\tau)+\phi(x,\tau'))\right\}\right]}{|\tau-\tau'|^{1+s}} \end{aligned} \tag{2.2}$$

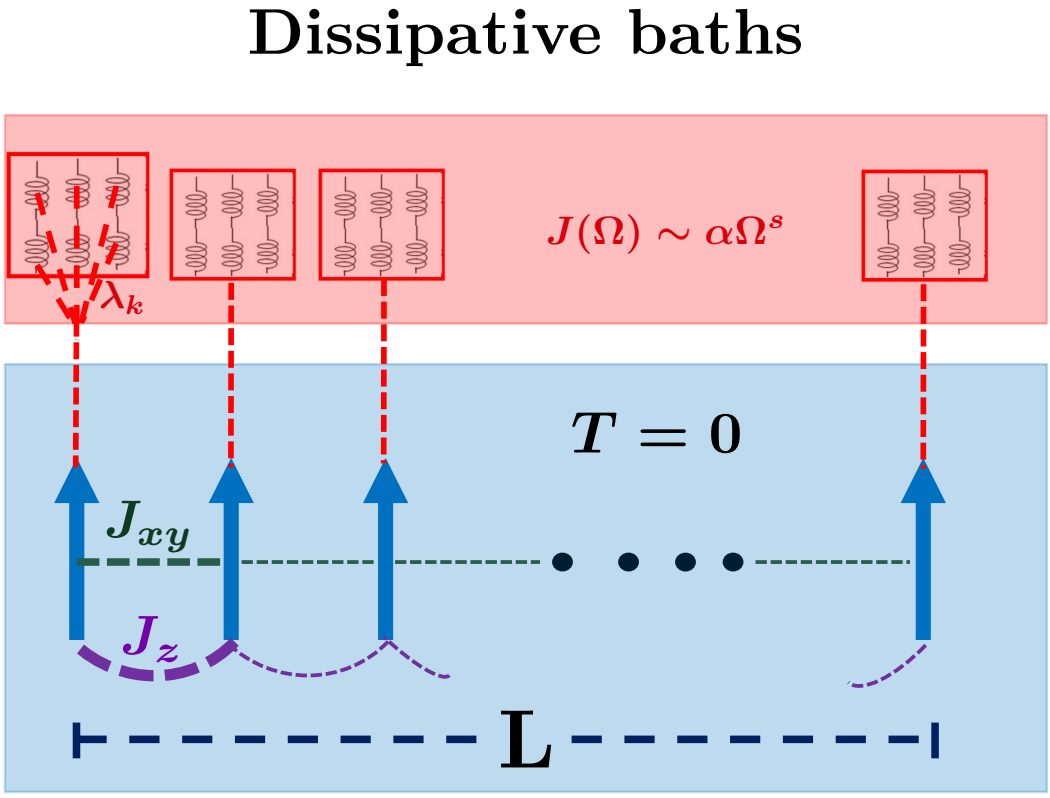

Figure 2.1: Schematic diagram of the microscopic system, i.e. a 1D XXZ spin chain (blue arrows) of length L coupled with spatially uncorrelated dissipative baths (red boxes). The system and the baths are kept at zero temperature. The spins have nearest-neighbour interaction J_{xy} in the XY plane and J_z along the z-axis. The baths are collections of simple harmonic oscillators, and the kth oscillator is coupled to the corresponding spin with strength λ_k. The bath is characterized by its spectral density function $J(\Omega) \sim \alpha\Omega^s$ (see text in Chapter 1).

After the derivation of the action, we describe the well-known properties of the system in the absence of the baths.

2.1 Microscopic model

From the beginning, we work in a system of units where $\hbar = c = k_B = 1$. The microscopic model that we consider here is a one-dimensional XXZ spin-1/2 chain with N spins in the presence of local dissipative baths at zero temperature. The hamiltonian of the full system is

given by:

$$\mathcal{H}_{\mathrm{XXZ}} = J_{\mathrm{xy}} \sum_{j=1}^{N} \left(\sigma_j^x \sigma_{j+1}^x + \sigma_j^y \sigma_{j+1}^y \right) + J_{\mathrm{z}} \sum_{j=1}^{N} \sigma_j^z \sigma_{j+1}^z + H \sum_{j=1}^{N} \sigma_j^z \tag{2.3}$$

$$\mathcal{H}_{\mathrm{B}} = \sum_{j=1,k}^{j=N} \frac{1}{2} \left(\frac{P_{jk}^2}{m_k} + m_k \Omega_k^2 X_{jk}^2 \right) \tag{2.4}$$

$$\mathcal{H}_{\mathrm{SB}} = \sum_{j=1}^{N} \sigma_j^z \sum_k \lambda_k X_{jk} \tag{2.5}$$

$$\mathcal{H}_{\mathrm{tot}} = \mathcal{H}_{\mathrm{S}} + \mathcal{H}_{\mathrm{B}} + \mathcal{H}_{\mathrm{SB}} \tag{2.6}$$

with the periodic boundary condition (PBC) $\sigma_{N+1} = \sigma_1$. The microscopic hamiltonian of the full system $\mathcal{H}_{\mathrm{tot}}$ consists of three parts: hamiltonian of the XXZ spin chain $\mathcal{H}_{\mathrm{XXZ}}$, hamiltonian of the dissipative baths $\mathcal{H}_{\mathrm{SB}}$, and the coupling between the baths and the spin chain $\mathcal{H}_{\mathrm{B}}$. In each site j, there is a quantum spin-1/2 and they can have a rotational configuration confined within a sphere of unit radius. They are denoted by the three-dimensional vector $\vec{\sigma_j} = \vec{S_j}/2$, where the components of $\vec{S_j}$ are the Pauli matrices:

$$S^x = \begin{pmatrix} 0 & 1 \\ 1 & 0 \end{pmatrix}, \; S^y = \begin{pmatrix} 0 & -i \\ i & 0 \end{pmatrix}, \; S^z = \begin{pmatrix} 1 & 0 \\ 0 & -1 \end{pmatrix}$$

The vector components of the spin-1/2 particles obey the following commutation relationship:

$$\left[\sigma_j^a, \sigma_{j'}^b \right] = i \delta_{j,j'} \epsilon_{abc} \, \sigma_j^c \tag{2.7}$$

Where $a, b, c \in (x, y, z)$ and, ϵ_{abc} is the totally antisymmetric tensor , i.e., $\epsilon_{abc} = 1 = -\epsilon_{bac}$ etc. and $\epsilon_{abc} = 0$ if any two indices are equal. The rotational symmetry between the XY plane and the Z axis is broken in this model by having two different interactions J_{xy} and J_z working on the x, y, and z components of the spins, respectively. When $J_{xy} = J_z$, this model reduces to the famous Heisenberg model. The spin chain is present in a magnetization $\vec{H} = g\mu_B h\hat{z}$, where g is the Lande factor, μ_B is Bohr magneton and h is a constant magnetic field along the z axis. Later, we will consider the cases $h \neq 0$ and $h = 0$ separately, as they lead to very different physical pictures.

We consider the dissipative baths à la Caldeira-Leggett, i.e., each bath is composed of a collection of simple harmonic oscillators. One important thing to note here: The baths are local to the spins and spatially uncorrelated to each other. This is clarified by eq. (2.4), where it can be observed that a spin located on a site j is acted upon by its own independent dissipative

bath, governed by the position degrees of freedom X_{jk} and momentum degrees of freedom P_{jk}. m_k and Ω_k denotes the mass and frequency of the k-th harmonic oscillator. Inspired by the Spin-Boson model [28], the z-component of the spin σ_j^z is coupled to X_{jk} via coupling energy λ_k. From the hamiltonian (eq. (2.5)), the effect of the bath can be viewed as a time-dependent annealed disorder $h_j(t) = \sum_k \lambda_k X_{jk}(t)$ present in the spin chain. The effect of quenched disorder in a one-dimensional many-body interacting system was already shown in [6, 7]. A schematic diagram of the system is represented by fig. (2.1).

This microscopic hamiltonian, as it is, is hard to analyze due to the presence of spin operators, numerous degrees of freedom, and many-body interactions. In the following sub-sections, we apply different techniques that get rid of these complications one by one and help us arrive at a field theory. This makes it easier for us to understand the zero-temperature, low-energy physics of this model.

2.2 Jordan-Wigner transformation

The first technique that we apply to our microscopic model is known as the Jordan-Wigner transformation. This transformation converts a spin-1/2 chain into a spinless fermionic chain, which automatically implies that $\mathcal{H}_{\rm B}$ (eq. (2.4)) will be unaltered after this procedure. Below, we first describe the general idea about the transformation, and then we apply them to eq. (2.6).

To understand this transformation, we first define two new spin operators :

$$\sigma_j^{\pm} \equiv \sigma_j^x \pm i\sigma_j^y \tag{2.8}$$

Using eq. (2.8) in eq. (2.3), we replace the σ^x and σ^y operators:

$$\begin{aligned} \frac{J_{xy}}{4}\sum_{j=1}^{N}\left[\left(\sigma_j^+ + \sigma_j^-\right)\left(\sigma_{j+1}^+ + \sigma_{j+1}^-\right) - \left(\sigma_j^+ - \sigma_j^-\right)\left(\sigma_{j+1}^+ - \sigma_{j+1}^-\right)\right] &= \frac{J_{xy}}{2}\sum_{j=1}^{N}\left(\sigma_j^+\sigma_{j+1}^- + \sigma_j^-\sigma_{j+1}^+\right) \\ \implies \mathcal{H}_{\rm XXZ} = \frac{J_{xy}}{2}\sum_{j=1}^{N}\left(\sigma_j^+\sigma_{j+1}^- + \sigma_j^-\sigma_{j+1}^+\right) + J_{\rm z}\sum_{j=1}^{N}\sigma_j^z\sigma_{j+1}^z &+ H\sum_{j=1}^{N}\sigma_j^z \end{aligned} \tag{2.9}$$

Note that the total magnetization $\sum_j \langle\sigma_j^z\rangle$ is conserved. If we don't restrict the system to some sector of magnetization, the dimension of the corresponding Hilbert space is 2^N as the eigenvalues of σ_z for a spin-1/2 particle correspond to either spin-up ($\sigma_z = 1/2$) or spin-

down ($\sigma_z = -1/2$) state. To map the spin-chain on a system of fermions, we first define the corresponding creation(destruction) operators $c_j^\dagger(c_j)$. These operators should obey the anti-commutation rule:

$$\left\{c_j, c_{j'}^\dagger\right\} = \delta_{j,j'},\ \{c_j, c_{j'}\} = \left\{c_j^\dagger, c_{j'}^\dagger\right\} = 0 \tag{2.10}$$

The system can now be diagonalized in the Fock space:

$$\begin{aligned} |n\rangle &= |n_1 n_2 \dots n_N\rangle \\ &= \left(c_1^\dagger\right)^{n_1} \left(c_2^\dagger\right)^{n_2} \dots \left(c_N^\dagger\right)^{n_N} |0\rangle \end{aligned} \tag{2.11}$$

where n_j denotes the number of fermions in the j-th site and $|0\rangle$ is the vacuum state. Assuming that a mapping between the spin-1/2 system and the fermionic system exists, it should obey the following conditions:

- The Fock space should also have a dimension of 2^N. This constraint hints at the fact that one can map the spin-up and spin-down states to a site with one fermion or zero fermion ($n_j = 0$ or 1), respectively. Thus, the Pauli exclusion principle also restricts the fermions to be spinless, as a one-dimensional system of fermions with spins has a fock space of dimension 4^N.

- Intuitively, one can understand that σ_j^+ (σ_j^-) and σ_j^z can be mapped onto $c_j^\dagger$ (c_j) and $n_j = c_j^\dagger c_j$, respectively. However, $\sigma_j^\pm$ on different sites commute, whereas the fermionic operators anti-commute.

In one dimension, this problem was first solved by P. Jordan and E. Wigner in [32], where they proposed the following mapping:

$$\sigma_j^+ \rightarrow c_j^\dagger \exp\left(i\pi \sum_{k=1}^{j-1} n_k\right) \tag{2.12}$$

$$\sigma_j^- \rightarrow c_j \exp\left(-i\pi \sum_{k=1}^{j-1} n_k\right) \tag{2.13}$$

$$\sigma_j^z \rightarrow n_j - \frac{1}{2} \tag{2.14}$$

$\exp\left(i\pi \sum_{k=1}^{j-1} n_k\right)$ is known as the string operator. From the fact that $\left[c_j^\dagger, n_k\right] = 0$ for $j \neq k$ and $\left\{c_j^\dagger, n_k\right\} = 0$ for $j = k$, it can be easily understood that the string operator commutes with all the fermionic operators out of the string and anti-commutes with the fermionic operators

inside the string. Applying the Jordan-Wigner transformation on eq. (2.9) and using the string operator commutation relationships, we see that:

$$\begin{aligned}\sigma_j^+\sigma_{j+1}^- &= c_j^\dagger \exp\left(i\pi\sum_{k=1}^{j-1} n_k\right)\exp\left(-i\pi\sum_{k=1}^{j} n_k\right)c_{j+1} \\ &= c_j^\dagger \exp\left(-i\pi n_j\right)c_{j+1} \end{aligned} \tag{2.15}$$

The factor of $\exp(-i\pi n_j)$ doesn't have any effect on the eigenbasis of the fermionic system, hence, $c_j^\dagger \exp\left(-i\pi n_j\right)c_{j+1} = c_j^\dagger c_{j+1}$. Similarly, it can be observed that $\sigma_j^-\sigma_{j+1}^+ = \left(\sigma_j^+\sigma_{j+1}^-\right)^\dagger = c_{j+1}^\dagger c_j$. Due to the PBC in the spin chain, the boundary terms such as $\sigma_N^+\sigma_1^-$ transform as $(-1)^{N+1}c_N^\dagger c_1$, etc. This affects the allowed values of momenta for the fermionic chain depending on the parity of the fermion number. However, as we are interested in the thermodynamic limit $L = Na \to \infty$, where L is the length of the spin chain and a is the lattice spacing, this boundary term's contribution becomes irrelevant. Applying the canonical transformation $c_i \to (-1)^i c_i$ (shifting the fermionic momenta by π), we obtain:

$$\boxed{\mathcal{H}_{\text{XXZ}} = -\frac{J_{xy}}{2}\sum_{j=1}^{N}\left(c_{j+1}^\dagger c_j + c_j^\dagger c_{j+1}\right) + J_z\sum_{j=1}^{N}\left(n_j - \frac{1}{2}\right)\left(n_{j+1} - \frac{1}{2}\right) + H\sum_{j=1}^{N}\left(n_j - \frac{1}{2}\right)} \tag{2.16}$$

Eq. (2.16) represents the hamiltonian of a one-dimensional chain of interacting fermions. For this model, J_{xy} acts as the hopping or kinetic energy of the system, and J_z acts as the nearest-neighbor interaction. The magnetic field h acts as a chemical potential for the fermionic chain. When $h = 0$, the average magnetization $\langle\sigma_j^z\rangle = 0$. In the fermionic language, this corresponds to $\langle n_j\rangle = 1/2$, which implies that the system is at half-filling and the corresponding fermi momentum is $k_F = \pi/2a$. The effect of h is to dope the system away from half-filling, which shifts the value of k_F. We will come back to this term at the end of Section 2.3 and show the effect of the finite magnetization more precisely.

Note that one can also map the XXZ spin chain on a one-dimensional system of interacting hard-core bosons via the mapping $\sigma_j^+ \to b^\dagger, \sigma_j^z \to n_b - 1/2$, where $b^\dagger$ and $n_b = b^\dagger b$ are the bosonic creation and number operators, respectively. In that case, the zero magnetization limit leads to a commensurate bosonic chain; finite magnetization destroys the commensuration of the system. This renders the XXZ spin chain as a quite generalized description of one-dimensional many-body systems. However, we limit our discussion here to Jordan-Wigner transformation as the fermionic description will be useful for the next step.

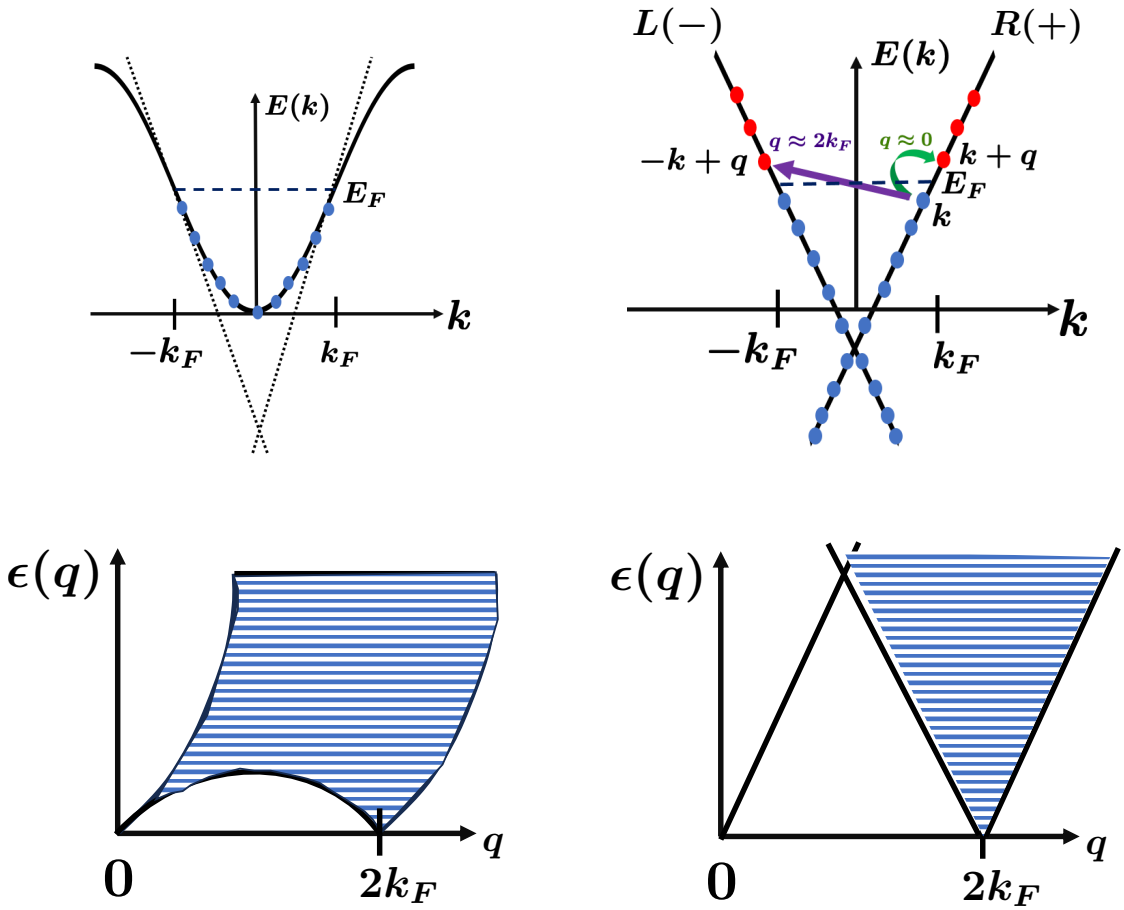

Figure 2.2: *Top*: The original cosine spectrum of the non-interacting spectrum (*left*). To analyze the low energy excitations, the spectrum is linearized at $E = E_F$ (*right*). Consequently, the spectrum has two bands: left ($-k_F$) and right (k_F). The excitations are majorly divided into two processes: $q \simeq 0$ or forward scattering (green arrow), and $q \simeq 2k_F$ or backward scattering (purple arrow). *Bottom*: The particle-hole excitation spectrum of the quadratic spectrum (*left*) and the linear spectrum (*right*). At small $q \sim 0$, the excitations have well-defined momenta and energy, and their energies depend only on q linearly.

2.3 Bosonization and Field theory

In general, many-body hamiltonians can't be diagonalized in the Fourier space due to the interaction term being quartic in fermionic operators. One has to apply certain techniques to understand the effect of interactions on a non-interacting system of fermions, also known as Fermi gas. For systems in two or higher dimensions and at zero or sufficiently low temperature, Fermi Liquid Theory (FLT) [33–36] captures these effects magnificently. In a nutshell, FLT proves that a system, in the presence of interaction, is extremely similar to Fermi gas: The ground state of the non-interacting system adiabatically goes to that of the interacting

system. The free fermions of Fermi gas are replaced by quasiparticles in an interacting system, and they remain essentially free (barring some residual interaction). These quasiparticles are fermions surrounded by particle-hole excitations and hence they are also fermionic in nature. Close to the fermi surface, the only parameter that changes is the mass of the quasiparticles. Even though one can reproduce these results via a perturbation of the interaction, FLT is not limited to only weak interactions.

However, FLT becomes invalid in one dimension. In this case, when a fermion wants to propagate, it must perturb its neighbors. This immediately points to the fact that in one-dimensional systems, excitations have to be collective in nature and the nearly free movements of quasiparticles are impossible. It can also be confirmed that a perturbation theory in interaction for one-dimensional many-body systems doesn't converge, which emphasizes the fact the ground state of the one-dimensional fermi sea drastically changes when an interaction is turned on in the system. Hence, one needs to find an alternative technique.

At low temperatures, the excitation in an interacting system is caused by the destruction of a particle with momentum k and the creation of a particle with momentum $k+q$ ($q>0$) below and above the fermi level, respectively. In one dimension, the fermi level of the system consists of only two points. Hence, a low-energy excitation is limited to $q=0$ and $q=2k_F$, where k_F is the fermi momentum of the system, and depends only on q. For example, in a one-dimensional system with quadratic dispersion $\epsilon_k = (k^2 - k_F^2)/2m$, the particle-hole excitation spectrum $E(q) = \epsilon_{k+q} - \epsilon_k$ for $q \simeq 0$ and $k \in [k_F - q, k_F]$ is well-defined and depends only on q via $E(q) = (k_F q)/m$ (fig. (2.2), *bottom left*). These excitations are composed of an even number of fermionic operators (one destruction and one creation operator), hence they are bosonic in nature. The bosonic quasiparticles can be used to analyze one-dimensional interacting systems and the technique is known as bosonization [37–39]. In the next subsection, we will apply the technique to our system (eq. (2.6)) and arrive at a field theory.

2.3.1 Bosonization of 1D XXZ spin chain

2.3.1.1 Non-interacting hamiltonian

Let's first focus on the non-interacting part of the hamiltonian which is responsible for the hopping of the fermions. I will denote this part as $\mathcal{H}_{\mathrm{XY}}$ from now on. Using Fourier transfor-

mation $c_j = \frac{1}{\sqrt{N}} \sum_k e^{ikx_j} c_k$ ($x_j = aj$), we can diagonalize the hamiltonian to calculate the energy dispersion:

$$\begin{aligned} \mathcal{H}_{\mathrm{XY}} &= -\frac{J_{xy}}{2N} \sum_{j=1}^{N} \sum_{k,k'} \left(e^{i(kx_j - k'x_{j+1})} + e^{-i(k'x_j - kx_{j+1})} \right) c_{k'}^\dagger c_k \\ &= -\frac{J_{xy}}{2} \sum_{k,k'} \left(e^{-ik'a} + e^{ika} \right) c_{k'}^\dagger c_k \delta_{k,k'} \\ &= -J_{xy} \sum_k \cos(ka)\, c_k^\dagger c_k \end{aligned} \tag{2.17}$$

The momenta k can take N values, and due to the PBC, $k = 2\pi n/(aN)$, where $n \in [-N/2, N/2)$. The energy dispersion $E(k) = -J_{xy}\cos(ka)$ and from here one can calculate the fermi velocity $v_F = \frac{dE(k)}{dk}|_{k=k_F} = aJ_{xy}\sin(ka)$.

We are interested in understanding the zero temperature, low-energy fluctuations of the hamiltonian in eq. (2.6), which is governed by particle-hole excitations close to the fermi surface. Hence, we first linearize the original dispersion relation at k_F (fig. (2.2), *top*). Note that this gives rise to two channels: The left channel (L) corresponds to the negative momenta, and the right channel (R) contains fermions of positive momenta. The non-interacting part of the system can thus be written as:

$$\mathcal{H}_{\mathrm{XY}} \simeq \sum_{\substack{k \\ r=\pm}} v_F (rk - k_F)\, c_{r,k}^\dagger c_{r,k} \tag{2.18}$$

Where $r = +$ corresponds to R and $r = -$ corresponds to L. This model is known as the Tomonaga-Luttinger model [40, 41]. The particle-hole excitations of this model, given by $v_F[r(k+q) - rK] = rv_F q$, are independent of k and well-defined (fig. (2.2), *bottom right*), hence we can convert the hamiltonian on this basis. Note that the $q \sim 0$ behavior of the excitations is linear in q, which mimics the particle-hole excitation spectrum of models with low-energy quadratic dispersion. We define the density fluctuation operators as:

$$\rho(q) = \sum_k c_k^\dagger c_{k+q}, \;\; \rho^\dagger(q) = \sum_k c_{k+q}^\dagger c_k \tag{2.19}$$

The density fluctuation operators have two fermionic operators in them, hence they are bosonic in nature. Hence, we will be able to define some bosonic operators b_q and $b_q^\dagger$ as the linear combinations of $\rho(q)$ and $\rho^\dagger(q)$. Before we proceed with the mapping, there is another detail to be noticed: In the linearized spectrum, the number of occupied states now extends to infinity. To

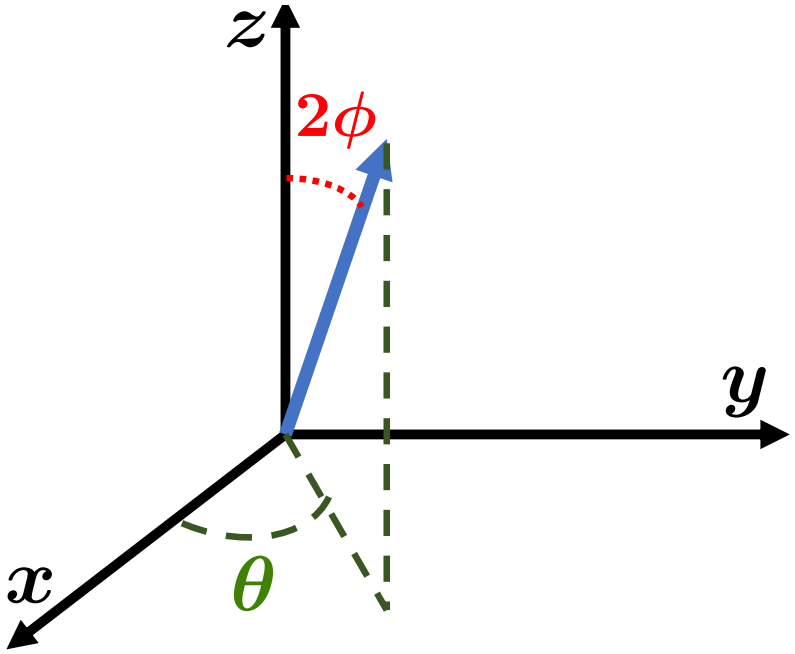

Figure 2.3: The physical interpretation of the fields ϕ and θ in context of the original microscopic system. The spin (blue arrow) can rotate in three dimensions. 2ϕ (red) is the angle it makes with the z-axis, and θ (green) represents the angle between x-axis and the spin's projection on the $x-y$ plane.

get rid of these divergences, we introduce normal-ordered operators: $:AB:=AB-\langle 0|\,AB\,|0\rangle$, where A and B are arbitrary operators. In Appendix A, we show that this procedure helps us ensure that the commutation relationship between the density fluctuation operators is bosonic in nature up to a normalization factor.

With these definitions, we are now ready to lay out a precise mapping of a fermionic chain to a bosonic field theory. It can be done in the two following steps:

- First, we convert the original fermionic operators to single-particle excitation operators close to the fermi momentum as follows:

$$c_j \simeq \frac{1}{\sqrt{N}} \sum_{k \simeq r k_F} e^{ikx} c_{r,k} = \sqrt{a} \sum_r \psi_r(x) \tag{2.20}$$

- Then, we convert these operators to two bosonic field operators $\phi(x)$ and $\theta(x)$ with the

following mappings (For more details, see Appendix A):

$$\begin{aligned}\psi_r(x) &= e^{irk_Fx}\widetilde{\psi}_r(x)\\ \widetilde{\psi}_r(x) &= \frac{U_r}{\sqrt{2\pi a}}e^{-i[r\phi(x)-\theta(x)]}\end{aligned} \tag{2.21}$$

Here U_r, etc. are known as the Klein factors, which follow majorana fermion-like anti-commutation rules:

$$\begin{aligned}\{U_r^\dagger, U_{r'}^\dagger,\} = \{U_r; U_{r'},\} = 0\\ \{U_r^\dagger, U_{r'}\} = 2\delta_{r,r'},\ U_r^\dagger U_r = U_r U_r^\dagger = 1\end{aligned} \tag{2.22}$$

$\psi_r(x)$ is fermionic in nature, and $\phi(x)$ and $\theta(x)$ are bosonic operators, hence the Klein factors are important for rigorous mapping of fermionic operators to bosonic ones. The fast oscillating part is contained within the e^{rik_Fx} factor and $\phi(x)$ and $\theta(x)$ are slowly varying bosonic fields. They are also related to each other: The canonical momentum $\Pi(x)$ conjugate to $\phi(x)$ is given by $\Pi(x) = \frac{1}{\pi}\nabla\theta(x)$.

The bosonic fields ϕ and θ have physical significance in the context of the XXZ spin chain. As the spins can rotate within a three-dimensional sphere, their rotational configuration can be described with ϕ and θ. The polar angle of the spin is represented by 2ϕ, and θ represents the azimuthal angle of the spin, as shown in fig. (2.3). With these definitions laid out, we are now ready to convert $\mathcal{H}_{\text{XY}}$ (eq. (2.18)) to a bosonic field theory. Applying eq. (2.20) on the k-dependent part of the linear hamiltonian, we obtain :

$$\begin{aligned}\mathcal{H}_{\text{XY}} &= v_F\sum_k c_{+,k}^\dagger\left(kc_{+,k}\right) + v_F\sum_k c_{-,k}^\dagger\left(-kc_{-,k}\right)\\ &= \frac{v_F}{Na}\sum_k\sum_{x,x'}\left[\psi_+^\dagger(x)\left(-i\partial_{x'}\right)\psi_+(x')e^{ik(x-x')} + \psi_-^\dagger(x)\left(i\partial_{x'}\right)\psi_-(x')e^{ik(x-x')}\right]\\ &= \frac{av_F}{2}\sum_x\left[\psi_+^\dagger(x)\left(-i\partial_x\right)\psi_+(x) + \psi_-^\dagger(x)\left(i\partial_x\right)\psi_-(x)\right]\end{aligned} \tag{2.23}$$

From eq. (2.21), we see that $i\partial_x\psi_r(x) = -\left(rk_F - r\nabla\phi(x) + \nabla\theta(x)\right)\psi_r(x)$. Before we proceed, there is one more observation we need to make. Using eq. (A.5) and (A.6), we see that in the thermodynamic limit via $\psi_+^\dagger\psi_+ = \left(\nabla\theta(x) - \nabla\phi(x)\right)/2\pi$ and $\psi_-^\dagger\psi_- = -\left(\nabla\theta(x) + \nabla\phi(x)\right)/2\pi$. In the continuum limit $a \to 0$, we can convert the sum over x to an integral via $\sum_x \to \frac{1}{a}\int_0^L dx$. Putting them back, we find:

$$\therefore\ \mathcal{H}_{\text{XY}} = \frac{v_F}{4\pi}\int dx\left[\left(\nabla\theta(x) - \nabla\phi(x)\right)^2 + \left(\nabla\theta(x) + \nabla\phi(x)\right)^2 - 2k_F\nabla\phi(x)\right] \tag{2.24}$$

The $2k_F\nabla\phi(x)$ term cancels the constant term in eq. (2.18). Hence, the bosonized version of the non-interacting hamiltonian is given by:

$$\boxed{\mathcal{H}_{XY} = \frac{v_F}{2\pi}\int_0^L dx\left[(\pi\Pi(x))^2 + (\nabla\phi(x))^2\right]} \tag{2.25}$$

2.3.1.2 Interacting part

Now, we bosonize the interaction which takes the following form (h.c. denotes hermitian conjugate):

$$\begin{aligned}
\mathcal{H}_{\mathrm{Z}} &= J_z\sum_j n_j n_{j+1} \\
&= a^2 J_z\sum_{x=a}^{Na}\left[\widetilde{\psi_+^\dagger}(x)\widetilde{\psi_+}(x) + \widetilde{\psi_-^\dagger}(x)\widetilde{\psi_-}(x) + \left(e^{-2ik_Fx}\widetilde{\psi_+^\dagger}(x)\widetilde{\psi_-}(x) + \text{h.c.}\right)\right] \\
&\times \left[\widetilde{\psi_+^\dagger}(x+a)\widetilde{\psi_+}(x+a) + \widetilde{\psi_-^\dagger}(x+a)\widetilde{\psi_-}(x+a) + \left(e^{-2ik_F(x+a)}\widetilde{\psi_+^\dagger}(x+a)\widetilde{\psi_-}(x+a) + \text{h.c.}\right)\right]
\end{aligned} \tag{2.26}$$

To simplify the multiplication, we use eq. (A.5) for the $\psi^\dagger\psi$ terms. We also drop the fastly oscillating e^{2ik_Fx} terms:

$$\begin{aligned}
\mathcal{H}_{\mathrm{Z}} &= \frac{a^2J_z}{\pi^2}\sum_{x=a}^{Na}\nabla\phi(x+a)\nabla\phi(x) + \frac{J_z}{4\pi^2}\sum_{x=a}^{Na}\left[e^{-2ik_Fa}e^{2i(\phi(x+a)-\phi(x))} + \text{h.c.}\right] \\
&+ \frac{J_z}{4\pi^2}\sum_{x=a}^{Na}\left(U_+^\dagger U_-\right)^2\left[e^{-2ik_F(2x+a)}e^{2i(\phi(x+a)+\phi(x))} + \text{h.c}\right]
\end{aligned} \tag{2.27}$$

In the continuum limit $a\to 0$, the first term becomes $(\nabla\phi(x))^2$ and $\phi(x+a)-\phi(x)\simeq a\nabla\phi(x)$. The exponential of the bosonic field in the second term can be expanded as $e^{2i(\phi(x+a)-\phi(x))}\simeq 1+2ai\nabla\phi(x)-2a^2(\nabla\phi(x))^2$. The constant term can be discarded and the linear terms of the hermitian conjugates cancel each other. Two different cases arise from the third term depending on the value of magnetization h:

- $\boldsymbol{h\neq 0}$: When the spin chain is at finite magnetization sector, the third term sums to zero because of the highly oscillating factor e^{4ik_Fx}. The second term, after summing the hermitian conjugates, becomes $-(a^2J_z/\pi)\cos(k_Fa)$. After summing up all the terms

and converting the sum over x to an integral, we find:

$$\boxed{\begin{aligned}\mathcal{H}_{\text{XXZ, incomm}} &= \frac{1}{2\pi}\int_0^L dx\left[\frac{u}{K}\left(\nabla\phi(x)\right)^2 + uK\left(\pi\Pi(x)\right)^2\right] \\ uK = v_F &= aJ_{xy}\sin(k_F a) \\ \frac{u}{K} &= v_F\left[1+\frac{2aJ_z}{\pi v_F}\left(1-\cos(k_F a)\right)\right]\end{aligned}} \tag{2.28}$$

- $\boldsymbol{h = 0}$: In this case, the first two terms behave exactly like the previous case with the replacement of $k_F = \pi/2a$. However, now $e^{\pm 4ik_F x}$ behaves as 1^x and hence the third term survives. In the continuum limit, $2\left(\phi(x+a)+\phi(x)\right) \simeq 2\phi(x)$. We drop the factors U_+ etc. because they are irrelevant for computing correlation functions and the hamiltonian is now given by

$$\boxed{\begin{aligned}\mathcal{H}_{\text{XXZ, comm}} &= \mathcal{H}_{\text{XXZ, incomm}} - \frac{g}{2\pi^2}\int_0^L dx\cos\left(4\phi(x)\right) \\ uK &= aJ_{xy} \\ \frac{u}{K} &= aJ_{xy}\left[1+\frac{4J_z}{\pi J_{xy}}\right] \\ g &= aJ_z\end{aligned}} \tag{2.29}$$

The effect of the magnetization can be observed from the bosonization perspective as well. We can map σ_j^z to the bosonic field operators via:

$$\begin{aligned}\sigma_j^z = n_j - \frac{1}{2} &= a\left[\psi_+^\dagger\psi_+ + \psi_-^\dagger\psi_- + \left(e^{-2ik_F x}\psi_+^\dagger + \psi_- + \text{h.c}\right)\right]] \\ &= \frac{1}{\pi}\left[-a\nabla\phi(x) + \cos\left(2\phi(x) - 2k_F x\right)\right]\end{aligned} \tag{2.30}$$

With this mapping, it's easy to see that the term with the magnetic field $H\sum_j n_j$ in the bosonized version is given by $-(H/\pi)\int dx\nabla\phi(x)$. In a fixed magnetization sector, this term can be absorbed into the quadratic hamiltonian by defining a new field $\widetilde{\phi}(x) = \phi(x) - (HKx/u)$. The magnetization M thus affects the fermi momentum as $k_F = \frac{\pi(1-(M/N))}{2a}$. At zero magnetization ($h = 0$), the fermi momentum $k_F = \pi/2a$ is commensurate with the lattice spacing, and hence we will be referring to this case as the '*commensurate model*'. Similarly, in a non-zero magnetization sector ($h \neq 0$), the model remains *incommensurate*.

2.3.2 Effective action: Path integral and integrating out the baths

Until now, we have only discussed the XXZ spin chain. With the help of bosonization, we have been able to get rid of the quartic interaction term; the bath degrees are still intact. Hence, we apply Feynmann Path Integral formalism to the bosonized hamiltonian. In a nutshell, this procedure maps an N dimensional quantum system to a $N+1$ dimensional classical system. Applying Path Integral allows us to integrate out the baths and arrive at an effective action of the system, where the effect of the bath is captured in a non-perturbative manner. The technical details of Path Integral itself was first discovered in [42] and can be found in [43, 44]. Here, we will restrict the discussion to the application of the formalism to our model.

Writing the Path Integral for the bosonized XXZ spin chain, we obtain

$$\begin{aligned} \mathrm{Tr} e^{-\beta \mathcal{H}_{\mathrm{XXZ}}} &= \int \mathcal{D}\Pi(x,\tau)\mathcal{D}\phi(x,\tau) e^{-S_{\mathrm{XXZ}}[\Pi,\phi]} \qquad (2.31) \\ S_{\mathrm{XXZ,IC}}[\Pi,\phi] &= \int_0^\beta d\tau \int_0^L dx \left[\frac{u}{2\pi}\left\{\frac{1}{K}\left(\nabla\phi(x,\tau)\right)^2 + K\left(\pi\Pi(x,\tau)\right)^2\right\} - i\Pi(x,\tau)\partial_\tau\phi(x,\tau)\right] \\ S_{\mathrm{XXZ,C}}[\Pi,\phi] &= S_{\mathrm{XXZ,IC}} - \frac{g}{2\pi^2}\int_0^\beta d\tau \int_0^L dx \cos\left(4\phi\left(x,\tau\right)\right) \end{aligned}$$

Where $S_{\mathrm{XXZ,IC}}$ corresponds to the microscopic system at $h=0$ and $S_{\mathrm{XXZ,CC}}$ corresponds to finite h. For the path integral, we integrate over all possible Π and ϕ, where ϕ satisfies periodic boundary conditions both in x and τ, i.e., $\phi(x,\tau+\beta)=\phi(x,\tau)$, $\phi(x+L,\tau)=\phi(x,\tau)$. τ is called the imaginary time. It acts as an additional dimension for the classical statistical action S_{XXZ} and has a length $\beta = 1/T$, where T is the temperature of the system. By sending both β and L to infinity, one can recover the thermodynamic limit of the microscopic model at zero temperature. One can re-write the quadratic part of the action ($S_{\mathrm{XXZ,IC}}$ of eq. (2.31)) in terms of only ϕ. To do so, we complete the square with $\Pi(x,\tau)$ and obtain

$$S_{\mathrm{XXZ,IC}} = \iint dx d\tau \left[\frac{u}{2\pi K}\left(\nabla\phi(x,\tau)\right)^2 + \frac{uK\pi}{2}\left(\Pi(x,\tau) + \frac{i}{\pi u K}\partial_\tau\phi(x,\tau)\right)^2 + \frac{1}{2\pi u K}\left(\partial_\tau\phi(x,\tau)\right)^2\right]$$

We define a new variable $\widetilde{\Pi}(x,\tau) = \Pi(x,\tau) + \frac{i}{\pi u K}\partial_\tau \phi(x,\tau)$, which can be integrated out as a gaussian variable. This gives us

$$\boxed{S_{\text{XXZ,IC}} = \frac{1}{2\pi K}\int_0^\beta d\tau \int_0^L dx \left[u\left(\nabla\phi(x,\tau)\right)^2 + \frac{1}{u}\left(\partial_\tau\phi(x,\tau)\right)^2\right]} \tag{2.32}$$

Similarly, one can write a Path Integral formulation for the dissipative baths and the coupling of the baths to the spin chain:

$$\begin{aligned}
\text{Tr}e^{-\beta(\mathcal{H}_\text{B}+\mathcal{H}_\text{SB})} &= \int \mathcal{D}\phi\,(x,\tau)\prod_k \mathcal{D}X_k(x,\beta)e^{-(S_\text{B}[\{P_k,X_k\}]+S_\text{SB}[\phi,\{X_k\}])} \\
S_\text{B}\left[\{P_k,X_k\}\right] &= \frac{1}{2}\int_0^\beta d\tau\int_0^L dx\sum_k \rho_k\left[\Omega_k^2 X_k^2(x,\tau) + \left(\partial_\tau X_k(x,\tau)\right)^2\right] \\
S_\text{SB}\left[\phi,\{X_k\}\right] &= \frac{1}{\pi}\int_0^\beta d\tau\int_0^L dx\left[-\nabla\phi(x,\tau) + \frac{1}{a}\cos\left(2\phi(x,\tau) - 2k_F x\right)\right]\sum_k \lambda_k X_k(x,\tau)
\end{aligned} \tag{2.33}$$

Where we have already taken the continuum limit $a \to 0$ and $\rho_k = m_k/a$ is the mass density of the oscillators. Now, we proceed to integrate out the bath degrees of freedom from the total action $S_\text{eff} = S_\text{XXZ} + S_\text{SB} + S_\text{B}$. We calculate the following normalized partition function:

$$\begin{aligned}
\frac{Z_\text{tot}}{Z_\text{B}} &= \int \mathcal{D}\phi e^{-S_\text{XXZ}}\frac{\int \mathcal{D}\phi\prod_k \mathcal{D}X_k e^{-S_\text{SB}}e^{-S_\text{B}}}{\int\prod_k \mathcal{D}X_k e^{-S_\text{B}}} \\
&= \int \mathcal{D}\phi e^{-S_\text{XXZ}}\langle e^{-S_\text{SB}}\rangle \\
&= \int \mathcal{D}\phi e^{-S_\text{XXZ}}e^{\frac{1}{2}\langle S_\text{SB}^2\rangle}
\end{aligned} \tag{2.34}$$

Where in the last line, we use the fact that the action is Gaussian in bath degrees of freedom. Inserting the form of S_SB in eq. (2.34), we obtain:

$$\begin{aligned}
S_\text{tot} &= S_\text{XXZ} - S_\text{int} \\
S_\text{int} &= \frac{1}{2\pi^2}\iint dxd\tau\left[-\nabla\phi(x,\tau) + \frac{1}{a}\cos\left(2\phi(x,\tau) - 2k_F x\right)\right]\left(\sum_{k,k'}\lambda_k\lambda_{k'}\left\langle X_k\left(x,\tau\right)X_k\left(x',\tau'\right)\right\rangle\right) \\
&\times \iint dx'd\tau'\left[-\nabla\phi(x',\tau') + \frac{1}{a}\cos\left(2\phi(x',\tau') - 2k_F x'\right)\right]
\end{aligned} \tag{2.35}$$

We know that the bath degrees of freedom are spatially uncorrelated from each other; however, they are correlated in τ, and it's given by

$$\langle X_k(x,\tau)X_k(x',\tau')\rangle = \frac{1}{\beta}\sum_{\omega_n}\frac{e^{-i\omega_n(\tau-\tau')}}{\rho_k\left(\omega_n^2+\Omega_k^2\right)}\delta\left(x-x'\right)\delta_{k,k'}$$

Where $\omega_n = 2\pi n/\beta,\ n\in[-\beta/2,\beta/2)$ is the fourier mode corresponding to τ and is known as Matsubara frequency. Using this relation and observing that $1/(\omega_n^2+\Omega_k^2) = \frac{1}{\Omega_k}\int d\Omega \frac{\Omega}{\omega_n^2+\Omega^2}\delta\left(\Omega-\Omega_k\right)$, we obtain:

$$\begin{aligned} S_{\text{int}} &= \frac{1}{2\pi^2}\iint dx d\tau\left[-\nabla\phi(x,\tau)+\frac{1}{a}\cos\left(2\phi(x,\tau)-2k_Fx\right)\right]D\left(\tau-\tau'\right) \\ &\times \int d\tau'\left[-\nabla\phi(x,\tau')+\frac{1}{a}\cos\left(2\phi(x,\tau')-2k_Fx\right)\right] \\ D\left(\tau-\tau'\right) &= \int d\Omega\left(\sum_k\frac{\lambda_k^2}{\rho_k\Omega_k}\delta\left(\Omega-\Omega_k\right)\frac{1}{\beta}\sum_{\omega_n}e^{-i\omega_n(\tau-\tau')}\frac{\Omega}{\omega_n^2+\Omega^2}\right) \end{aligned} \tag{2.36}$$

$D(\tau-\tau')$ is the kernel introduced due to the contribution of the dissipative baths. It depends on the spectral density of the baths (as described in Chapter 1), given by $J(\Omega) = (\pi/2)\sum_k\frac{\lambda_k^2}{\rho_k\Omega_k}\delta\left(\Omega-\Omega_k\right) = \pi\alpha\Omega^s\ \forall\ \Omega\in(0,\Omega_D)$, where Ω_D is the Debye frequency. Using that, one can find out that at times larger than a characteristic time scale τ_c, $D(\tau-\tau')\sim\alpha/\left|\tau-\tau'\right|^{1+s}$. Furthermore, we put $a=1$, which was there for dimensional purposes. With this, we are able to contract S_{int} as:

$$\begin{aligned} S_{\text{int}} &= \frac{\alpha}{2\pi^2}\int\frac{dxd\tau d\tau'}{\left|\tau-\tau'\right|^{1+s}}\left[-\nabla\phi(x,\tau)+\frac{1}{a}\cos\left(2\phi(x,\tau)-2k_Fx\right)\right] \\ &\times \left[-\nabla\phi(x,\tau')+\frac{1}{a}\cos\left(2\phi(x,\tau')-2k_Fx\right)\right] \end{aligned} \tag{2.37}$$

Expanding the multiplication, we make the following observations:

- The $\nabla\phi(\tau)\nabla\phi(\tau')$ term is the forward scattering term and can be neglected from power counting.
- The $\nabla\phi(\tau)\cos\left(2\phi(\tau')\right)$ terms oscillate rapidly due the presence of the $2k_Fx$ term for any magnetization.
- The $\cos\left(2\phi(\tau)\right)\cos\left(2\phi(\tau')\right)$ term survives, and we expand it into two cosine terms. One of these terms is $\cos\left(2\left(\phi(\tau)-\phi(\tau')\right)\right)$, and it's independent of the magnetization of the microscopic system. The other term is $\cos\left(2\left(\phi(\tau)+\phi(\tau')\right)+4k_Fx\right)$, and it only survives at zero magnetization or half-filling when $k_F=\pi/2a$.

Gathering all this information together, we arrive at the final action of the system. For the incommensurate case, the action is given by:

$$\boxed{\begin{aligned} S_{\text{tot}} &= S_{\text{XXZ}} - S_{\text{int}} \\ S_{\text{XXZ}} &= \frac{1}{2\pi K}\int d\tau dx \left[u\left(\nabla\phi(x,\tau)\right)^2 + \frac{1}{u}\left(\partial_\tau\phi(x,\tau)\right)^2\right] \\ S_{\text{int}} &= \frac{\alpha}{4\pi^2}\int dx d\tau d\tau' \frac{\cos\left[2\left\{(\phi(x,\tau)-\phi(x,\tau'))\right\}\right]}{|\tau-\tau'|^{1+s}} \end{aligned}}$$

Whereas for a commensurate spin chain, the action of the system is:

$$\boxed{\begin{aligned} S_{\text{tot,C}} &= S_{\text{XXZ,C}} - S_{\text{int,C}} \\ S_{\text{XXZ,C}} &= \frac{1}{2\pi K}\int d\tau dx \left[u\left(\nabla\phi(x,\tau)\right)^2 + \frac{1}{u}\left(\partial_\tau\phi(x,\tau)\right)^2\right] - \frac{g}{2\pi^2}\int dx d\tau \cos\left[4\phi(x,\tau)\right] \\ S_{\text{int,C}} &= \frac{\alpha}{4\pi^2}\int dx d\tau d\tau' \frac{\cos\left[2\left\{(\phi(x,\tau)-\phi(x,\tau'))\right\}\right] + \cos\left[2\left\{(\phi(x,\tau)+\phi(x,\tau'))\right\}\right]}{|\tau-\tau'|^{1+s}} \end{aligned}}$$

2.4 Luttinger liquid and sine-Gordon model

Before we proceed with analyzing the effect of the bath, we discuss the phase diagram of the original model without the bath present. Putting $\alpha = 0$ in eq. (2.1), we find that the 1D incommensurate XXZ spin chain can be described by the action:

$$S_{\text{LL}} = \frac{1}{2\pi K}\int d\tau dx \left[u\left(\nabla\phi(x,\tau)\right)^2 + \frac{1}{u}\left(\partial_\tau\phi(x,\tau)\right)^2\right] \tag{2.38}$$

In the literature, this is known as the Luttinger Liquid (LL) action [40, 41, 45, 46]. It is an effective low-temperature description of the massless regime for one-dimensional systems [47–49]. The occupation factor of LL has an exponential singularity at $k = k_F$ instead of a discontinuous jump, which is usually observed in higher dimensional interacting systems. This proves that the low-energy excitation is bosonic in nature in one dimension and not fermionic. LL has a gapless low-energy spectrum, is quasi-ordered, and the excitations in this phase are a mixture of diverging superfluid and charge density wave fluctuations [37]. At zero temperature, the conductivity of LL is a Drude peak, i.e., the system is perfectly conducting. We will discuss more properties of this phase, specifically certain thermodynamical responses, in Chapter 4 in more detail.

Bosonization shows us that this dissipative environment acts as a cosine potential along only the τ direction for an incommensurate spin chain. One can intuitively understand see that S_{LL}

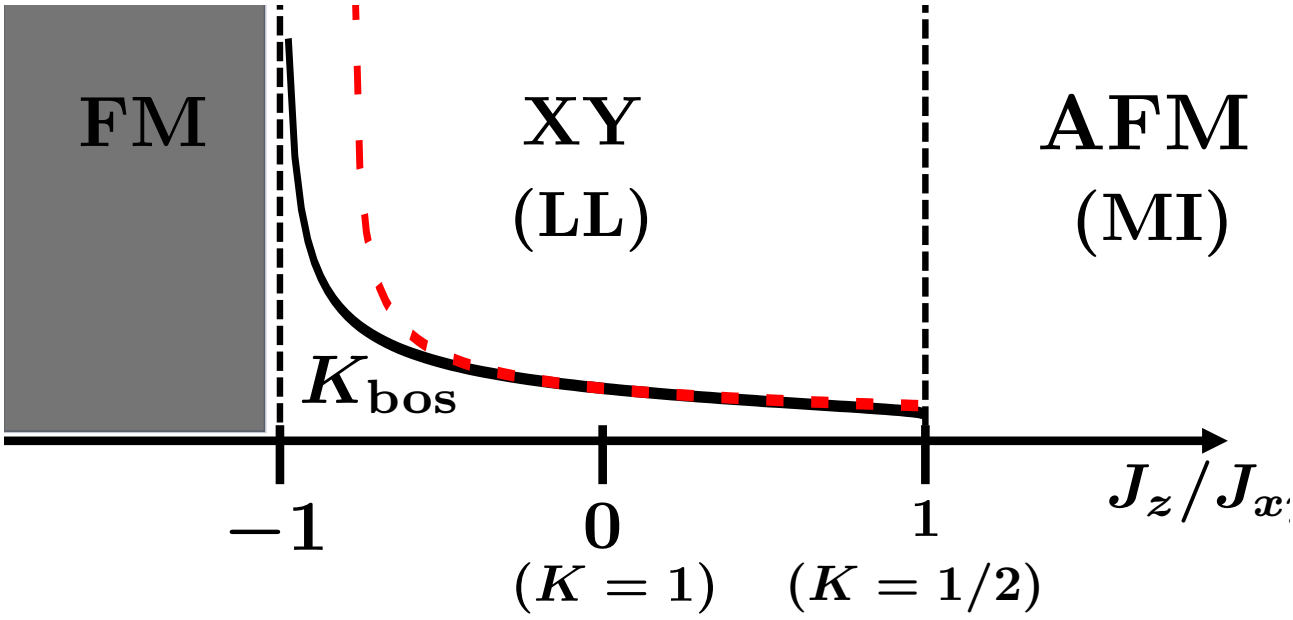

Figure 2.4: Phase diagram of 1D commensurate XXZ spin chain. The system can be solved exactly with Bethe Ansatz, and bosonization captures the XY phase (described by LL theory) and the AFM system (described by Mott Insulator theory). The LL parameter K calculated via bosonization K_{bos} (black solid line) matches well with the value obtained from Bethe Ansatz K_{BA} (red dashed line) in the region $J_z << J_{xy}$ and diverges at the Ferromagnetic transition.

contains the momenta $\Pi(x,\tau)$ conjugate to $\phi(x,\tau)$ and promotes fluctuations in the field that scales as the system size, resulting in unbounded fluctuations in the thermodynamic limit. On the other hand, the cosine potential tries to pin the field in one of its minima. This, along with the fact that S_{int} is long-range in imaginary time τ for $0 < s < 2$ [50], hints at the presence of a quantum phase transition at zero temperature. In the subsequent chapters, we locate this critical point and classify the behavior of the dissipation-induced phase using analytical and numerical techniques.

Note that when the spin chain is commensurate, the action of the XXZ spin chain is different and can be observed by putting $\alpha = 0$ in eq. (2.2):

$$S_{\mathrm{SG}} = S_{\mathrm{LL}} - \frac{g}{2\pi^2}\int dx d\tau \cos\left(4\phi(x,\tau)\right) \tag{2.39}$$

This action belongs to a class of model, popularly known as the two-dimensional Sine-Gordon model [51–53] and has been previously studied in context to many other physical systems such as the XY model [54, 55], the Thirring model [56, 57], models with spin and charge, etc. This model undergoes a phase transition [58], which belongs to the Berezinski-Kosterlitz-Thouless

universality class [59–62]. For K larger than a critical value $K_c = 1/2$ and for sufficiently large g, the system enters into a gapped Mott Insulator phase [63, 64] due to breaking of the discrete symmetry $\phi \to \phi + (2n+1)\pi/2,\ n \in \mathbb{Z}$. We will discuss the effect of the bath on this action in Chapter 6.

The one-dimensional XXZ model has also been solved exactly with the help of Bethe ansatz [65, 66]. The LL parameter K can also be calculated via this method (e.g., for a commensurate spin chain, $1/K_{\mathrm{BA}} = (2/\pi)\cos^{-1}(-J_z/J_{xy})$), which corresponds to that from bosonization (eq. (2.28) and (2.29)) at a small J_z/J_{xy} limit. The bosonization method is not able to capture the Ferromagnetic phase of the XXZ spin chain ($J_z/J_{xy} < -1$) due to the quadratic nature of energy dispersion $\omega \sim k^2$; however, the XY phase and the Ising AFM phase are well described by the LL phase and the Sine-Gordon Mott insulating phase, respectively (fig. (2.4), *left*). Note that For an incommensurate 1D XXZ spin-1/2 chain, the complete phase diagram of the microscopical system [67] is not described by only the LL action (eq. (2.32)). In this thesis, we focus on understanding the effect of the dissipation on the spin chain existing in the LL phase. In this regime, we are able to neglect oscillating terms such as $e^{4ik_F x}$ due to the system being sufficiently incommensurate (see derivation of eq. (2.28)). This assumption will be used multiple times in further calculations.

Chapter 3

Methods

In this chapter, we discuss the theories behind the numerical and analytical techniques that we will use in our thesis for analyzing our system. In a nutshell, we first talk about the perturbative Renormalization Group (RG) procedure, which is useful for detecting the critical point and the nature of the phase transition. Then we describe the procedure for variational ansatz, which effectively captures the behavior of the low-energy physics of the two phases. As an example, we show the applications of these techniques on the Sine-Gordon model (eq. (2.39)). These results will be useful to understand the application of the processes to our problem as well. Finally, we describe the numerical Langevin dynamics procedure, through which we simulate our action to explore the phase space of the action S_{tot}.

3.1 Perturbative Renormalization Group

As explained in Section 2.3, one of the biggest challenges in solving one-dimensional systems is the copious amount of singularities encountered, specifically at the low energy regime that we are interested in. For example, the effective interaction between two particles $\Gamma \sim g \ln(E/\omega)$ is logarithmically divergent at small frequencies [37, 68], where g is some microscopic coupling parameter. However, if ω is large, then the logarithmic quantity is of $O(1)$ and doesn't pose any problem. The fundamental idea of the RG procedure is to scale $g \to g'$ in such a way that the UV cut-off of the new theory is smaller than the previous one, with the condition that g' remains controlled. By doing so, one can get rid of unnecessary degrees of freedom and the theory becomes less divergent at a given scale of ω. From the behavior of the parameter flow as a function of the length scale, the critical point of a phase transition and its universality class can be detected.

Many different methods of perturbative RG have been discovered and well-established in the literature, such as the Kadanoff method [69], Wilson RG method [70] etc. However, the one we will use in this thesis is via calculating the correlation function of the form $\langle e^{ib\phi(x,\tau)} e^{-ib\phi(x',\tau')} \rangle$, where b is a constant. This is inspired by [71], where they investigated the phase transition in a two-dimensional planar Heisenberg model as a function of temperature. Furthermore, the same technique was used in [37] to analyze the aforementioned Sine-Gordon model (eq. (2.39)). We will not show the derivation of the RG equations for the Sine-Gordon model here, as it is very similar to the one done in Section 4.1; however, we will discuss the results to understand the nature of the phase transition and the location of the critical point.

3.1.1 Renormalization Group of Sine-Gordon model

The RG equations for the parameters K and g of eq. (2.39) is given by [37]:

$$\boxed{\frac{dK(l)}{dl} = -\frac{g^2(l)K^2(l)}{2}} \tag{3.1}$$

$$\boxed{\frac{dg(l)}{dl} = (2 - 4K(l))\, g(l)} \tag{3.2}$$

Where l is a dimensionless length scale, parametrized by $\Lambda(l) = \Lambda_0 e^{-l}$, Λ_0 being the bare high-energy cut-off of the theory (equivalently, $a(l) = a_0 e^{l}$, where a is a small length cut-off). It is evident from eq. (3.2) that the behavior of the RG flow of α depends on the initial value of K. When $K < K_c = 1/2$, the coefficient of $g(l)$ is positive in eq. (3.2). In this case, the flow of $g(l)$ is uncontrolled, i.e., the renormalized value $g(l = \infty) = g_r$ goes to infinity. This indicates that the system is in a new phase and in this phase, the cosine operator of eq. (2.39) is relevant. Due to the perturbative nature of the RG, the procedure fails to capture the renormalized values of the parameters in this phase. However, if $K \geq K_c$, for g smaller than or equal to a critical value of g_c, the system stays in the LL phase with finite $K(l = \infty) = K_r$ and $g_r = 0$ (irrelevant cosine potential). For larger values of g, the system enters into the other phase. The value of g_c turns out to be $K - K_c$ from the linear stability analysis of the RG equations; this determines the separatrix or the boundary of the phase transition. On the phase boundary, marked by the points (K_c, α_c), it can be shown that the system remains in the existing LL phase, which is a characteristic of the BKT universality class (fig. (3.1)). It can also be understood from the structure of the flow equations (eq. (3.1) and (3.2)) [62].

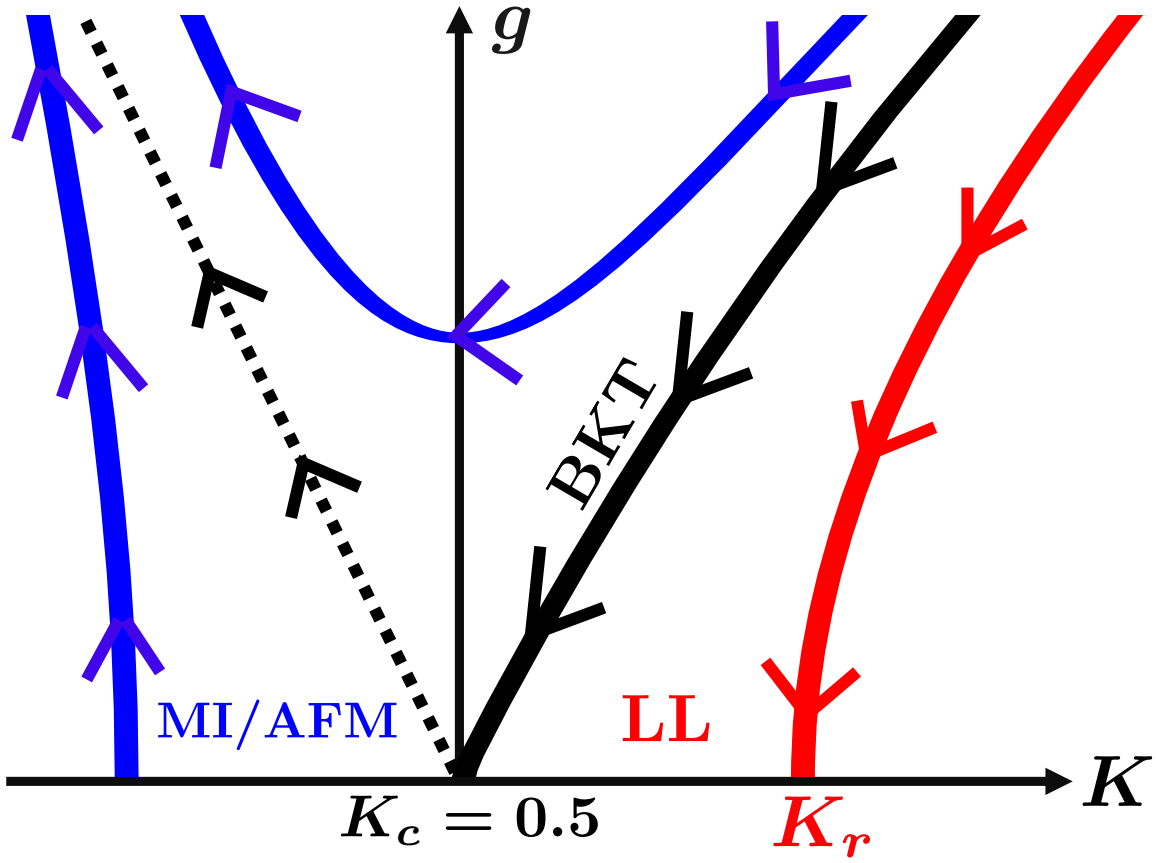

Figure 3.1: RG flow of Sine-Gordon model. The red line corresponds to the LL phase, where K_r is finite and $g_r = 0$ (see text). The separatrix is given by the solid black line $g_c = K - K_c$. For $g > g_c$ with $K \geq K_c$ and for any value of α with $K < K_c$, the cosine term becomes relevant as $g_r = \infty$ and $K_r = 0$, indicating the presence of a new phase. The arrowheads denote the direction of the flow.

The nature of the phase transition can also be determined from the RG equations via scaling arguments. One can approximate the cosine in eq. (2.39) via its quadratic expansion in the other phase as g goes to infinity and thus one can assume that the field ϕ is pinned in one of the minima of the cosine potential. By Fourier transforming this quadratic action, it can be observed that the other phase has a gap Δ in the low energy spectrum. This gap can be associated with a correlation length. The critical value of this correlation length ξ_c can be estimated as $\xi_c \sim e^{l^*}$, where l^* is a lengthscale such that $g(l^*) \simeq O(1)$. From dimensional analysis, it can be observed that near the critical point, the gap behaves as $\Delta \sim \xi_c^{-1} \simeq e^{-l^*}$.

With this information, one can now try to analyze how the gap behaves as a function of g

in the new phase in different regions of the phase. In the region $g << |K - K_c|$ (deep in the ordered phase) for small g, the flow is almost vertical, hence one can approximate that $dK/dl = 0$. From the RG flow, it can then be seen that $g(l) \simeq g_0 e^{(2-4K)l}$. Hence at the length scale l^*, $e^{l^*} \sim (1/g_0)^{1/(2-4K)}$, and the gap behaves as $\boldsymbol{\Delta \sim g_0^{1/(2-4K)}}$. As we will see in the next section, this behavior is the same as eq. (3.8); and we will use this as an argument for the validity of the variational ansatz.

However, one can also approach the critical line K_c from the symmetric phase. In this regime, the flow equations don't converge, but one can run the equation up to the length-scale $l = l^*$. In this regime, g is of order 1, and K flows as $Al = \tan^{-1}\left((K_0 - K_c)/A\right) - \tan^{-1}\left((K - K_c)/A\right)$, where $A = \sqrt{g_0^2 - (K_0 - K_c)^2}$ and $K_0 = K(l = 0)$. If one starts close to the critical line, $A \approx 0$. Following the blue flow line on the top in fig. (4.1), one can see that $K_0 - K_c > 0$ and $K(l^*) - K_c < 0$, hence $(K_0 - K_c)/A = +\infty$ and $(K - K_c)/A = -\infty$. Using the flow equation, we thus obtain that $l^* = \pi/A$, and hence the gap in this regime behaves as $\boldsymbol{\Delta \sim e^{-\pi/A}}$. From the definition of A, we see that this quantity is the square root of the distance of the point from the phase boundary; which means as one approaches the critical line, the gap vanishes exponentially. This result is highly non-perturbative.

3.2 Variational ansatz

Perturbative RG is an important technique to locate the critical point of a phase transition. It is also useful for analyzing the flow of parameters near the critical point in the symmetric phase. However, deep in the ordered phase, the coupling of the relevant term goes to infinity very fast. Hence, perturbative RG can't be used to analyze the physical properties of the ordered phase. There are other non-perturbative RG techniques that allow one to control the flow of parameters in the ordered phase, such as strong disorder RG [72, 73], functional RG [74] etc. However, here we use a method known as the variational method (or self-consistent harmonic approximation) to understand the two phases quantitatively and qualitatively away from the critical point. This method was first introduced in [75] to illustrate the usefulness of the path integral approach in condensed matter systems. Below, we describe the principles behind this method, and as an example, show its application to the Sine-Gordon model (eq. (2.39)).

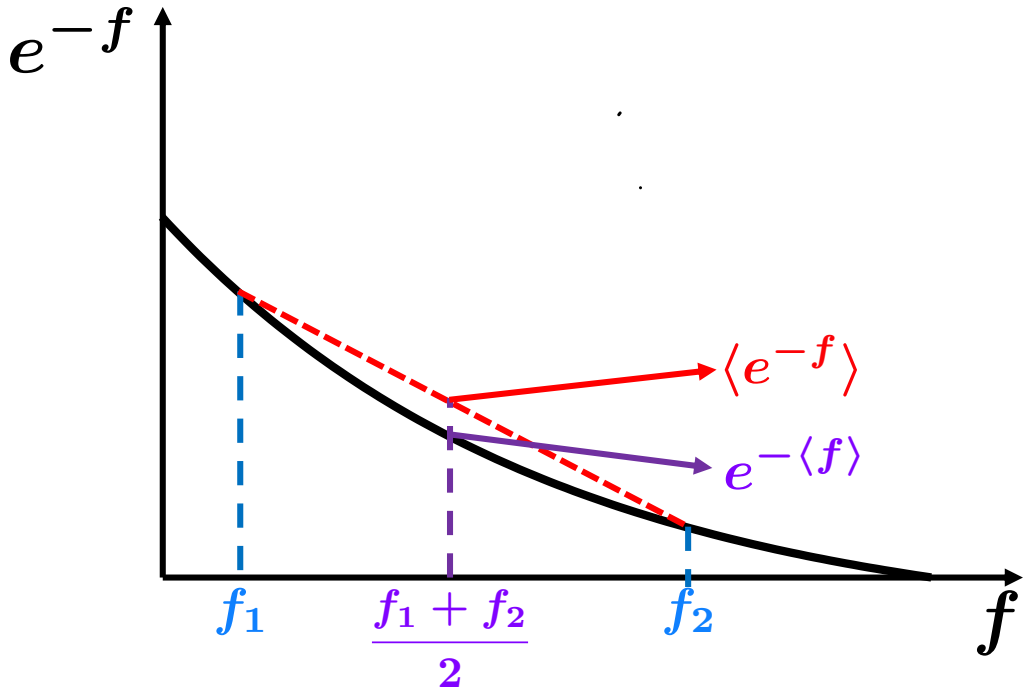

Figure 3.2: Geometrical interpretation of the inequality of $e^{-\langle f \rangle} < \langle e^{-f} \rangle$, where f is an arbitrary function. Due to the convex nature of the exponential, $e^{-\langle f \rangle}$ (marked in purple) is always smaller than $\langle e^{-f} \rangle$ (red).

3.2.1 Theory

Generally, the action of a system S can be non-gaussian, hence it is impossible to compute any correlation function or observable with this action. The main objective of the variational method is to obtain an effective gaussian action $S_{\text{var}} = \frac{1}{2\beta L} \sum_{q,\omega_n} \phi^*(q,\omega_n)\, G^{-1}_{\text{var}}\, \phi^*(q,\omega_n)$, where $\phi^*(q,\omega_n) = \phi(-q,-\omega_n)$ as $\phi(x,\tau)$ are real fields and $G^{-1}_{\text{var}}(q,\omega_n)$ is the propagator of the variational gaussian action in momentum and matsubara frequency. Note that for a general action $S(q,\omega_n)$, $G(q,\omega_n)$ is known as Green's function. The partition function Z of the action is given by:

$$\begin{aligned} Z &= \int \mathcal{D}\phi e^{-S} \\ &= \int \mathcal{D}\phi e^{-(S-S_{\text{var}})-S_{\text{var}}} \\ &= Z_{\text{var}} \langle e^{-(S-S_{\text{var}})} \rangle_{S_{\text{var}}} \end{aligned}$$

Where $Z_{\text{var}} = \int \mathcal{D}\phi e^{-S_{\text{var}}} \sim \prod_{q,\omega_n} \sqrt{G_{\text{var}}}$ (For more details of the derivation, see eq. (B.3)) and $\langle \ldots \rangle_{S_{\text{var}}}$ is averaged over the variational action. The variational ansatz can now be demonstrated in the following steps:

- The Free energy of the non-gaussian action F can be calculated as $F = -\frac{1}{\beta} \ln Z = F_0 - \frac{1}{\beta} \ln \langle e^{-(S-S_{\text{var}})} \rangle_{S_{\text{var}}}$, where $F_0 = -\frac{1}{\beta} \ln Z_{\text{var}}$.
- The following observation can be made: Due to the convexity of the function e^{-x}, the following inequality $e^{-\langle (S-S_{\text{var}}) \rangle} < \langle e^{-(S-S_{\text{var}})} \rangle$ is always satisfied (fig. (3.2)). We now define a quantity called Variational free energy $F_{\text{var}} = F_0 + \frac{1}{\beta} \langle (S - S_{\text{var}}) \rangle_{S_{\text{var}}}$. Using this inequality, it can be easily observed that F_{var} is an upper bound for the actual free energy F:

$$\begin{aligned} F &= F_0 - \frac{1}{\beta} \ln \langle e^{-(S-S_{\text{var}})} \rangle_{S_{\text{var}}} \\ &\leq F_0 - \frac{1}{\beta} \ln e^{-\langle (S-S_{\text{var}}) \rangle_{S_{\text{var}}}} \\ &= F_0 + \frac{1}{\beta} \langle (S - S_{\text{var}}) \rangle_{S_{\text{var}}} \\ \implies F &\leq F_{\text{var}} \end{aligned}$$

- Now, one can choose a convenient and quadratic form of S_{var} (or, alternatively G_{var}) which can be easily analyzed. Then, the variational free energy should be minimized $\frac{\partial F_{\text{var}}}{\partial G_{\text{var}}} = 0$ and the optimal parameters for the chosen G_{var} can be obtained.

This protocol is analogous to the variational method used in quantum systems [76], which is used to obtain the ground-state wave function and energy in complicated systems, such as molecular orbits [77].

3.2.2 Example: Sine-Gordon model

In this section, we will use the previously described variational ansatz to obtain the phase diagram of the sine-Gordon model described by eq. (2.39). Details of this calculation can be found in [57, 78]. The result of this analysis will later be used in Chapter 4 to highlight an important difference between the Sine-Gordon model and our incommensurate system (eq. (2.1)).

Assuming the previously mentioned quadratic form of S_{var}, it can be seen from eq. (B.3) that $F_0 = -\frac{1}{2\beta} \sum_{q,\omega_n} \ln G_{\text{var}}(q, \omega_n)$. $\langle S_{\text{var}} \rangle_{S_{\text{var}}}$ is a constant and can be discarded while taking

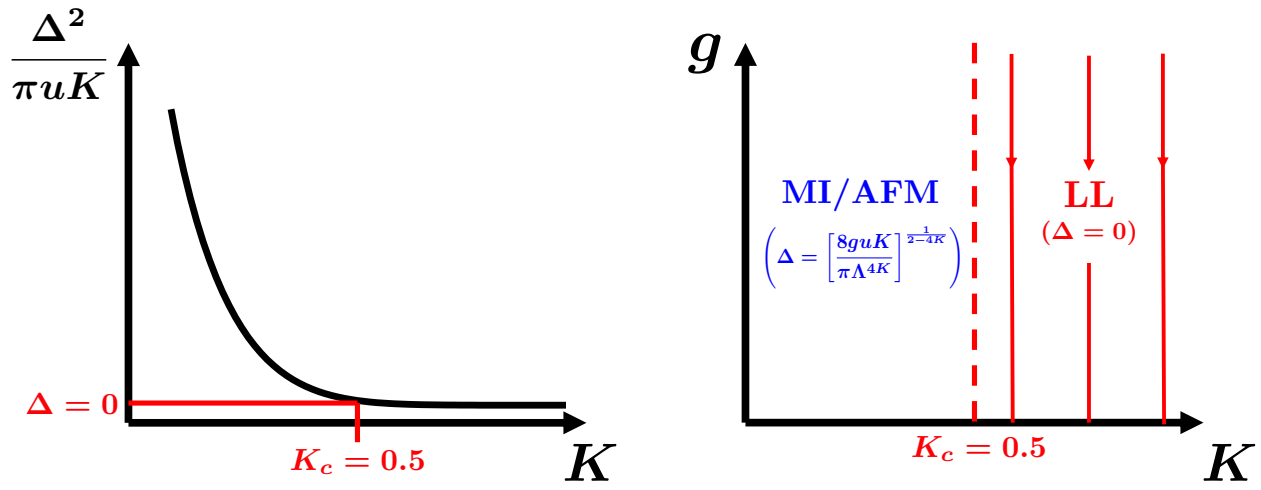

Figure 3.3: *Left*: Behaviour of $\frac{\Delta^2}{\pi u K}$ as a function of K, obtained from eq. (3.8). As K is increased, $\frac{\Delta^2}{\pi u K}$ monotonically decreases. The quantity goes to zero at $K = K_c = 0.5$. *Right*: Variational phase diagram of the Sine-Gordon model. The critical point obtained with this method $K_c = 0.5$ is the same as the perturbative RG. However, the shape of the phase boundary is not correctly captured (vertical instead of a tilted line). For $K \geq K_c$, the system stays in the LL phase (red) and K doesn't get renormalized. When $K < K_c$, the system enters into a phase with a finite gap (blue) and this phase is known as mott insulator or antiferromagnet.

the derivative with respect to G_{var}. Within the scope of the thesis, the action is generally of the form $S = S_{\text{LL}} + S_{\text{int}}$, where S_{int} contains the non-gaussian part. The quantity $\langle S_{\text{LL}} \rangle_{S_{\text{var}}}$ can be computed exactly and is given by $\frac{1}{2\pi K} \sum_{q,\omega_n} (uq^2 + \omega_n^2/u)\, G_{\text{var}}(q, \omega_n)$. Using the minimization condition for F_{var}, we obtain:

$$\boxed{\begin{aligned} &\cdot \frac{\partial}{\partial G_{\text{var}}} \left(-\frac{1}{2} \sum_{q,\omega_n} \ln G_{\text{var}} + \frac{1}{2\pi K} \sum_{q,\omega_n} \left(uq^2 + \frac{\omega_n^2}{u} \right) G_{\text{var}} + \langle S_{\text{int}} \rangle_{S_{\text{var}}} \right) = 0 \\ &\implies G_{\text{var}}^{-1} = \frac{1}{\pi K} \left(uq^2 + \frac{\omega_n^2}{u} \right) + 2 \frac{\partial \langle S_{\text{int}} \rangle_{S_{\text{var}}}}{\partial G_{\text{var}}} \end{aligned}} \tag{3.3}$$

Eq. (3.3) is a self-consistent equation for G_{var}. By using the proper form of S_{int} one can obtain the self-consistent equation for different systems. For Sine-Gordon action, $S_{\text{int}} = -\frac{g}{2\pi^2} \int dx d\tau \cos(4\phi(x,\tau))$. As S_{var} is gaussian, one can compute the derivative of $\langle S_{\text{int}} \rangle_{S_{\text{var}}}$

using eq. (B.22):

$$\begin{aligned}
\langle S_{\text{int}}\rangle_{S_{\text{var}}} &= -\frac{g\beta L}{2\pi^2}\exp\left(-8\langle\phi^2(x,\tau)\rangle\right) \\
&= -\frac{g\beta L}{2\pi^2}\exp\left(-\frac{8}{\beta L}\sum_{q',\omega_n'} G_{\text{var}}(q',\omega_{n'})\right) \\
\implies 2\frac{\partial\langle S_{\text{int}}\rangle_{S_{\text{var}}}}{\partial G_{\text{var}}(q,\omega_n)} &= \frac{8g}{\pi^2}\exp\left(-\frac{8}{\beta L}\sum_{q',\omega_n'} G_{\text{var}}(q',\omega_{n'})\right) \qquad (3.4)
\end{aligned}$$

The extra factor of βL in the first step of the equation comes from the integration over τ and x respectively in S_{int}. In the last step, it should be noted that the differentiation is done with respect to each fourier component of $G_{\text{var}}(q,\omega_n)$. Putting eq. (3.4) in eq. (3.3), we obtain:

$$G_{\text{var}}^{-1}(q,\omega_n) = \frac{1}{\pi K}\left(uq^2+\frac{\omega_n^2}{u}\right)+\frac{8g}{\pi^2}\exp\left(-\frac{8}{\beta L}\sum_{q',\omega_n'} G_{\text{var}}(q',\omega_{n'})\right) \qquad (3.5)$$

We now hypothesize that $\boldsymbol{G_{\text{var}}(q,\omega_n) = \pi K\left[uq^2+\frac{\omega_n^2}{u}+\frac{\Delta^2}{u}\right]^{-1}}$, where Δ is a constant term. Putting this ansatz in the self-consistent equation, in the thermodynamic zero temperature limit $\beta, L\to\infty$ where we can convert $\frac{1}{\beta L}\sum\limits_{q,\omega_n}\to\frac{1}{\pi^2}\int\limits_0^\infty\!\!\int dqd\omega_n$, we obtain:

$$\begin{aligned}
\frac{\Delta^2}{uK} &= \frac{8g}{\pi}e^{-\frac{8K}{\pi}\int\limits_0^\infty\!\!\int\frac{dqd\omega_n}{uq^2+\frac{\omega_n^2}{u}+\frac{\Delta^2}{u}}} \\
&= \frac{8g}{\pi}e^{-4K\int\limits_0^\infty\frac{d\omega_n}{\sqrt{\omega_n^2+\Delta^2}}} \qquad (3.6)
\end{aligned}$$

To compute the integration of the argument of the exponential, we first put a UV cut-off Λ on matsubara frequency to make the integral converge. This doesn't affect the low-energy physics of the system, which is governed by small ω_n. One can compute this integral exactly: $\int\limits_0^\Lambda\frac{d\omega_n}{\sqrt{\omega_n^2+\Delta^2}} = \frac{1}{2}\ln\left[1+\frac{2\Lambda\left(\Lambda+\sqrt{\Delta^2+\Lambda^2}\right)}{\Delta^2}\right]$, which can be approximated to $\ln(\Lambda/\Delta)$ for small Δ. Plugging it back, we find:

$$\Delta^2 = \frac{8guK}{\pi}\left(\frac{\Delta}{\Lambda}\right)^{4K} \qquad (3.7)$$

Eq. (3.7) is a self-consistent equation for Δ, which is the gap in the low-energy spectrum (mass of the low-energy fluctuations). The non-trivial solution of Δ given by:

$$\boxed{\Delta = \left[\frac{8guK}{\pi\Lambda^{4K}}\right]^{\frac{1}{2-4K}}} \qquad (3.8)$$

From eq. (3.8), it can be understood that $\Delta \neq 0$ only for $K < 0.5$ (fig. (3.3), *left*). Hence, the critical point for the phase transition of the Sine-Gordon model corresponding to a 1D commensurate XXZ spin chain is $K_c = 0.5$ (fig. (3.3), *right*). For $K < K_c$, the system exhibits a gapped phase, with the value of the gap given by eq. (3.8). This gapped phase corresponds to the antiferromagnet phase for a spin system or a mott insulator phase for a fermionic system. For $K \geq K_c$, the gap goes to zero and the system remains in the LL phase.

One can also verify that for the Sine-Gordon model, the LL propagator is a valid solution by assuming the ansatz $G^{-1}_{\text{var}} = \pi K_r \left[u_r q^2 + \frac{\omega_n^2}{u_r}\right]^{-1}$, where K_r and u_r are variationally renormalized Luttinger parameters. This ansatz produces the following self-consistent equation : $\frac{1}{\pi K_r}\left[u_r q^2 + \frac{\omega_n^2}{u_r}\right] = \frac{1}{\pi K}\left[u q^2 + \frac{\omega_n^2}{u}\right] + \frac{8g\Lambda^{-4K_r}}{\pi}$. For large Λ, the last term goes to zero, and we see that $K_r = K, u_r = u$. Hence, the variational ansatz keeps the flow of the Luttinger parameters vertical, which corresponds to their RG behaviors for small g and deep in the phase [37]. However, as we will see from Chapter 4, this is always not true. In the gapped phase, Δ vanishes as a power law, which is also equivalent to replacing the correct RG behavior with a vertical flow (fig. (3.3), *right*). However, variational ansatz helps us understand the behavior of the system deep inside the two phases.

3.3 Langevin dynamics

In this section, we discuss the main principle behind the numerical results in Chapter 5, which is solving the Langevin dynamics equation for the action S_{tot}. In a nutshell, the Langevin equation is a differential equation, which tells us how a system evolves under a combination of deterministic forces and random (stochastic) forces. This technique has been previously used particularly in statistical mechanics in many different contexts, e.g. - Brownian motion of a particle [79], thermal fluctuation inside an electrical circuit [80] etc. However, in our project, we use this method as a Monte Carlo technique to explore the configurational phase space of the action [81].

Let us start by directly writing the Langevin equation for the action that we solve numerically:

$$\boxed{\frac{d\phi(x,\tau;t)}{dt} = -\frac{\delta S_{\text{tot}}\left[\phi\right]}{\delta\phi\left(x,\tau;t\right)} + \eta\left(x,\tau;t\right)} \tag{3.9}$$

Here, t denotes the Langevin time, i.e., the time of the simulation. $\eta(t)$ is a Gaussian white noise with mean $\langle\eta(x,\tau;t)\rangle = 0$ and variance $\langle\eta(x,\tau;t)\eta(x',\tau';t')\rangle = 2\delta(x-x')\delta(\tau-\tau')\delta(t-t')$. Note that η is the noise that equilibrates the configuration and is different from the dissipative noise. The latter is already encoded in the action S_{tot}. Starting from eq. (3.9), we will now derive an expression for the probability distribution of stationary solutions $P(\phi_{\text{eq}})$ under Langevin dynamics.

Let's assume that t is discrete and each time step increment is denoted by dt. Then the increment in the deterministic part of eq. (3.9), given by $V[\phi] \equiv -\delta S_{\text{tot}}/\delta\phi$, is trivial and proportional to dt. However, we need to determine the increment of the noise, which we will denote by $\eta_{dt}(t)$. To maintain the white nature, one can safely assume that $\langle\eta_{dt}(t)\rangle = 0$ and is markovian in t. To deduce the dt-dependence of $\eta_{dt}(t)$, we set the $V[\phi]$ to zero. This reduces eq. (3.9) to $\phi(t+ndt) = \phi(t) + \eta_{dt}(t) + \eta_{dt}(t+dt) + \ldots + \eta_{dt}(t+(n-1)dt)$, where n is the number of steps in time. From this, one can determine the average mean square displacement of the field:

$$\begin{aligned}\langle[\phi(t+ndt)-\phi(t)]^2\rangle &= \langle[\eta_{dt}(t)+\eta_{dt}(t+dt)+\ldots+\eta_{dt}(t+(n-1)dt)]^2\rangle \\ &= \sum_{j=0}^{n-1}\langle\eta_{dt}^2(t+jdt)\rangle \\ &= n\langle\eta_{dt}^2(t)\rangle\end{aligned}$$

However, from Brownian motion, we know that the mean square displacement should be equal to $2ndt$ [82]. Comparing the results, we see that $\langle\eta_{dt}^2(t)\rangle = 2dt$. This result, coupled with the Gaussian nature of the noise, tells us that

$$P(\eta_{dt}) = \frac{1}{\sqrt{4\pi dt}}e^{-\frac{\eta_{dt}^2}{4dt}} \tag{3.10}$$

The increment in the noise is proportional to $P(\eta_{dt})\,dt \sim \sqrt{dt}$. $P(\eta_{dt})$ will be required to derive the probability of the field having a certain magnitude at (x,τ) coordinate at time $t+dt$, given by $P[\phi(x,\tau);t+dt]$, which we derive using the Kolmogorov-Chapman equation [83]. This equation is applied for integrating away dummy variables from a multivariate probability distribution. Applying this, we can write:

$$P[\phi(x,\tau);t+dt] = \int_{-\infty}^{\infty} W(\phi(x,\tau),\phi(x',\tau');dt)P[\phi(x',\tau');t]\,d\phi(x',\tau') \tag{3.11}$$

Where W is the probability that the field moves from (x', τ') at time t to (x, τ) at the time $t + dt$. This is only possible if $\phi(x', \tau') = \phi(x, \tau) + V[\phi(x', \tau')]dt + \eta_{dt}(t)$. Eq. (3.10) tells us that the probability of having such a value of η_{dt} is:

$$P(\eta_{dt} = \phi(x', \tau') - \phi(x, \tau) - V[\phi(x', \tau')]dt) = \frac{1}{\sqrt{4\pi dt}} e^{-\frac{\left(\phi(x', \tau') - \phi(x, \tau) - V[\phi(x', \tau')]\right)^2}{4dt}}$$

This probability is the same as W. Plugging it back in eq. (3.11), and expanding both sides in the first order of dt, we obtain:

$$\frac{\partial P\left[\phi(x, \tau; t)\right]}{\partial t} = -\frac{\partial}{\partial \phi}\left[V[\phi(x, \tau; t)] P\left[\phi(x, \tau; t)\right]\right] + \frac{\partial^2 P\left[\phi(x, \tau; t)\right]}{\partial \phi^2} \tag{3.12}$$

Eq. (3.12) is known as the Fokker-Planck equation, which describes the time evolution of probability density under stochastic noise [84, 85]. For ϕ to be equilibrated, the probability current should be zero, i.e., $\frac{\partial P[\phi(x,\tau);t]}{\partial t} = 0$. It can be then shown that the solution $P[\phi_{\text{eq}}]$, which satisfies eq. (3.12), is given by:

$$\boxed{P[\phi_{\text{eq}}(x, \tau)] = \frac{1}{Z} e^{-S_{\text{tot}}[\phi(x,\tau)]}} \tag{3.13}$$

From the result of eq. (3.13), we see that the configurations equilibrated under Langevin dynamics belong to the phase space of S_{tot}. The algorithm to solve eq. (3.9) and its implementation has been discussed in detail in Appendix C.

Chapter 4

The Incommensurate case: Phase diagram

For the next two chapters, we will focus on the problem of the incommensurate spin chain in the presence of local dissipative baths, which we will refer to as the "incommensurate dissipative spin chain" from now on. To start with our analysis, we apply the previously described perturbative RG and variational method to the action, described by eq. (2.1). The perturbative RG analysis establishes the existence of a BKT-type critical point at $K_c = 1 - (s/2)$ for small α, where s is the exponent of the bath spectral density. With the help of the variational ansatz, we discover that the "dissipative" phase is a gapless phase, whose low energy properties can be described by the following fractional propagator:

$$G^{-1}_{\text{diss}} = \frac{1}{\pi K_r}\left(u_r q^2 + \frac{\omega_n^2}{u_r} + \frac{\eta(\alpha)}{u_r}|\omega_n|^s\right) \tag{4.1}$$

Where η is a coefficient that depends on α and u_r and K_r are renormalized values of u and K. The variational method corroborates the RG analysis, identifying the phase transition at $K = K_c$ for small α. We also show that this variational method predicts the renormalization of the LL parameters in the LL phase, in contrast with the Sine-Gordon model. We argue that this is a consequence of the fact that the contribution of the bath is non-local in τ.

4.1 RG analysis of the Incommensurate case

To recall from Chapter 2, we are interested in locating the existence of phase transition in the following action:

$$S_{\text{tot}} = \frac{1}{2\pi K}\int\left[u(\nabla\phi(x,\tau))^2+\frac{1}{u}(\partial_\tau\phi(x,\tau))^2\right]-\frac{\alpha}{4a^2\pi^2}\int dxd\tau d\tau'\frac{\cos\left[2\left\{(\phi(x,\tau)-\phi(x,\tau'))\right\}\right]}{|\tau-\tau'|^{1+s}}$$

Where we have put the lattice spacing a back in the cosine part of the action, as we will use this small length cut-off to scale and extract the RG flow of the parameters. As described in Chapter 3, we will use a correlation function approach, where we will calculate:

$$R(r_1-r_2)=\langle e^{ib\phi(r_1)}e^{-ib\phi(r_2)}\rangle,\ r=(x,u\tau) \tag{4.2}$$

This section will be divided into two subsections. In the first part, we will show the derivation of the RG differential equations in detail. This part heavily follows the same steps as the Sine-Gordon action, whose details can be found in Section 2.3.2 of [37]. In the latter subsection, we will analyze the flow differential equations near the critical point.

4.1.1 Derivation of the RG flow equation

To check the RG flow of the parameters, we expand eq. (4.2) perturbatively in S_{int} as:

$$\begin{aligned} R(r_1-r_2) &= \langle e^{ib\phi(r_1)}e^{-ib\phi(r_2)}\rangle_{S_{\text{tot}}} \\ &= \frac{\sum_n \frac{(-1)^n}{n!}\langle e^{-ib\phi(r_1)}e^{ib\phi(r_2)}(S_{\text{int}})^n\rangle_{S_{\text{LL}}}}{\sum_n \frac{(-1)^n}{n!}\langle (S_{\text{int}})^n\rangle_{S_{\text{LL}}}} \end{aligned} \tag{4.3}$$

we now calculate $R(r_1-r_2)$ after perturbatively expanding the denominator at different orders of α. The 0th order quantity is simply $R_0(r_1-r_2)\langle e^{ib\phi(r_1)}e^{-ib\phi(r_2)}\rangle_{S_{\text{LL}}}$. From Appendix B (eq. B.17), it can be calculate as $R_0(r_1-r_2)=\exp(\frac{-b^2K}{2}F(r_1-r_2))$, where $F(r)=\log\left(\frac{x^2+(u|\tau|+a)^2}{a^2}\right)$.

The contribution from the first-order in α comes from the difference between two terms, namely $\langle e^{-ib\phi(r_1)}e^{ib\phi(r_2)}\rangle_{S_{\text{LL}}}\langle S_{\text{int}}\rangle_{S_{\text{LL}}}$ and $\langle e^{-ib\phi(r_1)}e^{ib\phi(r_2)}S_{\text{int}}\rangle_{S_{\text{LL}}}$. Note that this contribution is non-zero, which is different from the Sine-Gordon case where the first-order contribution is zero and the lowest order of renormalization starts at the second order of the coupling g. This is due to the fact that in our model, S_{int} is non-local and long-ranged. We will discuss the consequence of this observation in Section 4.2.2.

The 1st order terms can be separately calculated as:

$$1) \quad \langle e^{-ib\phi(r_1)} e^{ib\phi(r_2)} \rangle_{S_{\rm LL}} \langle S_{\rm int} \rangle_{S_{\rm LL}} = -\frac{\alpha}{4a^2\pi^2} e^{-\frac{b^2}{2}\langle [\phi(r_1)-\phi(r_2)]^2 \rangle} \int dx' d\tau' d\tau'' \frac{e^{-2\langle [\phi(x',\tau')-\phi(x',\tau'')]^2 \rangle}}{|\tau'-\tau''|^{1+s}}$$

$$= \quad -\frac{\alpha}{4a^2\pi^2} e^{-\frac{b^2 K}{2} F(r_1-r_2)} \int dx' d\tau' d\tau'' \frac{e^{-2KF(x'-x',\tau'-\tau'')}}{|\tau'-\tau''|^{1+s}}$$

$$2) \quad \langle e^{-ib\phi(r_1)} e^{ib\phi(r_2)} S_{\rm int} \rangle_{S_{\rm LL}} = \frac{\alpha}{4a^2\pi^2} \int dx' d\tau' d\tau'' \sum_{\epsilon=\pm} \frac{\langle e^{ib\phi(r_1)} e^{-ib\phi(r_2)} e^{2i\epsilon\phi(x',\tau')} e^{-2i\epsilon\phi(x',\tau'')} \rangle}{|\tau'-\tau''|^{1+s}}$$

$$= \quad \frac{\alpha}{8a^2\pi^2} e^{-\frac{b^2 K}{2} F(r_1-r_2)}$$

$$\times \quad \int dx' d\tau' d\tau'' \sum_{\epsilon=\pm} \frac{e^{-2KF(x'-x',\tau'-\tau'')} e^{bK\epsilon(F(x_1-x',\tau_1-\tau')-F(x_1-x',\tau_1-\tau'')-F(x_2-x',\tau_2-\tau')+F(x_2-x',\tau_2-\tau''))}}{|\tau'-\tau''|^{1+s}}$$

Writing all the terms together, we find :

$$. \quad R(r_1-r_2) = e^{\frac{-b^2 K}{2} F(r_1-r_2)} \left[1 + \frac{\alpha}{8\pi^2 u^2 a^2} \int d^2r' d^2r'' e^{-2KF(r'-r'')} \, D(\tau'-\tau'') \delta(x'-x'') \right.$$

$$\left. \times \quad \sum_{\epsilon=\pm} \left\{ e^{bK\epsilon(F(r_1-r')-F(r_1-r'')-F(r_2-r')+F(r_2-r''))} - 1 \right\} \right] \tag{4.4}$$

Where we have introduced the delta function $\delta(x'-x'')$ and converted the integral over $r' = (x', u\tau')$ and $r' = (x'', u\tau'')$. $D(\tau'-\tau'')$ denotes the long-range kernel in imaginary time $1/|\tau'-\tau''|^{1+s}$. Now we convert the integral to Center of Mass and relative coordinates via $r = r'-r''$, $R = \frac{r'+r''}{2}$. Now we can expand the functions F for small r value as following :

$$\begin{aligned} F(r_j - r') &= F(r_j - R - \frac{r}{2}) = F(-R) + \frac{r}{2} \nabla_R F(r_j - R) \\ F(r_j - r'') &= F(r_j - R + \frac{r}{2}) = F(-R) + \frac{3r}{2} \nabla_R F(r_j - R) \end{aligned}$$

Where $j = 1, 2$. Putting this back in eq. (4.4), we obtain

$$\begin{aligned} R(r_1-r_2) &= e^{\frac{-b^2 K}{2} F(r_1-r_2)} \left[1 + \frac{\alpha}{8\pi^2 u^2 a^2} \int d^2r d^2R \; e^{-2KF(r)} \, D(\tau) \delta(x) \right. \\ &\left. \times \quad \sum_{\epsilon=\pm} \left\{ e^{bK\epsilon(r.\nabla_R [F(r_1-R)-F(r_2-R)])} - 1 \right\} \right] \end{aligned}$$

Now, we expand the exponential inside the summation for a small value of r. The 0th order term cancels the constant and the first order terms cancel each other due to the sign difference

coming from ϵ. The lowest-order term that survives is the second-order term,

$$\begin{aligned} R(r_1 - r_2) &= e^{\frac{-b^2K}{2}F(r_1-r_2)}\Big[1 + \frac{\alpha}{8\pi^2u^2a^2}\int d^2r d^2R\; e^{-2KF(r)}\; D(\tau)\delta(x) \\ &\times \quad b^2K^2\left\{r.\nabla_R\left[F(r_1 - R) - F(r_2 - R)\right]\right\}^2\Big] \end{aligned} \tag{4.5}$$

The term with the gradient inside the square produces terms like :

$$r_i r_j(\nabla_{R_i}[F(r_1 - R) - F(r_2 - R)]))(\nabla_{R_j}[F(r_1 - R) - F(r_2 - R)]))$$

where i, j denotes the two possible coordinates $x, y = u\tau$. For the integral over d^2r and by symmetry $x \to -x, y \to -y$, only the diagonal $i = j$ terms survive. Like [6], our system is anisotropic. We can include the effect of this anisotropy with an additional term in F of the form $d\cos(2\theta)$, where θ is the angle between vector $(x, u\tau)$ and x axis and d is the measure of anisotropy. After expanding the gradient terms and integrating by parts over R, we obtain two terms $I_\pm$, where:

$$I_\pm = \int d^2R\left[F(r_1 - R) - F(r_2 - R)](\nabla_X^2 \pm \nabla_Y^2)[F(r_1 - R) - F(r_2 - R)\right]$$

The I_+ term renormalizes K and α, whereas I_- renormalizes the anisotropy which we are not interested in. Hence,

$$\begin{aligned} R(r_1 - r_2) &= e^{\frac{-b^2K}{2}F(r_1-r_2)}\left[1 - \frac{\alpha b^2K^2}{16\pi^2u^2a^2}\int r^2d^2r d^2R\; e^{-2KF(r)}\; D(\tau)\delta(x)\right. \\ &\times \quad \left.[F(r_1 - R) - F(r_2 - R)]\left(\nabla_X^2 + \nabla_Y^2\right)[F(r_1 - R) - F(r_2 - R)]\right] \end{aligned} \tag{4.6}$$

As F is a logarithmic function, we know that $(\nabla_X^2 + \nabla_Y^2)F(R) = 2\pi\delta(R)$, as is the case with the laplacian of 2D coulomb potential [86]. Using this, one can observe that $[F(r_1 - R) - F(r_2 - R)]\,(\nabla_X^2 + \nabla_Y^2)\,[F(r_1 - R) - F(r_2 - R)] = -4\pi F(r_1 - r_2)$. Note that terms such as $F(r_1 - r_1)$ can be discarded as they are finite, whereas $F(r_1 - r_2)$ are divergent for large distances. Plugging this back, we find:

$$R(r_1 - r_2) = e^{\frac{-b^2K}{2}F(r_1-r_2)}\left[1 + \frac{\alpha b^2K^2F(r_1 - r_2)}{4\pi u^2a^2}\int r^2d^2r\; e^{-2KF(r)}D(\tau)\delta(x)\right]$$

Now, we re-exponentiate the terms inside the bracket. This produces a correlation function $R(r_1 - r_2)$ of the form $\exp\left(-\frac{b^2K_{\text{eff}}}{2}F(r_1 - r_2)\right)$, where the K_{eff} is defined as:

$$K_{\text{eff}} = K - \frac{\alpha K^2}{2\pi a^2u^2}\int_{r>a} d^2r r^2 e^{-2KF(r)}D(\tau)\delta(x) \tag{4.7}$$

To simplify the equation above, we express d^2r and r^2 in terms of $x, u\tau$ and compute the integral over $\delta(x)$. We absorb a factor of $u^{s-1}a^{-s}$ into α to make it dimensionless. This produces

$$K_{\text{eff}} = K - \frac{\alpha K^2}{2\pi} \int_a^\infty \frac{dy}{a} \left(\frac{y}{a}\right)^{1-s-2K} \tag{4.8}$$

Eq. (4.8) should remain invariant with changing the lower cut-off. Sending a to $a' = a + da$, we find:

$$K_{\text{eff}} = K - \frac{\alpha K^2}{2\pi} \frac{da}{a} - \frac{\alpha K^2}{2\pi} \int_{a'}^\infty \frac{dy}{a} \left(\frac{y}{a}\right)^{1-s-2K} \tag{4.9}$$

To keep eq. (4.8) invariant, the condition that must be satisfied is:

$$K(a') = K(a) - \frac{\alpha(a) K^2(a)}{2\pi} \frac{da}{a} \tag{4.10}$$

Similarly, one obtains for α that:

$$\alpha(a') = \alpha(a) \left(\frac{a'}{a}\right)^{2-s-2K(a)} \tag{4.11}$$

The form of these differential equations prompts us to parametrize $a = a_0 e^l$, where a_0 is a microscopic bare constant. Substituting this, we obtain the following flow equations:

$$\boxed{\begin{aligned} \frac{dK}{dl} &= -\frac{\alpha K^2}{2\pi} \qquad (4.12) \\ \frac{d\alpha}{dl} &= (2 - s - 2K)\alpha \qquad (4.13) \end{aligned}}$$

Eq. (4.12) and (4.13) are the coupled differential equations for the RG flow of K and α. A similar action in the context of a 1D quantum wire coupled with a metallic gate was analyzed with perturbative RG in [87]. Their analysis corroborates with the value of K_c that we obtain from our RG calculation. However, in their case, the coefficient of α is different in the action. That doesn't change the physical properties of the systems, it only scales the value of α_c. In the next subsection, we will perform a linear stability analysis on them to locate the critical point.

4.1.2 Analysis of the RG flow equations

From eq. (4.13), we observe that for $K > 1 - \frac{s}{2}$, α remains controlled; whereas $K < 1 - \frac{s}{2}$, it diverges. Hence, we identify $K_c = 1 - \frac{s}{2}$ as the critical point of the transition for infinitesimally

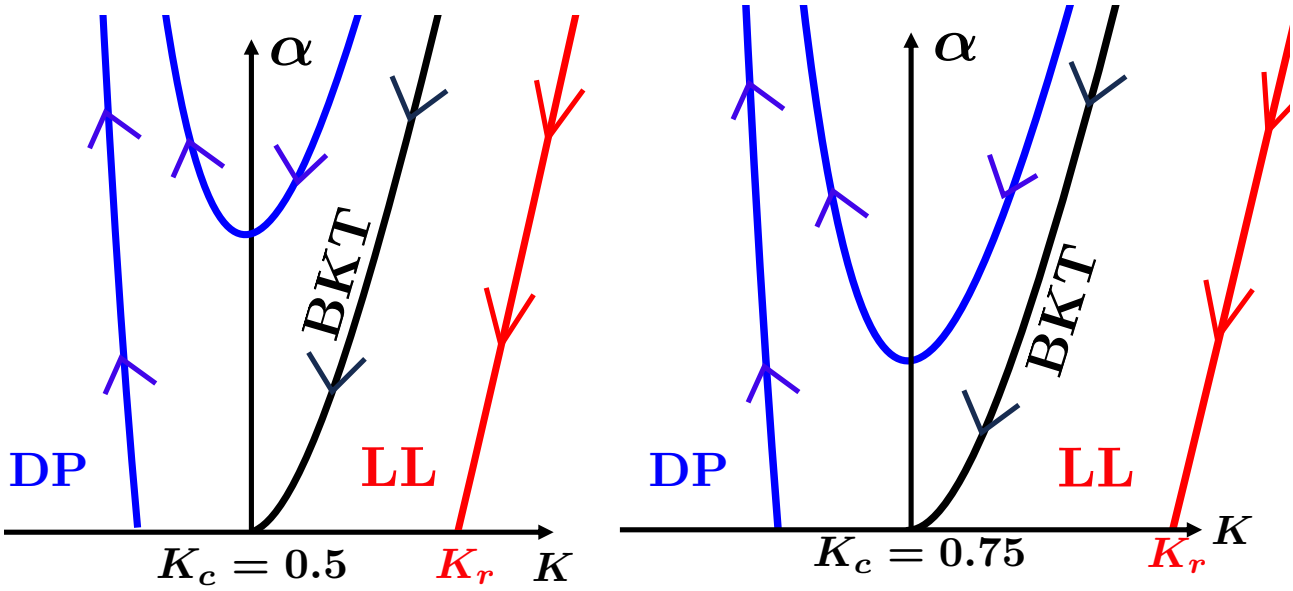

Figure 4.1: RG flow for the incommensurate case, obtained from the numerical solution of eq. (4.12) and eq. (4.13) for $s = 1$ (*left*) and $s = 0.5$ (*right*). For $s = 1$, $K_c = 0.5$ and for $s = 0.5$, $K_c = 0.75$; which match with the prediction of $K_c = 1 - \frac{s}{2}$ for a general bath exponent s. The phase boundaries are given by the black line and are parabolic in shape. For $K \geq K_c$ and $\alpha \leq \alpha_c$, K_r is finite and $\alpha_r = 0$ (red lines); and the system stays in the LL phase. For $K < K_c$, $\alpha_r \to \infty$, the cosine becomes relevant (blue lines) and the system enters into a new, dissipative phase (DP).

small α. To understand the behavior of K and α near K_c, we expand $K = K_c + K_\perp$. Putting this back in eq. (4.12) and (4.13) and keeping only the lowest-order terms, we find:

$$\frac{dK_\perp}{dl} = -\frac{K_c^2}{2\pi}\alpha \tag{4.14}$$

$$\frac{d\alpha}{dl} = -2K_\perp\alpha \tag{4.15}$$

Multiplying eq. (4.14) by $K_\perp$ on both sides and then substituting eq. (4.15), we obtain the constant of the RG, denoted as C^2:

$$K_\perp^2 - \frac{K_c^2}{2\pi}\alpha = C^2 \tag{4.16}$$

The form of the constant of motion tells us that the flow trajectory in this case is parabolic in nature, as opposed to the Sine-Gordon model where the trajectories are hyperbolic. The separatrix of the phase transition occurs when $C^2 = 0$, which implies that $\alpha_c = 2\pi((K/K_c)-1)^2$. We solve the flow equations in three different regions:

- $\mathbf{C^2 > 0}$: In this regime, eq. (4.14) and (4.15) can be re-written as:

$$\frac{dK_\perp}{dl} = C^2 - K_\perp^2 \tag{4.17}$$

$$\frac{d\alpha}{dl} = -2\alpha\sqrt{C^2 + \frac{K_c^2}{2\pi}\alpha} \tag{4.18}$$

In a region where $\alpha_c > \alpha > 0$, these equations can be exactly integrated. As an example, I show the solution of the eq. (4.17) here in detail. Note that in the region specified above, $C < K_\perp$. Hence,

$$\begin{aligned}
\int dl &= \int \frac{dK_\perp}{C^2 - K_\perp^2} \\
&= \frac{1}{2C}\left[\int \frac{dK_\perp}{C + K_\perp} + \int \frac{dK_\perp}{C - K_\perp}\right] \\
\implies l + c_1 &= \frac{1}{2C}\left[\ln|C + K_\perp| - \ln|C - K_\perp|\right] \\
&= \frac{1}{C}\tanh^{-1}\left(\frac{C}{K_\perp}\right)
\end{aligned}$$

Where c_1 is the integration constant. Assuming that $K_\perp(l = 0) = K_{\perp_0}$ is the bare coupling constant, it can be easily deduced that $c_1 = \tanh^{-1}\left(C/K_{\perp_0}\right)/C$. Putting this back, we obtain:

$$\begin{aligned}
\frac{1}{C}\tanh^{-1}\left(\frac{C}{K_\perp}\right) &= Cl + \frac{1}{C}\tanh^{-1}\left(\frac{C}{K_{\perp_0}}\right) \\
\implies K_\perp(l) &= \frac{C}{\tanh\left(Cl + \tanh^{-1}\left(\frac{C}{K_{\perp_0}}\right)\right)}
\end{aligned} \tag{4.19}$$

The flow equation for α can now be easily obtained from the constant of motion:

$$\begin{aligned}
\alpha(l) &= \frac{2\pi}{K_c^2}\left(K_\perp^2(l) - C^2\right) \\
&= \frac{2\pi}{K_c^2}\frac{C^2}{\sinh^2\left(Cl + \tanh^{-1}\left(\frac{C}{K_{\perp_0}}\right)\right)}
\end{aligned} \tag{4.20}$$

At $l \to \infty$ limit, the parameters flow to their stable renormalized values, given by $K_\perp(l = \infty) = C$ and $\alpha(l = \infty) = \alpha_r = 0$ respectively. This tells us that in this region the system remains in the LL phase with a renormalized finite value of K and the cosine is irrelevant. A diagrammatic representation of this flow can be seen by the red line in fig. (4.1).

- $\mathbf{C^2 = 0}$: This condition is fulfilled on the separatrix. Putting $C^2 = 0$ in eq. (4.17) and (4.18), we obtain by integrating:

$$K_\perp = \frac{K_{\perp_0}}{1 + K_{\perp_0} l} \tag{4.21}$$

$$\alpha = \frac{2\pi}{K_c^2} \left(\frac{K_{\perp_0}}{1 + K_{\perp_0} l} \right)^2 \tag{4.22}$$

In this case, when $l \to \infty$, $K_\perp(l = \infty) = \alpha(l = \infty) = 0$. Which implies that $K_r = K_c$ and $\alpha_r = 0$. This shows that $C^2 = 0$ is satisfied at the phase boundary, however, on this line the system still remains in the LL phase and the cosine term is marginally relevant. This is denoted by the black line in fig. (4.1).

- $\mathbf{C^2 < 0}$: This condition is satisfied in the region with the blue lines in fig. (4.1). In this region, the coefficient of α in eq. (4.13) is negative, hence α_r and K_r becomes infinity and 0, respectively. However, below a lengthscale l^* where $\alpha(l^*) \sim O(1)$, the flow equation for K can be integrated by substituting $C_1^2 = -C^2 = \frac{K_c^2}{2\pi}\alpha - K_\perp^2$, where $C_1^2 > 0$:

$$\begin{aligned} -\int dl &= \int \frac{dK_\perp}{C_1^2 + K_\perp^2} \\ \implies C_1 l &= \tan^{-1}\left[\frac{K_{\perp_0}}{C_1}\right] - \tan^{-1}\left[\frac{K_\perp}{C_1}\right] \end{aligned} \tag{4.23}$$

4.2 Variational analysis

Perturbative RG analysis of the incommensurate action (eq. (2.1)) tells us the existence of a phase transition at $K = K_c = 1 - \frac{s}{2}$. However, as the RG flow of α diverges in the dissipative phase, its properties can't be analyzed using the RG method mentioned above. Therefore, we will use the variational method, that we have previously described in Section 3.2 to analyze its zero-temperature behavior.

We will directly start from the self-consistent equation for G_{var}, given by eq. (3.3). In the incommensurate case, S_{int} is the long-range cosine function in eq. (2.1). Using eq. (B.22), we

obtain:

$$\begin{aligned}\langle S_{\text{int}}\rangle_{S_{\text{var}}} &= -\frac{\alpha L}{4\pi^2}\int d\tau d\tau' \frac{\langle \cos\left[2\left\{(\phi(x,\tau)-\phi(x,\tau')\right\}\right]\rangle_{S_{\text{var}}}}{|\tau-\tau'|^{1+s}} \\ &= -\frac{\alpha L}{4\pi^2}\int d\tau d\tau' \frac{e^{-2\left\langle[\phi(x,\tau)-\phi(x,\tau')]^2\right\rangle}}{|\tau-\tau'|^{1+s}} \end{aligned} \tag{4.24}$$

Where the factor of L in the numerator comes from integrating over x in the action S_{int}. Using eq. (B.5), we identify the argument of the exponential as the roughness function in the imaginary time direction $B(\tau-\tau')$. To compute the integral, we use eq. (B.8) and obtain:

$$\begin{aligned}\langle S_{\text{int}}\rangle_{S_{\text{var}}} &= -\frac{\alpha L}{4\pi^2}\int d\tau d\tau' \frac{e^{-\frac{4}{\beta L}\sum\limits_{q,\omega_n}(1-\cos(\omega_n(\tau-\tau')))G_{\text{var}}(q,\omega_n)}}{|\tau-\tau'|^{1+s}} \\ \implies 2\frac{\partial\langle S_{\text{int}}\rangle_{S_{\text{var}}}}{\partial G_{\text{var}}(q,\omega_n)} &= \frac{2\alpha}{\pi^2\beta}\int d\tau d\tau' \frac{(1-\cos(\omega_n(\tau-\tau')))\, e^{-\frac{4}{\beta L}\sum\limits_{q',\omega_{n'}}(1-\cos(\omega_{n'}(\tau-\tau')))G_{\text{var}}(q',\omega_{n'})}}{|\tau-\tau'|^{1+s}}\end{aligned}$$

Observing the fact that the integrals depend on only the difference $\tau-\tau'$, we convert the integral to relative and CoM coordinates $\tau_r=\tau-\tau'$ and $\tau_{CoM}=(\tau+\tau')/2$. Then we can integrate over τ_{CoM}, which cancels the factor of β in the denominator. Hence, the self-consistent equation for G_{var} for the incommensurate dissipative action is given by:

$$G^{-1}_{\text{var}}(q,\omega_n)=\frac{1}{\pi K}\left(uq^2+\frac{\omega_n^2}{u}\right)+\frac{2\alpha}{\pi^2}\int d\tau\tau^{-(1+s)}\left(1-\cos\left(\omega_n\tau\right)\right)e^{-\frac{4}{\beta L}\sum\limits_{q',\omega_{n'}}(1-\cos(\omega_{n'}\tau))G_{\text{var}}(q',\omega_{n'})} \tag{4.25}$$

Note that in eq. (4.25) the correction coming from the cosine part depends only on ω_n. Hence, we propose the following ansatz for $G^{-1}_{\text{var}}=\frac{1}{\pi K}\left[uq^2+\frac{\omega_n^2}{u}+\frac{F(\omega_n)}{u}\right]$. We can use this to reduce eq. (4.25) to the following form:

$$\frac{F(\omega_n)}{uK}=\frac{2\alpha}{\pi}\int d\tau\tau^{-(1+s)}\left(1-\cos\left(\omega_n\tau\right)\right)e^{-\frac{4K}{\pi}\int\limits_0^\infty dq' d\omega_{n'}\frac{1-\cos\left(\omega_{n'}\tau\right)}{uq'^2+\frac{\omega_{n'}^2}{u}+\frac{F(\omega_{n'})}{u}}} \tag{4.26}$$

Where in the exponential, we have converted $\frac{1}{\beta L}\sum\limits_{q,\omega_n}\to\frac{1}{\pi^2}\int\limits_0^\infty dqd\omega_n$ assuming thermodynamic and zero-temperature limit. In the following subsections, we will solve for the form of $F(\omega_n)$, both for the dissipative phase and the LL phase. We will show that in both phases, the variational solutions behave quite differently than the ones of the Sine-Gordon model.

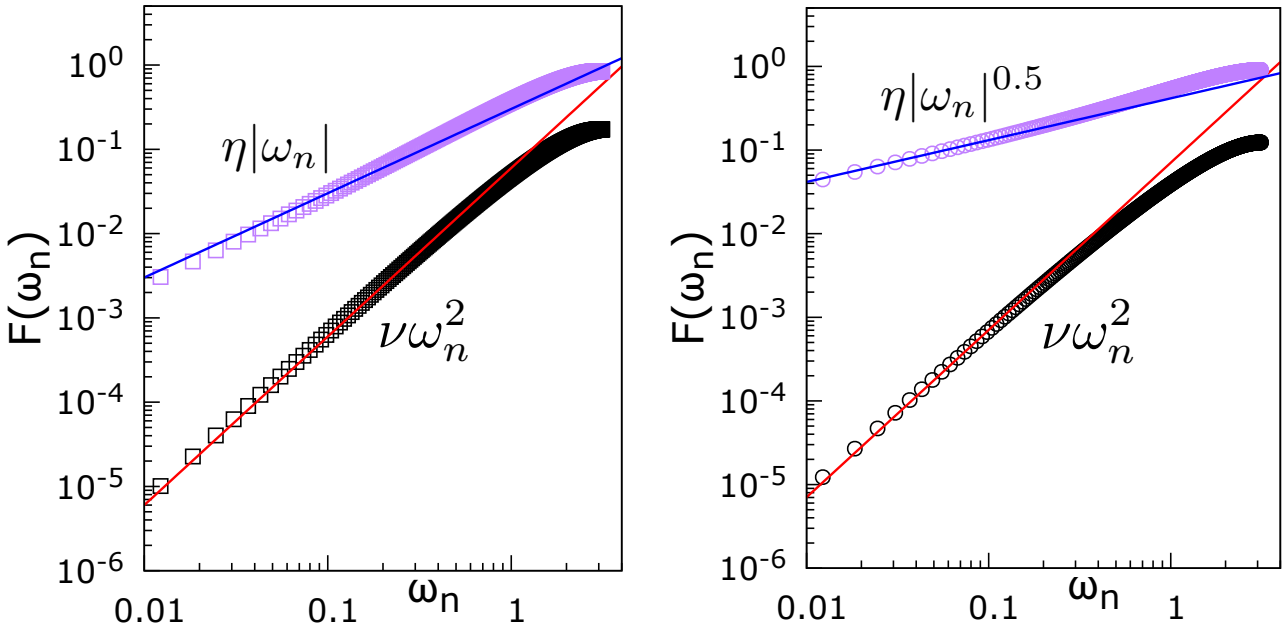

Figure 4.2: Behavior of $F(\omega_n)$ in different phases for $s = 1$ (*left*) and $s = 0.5$ (*right*), obtained from numerical solution of eq. (4.35) (with β=1024 and $\alpha = 5$). For $K < K_c = 1 - \frac{s}{2}$, $F(\omega_n)$ behaves as $0.301|\omega_n|$ for $s = 1, K = 0.15$ (*left*, purple square points), and for $s = 0.5, K = 0.3$, it behaves as $0.415\sqrt{|\omega_n|}$ (*right*, purple circular points). In the LL phase ($K = 1$), $F(\omega_n)$ always behaves as ω_n^2; particularly, $0.06\omega_n^2$ for $s = 1$ (*left*, black square points) and $0.054\omega_n^2$ for $s = 0.5$ (*right*, black circular points).

4.2.1 Dissipative phase

The first observation we make regarding the dissipative phase is that it can't be gapped. The RHS of eq. (4.26) tells us that the gap $\Delta = G_{\text{var}}^{-1}(q = \omega_n = 0) = 0$. Hence, a logical choice for the form of $F(\omega_n)$ would be $\boldsymbol{F(\omega_n) = \eta(\alpha)\,|\omega_n|^{\psi_1} + p(\alpha)\,|\omega_n|^{\psi_2}}$, where both ψ_1 and ψ_2 are non-zero. This expression is intended for small-ω_n. The reason for computing the sub-leading exponent is so that we can take account of finite size corrections to match with our numerical simulations in Chapter 5. Below, we will use this form of $F(\omega_n)$ to determine the value of the exponents and the coefficients.

- ***Determination of the exponents ψ***: We observe that the argument of the exponent in eq. (4.26) is independent of q except from the denominator, so one can easily integrate it out. Doing so produces:

$$\frac{\eta\omega_n^{\psi_1} + p\omega_n^{\psi_2}}{uK} = \frac{2\alpha}{\pi}\int d\tau\tau^{-(1+s)}\left(1 - \cos\left(\omega_n\tau\right)\right)e^{-2K\int_0^\infty d\omega_{n'}\frac{1-\cos\left(\omega_{n'}\tau\right)}{\sqrt{\omega_{n'}^2+\eta\omega_{n'}^{\psi_1}+p\omega_{n'}^{\psi_2}}}} \tag{4.27}$$

Where we have dropped the absolute sign from ω_n because the integral is limited to positive ω_n only. Now we make an assumption that $0 < \psi_1 < \psi_2 < 2$. In the large-τ limit, one can now compute the integral:

$$\begin{aligned}\int_0^{\Lambda_1} d\omega_{n'} \frac{1-\cos(\omega_{n'}\tau)}{\sqrt{\omega_{n'}^2 + \eta\omega_{n'}^{\psi_1} + p\omega_{n'}^{\psi_2}}} &\simeq \int_0^{\Lambda_1} d\omega_{n'} \frac{1-\cos(\omega_{n'}\tau)}{\sqrt{\eta}\omega_{n'}^{\psi_1/2}} + \int_{\Lambda_1}^{\Lambda} d\omega_{n'} \frac{1-\cos(\omega_{n'}\tau)}{\omega_{n'}} \\ &\overset{\text{large}-\tau}{\approx} C - \zeta\tau^{\frac{\psi_1}{2}-1}\end{aligned}$$

Where Λ_1 are Λ are frequency cut-offs, and C and ζ are constants. One can now expand the exponential with the large-τ assumption as $\psi_1/2 - 1$ is negative for the whole range of allowed values of ψ_1. Doing so reduces the self-consistent equation to:

$$\begin{aligned}\eta\omega_n^{\psi_1} + p\omega_n^{\psi_2} &\sim \int d\tau\tau^{-(1+s)}(1-\cos(\omega_n\tau))\left(1+\zeta\tau^{\frac{\psi_1}{2}-1}\right) \\ &= \omega_n^s \int dx x^{-(1+s)}(1-\cos x)\left(1+\zeta x^{\frac{\psi_1}{2}-1}\omega_n^{1-\frac{\psi_1}{2}}\right) \qquad (4.28)\end{aligned}$$

Where in the last line we have performed the change of variable $\omega_n\tau \to x$. Comparing the powers on both side, we find that $\boldsymbol{\psi_1 = s}$ and $\boldsymbol{\psi_2 = 1 + \frac{s}{2} > \psi_1 \forall s \in (0,2)}$. Hence, ψ_2 remains sub-leading in the region of s where the action is long-range in nature and accounts for finite-size corrections; however, the low-energy physics is governed by $|\omega_n|^s$. Note that this result is also consistent with the harmonic approximation, i.e., fourier transformation of the expansion of the cosine function up to quadratic order leads to the same result.

- ***Determination of the coefficient $\eta(\alpha)$***: After determining the exponents, we are now interested in understanding the behavior of the coefficient of the leading term, indicated by $\eta(\alpha)$ in the ansatz. From eq. (4.28), it can be observed that the $|\omega_n|^s$ is regulated by the constant term in the argument of the exponential; hence we will ignore the $\cos(\omega_{n'}\tau)$ while determining η. Using the leading terms, we find:

$$\begin{aligned}\int_0^{\Lambda} \frac{d\omega_{n'}}{\sqrt{\omega_{n'}^2 + \eta\omega_{n'}^{\psi_s}}} &\simeq \int_0^{\eta^{\frac{1}{2-s}}} \frac{d\omega_{n'}}{\sqrt{\eta}\omega_{n'}^{\psi_s/2}} + \int_{\eta^{\frac{1}{2-s}}}^{\Lambda} \frac{d\omega_{n'}}{\omega_{n'}} \\ &= \frac{2}{2-s} + \frac{1}{2-s}\ln\left(\frac{\Lambda^{2-s}}{\eta}\right) \qquad (4.29)\end{aligned}$$

At a small-η limit, the exponential is governed by the log term. Ignoring the constant,

the self-consistent equation takes the following form after integrating over τ:

$$\frac{\eta\omega_n^s}{uK} = \alpha' \left(\frac{\eta}{\Lambda^{2-s}}\right)^{\frac{2K}{2-s}} \omega_n^s \tag{4.30}$$

Where $\alpha' = -\frac{2\alpha\cos\left(\frac{\pi s}{2}\right)\Gamma(-s)}{\pi}$ is a positive, α dependent constant for $s \in (0,2)$. Comparing the coefficient of ω_n^s on both sides of eq. (4.30), it can be seen that η has a finite, non-zero solution for $K < 1 - \frac{s}{2}$, given by:

$$\boxed{\eta = \left(\frac{\alpha' uK}{\Lambda^{2K}}\right)^{\frac{2-s}{2-s-2K}}} \tag{4.31}$$

For $K \geq 1 - \frac{s}{2}$, the solution of eq. (4.30) is $\eta = 0$. From this, we can identify $K_c = 1 - \frac{s}{2}$ for infinitesimal α as the critical point for the phase transition, which also matches our RG prediction.

The variational analysis of the incommensurate dissipative action re-confirms our prediction about the location of the critical point K_c for small α and characterizes the low-energy spectrum of the dissipative phase as gapless and fractional in nature. However, this calculation only quantifies the lowest order of the ω_n-dependence. The next order of excitations are regulated by $|\omega_n|^{1+\frac{s}{2}}$ and $|\omega_n|^2$, and this will eventually renormalize the parameters u and K in the dissipative phase. We don't, however, analytically quantify the renormalization of the LL parameters in the scope of this thesis. We are working on this from the perspective of the commensurate case, which will be discussed in Chapter 6.

4.2.2 LL phase

To check the validity of the variational ansatz in the LL phase, we assume that in this phase, $\boldsymbol{F(\omega_n) = \nu\omega_n^2}$. To evaluate ν, we replace the G_{var} on the right-hand side of the eq. (4.25) with the bare LL propagator $G_{\text{LL}} = \pi K \left(uq^2 + \frac{\omega_n^2}{u}\right)^{-1}$. This step comes with the assumption that the variational correction ν is small compared to K, and we just provide an estimation for ν. By doing so, the self-consistent equation converts to:

$$\frac{\nu\omega_n^2}{uK} = \frac{2\alpha}{\pi}\int_{\tau_c}^{\infty} d\tau \frac{1-\cos\omega_n\tau}{\tau^{1+s}} e^{-2K\int_0^\Lambda d\omega_n' \frac{1-\cos\omega_n'\tau}{\omega_n'}} \tag{4.32}$$

Where τ_c is the time scale after which the system shows the LL behavior. The integral over $\omega_{n'}$ in the argument of the exponential can be exactly calculated as $\gamma_E + \ln(\Lambda\tau)$, where γ_E is the

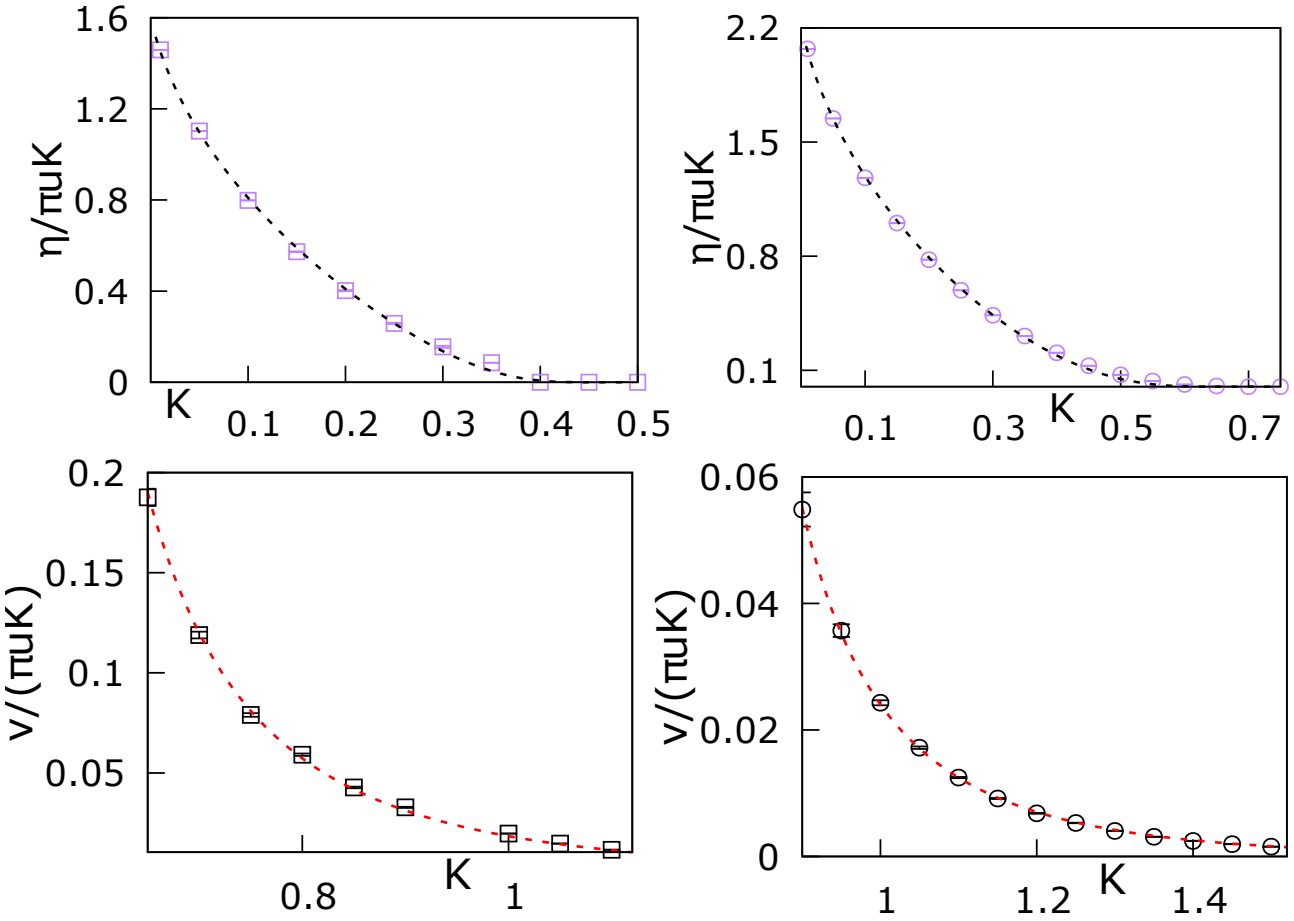

Figure 4.3: Behavior of η (*top*) and ν (*bottom*) for subohmic and ohmic bath, obtained from the solutions of eq. (4.35). For η, the fitting parameters are α' and Λ. For the ohmic case $s = 1$ (*left top*, purple square), $\alpha' = 10.096$ and $\Lambda = 1.963$, and for the subohmic case $s = 0.5$ (*right top*, purple circle), $\alpha' = 8.29$ and $\Lambda = 3.29$. For analyzing the behavior of ν, we use τ_c and Λ as fitting parameters. For $s = 1$ (*left bottom*, black square), $\tau_c = 1.68$ and $\Lambda = 0.272$; and for $s = 0.5$ (*right bottom*, black circle), $\tau_c = 1.241$ and $\Lambda = 0.415$. $\beta = 1024$ and $\alpha = 5$ for all the simulations.

Euler-gamma constant. Putting that back, and expanding $\cos\omega_n\tau$ for small ω_n upto quadratic order, we find:

$$\frac{\nu\omega_n^2}{uK} = \left(\frac{\alpha}{\pi}\frac{e^{-2K\gamma_E}}{\Lambda^{2K}}\int_{\tau_c}^{\infty} d\tau\tau^{1-s-2K}\right)\omega_n^2 \tag{4.33}$$

In the region of the parameter space where we do this calculation, $K > 1 - \frac{s}{2}$. In this limit, the exponent of τ in the integral is smaller than -1, so the integral is convergent within the

limit. Computing the integral and comparing coefficients from both sides, we obtain:

$$\boxed{\frac{\nu}{uK} = \frac{\tilde{\alpha} e^{-2K\gamma_E}}{\tilde{\Lambda}^{2K}\,(2K+s-2)}} \tag{4.34}$$

Where $\tilde{\alpha} = \frac{\alpha \tau_c^{s-2}}{\pi}$ and $\tilde{\Lambda} = \Lambda \tau_c$. Eq. (4.34) diverges at $K = K_c = 1 - \frac{s}{2}$, which indicates that the validity of this estimation is strictly limited by the lower bound of $K > K_c$. The effect of the correction ν is that it renormalizes K and u. If we denote the variational LL propagator as $G_{\text{LL,var}} = \pi K_{r,\text{var}} \left(u_{r,\text{var}} q^2 + \frac{\omega_n^2}{u_{r,\text{var}}} \right)$, then comparing with the bare LL propagator, we see that:

$$\begin{aligned} \frac{K_{r,\text{var}}}{u_{r,\text{var}}} &= \frac{K}{u} \\ \frac{1}{K_{r,\text{var}} u_{r,\text{var}}} &= \frac{1}{uK}\,(1+\nu) \end{aligned}$$

From these equations, one can deduce that $\boldsymbol{K_{r,\text{var}} = K/\sqrt{1+\nu}}$. As ν is always positive, the variational renormalization effectively decreases the bare value of K. The fact that ν is non-zero for the incommensurate dissipative spin chain is already a stark contrast to the Sine-Gordon model. This is a consequence of the fact that the variational method captures the RG up to the first order of the coupling. For the Sine-Gordon model, the contribution of the first order is zero; whereas, in the dissipative spin chain, K gets renormalized at the first order of α itself. As the action corresponding to the bath is non-local in τ, even the variational method captures the renormalization of K in the LL phase.

4.2.3 Numerical solution of the self-consistent equation

Until now, we have only provided different ansatz for the variational method and supported it with physical reasoning. To support our claims, we numerically solve the self-consistent equation for $F(\omega_n)$:

$$F(\omega_n) = \frac{2\alpha u K}{\pi} \sum_{\tau=1}^{\beta-1} D(\tau)(1-\cos\omega_n\tau)\; e^{-\frac{2\pi K}{\beta} \sum_{n'=-\frac{\beta}{2}}^{\frac{\beta}{2}-1} \frac{1-\cos\omega_{n'}\tau}{\sqrt{2\left(1-\cos\omega_{n'}\right)+F(\omega_{n'})}}} \tag{4.35}$$

Eq. (4.35) is the discretized and β-periodic version in the τ direction of eq. (4.26). $D(\tau) = \sum_{k=\beta/2}^{\beta/2-1} \mathcal{B}\left((\tau+k\beta) - \frac{s}{2}, s-1\right)$ ($\mathcal{B}$ is the Beta function) is discretized and $\beta/2$ symmetric version

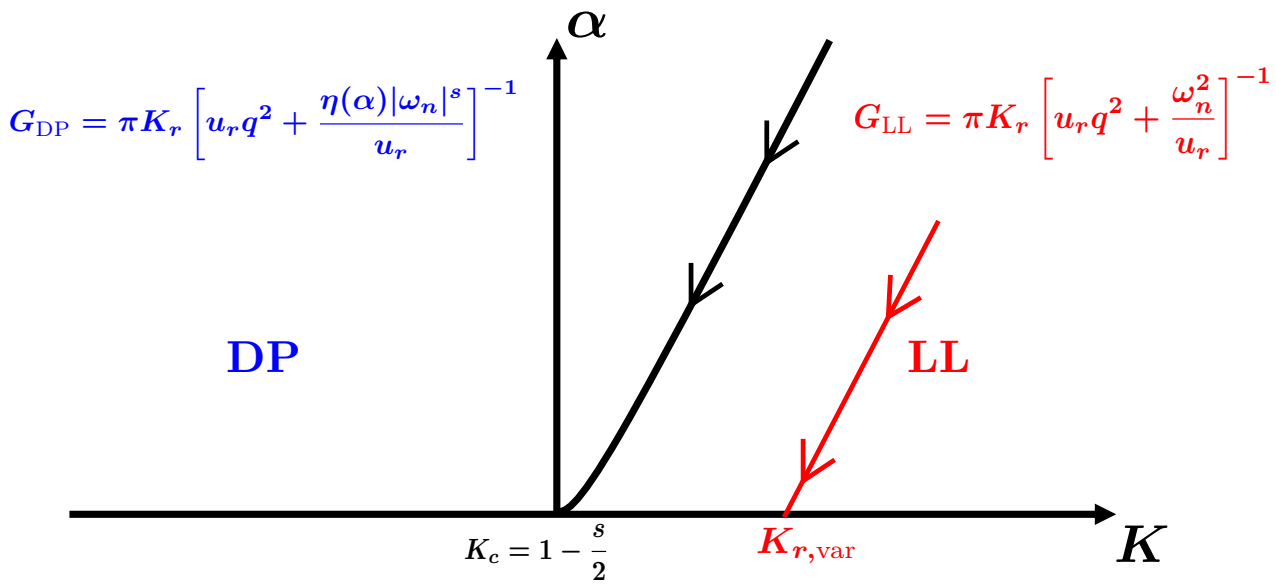

Figure 4.4: A sketch of the zero-temperature phase diagram of the system (eq. (2.1)), obtained from variational ansatz (not quantitative in nature). In the LL regime, this method predicts a renormalization of K to $K_{\mathrm{r,var}}$; which indicates the presence of a tilted phase boundary as opposed to the vertical boundary of Sine-Gordon model (fig. (3.3)). The low energy spectrum of the dissipative phase is governed by the fractional excitation $|\omega_n|^s$ and is gapless in nature.

of the long-range kernel $\tau^{-(1+s)}$ (For more details, see Appendix C). Due to the discretized nature, all integrals have been replaced with sums, and the ω_n^2 in the denominator of the argument of the exponential has been discretized to $2(1 - \cos \omega_n)$.

We solve eq. (4.35) for $s = 1$ (ohmic) and $s = 0.5$ (subohmic) for different values of K. First, we inspect the behavior of $F(\omega_n)$ as a function of ω_n. Then we extract η or ν, depending on which phase it is in, and try to fit those data according to eq. (4.31) or eq. (4.34). The results are shown in fig. (4.2) and fig. (4.3). The plots corroborate with our analytic predictions: The dissipative phase is indeed gapless, with the leading term behaving as $|\omega_n|^s$; and the estimation for η and ν are quite accurate.

4.3 Phase diagram

The first observation that we make from eq. (4.21) and eq. (4.22) that $K_r = K_c$ and $\alpha_r = 0$ on the critical line.. This means that at the phase boundary, the system still remains in the LL phase, which is a signature of the BKT phase transition.

From the variational method, we know that in the dissipative phase, the gap ω_n^2 of the LL phase is replaced by fractional excitations $\eta|\omega_n|^s$. We can associate a correlation length ξ_c to η and analyze how η behaves at different regimes. Comparing with the Sine-Gordon model, we observe that $\eta|\omega_n|^s$ has the dimension of L^{-2}, which implies that η has the dimensionality of L^{s-2}, which is negative for $0 < s < 2$. Now if we stop the RG at a lengthscale l^* where $\alpha(l^*) \sim O(1)$, then $\xi_c \sim e^{l^*}$ and hence $\eta \sim e^{-(2-s)l^*}$. Deep in the dissipative phase, where $dK/dl = 0$ (K is constant), $\alpha(l^*) = \alpha_0 e^{(2-s-2K)l^*} \implies e^{l^*} \sim (1/\alpha_0)^{\frac{1}{2-s-2K}}$. Hence, η behaves as $\boldsymbol{\eta \sim \alpha_0^{\frac{2-s}{2-s-2K}}}$, which is what we find from our variational calculation (eq. (4.31)).

One can also check the behavior of η near the critical line, where $C_1 \approx 0$. In this regime, $K_{\perp_0}/C_1 = \infty$ and $K_\perp/C_1 = -\infty$. Hence, from eq. (4.23), we see that $l^* = \pi/C_1$. As C_1^2 is a constant of the RG flow, we can choose it to be $\frac{K_c^2}{2\pi}\alpha_0 - K_{\perp_0}^2$. Hence, η behaves in this regime as $\boldsymbol{\eta \sim e^{-(2-s)/\sqrt{\frac{K_c^2}{2\pi}\alpha_0 - K_{\perp_0}^2}}}$, which is similar to the non-perturbative behaviour of Δ in the gapped phase of Sine-Gordon model.

The correspondence between the variational ansatz and the RG for the incommensurate dissipative spin chain is quite similar to that of the Sine-Gordon model. However, in the LL phase, the variational method does hint at a renormalization of K. Just like the RG, it shows that the $K_{r,\text{var}} = K/(\sqrt{1+\nu})$ is smaller than the bare K. This hints at a *tilted phase boundary*, rather than a vertical one like the Sine-Gordon model (fig. (4.4)).

Chapter 5

The Incommensurate case: Thermodynamics and Transport

To briefly recall, we establish a phase diagram of the Incommensurate dissipative spin chain (eq. (2.1)) using perturbative RG and variational ansatz. With these techniques, the existence of a BKT type critical point $K_c = 1 - \frac{s}{2}$ for an infinitesimally small value of α is established. We also understand that deep within the phases, the low-energy excitation physics can be captured by a gaussian action with the following propagators:

$$G^{-1}_{\mathrm{LL}}(q, \omega_n) = \frac{1}{\pi K_r}\left(u_r q^2 + \frac{\omega_n^2}{u_r}\right) \tag{5.1}$$

$$G^{-1}_{\mathrm{diss}}(q, \omega_n) = \frac{1}{\pi K_r}\left(u_r q^2 + \frac{\eta|\omega_n|^s}{u_r}\right) \tag{5.2}$$

In this section, we will compute different thermodynamic and dynamic quantities with these propagators, which help us to physically characterize the dissipative phase. In particular, we show that the dissipative phase has unaltered susceptibility (also known as compressibility) and vanishing spin stiffness. We also define an order parameter to identify the two phases, given by $\mathcal{O} = \langle \cos(2\phi(x,\tau))\rangle$. With the help of bosonization mapping, we are able to relate this order parameter to the amplitude of a Spin Density Wave (SDW). Thus, we discover that the dissipative phase is a gapless SDW with long-range order, which is the result of the spontaneous breaking of the continuous symmetry $\phi \to \phi + c$ due to the long-range nature of the action

coming from the bath.

To support our theoretical predictions, we numerically simulate the original action (eq. (2.1)) via Langevin dynamics (as described in Chapter 3) to generate equilibrated configurations. From these configurations, we numerically calculate the same correlation functions and match them against our analytical formulations to verify our predictions. Specifically, we do the simulations for ohmic ($s = 1$) and subohmic ($s = 0.5$) baths. For each type of bath, we take a $K > K_c$ and simulate the configurations for different values of α. This enables us to predict a phase diagram of the system for different values of the parameters.

5.1 Thermodynamical properties

We start our phase characterization with the calculation of two thermodynamic quantities for the different phases, Namely: a) The susceptibility χ and b) the order parameter $\langle \cos 2\phi \rangle$ of the spin chain. In the next two sections, we will relate these quantities to the bosonized field theory via the two-point correlation function and calculate them for the two different phases.

5.1.1 Susceptibility

The susceptibility χ of a 1D spin chain is defined as the response of the system when a finite magnetic field $h(x,t)$ is added to the system. In general, the magnetic field can be time and space-dependent; however, for our purpose, we will consider it to be a constant field $h(x,t) = h$.

Adding a constant magnetic field to the XXZ spin chain adds a term of the form $h\sum_i \sigma_i^z$. As we have seen already in Chapter 2, Section 2.3 under the discussion of the commensurability of the spin chain, the microscopic magnetic term is equal to a contribution of $S_h = -\frac{h}{\pi}\int dx d\tau \, (\nabla\phi(x,\tau))$ to the bosonized action. Note that the integral over the $\cos(2\,(\phi - q_F x))$ term goes to zero as the field h is constant in space and cosine oscillates rapidly. This can also be understood as changing the density of the system $\rho(x,\tau)$ via the addition of a chemical potential h; hence the thermodynamic limit of the susceptibility χ of the spin chain is equivalent to the compressibility of the bosonic field κ. Note that the standard definition of κ in the literature is $\kappa_{\mathrm{T}} = (1/\rho^2)(\partial\rho/\partial h)$, however here we will calculate $\kappa = (\partial\rho/\partial h)$ as they are directly related to each other. With this definition, from linear response theory [37, 88], χ can

be calculated from the response to the density-density correlation function via:

$$\chi(x,\tau) = \langle T_\tau \delta\rho(x,\tau)\delta\rho(0,0)\rangle \tag{5.3}$$

Where $\langle T_\tau \ldots\rangle$ denotes time-ordered correlation to respect the causality of the response. From the form of our perturbation S_h, we understand that $\delta\rho(x,\tau) \simeq -\frac{1}{\pi}\nabla\phi(x,\tau)$. Fourier transforming both sides of eq. (5.3), we obtain:

$$\begin{aligned}
\frac{1}{\beta L}\sum_{q,\omega_n}\chi(q_1,\omega_{n_1})e^{i\left(q_1 x-\omega_{n_1}\tau\right)} &= \frac{1}{(\beta L)^2}\sum_{\substack{q_1,\omega_{n_1}\\ q_2,\omega_{n_2}}}\langle\delta\rho(q_1,\omega_{n_1})\delta\rho(q_2,\omega_{n_2})\rangle e^{i\left(q_1 x-\omega_{n_1}\tau\right)} \\
\implies \chi(q,\omega_n) &= \frac{1}{\beta L}\sum_{q_2,\omega_{n_2}}\langle\delta\rho(q,\omega_n)\delta\rho(q_2,\omega_{n_2})\rangle
\end{aligned} \tag{5.4}$$

The Fourier components of $\delta\rho(q,\omega_n)$ are given by $-(1/\pi)(iq)\phi(q,\omega_n)$. Substituting this in the previous equation, we obtain:

$$\boxed{\chi(q,\omega_n) = -\frac{q}{(\pi)^2\beta L}\sum_{q_2,\omega_{n_2}} q_2\langle\phi(q,\omega_n)\phi(q_2,\omega_{n_2})\rangle} \tag{5.5}$$

We can use eq. (5.5) to compute the susceptibility in both phases now, whose quadratic description we have obtained using the variational method. Let's compute them in both phases now:

- **LL:** In this phase, $S_{\text{LL}} = \frac{1}{2\pi K\beta L}\sum_{q,\omega_n}\phi^*(q,\omega_n)(uq^2+\omega_n^2/u)\phi(q,\omega_n)$. Hence, using eq. (B.6), the susceptibility can be calculated as:

$$\begin{aligned}
\chi_{\text{LL}} &= -\frac{qK_r}{\pi}\sum_{q_2,\omega_{n_2}}\frac{q_2}{u_r q_2^2+\frac{\omega_{n_2}^2}{u_r}}\delta_{q,-q_2}\delta_{\omega_n,-\omega_{n_2}} \\
&= \frac{K_r}{\pi}\frac{q^2}{u_r q^2+\frac{\omega_n^2}{u_r}}
\end{aligned} \tag{5.6}$$

  We are interested in the thermodynamic limit of χ, which we obtain by taking $\omega_n \to 0$ limit (static perturbation) first, and then $q \to 0$ (spatially independent perturbation). Doing so, we find:

$$\boxed{\chi_{\text{LL}}(q\to 0) = \frac{K_r}{u_r\pi}} \tag{5.7}$$

- **Dissipative phase:** The dissipative phase is described by the variational action $S_{\text{diss}} =$

$\frac{1}{2\pi K\beta L}\sum_{q,\omega_n}\phi^*(q,\omega_n)(uq^2+\eta|\omega_n|^s/u)\phi(q,\omega_n)$. Similarly as the LL phase, we see that:

$$\begin{aligned}\chi_{\text{diss}} &= -\frac{qK_r}{\pi}\sum_{q_2,\omega_{n_2}}\frac{q_2}{u_r q_2^2+\frac{\eta|\omega_{n_2}|^s}{u_r}}\delta_{q,-q_2}\delta_{\omega_n,-\omega_{n_2}}\\ &= \frac{K_r}{\pi}\frac{q^2}{u_r q^2+\frac{\eta|\omega_n|^s}{u_r}}\\ \implies &\boxed{\chi_{\text{diss}}(q\to 0)=\frac{K_r}{u_r\pi}}\end{aligned} \tag{5.8}$$

Eq. (5.7) and (5.8) tell us that the susceptibility remains unaltered in both the phases and proportional to the initial value of K/u, as we have seen from our variational calculation of the phases. This might seem shocking at a first glance; however, this phenomenon occurs due to the fact that the dissipative action is invariant under statistical tilt symmetry (STS) [89, 90]. We dedicate the next part to the discussion of this symmetry.

5.1.1.1 Statistical Tilt Symmetry

To understand the STS, we need to go back to the statistical point of view. The partition function of the system in the presence of a magnetic field h is given by:

$$Z[h]=\int\mathcal{D}\phi e^{\left[-S_{\text{LL}}-S_{\text{int}}+\frac{h}{\pi}\int dxd\tau\nabla\phi(x,\tau)\right]} \tag{5.9}$$

One can now complete the square with the $(\nabla\phi)^2$ term from the LL : $-\frac{u}{2\pi K}\int(\nabla\phi)^2+\frac{h}{\pi}\int(\nabla\phi)=-\frac{u}{2\pi K}\int\left(\nabla\left(\phi-\frac{hKx}{u}\right)\right)^2+\frac{h^2K\beta L}{2\pi u}$. We now define a new field $\tilde{\phi}=\phi-\frac{hKx}{u}$ and re-write the whole action in terms of $\tilde{\phi}$. The key observation here is that S_{int} remains invariant due to this tilt transformation. Eq. (5.9) can be written as:

$$Z[h]=\int\mathcal{D}\phi e^{\left[-S_{\text{LL}}[\tilde{\phi}]-S_{\text{int}}[\tilde{\phi}]+\frac{h^2K\beta L}{2\pi u}\right]} \tag{5.10}$$

The compressibility of this system (or static limit of susceptibility of the spin chain $\chi(q\to 0)$) can be now computed via the following calculation:

$$\begin{aligned}\chi &= \frac{1}{\beta L}\frac{\partial^2}{\partial^2 h}\ln Z[h]\\ &= \frac{1}{\beta L}\frac{\partial^2}{\partial^2 h}\left(\ln Z\left[S_{\text{tot}}\left[\tilde{\phi},h=0\right]\right]+\frac{h^2K\beta L}{2\pi u}\right)\\ &= \frac{K}{\pi u}\end{aligned} \tag{5.11}$$

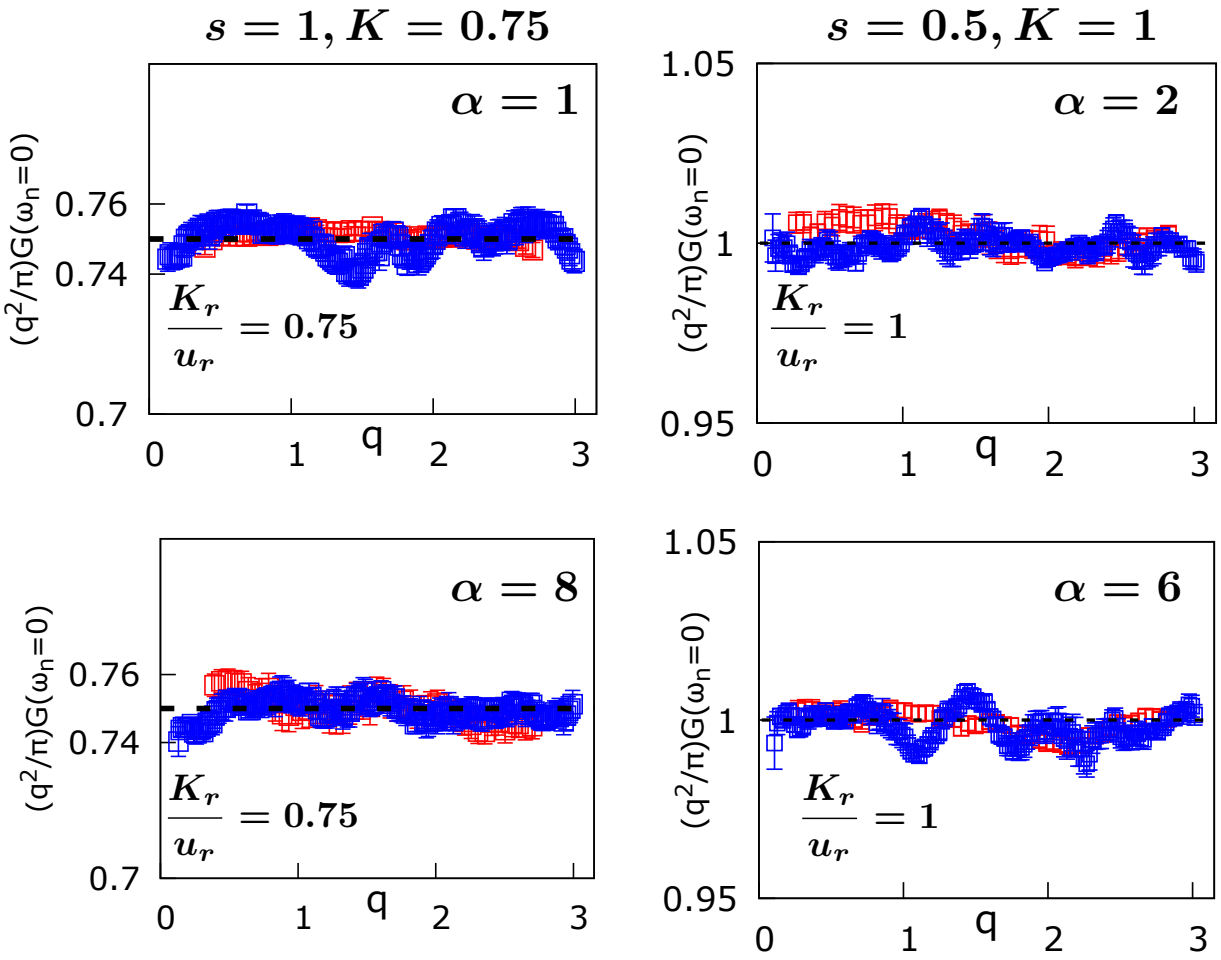

Figure 5.1: Numerical results for χ for ohmic ($s = 1$) (*left*) and subohmic ($s = 0.5$) (*right*) bath. For the ohmic case, the initial K/u value is 0.75, and this remains invariant for both $\alpha = 1$ (LL phase) and $\alpha = 8$. Similarly for the subohmic bath, $K_r/u_r = K/u = 1$ for both $\alpha = 2$ (LL phase) and $\alpha = 6$ (dissipative phase). For both baths, the red points indicate a system size of $L = \beta = 128$. The blue points indicate a system size of $L = \beta = 384$ for $s = 1$ and $L = \beta = 320$ for $s = 0.5$.

From this calculation, it can be understood that even though local dissipative baths can induce a phase transition in a one-dimensional many-body incommensurate system, the susceptibility of the system remains invariant and independent of the dissipative coupling. As the coupling is increased, both K and u get renormalized in such a way that the ratio K/u stays constant and equal to the initial value.

5.1.2 Order Parameter

This section will be very crucial in understanding the true form of the dissipative phase. From eq. (2.30), we observe that the average value of the z-component of the spin is given by:

$$\begin{aligned}\langle\sigma^z(x)\rangle &= \frac{1}{\pi a}\left(-a\nabla\langle\phi(x,\tau)\rangle + \langle\cos\left(2\phi(x,\tau) - 2q_F x\right)\rangle\right) \\ &= \frac{1}{\pi a}\left(-a\nabla\langle\phi(x,\tau)\rangle + \langle\cos(2\phi(x,\tau))\rangle\cos 2q_F x + \langle\sin(2\phi(x,\tau))\rangle\sin 2q_F x\right) \quad (5.12)\end{aligned}$$

Where q_F is the fermi momentum of the system and we have put back the lattice spacing a to explicitly show the dimensionless nature of the quantity. Now we make a key observation: eq. (5.12) is extremely similar to the formation of a **spin density wave (SDW)** $\boldsymbol{\langle\sigma^z(x)\rangle = \sigma_0 + \sigma_1\cos\left(2q_F x\right)}$, where σ_0 is the average magnetization M/N and σ_1 is the amplitude of the SDW [91]. The periodicity of the SDW is π/q_F. One can determine the values of σ_0 and σ_1 via multiple physical arguments:

- Firstly, we observe that $\boldsymbol{\sigma_0 = 0}$. This is due to the fact that the effect of the finite polarization in the spin chain simply offsets the fermi momentum q_F of the system to incommensuration, which is already encoded in our bosonization procedure. Hence, in this bosonized action, the average magnetization is 0. This also supports the fact that the parity symmetry of the field $\phi \to -\phi$ is not broken, hence $\boldsymbol{\pi\sigma_0 = -\nabla\phi = 0}$.

- As the parity symmetry is preserved, it's easy to see that the last term in eq. (5.12) also goes to 0. Hence, comparing the form of the SDW with the surviving terms of eq. (5.12), the amplitude of the SDW is given by $\boldsymbol{\sigma_1 = \frac{1}{\pi a}\langle\cos(2\phi)\rangle}$, which is the quantity we will use as an order parameter for the phase transition. In the following part of this subsection, we will show that in the LL phase, σ_1 goes to 0 at zero temperature and thermodynamic limit, whereas in the dissipative phase, it goes to a constant.

- The formation of the SDW in this system doesn't correspond to the standard Peierls mechanism [92], where the amplitude σ_1 opens a gap in the low-energy spectrum of the system. Indeed, in our case, the system is gapless: The SDW excitations are the gapless Goldstone modes corresponding to the *spontaneous breaking of the continuous translational symmetry* of the field $\boldsymbol{\phi \to \phi + c}$. In the incommensurate dissipative spin chain, this symmetry breaking becomes possible due to the long-range nature of the action corresponding to the local dissipative baths.

- The global shift $\phi \to \phi + c$ doesn't cost any energy; however in the dissipative phase, the

symmetry is broken in the presence of any impurity or local field. Hence, it's convenient to fix the constant by setting the center of the mass of the field $\phi_{\text{CoM}} = \phi(q = 0, \omega_n = 0)$ to 0.

- As the action is symmetric under $\phi \to \phi + c$ for all values of c, one can choose different order parameters to identify the phase transition. For example, by setting $c = \pi$, it can be easily observed that a choice of the order parameter can be $\langle \cos\phi \rangle$ ($\langle \cos\phi \rangle = \langle \cos(\phi + \pi) \rangle \implies \langle \cos\phi \rangle = 0$ unless the symmetry is broken). We will mostly stick to the choice of $\langle \cos 2\phi \rangle$ as the order parameter as it holds the most physical relevance in understanding the characteristics of the dissipative phase, however $\langle \cos\phi \rangle$ will be relevant in understanding some parts of the numerical results in Section 5.3.

With these motivations detailed above, we will now proceed with the calculation of the order parameter $\sigma_1 = \frac{1}{\pi a}\langle \cos 2\phi \rangle$ in the LL phase (eq. (5.1)) and in the dissipative phase (eq. (5.2)) with their corresponding variational propagators. As both the propagators are gaussian in nature, the order parameter can be simplified in fourier space in terms of the propagator using eq. (B.22):

$$\begin{aligned} \frac{1}{\pi a}\langle \cos 2\phi \rangle &= \frac{1}{\pi a} e^{-2\langle \phi^2(x,\tau) \rangle} \\ &= \frac{1}{\pi a} e^{-\frac{2}{(\beta L)^2} \sum\limits_{\substack{q_1,\omega_{n_1} \\ q_2,\omega_{n_2}}} \left\langle \phi(q_1,\omega_{n_1})\phi(q_2,\omega_{n_2}) \right\rangle e^{i\{(q_1+q_2)x - (\omega_{n_1}+\omega_{n_2})\tau\}}} \\ &= \frac{1}{\pi a} e^{-\frac{2}{\beta L} \sum\limits_{q,\omega_n} G(q,\omega_n)} \end{aligned} \tag{5.13}$$

Where the sum over q and ω_n is to be understood without the $q = \omega_n = 0$ mode. Hence, at zero temperature ($\beta \to \infty$) and in the thermodynamic limit ($L \to \infty$) the true value of the order parameter is given by:

$$\sigma_1 = \frac{1}{\pi a} e^{-\frac{2}{\pi^2} \int_0^\Lambda d\omega_n \int_0^\infty dq \; G(q,\omega_n)} \tag{5.14}$$

However, it is imperative for us to understand the effect of finite size and temperature on the order parameter, hence we will calculate the quantity from eq. (5.13), and we will denote this quantity as $\langle \cos 2\phi \rangle_{L,\beta}$ from now on. The summation in the exponential of eq. (5.13) can be broken down into three different types of terms:

- The contribution from $\omega_n = 0, q \neq 0$ terms, which account for finite size effect.
- The contribution from $\omega_n \neq 0, q = 0$ terms, which demonstrate the effect of finite

temperature.

- The contribution from $\omega_n \neq 0, q \neq 0$ terms, which can be approximated by σ_1 (eq. (5.14)) with sub-leading corrections.

5.1.2.1 LL phase

In the LL phase, the propagator is given by $G_{\rm LL} = \pi K_r \left(u_r q^2 + \frac{\omega_n^2}{u_r}\right)^{-1}$, where $K_r = K/\sqrt{1+\nu}$ and $u_r = u/\sqrt{1+\nu}$. Using this, one can show that:

$$\begin{aligned} \frac{2}{\beta L}\sum_{q\neq 0} G_{\rm LL}(q,0) &= \frac{4\pi K}{u\beta L}\sum_{m=1}^{\infty}\frac{1}{\left(\frac{2\pi m}{L}\right)^2} \\ &= \frac{\pi K L}{6u\beta} \end{aligned} \tag{5.15}$$

$$\begin{aligned} \frac{2}{\beta L}\sum_{\omega_n\neq 0} G_{\rm LL}(0,\omega_n) &= \frac{4\pi K u}{(1+\nu)\beta L}\sum_{n=1}^{\infty}\frac{1}{\left(\frac{2\pi n}{L}\right)^2} \\ &= \frac{\pi u K \beta}{6(1+\nu)L} \end{aligned} \tag{5.16}$$

The third term with the sum over non-zero q and ω_n, given by $\frac{2}{\beta L}\sum_{q\neq 0,\omega_n\neq 0} G(q,\omega_n)$ is slightly more tricky to calculate. One can estimate this sum by converting it into an integral $\frac{2K}{\pi}\int_{2\pi/L}^{\Lambda_1} dq \int_{2\pi/\beta}^{\Lambda_2} \frac{d\omega_n}{uq^2+\frac{\omega_n^2}{u}(1+\nu)}$ (Λ_1 and Λ_2 are UV cut-offs) and observing that if the lower and upper limit of the integral over q is sent to 0 and ∞ respectively, the integral is approximated by $K/\sqrt{1+\nu}\ln(\Lambda_2\beta)$; similarly, when the limit of ω_n is sent to 0 and ∞, the integral approximately equals to $K/\sqrt{1+\nu}\ln(\Lambda_1 L)$. From this, it can then be estimated that :

$$\frac{2}{\beta L}\sum_{q\neq 0,\omega_n\neq 0} G_{\rm LL}(q,\omega_n) \sim \frac{K}{\sqrt{1+\nu}}\ln\min(L,\beta) \tag{5.17}$$

Putting all the terms together, it can then be seen that:

$$\boxed{\langle\cos 2\phi\rangle^{\rm LL}_{L,\beta} \sim e^{-\frac{\pi^2}{6}\left(\chi\frac{L}{\beta}+\rho_s\frac{\beta}{L}\right)-K_r\ln\min(\beta,L)}} \tag{5.18}$$

Where $\rho_s = u_r K_r/\pi$ is the spin-stiffness (superfluid density) or charge stiffness of the system, which we will discuss in Section 5.2.3.

5.1.2.2 Dissipative phase

In the dissipative phase, the variational propagator is given by $G_{\text{diss}} = \pi K_r \left(u_r q^2 + \frac{\eta|\omega_n|^s}{u_r}\right)^{-1}$. The summation over $\omega_n = 0, q \neq 0$ is the same as that in the LL phase (eq. (5.15)). The sum over $q = 0$ terms are given by:

$$\frac{2}{\beta L}\sum_{\omega_n\neq 0} G_{\text{diss}}(0,\omega_n) = \frac{2u_r K_r}{\eta}\sum_{n=1}^{\infty}\frac{\frac{2\pi}{\beta}dn}{\left(\frac{2n\pi}{\beta}\right)^s} \tag{5.19}$$

Where $dn = 1$. One can convert the summation into an integral over $\omega_n = (2\pi n)/\beta$, given by $\int_{2\pi n/\beta}^{\Lambda_1} d\omega_n\ \omega_n^{-s}$. Note that this cut-off Λ_1 is necessary in eq. (5.19) when the bath is subohmic or ohmic in nature. This integral behaves differently for different values of s, and after taking the leading order term for large β, we see that:

$$\frac{2}{\beta L}\sum_{\omega_n\neq 0} G_{\text{diss}}(0,\omega_n) = \frac{2u_r K_r}{\eta}\frac{b_0(s)}{(2\pi)^{s-1}}\frac{\beta^{f(s)}}{L} \tag{5.20}$$

Where $f(s) = 0$ and $b_0(s) \sim \frac{1}{1-s}$ for subohmic bath ($0 < s < 1$), and $f(s) = s - 1$ and $b_0(s) = \zeta(s)$ for superohmic bath ($1 < s < 2$). For an ohmic bath ($s = 1$), $b_0(s)\beta^{f(s)}$ is replaced by $\ln(\beta) + \gamma_E$. The contribution of the third term can now be calculated for large-β as:

$$\begin{aligned}\frac{2}{\beta L}\sum_{q\neq 0,\omega_n\neq 0} G_{\text{diss}}(q,\omega_n) &= \frac{2K_r}{\pi}\int_{2\pi/L}^{\infty} dq \int_{2\pi/\beta}^{\Lambda_1}\frac{d\omega_n}{uq^2 + \frac{\eta\omega_n^s}{u_r}} \\ &\approx c_0 - c_1\beta^{\frac{s}{2}-1}\end{aligned} \tag{5.21}$$

Where c_0 and c_1 are positive constants that depend on K_r, u_r, η, s and Λ_1. Hence in the dissipative phase, we obtain:

$$\boxed{\langle\cos 2\phi\rangle_{L,\beta}^{\text{diss}} \sim \sigma_1 e^{-\chi\frac{\pi^2}{6}\frac{L}{\beta} - \frac{2u_r K_r}{\eta}\frac{b_0(s)}{(2\pi)^{s-1}}\frac{\beta^{f(s)}}{L} + c_1\beta^{s/2-1}}} \tag{5.22}$$

Where we understand that $\sigma_1 = e^{-c_0}$ is the true order parameter from eq. (5.14).

5.1.2.3 Behaviour of the order parameter

From eq. (5.18) and eq. (5.22), We can now extract the behavior of the order parameter in both phases in different limits.

- In the thermodynamic limit $L \to \infty$ and finite temperature, the order parameter in both

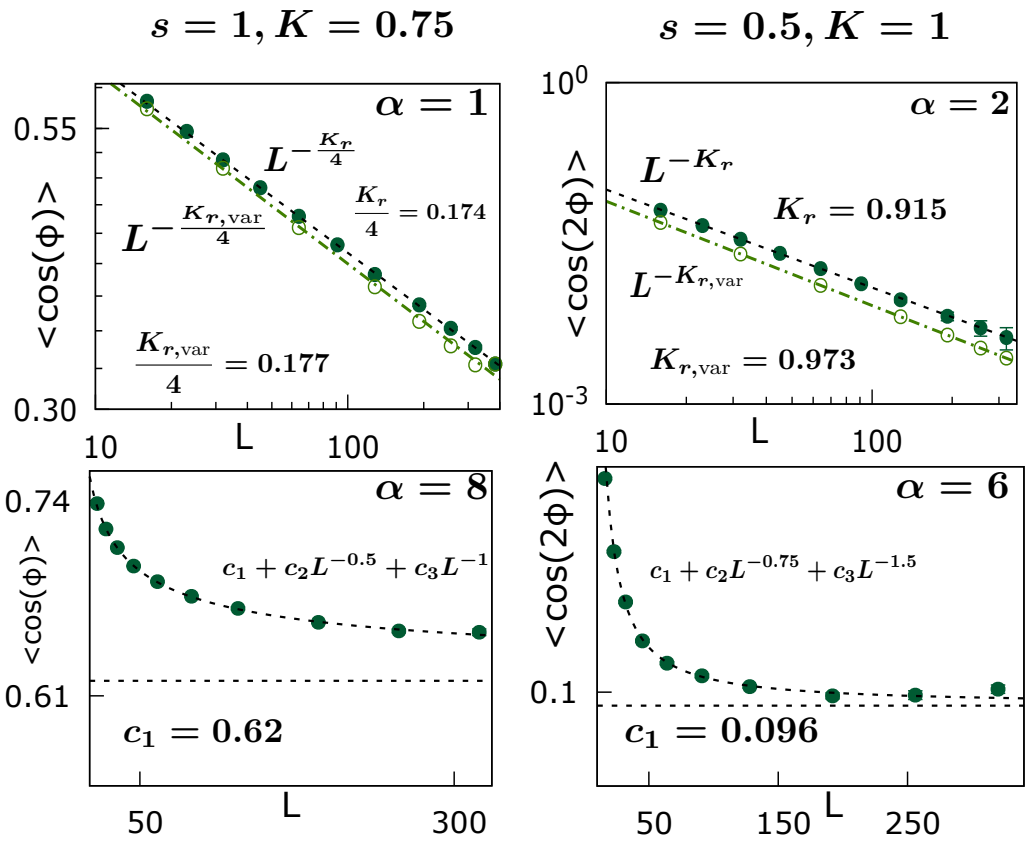

Figure 5.2: Behavior of the order parameter for the ohmic bath (*left*) and the subohmic bath (*right*). $\langle \cos\phi \rangle$ for $s = 1, \alpha = 1$, and $\langle \cos 2\phi \rangle$ $s = 0.5, \alpha = 2$ (*top*) (*deep green*) decay as power laws, from which we can extract $K_r/4 = 0.174$ for the ohmic and $K_r = 0.915$ for the subohmic bath, respectively. For $s = 1, \alpha = 8$ and $s = 0.5, \alpha = 6$, however, the order parameters saturate to a constant. From fitting, we obtain $c_1 = 0.62, c_2 = 0.603, c_3 = -0.531$ for the ohmic and $c_1 = 0.096, c_2 = 0.112, c_3 = 3.37$ for the subohmic case. From the variational self-consistent solution, we find good quantitative matches in the LL liquid, where it predicts $K_{r,\mathrm{var}}/4 = 0.177$ for the ohmic and $K_{r,\mathrm{var}} = 0.973$ for the ohmic bath.

the phases vanishes **exponentially as** $\sim e^{-\chi \frac{\pi^2}{6} \frac{L}{\beta}}$.

- The zero temperature limit $\beta \to \infty$ and finite size regime is more interesting. In the LL regime, the order parameter $\langle \cos 2\phi \rangle^{\mathrm{LL}}_{L,\infty}$ **vanishes again exponentially as** $\sim e^{-\rho_s \frac{\pi^2}{6} \frac{\beta}{L}}$. In the dissipative phase, however, $\langle \cos 2\phi \rangle^{\mathrm{diss}}_{L,\infty}$ either vanishes as a **stretch exponential** $\sim e^{-\frac{\beta^{s-1}}{L}}$ **for superohmic bath**, or it **saturates to a constant for subohmic bath**. This is evidence of the fact that order is established even at finite size in the XXZ spin chain at zero temperature when the baths are subohmic in nature and it is destroyed when the baths are superohmic in nature. This ordering phenomenon can be related to the phase transition observed in the Spin-boson (single particle) model in the presence

of a subohmic bath [93, 94].

- For our numerical simulations, we set $L = \beta$ and send $\beta \to \infty$. In this limit, one can observe that:

$$\boxed{\begin{aligned} \langle \cos 2\phi \rangle^{\text{LL}}_{L=\beta=\infty} &\sim L^{-K_r} && (5.23) \\ \langle \cos 2\phi \rangle^{\text{diss}}_{L=\beta=\infty} &\sim \sigma_1 e^{-\frac{\pi^2}{6}\chi} \left(1 + c_1 L^{\frac{s}{2}-1} + c_2 L^{s-2}\right) && (5.24) \end{aligned}}$$

  where c_2 is also a positive constant and accounts for finite-size corrections. Note that for a generalized choice order parameter $\langle \cos n\phi \rangle$, $n \in \mathbb{Z}$, it decays as $L^{-\frac{n^2 K_r}{4}}$ in the LL phase. In the dissipative phase, however, the algebraic decay retains the same exponentials and only the constants σ_1, c_1, and c_2 get modified.

5.1.3 Spin-spin correlation

In this section, we calculate the spin-spin correlations, which tell us about the nature of the order established due to the quantum phase transition in the system. The two-point spin correlators, using eq. (2.30), are defined as:

$$\boxed{\begin{aligned} \langle \sigma^z_{x,\tau} \sigma^z_{0,\tau} \rangle &\sim \langle e^{2i\phi(x,\tau)} e^{-2i\phi(0,\tau)} \rangle \cos(2q_F x) && (5.25) \\ \langle \sigma^z_{x,\tau} \sigma^z_{x,0} \rangle &\sim \langle e^{2i\phi(x,\tau)} e^{-2i\phi(x,0)} \rangle && (5.26) \end{aligned}}$$

While writing the definitions of the spatial and imaginary-time spin correlations, we use the fact that the correlations will be governed by the behavior of the $2q_F$ components, namely the cos functions; and the $\nabla\phi - \nabla\phi$ correlations add insignificant corrections to the calculation. As our variational propagators are quadratic in the fourier space, using eq. (B.22) with eq. (B.4) and (B.5) respectively, the spatial spin-spin correlation can be re-written as $e^{-2\langle[\phi(x,\tau)-\phi(0,\tau)]^2\rangle} = e^{-2B(x)}$ and similarly the imaginary time spin-spin correlation is equal to $e^{-2\langle[\phi(x,\tau)-\phi(x,0)]^2\rangle} = e^{-2B(\tau)}$. Hence, we need to compute the roughness functions in the different phases to understand the spin-spin correlations. We will divide the roughness function according to the contributions from zero and non-zero q and ω_n components.

5.1.4 Spatial spin-spin correlation

To recall from eq. (B.7), the spatial roughness function in the fourier space is given by:

$$B(x) = \frac{2}{\beta L} \sum_{q,\omega_n} (1 - \cos(qx))\, G(q, \omega_n) \tag{5.27}$$

One can immediately observe that the $q = 0, \omega_n \neq 0$ terms go to 0 due to the $\cos qx$ term in the numerator. The $\omega_n = 0, q \neq 0$ contributions are the same for both the LL and the dissipative phase:

$$\begin{aligned} \frac{2}{\beta L}\sum_{q\neq 0}\left(1-\cos\left(qx\right)\right)G(q,0) &= \frac{4\pi\chi}{\beta L}\sum_{m=1}^{\infty}\frac{1-\cos qx}{q^2} \\ &\sim \frac{\pi^2\chi|x|}{\beta} \end{aligned} \tag{5.28}$$

The $q \neq 0, \omega_n \neq 0$ term is different for the two different phases. For the LL phase, we can see that this term will behave as $\sim K_r \ln x$ for large x by replacing K with K_r and putting $\tau = 0$ in eq. (B.17). In the dissipative phase, this contribution is given by:

$$\begin{aligned} \frac{2}{\beta L}\sum_{q,\omega_n}\left(1-\cos\left(qx\right)\right)G_{\text{diss}}(q\neq 0,\omega_n\neq 0) &= \frac{2K_r}{\pi}\int_0^{\infty}d\omega_n\int_0^{\Lambda}dq\frac{1-\cos\left(qx\right)}{u_r q^2+\frac{\eta\omega_n^s}{u_r}} \\ &\sim c_0 - a_2|x|^{1-\frac{2}{s}} \end{aligned} \tag{5.29}$$

Where $a_2 = \frac{2K_r u_r^{\frac{2}{s}-1}\eta^{-\frac{1}{s}}\Gamma\left(\frac{2}{s}-1\right)}{s}$ is a positive constant and c_0 is the same constant from the order parameter calculation. Putting all the terms together, we find for finite temperature in the thermodynamic limit for large x, the spatial spin-spin correlators behave as:

$$\boxed{\begin{aligned} \langle\sigma^z_{x,\tau}\sigma^z_{0,\tau}\rangle_{\text{LL}} &\sim e^{-\frac{2\pi^2\chi x}{\beta}}x^{-2K_r}\cos(2q_F x) && (5.30)\\ \langle\sigma^z_{x,\tau}\sigma^z_{0,\tau}\rangle_{\text{diss}} &\sim \sigma_1^2 e^{-\frac{2\pi^2\chi x}{\beta}}\left(1+a_2x^{1-\frac{2}{s}}\right)\cos(2q_F x) && (5.31)\end{aligned}}$$

Where for the dissipative phase, we have expanded the exponential term $e^{a_2x^{1-\frac{2}{s}}}$ under the large-x assumption up to the first order.

5.1.5 Imaginary time spin-spin correlation

The imaginary-time spin-spin correlation, just like the spatial one, can be expressed in Fourier space as:

$$B(\tau) = \frac{2}{\beta L}\sum_{q,\omega_n}\left(1-\cos\left(\omega_n\tau\right)\right)G(q,\omega_n) \tag{5.32}$$

In this case, the $\omega_n = 0, q \neq 0$ terms vanish due to the $\cos\omega_n\tau$ in the numerator. The summation over $q = 0, \omega_n \neq 0$ terms is different in the LL phase and the dissipative phase. For the LL

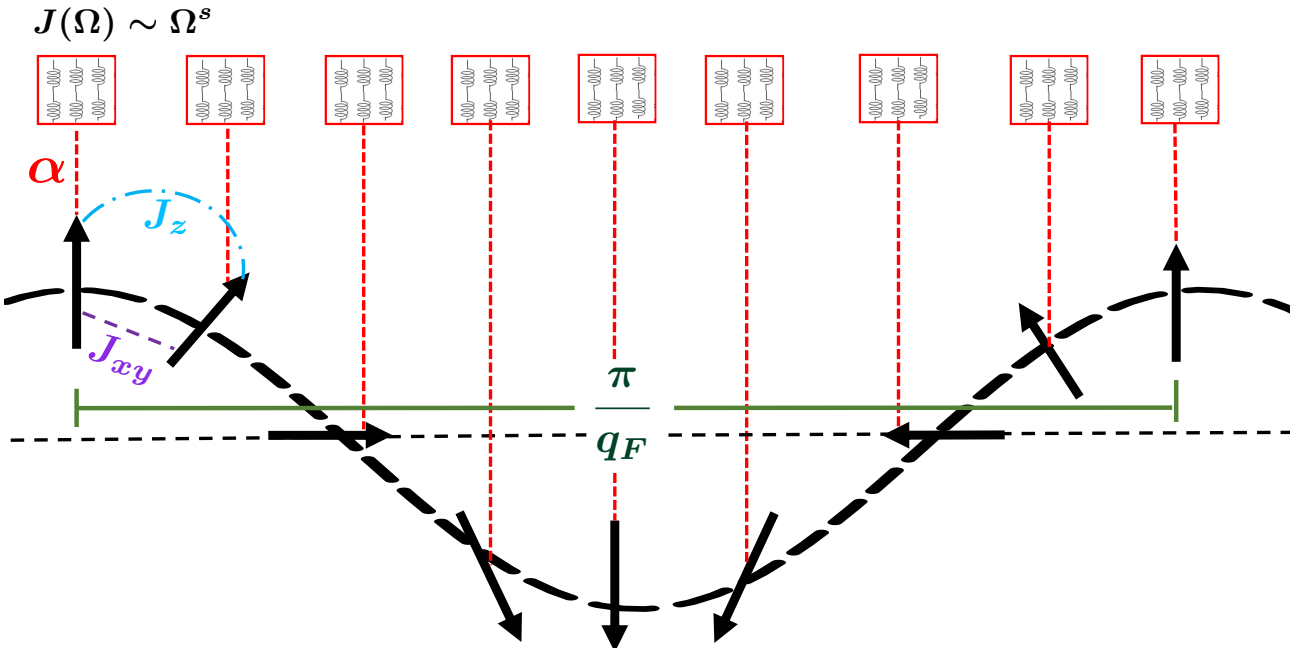

Figure 5.3: A schematic diagram of the dissipative phase. The black arrows denote the spins and the red boxes are the dissipative Caldeira-Leggett baths. The dissipative phase is a gapless SDW with long-range order with periodicity π/q_F.

phase, it can be calculated as:

$$\begin{aligned} \frac{2}{\beta L}\sum_{\omega_n\neq 0}\left(1-\cos\left(\omega_n\tau\right)\right)G_{\mathrm{LL}}(0,\omega_n) &= \frac{4\pi K_r u_r}{\beta L}\sum_{n=1}^{\infty}\frac{1-\cos(\omega_n\tau)}{\omega_n^2} \\ &\sim \frac{\pi^2\rho_s\tau}{L} \end{aligned} \tag{5.33}$$

And for the dissipative phase, it's given by:

$$\begin{aligned} \frac{2}{\beta L}\sum_{\omega_n\neq 0}\left(1-\cos\left(\omega_n\tau\right)\right)G_{\mathrm{diss}}(0,\omega_n) &= \frac{4\pi K_r u_r}{\beta L\eta}\sum_{n=1}^{\infty}\frac{1-\cos(\omega_n\tau)}{\omega_n^s} \\ &\sim \frac{K_r u_r}{\eta}\frac{\tau^{f_1(s)}}{L} \end{aligned} \tag{5.34}$$

Where $f_1(s)=0$ for subohmic bath and $f_1(s)=1-s$ for superohmic bath. For ohmic bath, $\tau^{f_1(s)}$ is replaced by $\ln\tau$. The contribution of the third term with $q\neq 0,\omega_n\neq 0$ terms for the LL phase can be calculated to be $K_r\ln\left(u_r\tau\right)$ from eq. (B.17). For the dissipative phase, it can be calculated as:

$$\begin{aligned} \frac{2}{\beta L}\sum_{q\neq 0,\omega_n\neq 0}\left(1-\cos\left(\omega_n\tau\right)\right)G(q,\omega_n) &= \frac{2K_r}{\pi}\int_0^{\Lambda}d\omega_n\int_0^{\infty}dq\frac{1-\cos(\omega_n\tau)}{u_r q^2+\frac{\eta\omega_n^s}{u_r}} \\ &\sim c_0 - a_1\tau^{\frac{s}{2}-1} \end{aligned} \tag{5.35}$$

Where $a_1 = \frac{K}{\eta}\Gamma\left(1-\frac{s}{2}\right)\sin\left(\frac{\pi s}{4}\right)$. Combining all the terms together, we find that for zero temperature and finite L at large τ, the imaginary time correlations are given by:

$$\boxed{\langle\sigma^z_{x,\tau}\sigma^z_{x,0}\rangle_{\text{LL}} \sim e^{-\frac{2\pi^2\rho_s\tau}{L}}\left(u_r\tau\right)^{-2K_r}} \tag{5.36}$$

$$\boxed{\langle\sigma^z_{x,\tau}\sigma^z_{x,0}\rangle_{\text{diss}} \sim \sigma_1^2 e^{-\frac{Ku\tau f_1(s)}{\eta L}}\left(1+a_1\tau^{\frac{s}{2}-1}\right)} \tag{5.37}$$

5.1.6 Nature of the dissipative phase

From the order parameter analysis, we already understood that symmetry is broken in the dissipative phase at zero temperature, and even at finite temperature for subohmic bath. From eq. (5.31), we understand that the order starts decaying exponentially fast after a length scale of $\sim \beta/(2\pi^2\chi)$ at finite β in the dissipative phase. However, at 0 temperature ($\beta \to \infty$), the connected spatial and imaginary time correlations exhibit a decay in power-law fashion, and the exponents increase as s decreases, i.e., the bath becomes slower in nature. In particular, at large-x we see the signature of spatial long-range order :

$$\boxed{\lim_{x\to\infty}\langle\sigma^z_{x,\tau}\sigma^z_{0,\tau}\rangle_{\text{diss}} = \sigma_1^2\cos(2q_F x)} \tag{5.38}$$

All these pieces of evidence point towards the fact that there is, indeed, a quantum phase transition (phase transition at 0 temperature) induced in the LL phase by the dissipative environment. The new, dissipative phase is a **SDW with spatial long-range order of period $\pi/\mathbf{q_F}$** (fig. (5.3)). The order is established by the spontaneous breaking of the symmetry $\phi \to \phi + c$ due to the long-range nature of the contribution from the baths. The SDW excitations are bosonic modes resulting from the symmetry breaking, and as the symmetry is continuous in nature, these modes are gapless, obeying the Goldstone theorem.

5.2 Dynamical properties: Conductivity and Charge stiffness

We have discussed the thermodynamical properties of the incommensurate dissipative spin chain until now. In this section, we will analyze various dynamical properties of the system. In particular, we will focus on two quantities: Charge stiffness and DC Conductivity of the dissipative phase. In the following calculations, we will use the concepts of analytical continuation

and response function formalism heavily. More details can be found in [37, 88].

We start with the microscopic Ohmic law, which makes a correlation between current density, conductivity, and electric field respectively via $j(q,\omega) = \sigma(q,\omega)E(q,\omega)$. Note that ω corresponds to the frequency modes corresponding to real-time t. Using the Kubo procedure, we apply an electric field $E(t) = E_0 e^{-i(\omega+i\epsilon)t}$ to the system, where $\epsilon = 0^+$ is a small positive quantity. This electric field can be associated with a time-dependent potential $E(x,t) = -\partial A(x,t)/\partial t$. The current operator can thus be derived as a functional derivative of the Hamiltonian (not the action) of the system, given by $j(x,\tau) = -\partial\mathcal{H}/\partial A(x,t)$.

Considering response up to the linear order in A, one can show that the average current density is given by:

$$\langle j(x,t)\rangle = \int dx'dt' \left[\frac{\partial^2\mathcal{H}}{\partial A(x,t)\partial A(x',t')}\bigg|_{A=0} - \langle j(x,t)j(x',t')\rangle_{\text{ret}}\right] A(x',t') \tag{5.39}$$

Where $\langle\ldots\rangle_{\text{ret}}$ denotes retarded correlation function. The first term is known as the diamagnetic term. In our case, the Hamiltonian of the spin chain $\mathcal{H}$, given by eq. (2.25) is quadratic in $\Pi(x)$. In the presence of the vector potential A, one needs to substitute $\Pi \to \Pi - \frac{eA}{\pi}$; and thus the diamagnetic term D can be computed by:

$$\begin{aligned} D &= \frac{uK}{2\pi}\frac{\partial^2}{\partial A(x,t)\partial A(x',t')}\int dx \left[\left(\pi\Pi(x) - \frac{eA}{\pi}\right)^2 + (\nabla\phi(x))^2\right]\Big|_{A=0} \\ &= \frac{uKe^2}{\pi}\delta(x-x')\delta(\tau-\tau') \end{aligned} \tag{5.40}$$

The 2nd term in eq. (5.39) is easier to compute in the imaginary time formalism as $\langle j(x,t)j(x',t')\rangle_{\text{ret}} = -\langle j(x,\tau)j(x',\tau')\rangle = -(euK)^2\langle\Pi(x,\tau)\Pi(x',\tau')\rangle$, as $j(x,\tau) = e(uK)\Pi(x,\tau)$. The action S is quadratic in $\Pi(x,\tau)$ as well (eq. (2.31)), hence one can complete the square with $\Pi(x,\tau)$ to obtain a gaussian action with average $\frac{i}{uK\pi}\partial_\tau\phi$ and variance $\frac{1}{\pi uK}\delta(x-x')\delta(\tau-\tau')$. Thus, the correlation function is given by:

$$(euK)^2\langle\Pi(x,\tau)\Pi(x',\tau')\rangle = \frac{uKe^2}{\pi}\delta(x-x')\delta(\tau-\tau') - \frac{e^2}{\pi^2}\langle\partial_\tau\phi(x,\tau)\partial_{\tau'}\phi(x,\tau')\rangle \tag{5.41}$$

Thus, the first term from eq. (5.41) cancels the diamagnetic term exactly, the surviving correlation term determines the behavior of the conductivity in the system. In eq. (5.39), using the relationship between the electric field and the vector potential in the fourier space

$A(q,\omega) = \frac{-i}{\omega+i\epsilon}E(q,\omega) = \frac{-1}{\omega_n}E(q,\omega_n)$, we see that:

$$\langle j(q,\omega)\rangle = \frac{e^2}{\pi^2\beta L}\left[\omega_n\langle\phi(q=0,\omega_n)\phi^*(q=0,\omega_n)\rangle\right]_{i\omega_n\to\omega+i\epsilon}E(q,\omega_n)$$

$$\implies \boxed{\sigma(\omega) = \frac{e^2}{\pi^2\beta L}\left[\omega_n\langle\phi(q=0,\omega_n)\phi^*(q=0,\omega_n)\rangle\right]_{i\omega_n\to\omega+i\epsilon}} \tag{5.42}$$

Where we have used the standard analytical continuation between real frequency ω and matsubara frequency ω_n, given by $i\omega_n \to \omega + i\epsilon$. Note that the conductivity depends only on the 0 mode of the momentum as it is independent of the position x. This derivation is powerful as it relates the conductivity of the system to the $\phi - \phi$ correlator. Even in the presence of the dissipative bath, this derivation remains unchanged because the contribution of the bath is independent of $\Pi(x)$, so we can use this formulation to compute the conductivity of both the LL phase and the dissipative phase.

5.2.1 LL phase

In the LL phase, $\langle\phi(q=0,\omega_n)\phi^*(q=0,\omega_n)\rangle = \beta L\frac{\pi u_r K_r}{\omega_n^2}$. Substituting this in eq. (5.42), we find:

$$\begin{aligned}\sigma(\omega)_{\text{LL}} &= (u_rK_r)\frac{e^2}{\pi}\left(\frac{1}{\omega_n}\right)\Big|_{i\omega_n\to\omega+i\epsilon} \\ &= \frac{ie^2}{\pi}(u_rK_r)\frac{\omega-i\epsilon}{\omega^2+\epsilon^2}\end{aligned} \tag{5.43}$$

When the applied electric field is constant in time $E(t) = E_0$, the relevant physical observable is DC conductivity, given by $\sigma_{\text{DC}} = \lim_{\omega\to 0}\text{Re}[\sigma(\omega)]$, where Re[...] denote the real part of the quantity. Setting $\omega \to 0$, we can see that for $\epsilon = 0^+$:

$$\boxed{\lim_{\omega\to 0}\text{Re}[\sigma(\omega)] = e^2(u_rK_r)\delta(\omega)} \tag{5.44}$$

The DC conductivity in the LL phase displays a Drude peak [95, 96], which indicates that the system is perfectly conducting in nature with infinite DC conductivity. The quantity $(u_rK_r)/\pi$ is known as the charge stiffness [97] and we will discuss it in more detail in the last section.

5.2.2 Dissipative phase

In the dissipative phase, the two-point correlation function is given by $\langle\phi(q=0,\omega_n)\phi^*(q=0,\omega_n)\rangle = \beta L\frac{\pi u_r K_r}{\eta|\omega_n|^s}$. Using eq. (5.42), We find that:

$$\begin{aligned}\sigma(\omega)_{\text{diss}} &= \frac{e^2}{\pi}\left(\frac{u_r K_r}{\eta}\right)\left(\frac{\omega_n}{|\omega_n|^s}\right)\Bigg|_{i\omega_n\to\omega+i\epsilon} \\ &= \frac{e^2}{\pi}\left(\frac{u_r K_r}{\eta}\right)\frac{\epsilon-i\omega}{(\omega^2+\epsilon^2)^{s/2}}\end{aligned} \tag{5.45}$$

Just like the LL phase, the static limit or the DC conductivity can be calculated by taking the real part of the conductivity and going to the $\omega\to 0$ limit. That gives us:

$$\boxed{\sigma_{\text{DC}}^{\text{diss}} = \frac{e^2}{\pi}\left(\frac{u_r K_r}{\eta}\right)\epsilon^{1-s}} \tag{5.46}$$

Eq. (5.46) is very interesting. It tells us that the DC conductivity of the dissipative phase behaves very differently depending on the bath exponent s.

- If the bath is superohmic ($s>1$), the exponent of the ϵ is negative. This means that **the static conductivity diverges**, and it diverges slower compared to the Drude peak in the LL phase. However, the system still remains conducting in nature.

- For an ohmic bath, $\boldsymbol{\sigma_{\text{DC}}^{\text{LL}} \sim \frac{e^2}{\eta(\alpha)}}$ is a constant. The static conductivity is finite and inhibited, and it decreases as the coupling to the bath is increased.

- The most interesting case corresponds to the subohmic bath ($s<1$). In that case, the DC conductivity **vanishes to 0**, which is the signature of an insulating phase.

The absence of DC conductivity in the dissipative phase can also be interpreted as a signature of "*localization*". This localization phenomenon is different than the famous Anderson localization [1], in which case the spatial two-point correlation decays exponentially (Recall that in the dissipative phase, they are long-range ordered with power-law decay). It would also be interesting to investigate the conductivity of this phase at a finite temperature. The true nature of this localization is yet to be understood.

5.2.3 Charge stiffness

Here we discuss the charge stiffness of the system D, which is a measure of the system's ability to sustain current. It can be derived in many different ways, e.g. - by considering the system as a ring and measuring the current in it when a magnetic flux is present or by taking double derivative of the ground state energy of the system with respect to the magnetic flux [98, 99], etc. However, here we show the simplest derivation from the correlation function perspective. This is very similar to the derivation of susceptibility χ (Section 5.1.1), so we don't show it separately here and provide the final result. The charge stiffness is given by:

$$\boxed{D = \lim_{\omega_n \to 0} \lim_{q \to 0} -\frac{\omega_n}{\pi^2 \beta L} \sum_{q_2, \omega_{n_2}} \omega_{n_2} \langle \phi(q, \omega_n) \phi(q_2, \omega_{n_2}) \rangle} \tag{5.47}$$

Note that to calculate D, one needs to first take the $q \to 0$ limit and then the $\omega_n \to 0$ limit as this is a transport-related quantity. Just like previous calculations, one can see that in the LL phase $\boldsymbol{D}_{\mathrm{LL}} = (\boldsymbol{u_r K_r})/\boldsymbol{\pi}$, whereas in the dissipative phase for any $s < 2$, $\mathbf{D}_{\mathrm{diss}} = \mathbf{0}$. This signifies that the Drude peak vanishes in the dissipative phase, which we have already seen from the conductivity calculation.

At zero temperature, the charge stiffness is equal to another quantity known as **spin stiffness** or **superfluid density** $\boldsymbol{\rho_s}$ [100]. A finite value of ρ_s indicates the presence of superfluid excitations in the system. As we already know, the LL phase contains superfluid excitations, hence $\boldsymbol{\rho}_{s_{\mathrm{LL}}} = \boldsymbol{u_r K_r/\pi}$ is finite in this phase. In the dissipative phase, the excitations are SDW, hence $\boldsymbol{\rho}_{s_{\mathrm{diss}}} = \mathbf{0}$.

5.3 Numerical results

In this section, we will discuss the results of the numerical simulations of the incommensurate dissipative system, specifically, of the action given by eq. (2.1). As we have discussed in Section 3.3 and Appendix C, we numerically simulate the Langevin dynamics of the action to generate equilibrated configurations. We calculate various correlation functions on these configurations, and then we verify their behaviors against the analytical predictions. For the simulations, we chose an ohmic bath ($s = 1$) and a subohmic bath ($s = 0.5$). For the ohmic case, $K_c = 0.5$, and we chose the initial value of $K = 0.75$. On the other hand, $K_C = 0.75$ for $s = 0.5$, and here we took the initial value to be $K = 1$. We traverse the $K - \alpha$ phase space by fixing the value

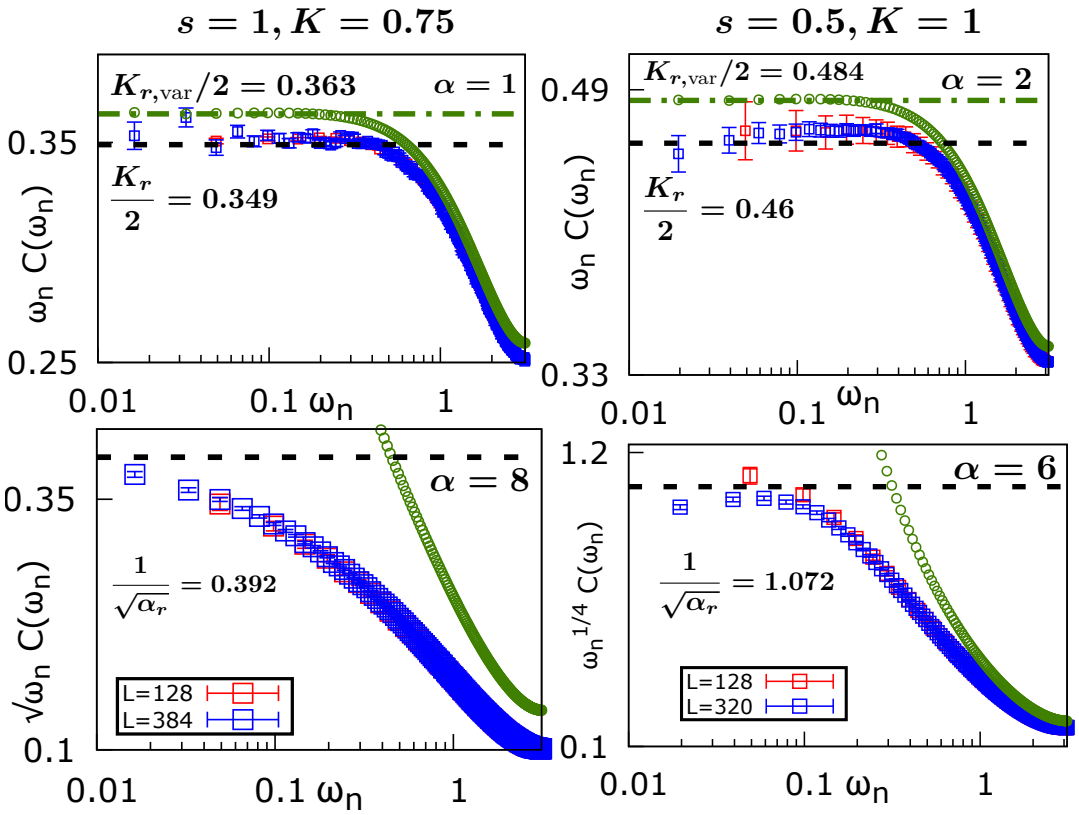

Figure 5.4: Behavior of $C(\omega_n)$ in the two different phases for the ohmic (*left*) and the subohmic bath (*right*). For $s = 1, \alpha = 1$ and $s = 0.5, \alpha = 2$ (*top*), $\omega_n C(\omega_n)$ converges to a constant for small ω_n. The extracted value of $K_r = 0.698$ for the ohmic and $K_r = 0.92$ for the subohmic bath from this analysis. However, $\sqrt{\omega_n} C(\omega_n)$ and $\omega_n^{1/4} C(\omega_n)$ goes to constant $1/\sqrt{\alpha_r} = 0.392$ and $1/\sqrt{\alpha_r} = 1.072$ for small-ω_n for $s = 1, \alpha = 8$ and $s = 0.5, \alpha = 6$ (*bottom*), respectively. The averages were done over 6000 to 12000 configurations. The variational analysis (green points) has a good quantitative prediction in the LL phase with $K_{r,\mathrm{var}} = 0.726$ for the ohmic and $K_{r,\mathrm{var}} = 0.968$ for the subohmic bath. However, it overestimates the prediction and doesn't capture the dissipative phase quantitatively.

of K and then increasing the value of α. For each value of α, we simulate configurations of different sizes while keeping $\beta = L$, i.e., the configurations are square-shaped. We also enforce periodic boundary conditions on both x and τ direction. The value of u is fixed to be 1 for all the simulations. Keeping all these parameters in mind, let us now look at the numerical results:

- ***Calculation of χ***: Instead of directly calculating χ, we instead calculate $q^2 G(q, \omega_n = 0)$ as a function of q, where $G(q, \omega_n) = \beta L \langle \phi^*(q, \omega_n) \phi(q, \omega_n) \rangle$. From eq. (5.5), one can see that this quantity is equal to the ratio $\pi\chi = K_r/u_r$. From fig. (5.1), we see that $q^2 G(q, \omega_n = 0)$ is equal to the initial value of K/u for all values of q, which is equal to 0.75 for the ohmic case and 1 for the subohmic case. Thus, we are able to numerically

establish the existence of statistical tilt symmetry in the action.

- ***Calculation of $C(\omega_n)$***: One of the fundamental results that we found during our analysis is that the low-energy propagator of the dissipative phase has a gapless $|\omega_n|^s$ dependence. To see this behavior explicitly, we definite a quantity $C(\omega_n) = \frac{1}{\pi L}\sum_q G(q, \omega_n)$. Using eq. (5.1) and eq. (5.2), one can average over the q modes of the variational propagators of both phases in the thermodynamic limit. The small-ω_n behavior of $C(\omega_n)$ is then given by:

$$\boxed{\begin{aligned} C(\omega_n \to 0)_{\text{LL}} &= \frac{K_r}{2\omega_n} \qquad (5.48)\\ C(\omega_n \to 0)_{\text{diss}} &= \frac{1}{\sqrt{\alpha_r \omega_n^s}} \qquad (5.49)\end{aligned}}$$

  Where in eq. (5.49), $\alpha_r = 4\eta/K_r^2$. From fig. (5.4), *top*, we see that indeed for $s = 1, \alpha = 1$ and $s = 0.5, \alpha = 2$, $\omega_n C(\omega_n)$ goes to a constant. From eq. (5.49), we see that this constant is $K_r/2$. Thus we are able to extract K_r in the LL phase from the numerical solution. However, for $s = 1, \alpha = 8$ and $s = 0.5, \alpha = 6$ (fig. (5.4), *bottom*), we see that the convergence at small ω_n is obtained from $\omega_n^{\frac{s}{2}} C(\omega_n)$. In this phase, the physical meaning of K_r is lost as we understood from the RG and variational analysis; instead, the quantities that regulate the phase are K_r/u_r and α_r. From the saturation value of the plot $1/\sqrt{\alpha_r}$, we can extract this quantity as well.

We also numerically simulated the self-consistent equation (eq. (4.35)) for the same values of s, K, and α to check how good the variational ansatz quantitatively is. Fig. (5.4), *top* tells us that in the LL phase for moderate values of α, the variational ansatz is pretty good in predicting the renormalized values of the LL parameters. However, as α is increased, the quantification starts becoming more and more unreliable. Specifically, the variational method overestimates the phase transition. We can understand from fig. (5.4), *bottom* that the variational method predicts that the system is still in the LL phase, whereas the actual simulation indicates that the system is in the dissipative phase.

Note that another quantity that trivially comes to mind for analyzing the ω_n-dependence of the propagator is $G(q = 0, \omega_n)$. We started our analysis with this quantity; however, the simulation data for $G(q = 0, \omega_n)$ turned out to be extremely noisy. However, integrating out the q modes reduces the noise, thus making it easier for us to understand the saturation of the above-mentioned quantities and to extract the renormalized values

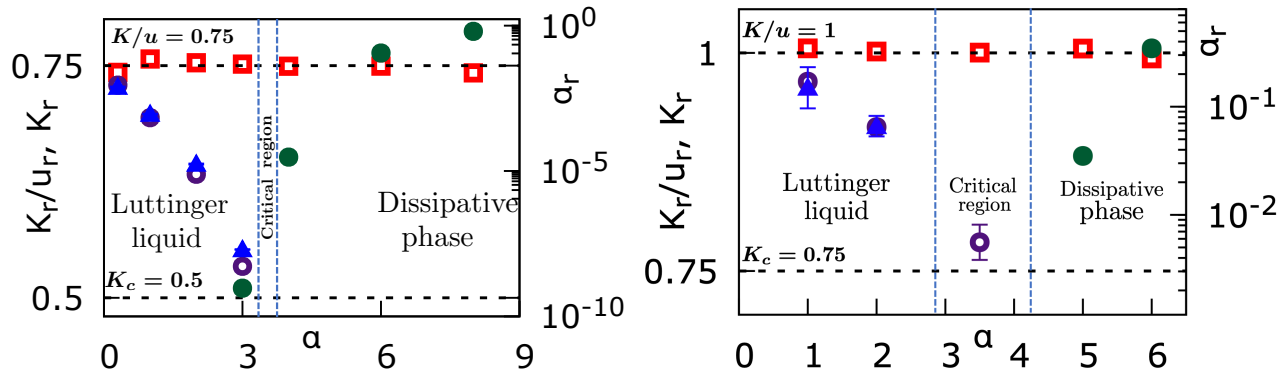

Figure 5.5: Phase diagram for the ohmic bath (*left*) and the subohmic bath(*right*). The ratio K_r/u_r (*red squares*) remains constant for all values of α. As α increases, K_r, both obtained from $\langle \cos 2\phi \rangle$ (*purple circles*) and $C(\omega_n)$ (*blue triangle*) decreases and approaches $K_c = 1 - (s/2)$. In the dissipative phase, α_r increases (*green solid circles*) rapidly as α increases. We identify the critical regime for both cases to be $\alpha_C \in (3, 4)$.

of the parameters.

- ***Calculation of order parameter***: Finally, we calculate the order parameter $\langle \cos n\,(\phi - \phi_{\text{CoM}}) \rangle$ with $n = 1$ for the ohmic case and $n = 2$ for the subohmic case. Recall that ϕ_{CoM} is the same as $\phi(q = \omega_n = 0)$, which we set to zero in our analytical calculation as well (Section 5.1.2). As we took $L = \beta$, the analytical predictions for the LL and the dissipative phase are given by eq. (5.23) and eq. (5.24), respectively. Indeed, from fig. (5.2), *top*, we see that for $s = 1, \alpha = 1$, $\langle \cos((\phi - \phi_{\text{CoM}}))_{\text{LL}} \rangle \sim L^{-K_r/4}$, and for $s = 0.5, \alpha = 2$, $\langle \cos(2\,(\phi - \phi_{\text{CoM}}))_{\text{LL}} \rangle \sim L^{-K_r}$. We are also able to extract the value of K_r from this fitting, and they match quite closely with the ones extracted from the $C(\omega_n)$ analysis. On the other hand, for $s = 1, \alpha = 8$ and $s = 0.5, \alpha = 6$, the order parameter saturates to a constant with an algebraic decay as $\langle \cos(n\,(\phi - \phi_{\text{CoM}}))_{\text{diss}} \rangle \sim c_1 + c_2 L^{1-\frac{s}{2}} + c_3 L^{2-s}$ (fig. (5.2), bottom), which is exactly the decay that was predicted by the variational method. We also calculated the order parameter from the variational self-consistent equation for the LL phase (as we saw before, it overestimates the transition in the dissipative phase), and as expected, the ansatz is quantitatively close to the actual simulations.

The numerical results in Section 5.3 confirm our predictions about the behavior of the two phases. We see that the system either remains in the LL phase with renormalized values of K_r (and thus u_r as K_r/u_r remains invariant and equal to K/u), or it enters into a gapless ordered phase with a fractional low-energy behavior of $|\omega_n|^s$. We also plot K_r and α_r as a function

of α for both ohmic and subohmic cases (fig. (5.2)). From these results, we can see the flow of the parameter as the coupling to the dissipative environment is increased. We see that for both the ohmic and the subohmic case, K_r/u_r always remains constant obeying the statistical tilt symmetry. However, as α is increased, K_r starts to decrease and approach $K_c = 1 - s/2$. It can then be inferred that u_r also decreases, hence the spin stiffness and charge stiffness $\rho_s = D = u_r K_r/\pi$ decreases as the system approaches the critical point. In the dissipative phase, K_r loses physical meaning. However, α_r starts rapidly increasing as α increases and the phase becomes more dissipative in nature. From the plots, we identify the critical regime as $\alpha_c \in (3, 4)$ for the ohmic bath and the subohmic bath.

5.4 Discussion

This section is dedicated to a comprehensive discussion of our results in comparison to some of the other important contemporary works that have been done on similar open quantum systems. While doing a bibliographical survey, we found two important papers that turned out to be extremely relevant to this work. The first one was [87], where they studied the quantum phase transition in a one-dimensional quantum wire coupled with a dissipative metallic gate. The study was fully analytical in nature with an emphasis on the bosonization method which they used to arrive at a similar $1+1$ dimensional long-range cosine potential coming from the gate, and the perturbative RG method which results in the same flow equations as our incommensurate system (eq. (4.12) and eq. (4.13)). They predicted the dissipative phase to be gapless and spatially long-range ordered and also commented about the dissipative phase having finite DC conductivity for an ohmic bath; however, their analysis lacked numerical evidence and a deeper insight into the physical nature of the dissipative phase. The other relevant work [101] was fully numerical in nature: Quantum Monte-Carlo techniques were implemented on a one-dimensional system of many-body interacting hardcore bosons with local Caldeira-Leggett type baths, and the authors found the dissipative phase (referred in the letter as bath induced Bose Liquid) to have increased susceptibility, non-zero conductivity, and zero gap. Moreover, they deemed the phase transition to have a dynamical exponent $z = 2$, which contradicts the results of [87] where the transition was found to be of BKT type ($z = 1$).

This motivated us to do a thorough study of the system with both numerical and analytical techniques that, first of all, would be self-contained, and would also be able to corroborate

the previously mentioned studies. Analytically, we chose a variational approach, which is more powerful than the harmonic expansion done in [87]; the self-consistent nature of this technique allowed us to verify the location of the critical point, and arrive at a powerful low-energy description of the dissipative phases with additional finite size corrections which allows us to be more precise regarding our numerical analysis. Additionally, we were able to observe a variational renormalization of the LL parameters in the LL phase. To be able to properly characterize the dissipative phase against the existing LL phase, we wanted to calculate both thermodynamical and dynamical (transport-related) quantities. With a simple statistical tilt symmetry argument, we showed the invariance of χ in the dissipative phase, which refuted the claim of the numerical work. We also defined an order parameter for this transition $\langle \cos 2\phi \rangle$ and related it to a physical observable (amplitude of an SDW), thus being able to pinpoint the exact nature of the dissipative phase. Our analyses also showed that the system has spatial long-range order and gapless fractional low-energy excitation in ω_n, however, we made additional arguments regarding the presence or absence of the order at the finite size and finite temperature limit of the system for different types of baths. Finally, from our transport analysis, we showed that the dissipative phase is specifically insulating when the baths are subohmic. This observation was missing from the previous works. However, The authors claimed the existence of a third gapped, Bose-Einstein condensation-like phase in [87] by performing a large-N approximation of the action, which we don't find via our analysis.

Our work fortifies the results of [87] accompanied by additional observations and refutes some of the claims in [101]. We have certain hypotheses regarding the disparities. One possibility is that the incommensuration parameter that they used in their simulations is really small, which could have resulted in a different kind of phase transition than the one observed in our system. Also, the system sizes in the Monte Carlo simulations were quite small, which could potentially give rise to large finite-size effects. The implementation of the bosonization method ensured that the system was incommensurate enough, and the numerical Langevin analysis enabled us to arrive at much larger system sizes. Also, in [101], they perform the numerical analyses on the microscopical system itself, whereas we map the system onto a classical system; so there could be some microscopic phenomenon that might not have been captured by the bosonization procedure. However, this possibility remains remote.

The discussions and results until now (from Chapter 2 to 5) have resulted in one publication [11] and one pre-print in Arxiv [12]. For the convenience of the readers, we have put the

two papers before the bibliography. In the final chapter (Chapter 6), we will briefly discuss our analysis of the commensurate case, which is an ongoing work.

Chapter 6

Commensurate Phase

In this chapter, we discuss the zero-temperature phase diagram of the 1D XXZ spin chain at zero magnetization coupled with local dissipative baths. As it has already been derived in Chapter 2, this system can also be mapped onto a classical action, given by eq. (2.2). This is an ongoing work with O. Bouverot-Dupuis, L. Foini, and A. Rosso, and here we describe only certain important developments that we have made. Specifically, we show that just like the incommensurate model, there exists a BKT phase transition in the commensurate case. However, the location of the critical point $K_c = 1 - \frac{s}{2}$ for subohmic bath, and $K_c = 1/2$ for ohmic and superohmic bath. We also find that here, the previously described gapless SDW phase is replaced by a gapped AFM phase, described by the effective gaussian action:

$$S_{\text{diss,comm}} = \frac{1}{2\pi K_r}\left(u_r q^2 + \frac{\omega_n^2}{u_r} + \frac{\Delta^2}{u_r}\right) \tag{6.1}$$

Where Δ has the dimension of energy (in natural units, L^{-1}) and is independent of ω_n or q. It represents the mass of the excitations or the gap in the low energy spectrum of the system.

6.1 Variational analysis

To recall from before, the action of the commensurate spin chain in the presence of local dissipative baths is given by:

$$\begin{aligned} S_{\text{tot,C}} &= S_{\text{SG}} + S_{\text{int}} + S_{int,C} \\ S_{\text{SG}} &= \frac{1}{2\pi K}\int dxd\tau \left[u(\nabla\phi(x,\tau))^2 + \frac{1}{u}(\partial_\tau\phi(x,\tau))^2\right] - \frac{g}{2\pi^2}\int dxd\tau \cos\left(4\phi(x,\tau)\right) \\ S_{\text{int}} &= -\frac{\alpha}{4\pi^2}\int dxd\tau d\tau' \frac{\cos\left[2\left\{(\phi(x,\tau)-\phi(x,\tau'))\right\}\right]}{|\tau-\tau'|^{1+s}} \\ S_{\text{int,C}} &= -\frac{\alpha}{4\pi^2}\int dxd\tau d\tau' \frac{\cos\left[2\left\{(\phi(x,\tau)+\phi(x,\tau'))\right\}\right]}{|\tau-\tau'|^{1+s}} \end{aligned} \tag{6.2}$$

A perturbative RG analysis of a similar action was done in [102] in the context of superfluid to mott insulator transition in a mixture of heavy bosons confined to move in one dimension and light fermions acting as ohmic dissipative baths for the bosons. The existence of a BKT phase transition was discovered in this system in the parametric plane of $K-g$, and the dissipative phase was found to be a fractional mott phase. However in our case, we investigate the system in the presence of a bath with general exponent s, and we are interested in understanding the phase diagram in the $K-\alpha$ plane. To do that, we once again rely on the variational method to understand the nature of the dissipative phase.

We start from eq. (3.3), where we replace S_{int} with $S_{\text{SG}} + S_{\text{int}} + S_{\text{int,c}}$ from eq. (2.2). We have already done these averages previously in the thesis. $\langle S_{\text{int}}\rangle_{S_{\text{var}}}$ has been calculated in the discussion of the variational method of the Sine-Gordon model (eq. (3.4)), and similarly the average $\langle S_{\text{int}}\rangle_{S_{\text{var}}}$ is discussed in the variational analysis of the incommensurate spin chain (eq. (4.24)). For $\langle S_{\text{int,C}}\rangle_{S_{\text{var}}}$, it will be the same term as the incommensurate term, with $1+\cos\omega_n\tau$ in the argument of the exponential instead of $1-\cos\omega_n\tau$. Putting all these terms together, we find that in the thermodynamic limit,

$$\begin{aligned} G_{\text{var}}^{-1} = \frac{1}{\pi K}\left(uq^2 + \frac{\omega_n^2}{u}\right) + \frac{2\alpha}{\pi^2}\int d\tau \frac{(1-\cos\omega_n\tau)}{\tau^{1+s}} e^{-\frac{4}{\pi^2}\int_0^\infty dq' d\omega_{n'} G_{\text{var}}(q',\omega_{n'})(1-\cos\omega_{n'}\tau)} \\ + \frac{8g}{\pi^2} e^{-\frac{8}{\pi^2}\int_0^\infty dq' d\omega_{n'} G_{\text{var}}(q',\omega_{n'})} + \frac{2\alpha}{\pi^2}\int d\tau \frac{(1+\cos\omega_n\tau)}{\tau^{1+s}} e^{-\frac{4}{\pi^2}\int_0^\infty dq' d\omega_{n'} G_{\text{var}}(q',\omega_{n'})(1+\cos\omega_{n'}\tau)} \end{aligned} \tag{6.3}$$

Let us assume that the dissipative phase of this system is described by the following variational propagator $\boldsymbol{G_{\text{var}} = \pi K_r\left[u_r q^2 + \frac{\eta|\omega_n|^s}{u_r} + \frac{\Delta^2}{u_r} + \frac{\omega_n^2}{u_r}\right]^{-1}}$, as it was suggested in [102]. One can

expect in general a ω_n^2 term coming from the $\cos\omega_n\tau$ terms in eq. (6.3) which will eventually renormalize the LL parameters to K_r and u_r. Now we analyze eq. (6.3) to understand the behavior of η and Δ.

- ***Determination of η***: Let us first try to analyze the coefficient of the fractional term η and understand what contributes to this coefficient. In the argument of the exponential in the 2nd and the 4th term in eq. (6.3), the integrals produce a constant and a τ-dependent term. The constant, multiplied with the $\cos\omega_n\tau$ produces the $|\omega_n|^s$ term when integrated over τ. However, the two $\cos\omega_n\tau$ terms, corresponding to the 2nd and the 4th term, have the same coefficient and with opposite signs. Thus, they must cancel each other, resulting in $\boldsymbol{\eta = 0}$, implicating that the fractional excitation term $|\omega_n|^s$ is absent in the commensurate dissipative spin chain.

- ***Behavior of Δ***: Before we proceed to analyze the behavior of the gap, let us first elaborate on the reasoning behind putting a gap term in the variational ansatz. The third term in eq. (6.3) is the same term that is responsible for the gap in the Sine-Gordon model. Thus, we can expect it to do the same in the commensurate dissipative case. To calculate the analytical form of Δ, we set $q = \omega_n = 0$ on both sides of eq. (6.3). The 1st and the 2nd term vanish and we obtain a self-consistent equation for the gap:

$$\frac{\Delta^2}{u_r K_r} = \frac{8g}{\pi} e^{-\frac{8}{\pi^2}\int_0^\infty dq' d\omega_{n'} G_{\text{var}}(q',\omega_{n'})} + \frac{4\alpha}{\pi}\int \frac{d\tau}{\tau^{1+s}} e^{-\frac{4}{\pi^2}\int_0^\infty dq' d\omega_{n'} G_{\text{var}}(q',\omega_{n'})(1+\cos\omega_{n'}\tau)} \tag{6.4}$$

Now we can compute the integrals in the exponential functions in eq. (6.4) using $G_{\text{var}} = \pi K_r \left[u_r q^2 + \frac{\Delta^2}{u_r} + \frac{\omega_n^2}{u_r}\right]^{-1}$ (where we have already put $\eta = 0$) to understand the behavior of Δ. Just like before, we integrate out the q' modes, and find:

$$\frac{\Delta^2}{u_r K_r} = \frac{8g}{\pi} e^{-4K_r\int_0^\Lambda \frac{d\omega_{n'}}{\sqrt{\Delta^2+\omega_{n'}^2}}} + \frac{4\alpha}{\pi}\int \frac{d\tau}{\tau^{1+s}} e^{-2K_r\int_0^\Lambda d\omega_{n'}\frac{1+\cos\omega_{n'}\tau}{\sqrt{\Delta^2+\omega_{n'}^2}}} \tag{6.5}$$

Where Λ is a high-energy cut-off. The first integral on the right-hand side was already computed in Section 3.2.2 and it is approximately equal to $\ln(\Lambda/\Delta)$ for small-Δ expansion. Similarly, the second integral produces $\ln(\Lambda/\Delta^2) - \ln\tau - \gamma_E$. Putting all the terms

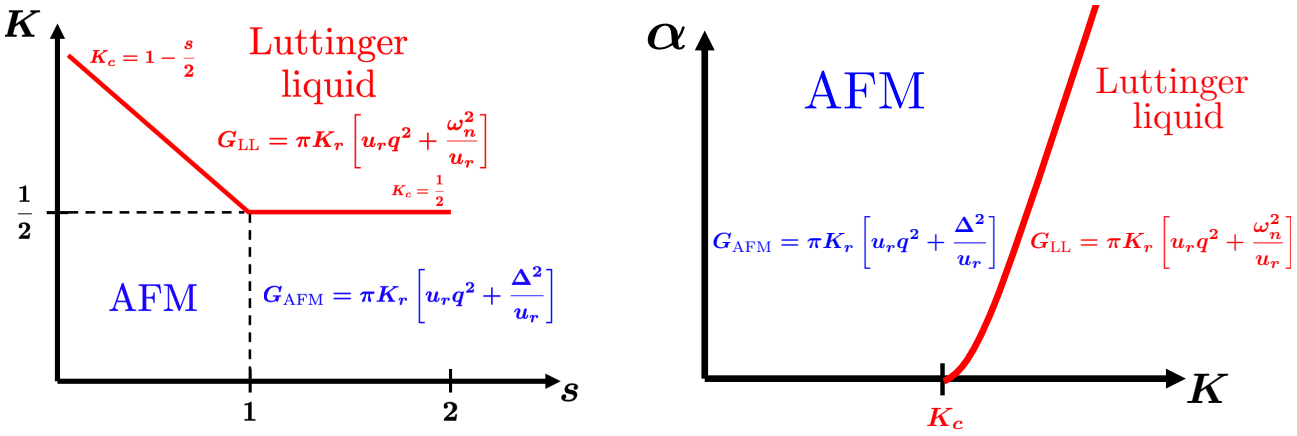

Figure 6.1: Tentative phase diagram for the commensurate dissipative spin chain. *left*: In the $K - s$ plane for small α, the system is in the dissipative phase for $K < K_c = 1 - (s/2)$ for subohmic bath $0 < s < 1$ and for $K < K_c = 1/2$ for ohmic and superohmic bath ($s \geq 1$), and remains in the LL phase for $K \geq K_c$. *right*: For a fixed value of s, the commensurate dissipative spin chain is in the LL phase for $K \geq K_c, \alpha \leq \alpha_c$. For $K < K_c$ or $K > K_c, \alpha > \alpha_c$, the system enters into a gapped antiferromagnetic phase.

together, we find:

$$\cdot \frac{\Delta^2}{u_r K_r} = \frac{8g}{\pi}\left(\frac{\Delta}{\Lambda}\right)^{4K_r} + \frac{4\alpha}{\pi} e^{2K_r\gamma_E}\left(\frac{\Delta^2}{\Lambda}\right)^{2K_r}\int_{\tau_c}^{1/\Delta} d\tau^{2K-1-s}$$

$$\Longrightarrow \boxed{\frac{\Delta^2}{u_r K_r} = \frac{8g}{\pi}\left(\frac{\Delta}{\Lambda}\right)^{4K_r} + \frac{4\alpha}{\pi} e^{2K_r\gamma_E}\left(\frac{\Delta^2}{\Lambda}\right)^{2K_r}\frac{\Delta^{s-2K_r} - \tau_c^{2K_r-s}}{2K_r - s}} \tag{6.6}$$

Where τ_c is the timescale after which the bath behaves as the power law. Eq. (6.6) can be reformulated and simplified as $\mathbf{\Delta^2 \sim a_1 \Delta^{4K_r} a_1 - \frac{a_2}{s-2K_r}\Delta^{4K_r+(s-2K_r)}}$ (I have written the exponents in this form for a better understanding of the discussions in the following paragraphs), where $a_1 = \frac{8g}{\pi\Lambda^{4K_r}} + \frac{4\alpha\tau_c^{2K_r-s}e^{2K_r\gamma_E}}{\pi(s-2K_r)\Lambda^{2K_r}}$ and $a_2 = \frac{4\alpha e^{2K_r\gamma_E}}{\pi\Lambda^{2K_r}}$ are constants smaller than 1. A careful examination of this equation tells us the value of the critical point K_c for small values of α and g.

6.2 Phase diagram

In this section, we analyze the self-consistent equation for the gap Δ (eq. (6.6)) for different types of baths, which lets us sketch out a plausible phase diagram of this system.

- $\mathbf{s - 2K_r > 0}$: When $K_r < s/2$, the right hand side of eq. (6.6) is dominated by the first term with Δ^{4K_r}. In this case, the non-trivial finite solutions for Δ are given by

$\boldsymbol{\Delta \sim a_1^{\frac{1}{2-4K_r}}}$. The form of the exponential tells us that the critical point $\boldsymbol{K_c = 1/2}$ for the phase transition, i.e., Δ is finite only for $K_r < 1/2$. We also understand that for the gapped phase, $2K_r < 1 \implies -2K_r > -1$, hence $\mathbf{1 < s < 2}$ to satisfy the initial condition of $s - 2K_r > 0$. Thus, this solution is valid for superohmic baths.

- $\mathbf{s - 2K_r < 0}$: On the other hand for $K_r > s/2$, $4K_r > 4K_r + (s - 2K_r)$. Thus, the leading term on the right-hand side of eq. (6.6) is $\Delta^{4K_r+(s-2K_r)} = \Delta^{s+2K_r}$. Now, the finite non-trivial solution of Δ is given by $\boldsymbol{\Delta \sim a_2^{\frac{1}{2-s-2K_r}}}$, signifying that $\boldsymbol{K_c = 1 - \frac{s}{2}}$ and Δ is non-zero only for $K_r < K_c$. We also see that in this regime, $s < 2K_r < 2 - s$, and this condition is only satisfied when $\mathbf{0 < s < 1}$. Hence, we understand that this behavior of Δ is satisfied only for subohmic baths.

- $\mathbf{s = 2K_r}$: From the previous two cases, we see that they are continuous and match with each other for $s = 1, K_c = 1/2$, and this corresponds to $s = 2K_r$. However, in this case, the denominator $s - 2K_r$ in eq. (6.6) blows up, leading us to believe that there is a small logarithmic correction for K_c that regulates this divergence. Indeed, expanding the 2nd term as $a^{s-2K_r} \approx 1 + (s - 2K_r) \ln a$ for small $s - 2K$, we find:

$$\begin{aligned} \Delta^2 &\approx g\Delta^{4K_r} + \frac{\alpha\Delta^{4K_r}}{2K_r - s}\left[(1 + (s - 2K_r)\ln\Delta) - (1 + (2K_r - s)\ln\tau_c)\right] \\ &= \Delta^{4K_r}\left(g + 2\alpha \ln \Delta\tau_c\right) \end{aligned} \tag{6.7}$$

  Thus the second term leads to a small logarithmic correction, which needs to be investigated more.

From these results, we understand that in the commensurate case, the dissipative phase is a gapped phase and expect fig. (6.1) to be the tentative phase diagram of the commensurate dissipative system in $K - s$ plane for $\alpha \to 0$ (*left*) and in the $\alpha - K$ plane for a fixed value of s (*right*).

6.3 Numerical Results

With the variational analysis done above, we are currently doing the numerical simulation of the commensurate dissipative spin chain as before. In this section, we show the results for the superohmic bath ($s = 1.5$), $K = 0.75 > K_c = 0.5$ and $g = 1$. For all values of α, we increase L as β. As the symmetric phase of the commensurate action is still LL, we expect the behavior

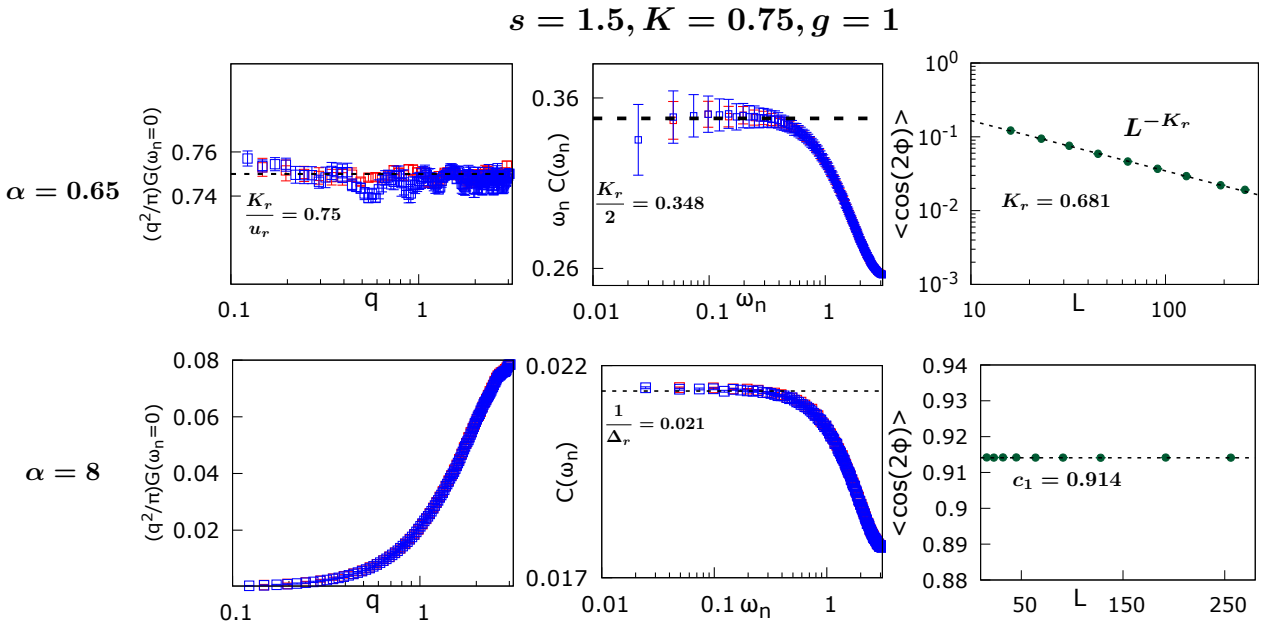

Figure 6.2: Different correlation functions and the order parameter in the commensurate case for superohmic bath ($s = 1.5$) for $\alpha = 0.65$ (*top row*) and $\alpha = 8$ (*bottom row*). The values of the parameters are $K = 0.75$, $g = 1$, and $u = 1$, respectively. *left*: $\pi\chi$ is finite and equal to the initial value 0.75 for $\alpha = 0.65$ and vanishes for $\alpha = 8$. *middle*: For $\alpha = 0.65$, $\omega_n C(\omega_n)$ saturates to $K_r/2 = 0.348$, whereas for $\alpha = 8$, $C(\omega_n)$ saturates to $1/\Delta_r = 0.021$ for small ω_n. *right*: The order parameter $\langle\cos 2\phi\rangle$ decays with size as a power law L^{-K_r} with $K_r = 0.681$ for $\alpha = 0.65$, whereas it remains constant $c_1 = 0.914$ for $\alpha = 8$.

of the correlation functions as we have discussed in Chapter 5. In the upcoming sections, we will show that indeed the dissipative phase in this case is a gapped AFM phase with vanishing susceptibility.

- ***Calculation of χ***: Using the formulations of eq. (5.5), We see that in the dissipative phase:

$$\begin{aligned}\chi_{\text{diss,com}} &= -\frac{qK_r}{\pi}\sum_{q_2,\omega_{n_2}}\frac{q_2}{u_r q^2 + \frac{\omega_n^2}{u_r} + \frac{\Delta^2}{u_r}}\delta_{q_1,-q_2}\delta_{\omega_{n_1},-\omega_{n_2}} \\ &= \frac{K_r}{\pi}\frac{q^2}{u_r q^2 + \frac{\omega_n^2}{u_r} + \frac{\Delta^2}{u_r}} \end{aligned} \tag{6.8}$$

This shows that in the dissipative phase in the thermodynamic limit, $\boldsymbol{\chi(q \to 0, \omega_n \to 0)_{\text{diss,com}} = 0}$. Indeed, it can be observed from eq. (2.2) that the action of the system $S_{\text{tot,C}}$ is not invariant under the statistical tilt symmetry $\nabla\phi \to \nabla\phi + c$, hence χ is not preserved in the dissipative phase, unlike the incommensurate case. From fig. (6.2), *left*, we see that for small α, the susceptibility χ is finite and equal to the bare

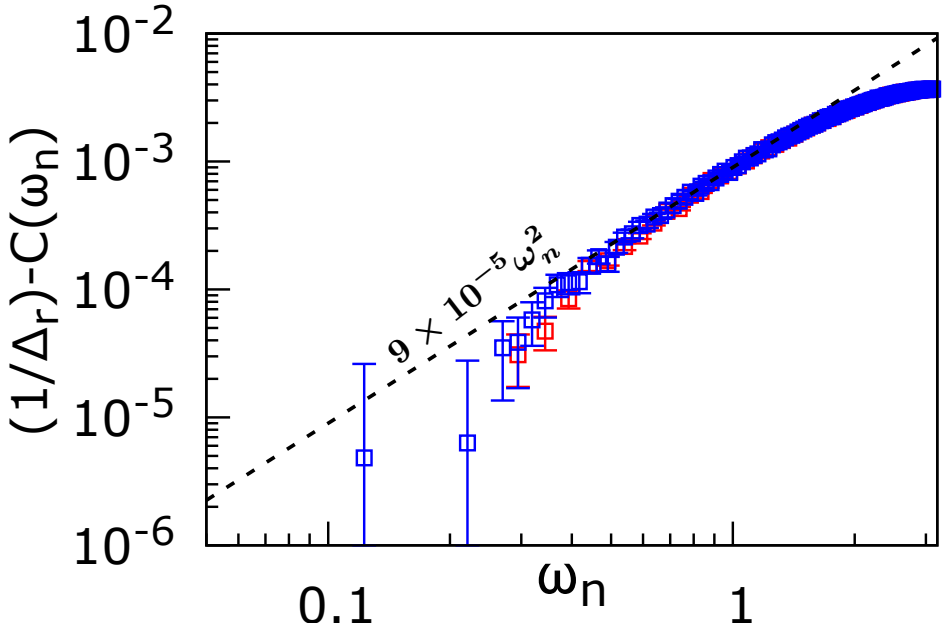

Figure 6.3: $(1/\Delta_r) - C(\omega_n)$ for the dissipative phase ($s = 1.5, K = 0.75, g = 1, \alpha = 8$). This quantity fits well with $9 \times 10^{-5}\omega_n^2$ for small ω_n, which is the sub-leading ω_n dependence of the propagator in the commensurate dissipative phase.

value $K/u = 0.75$, indicating that the system is in the LL phase. However, for $\alpha = 8$, $\chi(q \to 0)$ vanishes rapidly, which corresponds to the dissipative phase.

- ***Calculation of $C(\omega_n)$***: Just like the incommensurate case, one can calculate $C(\omega_n) = \frac{1}{\pi L}\sum_q G(q, \omega_n)$ for the commensurate case as well. In this case, we see that

$$\boxed{C(\omega_n \to 0)_{\text{LL}} = \frac{K_r}{2\omega_n}} \tag{6.9}$$

$$\boxed{C(\omega_n \to 0)_{\text{diss}} = \frac{1}{\Delta_r}} \tag{6.10}$$

where $\Delta_r = 2\Delta/K_r$. Thus, in the commensurate dissipative case, $C(\omega_n)$ itself goes to a constant due to the presence of the gap for small values of ω_n. Indeed, from fig. (6.2), *middle*, we see that for $\alpha = 0.65$, $\omega_n C(\omega_n)$ saturates to a constant $K_r/2$; whereas for $\alpha = 8$, $C(\omega_n)$ plateaus, which is a signature of the dissipative phase having a gap.

We also previously argued that the fractional term $|\omega_n|^s$ is absent in this system. To extract the sub-leading ω_n-dependence, we subtract the constant $1/\Delta_r$ from $C(\omega_n)$. For

small-ω_n, one can see that,

$$\begin{aligned}\frac{1}{\Delta_r} - \frac{K_r}{2\sqrt{\Delta^2+\omega_n^2}} &\approx \frac{1}{\Delta_r} - \frac{K_r}{2\Delta}\left[1 - \frac{1}{2}\left(\frac{\omega_n}{\Delta}\right)^2\right] \\ &= \frac{1}{\Delta_r}\left(\frac{\omega_n}{\Delta}\right)^2\end{aligned}$$

In fig. (6.3), we plot $(1/\Delta_r) - C(\omega_n)$ as a function of ω_n in log-log scale. This quantity, for the small-ω_n range, fits well with ω_n^2, which points to the fact the sub-leading ω_n behavior is indeed ω_n^2 and the fractional laplacian term $|\omega_n|^s$ is absent.

- ***Calculation of*** $\langle \cos 2(\phi - \phi_{CoM})\rangle$: Without calculating explicitly, we expect the order parameter of the phase transition to decrease in the symmetric phase and saturate to a constant in the ordered phase as system size L and β is increased. From fig. (6.2), *right* we expect that for $\alpha = 0.65$, $\langle \cos 2(\phi - \phi_{\rm CoM})\rangle \sim L^{-K_r}$ indeed decreases as a power law, whereas for $\alpha = 8$ it remains constant and finite for all values of L. The value of K_r extracted from the order parameter analysis 0.681 is also quite close to that from the $C(\omega_n)$ analysis 0.696. All this information points towards the fact that in the commensurate case, the dissipative phase is gapped and has vanishing susceptibility.

6.4 Discussion

In this section, we make a couple of remarks regarding the commensurate dissipative phase. Firstly, unlike the incommensurate case, the action of the commensurate case (eq. (2.2)) is invariant under the discrete symmetric transformation $\phi \to \phi + \pi/2$. This is the same symmetry that gets broken in the Sine-Gordon model, leading to a gapped antiferromagnetic case; and one can expect the same scenario to happen in the commensurate dissipative spin chain. But how to draw parallels with the incommensurate system? Putting $q_F = \pi/2a$ in eq. (5.12), we see that in the commensurate case, $\langle \sigma^z(x)\rangle = \sigma_0 + (-1)^j \langle \cos 2\phi\rangle$, where we have assumed the system is described by $x = x_j = aj$ on a discrete lattice. In the dissipative phase, when the $\phi \to \phi + \pi/2$ symmetry is broken, $\langle \cos 2\phi\rangle$ is finite, and the alternatively changing sign $(-1)^j$ signifies the presence of an antiferromagnetic phase.

Physically, one can view the effect of the $\cos(2\phi(\tau) + 2\phi(\tau'))$ term coming from the dissipative bath as an enhancer to the already existing $\cos 4\phi$ term. This can be understood in two ways. Firstly, for $\tau \approx \tau'$, $\cos(2\phi(\tau) + 2\phi(\tau')) \approx \cos 4\phi(\tau)$ is the same as the sine-gordon

term. This claim is also supported by [103], where a 1D XXZ spin chain coupled with optical phonons was studied using bosonization, perturbative RG, and variational ansatz. In the commensurate case, the bosonized action coming from the phonons in their work is given by $\sum_{r=\pm} \iint dx d\tau d\tau' \cos\left[2\left(\phi(x,\tau) - r\phi(x,\tau')\right)\right] D(|\tau-\tau'|)$, where $D(|\tau-\tau'|) \sim e^{-|\tau-\tau'|}$. Even in the absence of the Sine-Gordon term, the existence of a gap was found with the variational analysis of the action as the dissipative kernel $D(|\tau-\tau'|)$ is short-range in this case and the exponential decay restricts the majority of the contribution for $\tau \approx \tau'$, which effectively turns the contribution of the bath into a Sine-Gordon term. Secondly, we can see from eq. (6.6) that Δ depends on $\alpha + g$ and α in the superohmic and the subohmic cases, respectively. This shows that for superohmic baths, α assists g to create the gap; and for subohmic baths, the shifting of K_c away from $1/2$ is solely regulated by the α term.

From our variational analysis, it may initially seem that they don't match with the results from [102] as they reported the variational propagator of the ordered phase to also have the fractional term $|\omega_n|^s$ (fractional with respect to the laplacian). However in their case, the coupling strengths α_1 and α_2 for the two long-range terms, given by $\cos(2\phi(\tau) - 2\phi(\tau'))$ and $\cos(2\phi(\tau)+2\phi(\tau'))$ respectively, are different. Indeed, in that case the coefficient of $|\omega_n|^s$, which is proportional to $\alpha_1 - \alpha_2$, is finite. The dissipative commensurate spin chain is a more special limit of their model where $\alpha_1 = \alpha_2$, and thus the fractional term $|\omega_n|^s$ disappears completely, rendering the system to be a standard antiferromagnetic phase. This is also supported by eq. (32) of [103], where the variational propagator of the system is free of any such fractional laplacian term. Note that the usage of the term 'fractional' here shouldn't be confused with excitations with fractional charges, which can arise from soliton-anti soliton excitations in such systems. Such excitations may be present in the commensurate dissipative spin chain system described here due to the sine-Gordon potential [104, 105] and the variational analysis is unable to capture them. We are also separately investigating the possibility of excitations of such a nature.

Regarding the ongoing work, we are currently in the process of properly quantifying the renormalization of the LL parameters u_r and K_r in both the dissipative phase and the LL phase. This process is much more complicated for the dissipative phase in the incommensurate case and ultimately qualitatively not so interesting, that's why we skipped it in the previous chapters. We are also producing more numerical Langevin simulations for this system in the presence of subohmic and ohmic baths.

Conclusion

The works on the Spin-Boson model by Leggett et al inspired us to extend the results to a generalized description of one-dimensional many-body systems and understand the effect of dissipation on an interacting system. With bosonization, we were able to map the quantum system on a two-dimensional interface, where the dissipation acts as a long-range cosine potential. A perturbative RG analysis of the action shows the existence of a BKT-type critical point, and with the help of the variational method, we predicted the low-energy spectrum of the dissipative phase to be gapless with fractional excitation. We were also able to show the existence of a quantum BKT phase transition as a function of the dissipation strength, the new dissipative phase being a gapless SDW with inhibited conductivity for an incommensurate spin chain and back up our claims with numerical simulation of the Langevin dynamics equation associated to the field theory. Particularly for a subohmic bath, the conductivity completely vanishes, rendering the system into an insulator, which can be interpreted as a dissipation-induced localization in one-dimensional interacting systems. Apart from the ongoing work regarding the commensurate dissipative spin chain, we also have certain extensions in mind that could be interesting to tackle.

A very interesting aspect would be to study the characteristics of the dissipative phase in finite temperature. In the original Spin-Boson model, it was shown that the localized phase can relax (mostly exponentially) depending on the temperature and the nature of the bath [28]. It would be interesting to calculate the conductivity of the incommensurate dissipative phase as a function of frequency at zero temperature and as a function of temperature at finite temperature. In the commensurate case, we suspect the dissipative phase to be a Mott Insulator and its conductivity has been already thoroughly investigated in different temperature and frequency regimes [37]. We believe our approach is prepared to handle this question as bosonization has been used previously to investigate transport properties at finite temperatures on one-dimensional systems connected to semi-infinite non-interacting leads [106, 107].

Another angle that we would like to address in the future is the investigation of the phase transition and signature of localization when the baths are coupled differently to the system. In our work, the baths are connected to the σ^z component of the spin as in the original Caldeira-Leggett work. it would be interesting to analyze the system with the baths being coupled to the σ^x and σ^y components as well, which will be equivalent to coupling to the $\theta(x, \tau)$ fields in the bosonized language. We believe that this scheme can lead to the genesis of the third disordered phase reported in [87].

A different limit of the dissipation, in which case the bath is global (spatially correlated to each other), should be investigated thoroughly. One can also investigate the effect of annealed disorder coming from dissipation on a pre-existing quenched disordered system. For example, previously a study was conducted on the effect of ohmic dissipation on a random-field transverse ising model in [108, 109], where it was shown, using real space RG and SDRG, that dissipation can affect thermodynamic quantities such as susceptibility and specific heat in a strongly disordered model.

Finally, we are interested in understanding the connection between Zeno localization and localization induced by Caldeira-Leggett baths. In the beginning, they seem to be the opposite poles of a spectrum: Measurement acts in a markovian way on the system, whereas the localization induced due to the Caldeira-Leggett baths happens when the dissipation is extremely non-markovian and has a slow time dynamics. However, recently in [110] the authors have studied the entanglement transition in a many-body system in the presence of a non-markovian bath, and their protocol can be used to bridge the gap between these two types of localization by analyzing the quantum dynamics of our system.

Publications

Bath-induced phase transition in a Luttinger liquid

Saptarshi Majumdar,[1,*] Laura Foini,[2] Thierry Giamarchi,[3] and Alberto Rosso[1]
[1]*Université Paris Saclay, CNRS, LPTMS, 91405, Orsay, France*
[2]*IPhT, CNRS, CEA, Université Paris Saclay, 91191 Gif-sur-Yvette, France*
[3]*Department of Quantum Matter Physics, University of Geneva, 24 Quai Ernest-Ansermet, CH-1211 Geneva, Switzerland*

(Received 21 October 2022; revised 9 March 2023; accepted 21 March 2023; published 7 April 2023)

We study an XXZ spin chain, where each spin is coupled to an independent ohmic bath of harmonic oscillators at zero temperature. Using bosonization and numerical techniques, we show the existence of two phases separated by a Kosterlitz-Thouless transition. At low coupling with the bath, the chain remains in a Luttinger liquid (LL) phase with a reduced but finite spin stiffness, while above a critical coupling, the system is in a dissipative phase characterized by a vanishing spin stiffness. We argue that the transport properties are also inhibited: The LL is a perfect conductor, while the dissipative phase displays finite resistivity. Our results show that the effect of the bath can be interpreted as annealed disorder-inducing signatures of localization.

DOI: 10.1103/PhysRevB.107.165113

I. INTRODUCTION

Localization is a spectacular quantum effect in which transport properties are totally suppressed. It is mainly due to the presence of quenched impurities, as predicted by Anderson [1] for free fermions and recently argued to persist in the presence of interactions via the so-called many-body localization (MBL) [2–7]. However, localization can also be induced by quantum measurements or by the presence of an external bath. The first case gives rise to the Zeno effect, originally introduced as the mechanism that froze the dynamics of a two-level system [8,9]. Today, it is generalized to many-body systems in which the frequency of quantum measurement is at the origin of phase transitions from a volume law to an area law for entanglement entropy [10–19]. Localization induced by external bath is much less studied. It is known that a subohmic bath at zero temperature can freeze the quantum dynamics of simple systems, such as a single spin or particle [20–23]. In this paper, we investigate if these mechanisms are also relevant in a many-body system. We show that a bath that produces local phonons is a source of annealed disorder and study how this disorder affects the transport properties. We focus on a one-dimensional (1D) system that can be mapped to a two-dimensional (2D) field theory, already studied by bosonization [24] and Monte Carlo techniques [25] in a different context. However, its phase diagram remains controversial, and it is not clear how many phases appear varying the strength of the coupling between the bath and the system. Here, we introduce an approach which directly simulates the bosonized action and allows us to reach large system sizes. Our results show a simple scenario of two phases with a Kosterlitz-Thouless (KT) transition between them. Increasing the coupling strength, a dissipative phase with suppressed transport takes over a perfectly conducting Luttinger liquid (LL) phase.

*saptarshi.majumdar@universite-paris-saclay.fr

II. MODEL

We consider an XXZ spin chain with the Hamiltonian $H_S = \sum_{j=1}^{N} J_z S_j^z S_{j+1}^z + J_{xy}(S_j^x S_{j+1}^x + S_j^y S_{j+1}^y)$ and $J_z/J_{xy} \in (-1, 1)$. This model displays a gapless low-energy spectrum, and it is in a perfectly conducting phase known as LL [26]. Each spin j of the chain is in contact with its own independent bath of harmonic oscillators with the Hamiltonian $H_B = \sum_{jk} \frac{P_{jk}^2}{2m_k} + \frac{m_k \Omega_k^2}{2} X_{jk}^2$ (see Fig. 1). A different choice for local baths was studied in Ref. [27]. The complete Hamiltonian is given by

$$H = H_S + H_B + H_{SB},$$
$$H_{SB} = \sum_{j=1}^{N} S_j^z \sum_k \lambda_k X_{jk}. \tag{1}$$

Note that the coupling term $h_j(t) = \sum_k \lambda_k X_{jk}$ is equivalent to a time-dependent magnetic field interacting with the spins. The time-independent limit $h_j(t) = h_j$ corresponds to a quenched disordered magnetic field. This case is well studied by bosonization [28] or powerful simulation techniques [29], and a zero temperature localization transition from LL toward a Bose glass phase takes place by varying the disorder strength. Here, we employ bosonization to study the time-dependent (annealed disorder) case. To fully characterize the bath, we need to specify the low-frequency behavior of the spectral function, defined as

$$J(\Omega) = \frac{\pi}{2} \sum_k \left(\frac{\lambda_k^2}{m_k \Omega_k} \right) \delta(\Omega - \Omega_k). \tag{2}$$

In general, one has $J(\Omega) = \pi \alpha \Omega^s$ for $\Omega \in (0, \Omega_D)$. Here, α denotes the effective coupling strength with the bath, the cutoff Ω_D is the Debye frequency, and s sets the nature of the bath. For our study, we take $s = 1$, which corresponds to an ohmic bath.

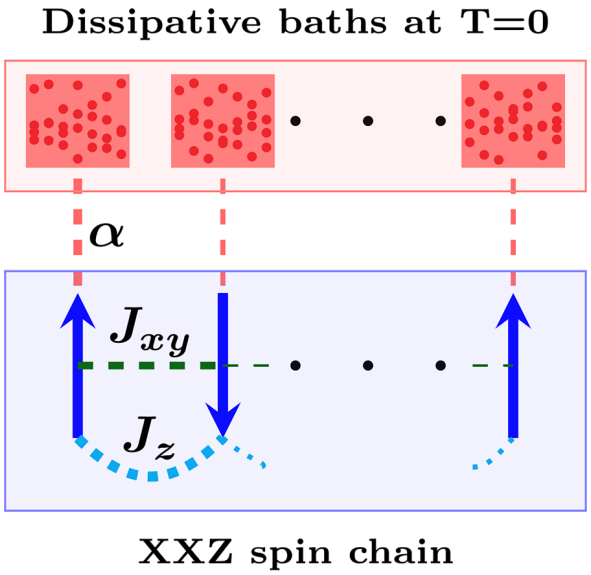

FIG. 1. Schematic representation of the microscopic system: A one-dimensional XXZ spin chain (blue color) with each spin coupled to its individual dissipative bath (red color). The baths are described by a collection of simple harmonic oscillators kept at zero temperature. The parameter α is a measure of the coupling strength between the bath and the associated spin.

III. BOSONIZED ACTION

The bosonization procedure of the XXZ spin chain is well known [26]. We map the chain with periodic condition into a 1D fermionic system using Jordan-Wigner transformation. For $J_z = 0$, we recover the free-fermion problem that can be diagonalized in the momentum space $q = 2\pi l/(Na)$ with a as lattice spacing and $l \in (-N/2, N/2)$. The Fermi momentum depends on the total magnetization M of the spin chain, namely, $q_F = \pi(N - M)/(2Na)$, where q_F is the Fermi momentum of the spin chain and a is the lattice spacing kept for dimensional matching reasons. Two cases should be distinguished: In the zero sector of magnetization, q_F is commensurate with the lattice space, while it is incommensurate for the nonzero magnetization sector. Here, we focus on the incommensurate case. Away from the sector of zero magnetization, by linearizing the spectrum around q_F, one recovers the action for the well-known LL model:

$$S_{\rm LL} = \frac{1}{2\pi}\int dx d\tau \left\{\frac{1}{uK}[\partial_\tau \phi(x,\tau)]^2 + \frac{u}{K}[\partial_x \phi(x,\tau)]^2\right\}. \tag{3}$$

Here, $\phi(x,\tau)$ is a 2D field living in the physical space $x \in (0, L)$ and in imaginary time $\tau \in (0, \beta)$, β being the inverse temperature of the system. At zero magnetization, there is an extra term in the action $S_{\cos} = -\frac{J_z}{2\pi^2}\int dx d\tau \cos[4\phi(x,\tau)]$, which is irrelevant for $K > \frac{1}{2}$. The constants u and K are called LL parameters, and they depend on J_{xy} and J_z. These parameters can be exactly calculated from the Bethe ansatz (e.g., $K^{-1}_{\text{Bethe ansatz}} = (2/\pi)\arccos[-J_z/J_{xy}]$), and they match with the bosonization prediction in the regime $J_z \ll J_{xy}$ ($K^{-1}_{\text{bosonization}} = \sqrt{1 + 4J_z/\pi J_{xy}}$). However, away from half-filling (nonzero magnetization sector), the bosonization prediction between the LL parameters and the spin chain are slightly more complicated and given by $uK = aJ_{xy}\sin(q_F a)$ and $u/K = uK\{1 + \frac{2aJ_z}{\pi v_F}[1 - \cos(2q_F a)]\}$.

To tackle the dissipative problem, there are two different approaches. Here, we map to an equivalent fermionic system via Jordan-Wigner transformation and apply bosonization to arrive at a 2D field theory. Alternatively, the quantum Hamiltonian can be mapped onto a hard-core bosonic system via Holstein-Primakoff transformation and then numerically simulated via quantum Monte Carlo methods (indeed, bosons do not suffer from the sign problem). In both cases, to integrate the bath degrees of freedom, one must introduce the path integral description of the system. The action associated with the bath and the interaction between the bath and the system are identical for bosons and fermions and are given by

$$S_{\rm B} + S_{\rm SB} = \int_0^\beta d\tau \sum_{j=1}^N \left[n_j(\tau) - \frac{1}{2}\right]\sum_k \lambda_k X_{kj} + \sum_{j=1}^N \sum_k \left(m_k \dot{X}_{kj}^2 + \frac{m_k \Omega_k^2}{2} X_{kj}^2\right), \tag{4}$$

where $n_j = S_j^z + \frac{1}{2}$ is the density operator. Now, we can integrate out the bath degrees of freedom and arrive at an effective action for the system degrees of freedom only, where the effect of the bath is encoded in the interacting part $S_{\rm int}$:

$$S_{\rm int} = -\iint_0^\beta d\tau d\tau' \sum_{j=1}^N \left[n_j(\tau) - \frac{1}{2}\right] \times D(\tau - \tau')\left[n_j(\tau') - \frac{1}{2}\right]. \tag{5}$$

Here, $D(\tau - \tau')$ is the dissipative kernel which is produced from integrating over the bath modes. Its Fourier transform can be expressed in terms of the bath spectral function $J(\Omega)$:

$$D(\omega_n) = \frac{2}{\pi}\int_0^\infty J(\Omega)\frac{\Omega}{\omega_n^2 + \Omega^2}. \tag{6}$$

Using the form $J(\Omega) = \pi\alpha\Omega$ ($s = 1$), we get $D(\tau - \tau') \sim \alpha|\tau - \tau'|^{-2}$.

To bosonize Eq. (5), we recall that the bosonized version of S_j^z is given by

$$\hat{S}^z = -\frac{1}{\pi}\nabla\phi + \frac{1}{\pi a}\cos(2\phi - 2q_F x). \tag{7}$$

Using Eq. (5), the dissipative part of the action is given by

$$S_{\rm int} = -\frac{1}{2\pi^2}\int_0^L dx \iint_0^\beta d\tau d\tau' \times \left\{-\nabla\phi(x,\tau) + \frac{1}{a}\cos[2\phi(x,\tau) - 2q_F x]\right\} \times D(\tau - \tau')\left\{-\nabla\phi(x,\tau') + \frac{1}{a}\cos[2\phi(x,\tau') - 2q_F x]\right\}. \tag{8}$$

After multiplying all the terms, one can put $a = 1$, which was there for dimensional purposes. For the expansion, we will be making a few observations here:

(1) At equal time ($\tau = \tau'$), the dissipative action is $(S_j^z)^2$, which is identity. Hence, this term does not contribute anything to the physics, and we can neglect the constant term in $D(\tau - \tau')$.
(2) The terms of the form $\nabla\phi(\tau)\cos[2\phi(\tau') - 2q_F x]$ will oscillate rapidly for nonzero magnetization due to the $2q_F x$ term, and hence, it will integrate to zero. Similarly, the $\cos[2\phi(\tau) - 2q_F x]\cos[2\phi(\tau') - 2q_F x]$ term can be broken up into two terms; one of these terms will be of the form $\cos\{2[\phi(\tau) + \phi(\tau')] - 4q_F x\}$. This term can also be integrated to zero due to the rapidly oscillating term $4q_F x$.
(3) The $\nabla\phi(\tau)\nabla\phi(\tau')$ term is the forward scattering term and is irrelevant by power counting.

Hence, the action of the full system turns out to be

$$S_{\text{tot}} = S_{\text{LL}} + S_{\text{int}}, \tag{9}$$

$$S_{\text{int}} = -\frac{\alpha}{4\pi^2}\int dx d\tau d\tau' \frac{\cos\{2[\phi(x,\tau) - \phi(x,\tau')]\}}{|\tau - \tau'|^2}. \tag{10}$$

IV. OBSERVABLES AND BOSONIZATION

Thermodynamic quantities of the spin chain can be expressed in terms of the correlation functions of the field ϕ. The propagator $G(q,\omega_n) = \langle\phi(q,\omega_n)\phi(-q,-\omega_n)\rangle$ can be related to the susceptibility χ and spin stiffness ρ_s by the two equations:

$$\chi = \lim_{q\to 0}\lim_{\omega_n\to 0}\frac{q^2}{\pi^2}G(q,\omega_n), \tag{11}$$

$$\rho_s = \lim_{\omega_n\to 0}\lim_{q\to 0}\frac{\omega_n^2}{\pi^2}G(q,\omega_n). \tag{12}$$

Here, $\omega_n = 2\pi n/\beta, n \in (-\infty,\infty)$ are the Matsubara frequencies. In the LL phase, $G_{\text{LL}}(q,\omega_n) = \pi K/(\omega_n^2/u + uq^2)$, and hence, $\chi = K/(u\pi)$ and $\rho_s = uK/\pi = K^2/(\pi^2\chi)$. The bath introduces a long-range cosine interaction in the τ direction only, and the strength of this potential is controlled by the parameter α. A perturbative renormalization group study [24] shows that, for $K < K_c = 0.5$, the cosine term is relevant, and the LL phase is destroyed, whereas for $K > K_c$ and small α, the system stays in the LL phase but with renormalized LL parameters K_r and u_r. For $K \gtrsim K_c$, the transition is of the KT type: The critical point $\alpha_c(K)$ is still LL with $K_r = K_c = 0.5$. The nature of the dissipative phase is not clear: For moderate K and very large α, the action should be gapless and harmonic, obtained by the quadratic expansion of the cosine term. For $K \gg K_c$, a large-N argument suggests the existence of a gapped disordered phase. Monte Carlo simulations [25] were performed on the 1D hard-core bosonic chain, which can be mapped to free fermions ($K = 1$). Increasing α, they found that χ increases, and at α_c, the system undergoes a continuous second-order phase transition with vanishing ρ_s. Below, we propose a simple scenario able to conciliate the puzzle of contradictory results.

V. METHODS

To make progress, on one side, we compute the correlation function $G(q,\omega_n)$ numerically by generating equilibrated configurations $\phi(x,\tau)$ from the action in Eq. (9) with the help of Langevin dynamics (see Appendix C). The long-distance, low-energy behavior of this correlation function allows us to classify the system in two possible phases. One possibility is that the system remains in the LL phase with renormalized values of u and K. The second possibility is the appearance of a new dissipative phase, where α becomes relevant. The analytical behavior of $G(q,\omega_n)$ in this new phase was proposed in Ref. [24] using a harmonic expansion around the cosine potential. Here, we use a variational approach and propose an improved expression of the correlation function in the dissipative phase:

$$G_{\text{var}}^{-1}(q,\omega_n) = \frac{u_r q^2}{2\pi K_r} + \frac{\alpha_r}{\pi^2}|\omega_n| + a_1|\omega_n|^{3/2} + a_2\omega_n^2. \tag{13}$$

The macroscopic behavior of this phase depends only on the two parameters u_r/K_r and α_r. The parameters a_1 and a_2 are introduced to account for finite-sized effects. From the analysis of our result, we will show that, by varying α, the long-distance properties are always captured either by the LL or by the variational propagator [Eq. (13)] with renormalized parameters u_r, K_r, and α_r.

A. Variational ansatz

To derive the correlation function of Eq. (13), we need to find an effective quadratic action of the form $S_{\text{var}} = \frac{1}{2\beta L}\sum_{q,\omega_n}\phi^*(q,\omega_n)G_{\text{var}}^{-1}(q,\omega_n)\phi(q,\omega_n)$. We use the variational method: We minimize the free energy $F_{\text{var}} = -\frac{1}{\beta}\sum_{q,\omega_n}\log G_{\text{var}} + \frac{1}{\beta}\langle S - S_{\text{var}}\rangle_{S_{\text{var}}}$ [with $(S - S_{\text{var}})$ averaged over S_{var}] with respect to the variational Green's function:

$$G_{\text{var}}^{-1} = \frac{1}{2\pi K}\left(uq^2 + \frac{\omega_n^2}{u}\right) + \frac{\alpha}{\pi^2}\int d\tau D(\tau)(1 - \cos\omega\tau) \times \exp\left\{\left[-\frac{1}{\pi^2}\int_{-\infty}^{\infty} dq d\omega\, G_{\text{var}}(q,\omega)(1 - \cos\omega\tau)\right]\right\}. \tag{14}$$

We try to solve this self-consistent equation by making the following ansatz: $G_{\text{var}}^{-1}(q,\omega) = \frac{1}{2\pi K}(uq^2 + \frac{\omega_n^2}{u}) + \frac{\alpha}{\pi^2}F(\omega)$, where $F(\omega) = a(\alpha)|\omega|^{\psi} + b(\alpha)|\omega|$. With this assumption, for large τ, the behavior of $G(\omega)$ is governed by the $|\omega|$ term. It can be easily shown that $\int_{\infty}^{\infty} dq d\omega\, G_{\text{var}}(q,\omega)(1 - \cos\omega\tau) \approx C(\alpha) - [\frac{\tau_c(\alpha)}{\tau}]^{1/2}$, where $C(\alpha)$ and $\tau_c(\alpha)$ are α-dependent constants. For a more systematic expansion in powers of $1/\tau$, one can use the results in Ref. [30]. Putting this back into the self-consistent equation for $F(\omega)$, we obtain

$$\begin{aligned} a(\alpha)|\omega|^{\psi} + b(\alpha)|\omega| &= \int d\tau D(\tau)(1 - \cos\omega\tau) \times \exp\left(-\left\{C(\alpha) - \left[\frac{\tau_c(\alpha)}{\tau}\right]^{1/2}\right\}\right) \\ &\overset{\text{large }\tau}{\approx} \int d\tau D(\tau)(1 - \cos\omega\tau) \times e^{-C(\alpha)}\left\{1 + \left[\frac{\tau_c(\alpha)}{\tau}\right]^{1/2}\right\}. \end{aligned} \tag{15}$$

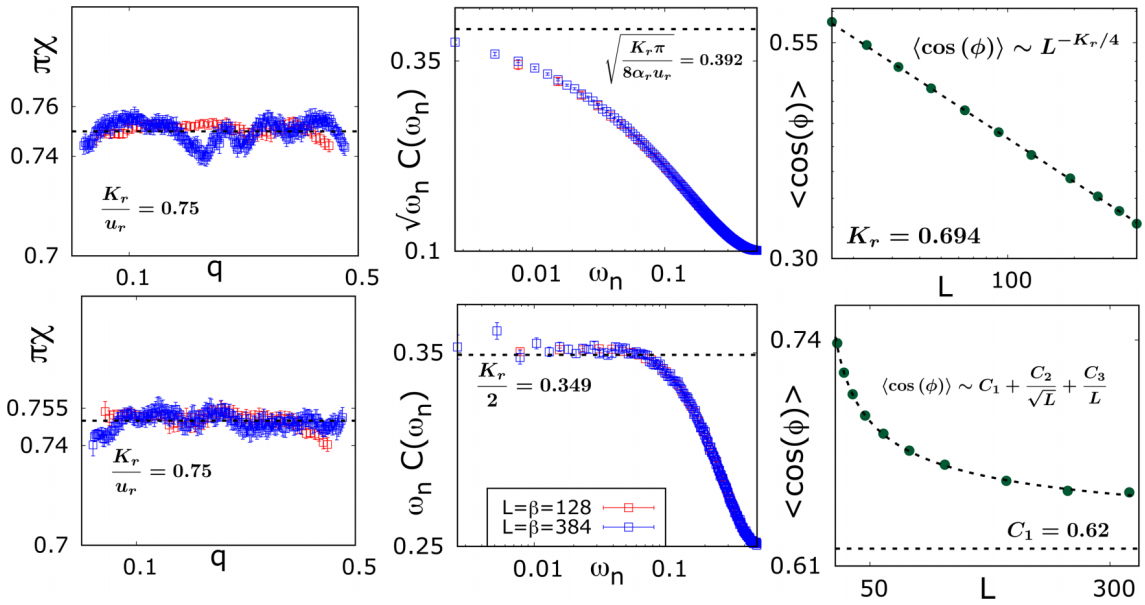

FIG. 2. Calculation of different quantities for $K = 0.75$ that characterizes Luttinger liquid (LL; $\alpha = 1$, top row) and dissipative phase ($\alpha = 8$, bottom row). Blue and red points correspond to $L = \beta = 384$ and 128, respectively. The average is performed over 6000 to 12 000 configurations. (left) Due to symmetry, $\pi\chi = K_r/u_r$ is equal to $K/u = 0.75$ for all values of α and all length scales. (middle) For $\alpha = 1$, $\omega_n C(\omega_n)$ saturates to $K_r/2 = 0.349$ as $\omega_n \to 0$; whereas for $\alpha = 8$, $\sqrt{\omega_n}C(\omega_n)$ saturates to $[K_r\pi/(8\alpha_r u_r)]^{1/2} = 0.392$. The other fitting constants are $a_1 = 0.2493$ and $a_2 = 3.572$. (right) For $\alpha = 1$, $\langle\cos(\phi)\rangle$ decays as a power law, which allows us to extract $K_r = 0.694$, consistent with the fit of $\omega_n C(\omega_n)$. For $\alpha = 8$, it saturates to a constant, as predicted by the variational ansatz (the fit gives $c_1 = 0.62$, $c_2 = 0.603$, and $c_3 = -0.531$).

The ω dependence can be easily extracted from these equations, which turns out to be $|\omega|$ and $|\omega|^{3/2}$. The coefficient of $|\omega|$ should be determined self-consistently, and in our analysis, we take it as a fitting parameter α_r/π^2. The coefficient in front of ω^2 will be renormalized by higher-order terms from variational analysis. Hence, the variational propagator is given at low order in ω by Eq. (13).

VI. RESULTS

A. Phase diagram

In the following, we present our results for the correlation functions of the action $S = S_{\rm int} + S_{\rm LL}$, with $u = 1$, $K = 0.75$, and different α. For our simulations, we set $\beta = L$. The first observation is that the action of Eq. (10) is invariant under tilt transformation (see Appendix B). As a consequence, χ is not affected by the presence of $S_{\rm int}$. We measure K_r/u_r both at low and high α, as shown in Fig. 2, left. Note that the susceptibility corresponds to the $q \to 0$ limit, but due to the symmetry, K_r/u_r is invariant at all length scales and all values of α. We conclude that $K_r/u_r = K/u$ for all values of α. In Fig. 2, middle, we present our results for $C(\omega_n) = (1/\pi L)\sum_q \langle|\phi(q,\omega_n)|^2\rangle = \frac{1}{\pi L}\sum_q G(q,\omega)$. Using the LL and the variational propagator, we find that

$$C(\omega_n \to 0) = \begin{cases} \frac{K_r}{2\omega_n} & \text{LL} \\ \sqrt{\frac{K_r\pi}{8\alpha_r u_r}}\frac{1}{\sqrt{\omega_n}} & \text{variational.} \end{cases} \tag{16}$$

We see that, indeed, for small α, $C(\omega_n)$ behaves as expected for the LL phase, while for large α, $C(\omega_n)$ shows an agreement with the variational approach. To confirm our prediction, we compute an independent quantity, namely, $\langle\cos(\phi)\rangle$. This quantity decreases with a characteristic finite-sized behavior: It goes to zero as $\langle\cos(\phi)\rangle_{\rm LL} \sim L^{-K_r/4}$ in the LL phase and saturates to a constant as $\langle\cos(\phi)\rangle_{\rm var} \sim c_1 + c_2/\sqrt{L} + c_3/L$ within the variational ansatz (here, c_1, c_2, and c_3 are fitting cutoff-dependent parameters, see Appendix A). Figure 2, right, confirms the scenario of a transition between a LL to a dissipative phase described by the variational ansatz. Moreover, the value of K_r extracted from $\langle\cos(\phi)\rangle$ matches nicely with the prediction of $C(\omega_n)$. In Fig. 3, we rationalize our results of the renormalized parameters, obtained by varying α. For $K = 0.75$, we observe that the stiffness decreases with α in the LL phase and vanishes in the critical region $\alpha \in (3, 4)$. Moreover, just before the transition, K_r approaches $K_c = 0.5$ and $\rho_{s_c} = 1/(4\pi^2\chi)$, as predicted by the KT transition. In the Appendix, we provide further results for $u = 1$, $K = 0.55$ (see Fig. 4), which are also in agreement with this picture.

B. Transport properties

With our approach, one can compute thermodynamic quantities without direct access to transport properties. However, via Wick rotation, the conductivity can be related to the propagator:

$$\sigma(\omega) = \frac{e^2}{\pi^2\hbar}[\omega_n G(q=0,\omega_n)]_{i\omega_n\to\omega+i\epsilon}.$$

For LL, the DC conductivity $\sigma_{\rm DC} \equiv {\rm Re}[\sigma(\omega \to 0)] = (e^2 uK/\hbar)\delta(\omega)$, which shows the system is perfectly conducting. For the dissipative phase, we use Eq. (13) for Wick rotation and get $\sigma_{\rm DC} = e^2/\hbar\alpha_r$, proving that the system has finite conductivity. For a generic bath, $G(q=0,\omega_n) \sim 1/(\alpha_r|\omega_n|^s)$,

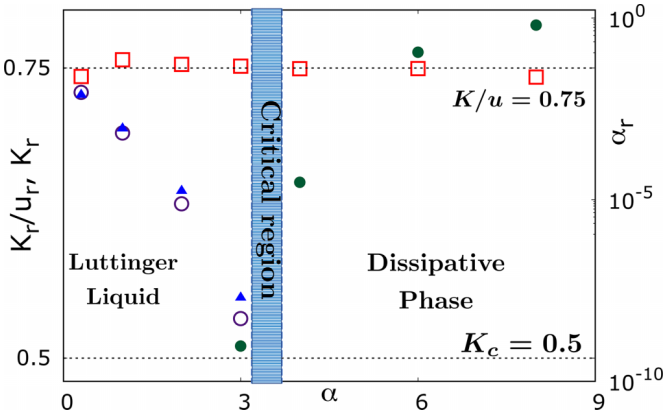

FIG. 3. Behavior of different renormalized parameters as a function of dissipative coupling α. K_r/u_r (red square points) remains constant and equal to $K/u = 0.75$ for all values of α. K_r, extracted from $\langle\cos(\phi)\rangle$ analysis (purple circular points) agrees with the one from the $C(\omega_n)$ analysis (blue triangular points). It approaches $K_c = 0.5$ as α reaches the critical point. The parameter α_r (green circular points) starts to be defined in the dissipative phase and increases rapidly with increase in α. This behavior of the parameter allows us to locate the different phases: For $\alpha < 3$, the system is in Luttinger liquid (LL) phase, whereas for $\alpha > 4$, the system is in dissipative phase. The phase transition takes place for $\alpha \in (3, 4)$.

and hence, $\mathrm{Re}[\sigma(\omega)] = (e^2/\hbar\alpha_r)(\epsilon/(\omega^2+\epsilon^2)^{s/2})$. Especially when the bath is subohmic ($s < 1$), the DC conductivity of the system goes to zero, which is a signature of bath-induced localization in the system.

VII. DISCUSSION AND CONCLUSIONS

It remains important to clarify how to conciliate our observations of a KT transition with $K_c = 0.5$ and the hard-core bosonic Monte Carlo simulations (at $K = 1$ instead of $K = 0.75$) that show a vanishing stiffness at the transition [25]. A possibility is that it is an artifact of the commensurate-incommensurate crossover of the system as the system size, as well as the incommensurate parameter, used in the Monte Carlo study is small. Another possibility remains that our action misses some term that is relevant for the microscopic lattice model.

On a more general framework, many efforts are currently being made to observe localization transition in open quantum systems. The most popular approach is to consider the bath as a perturbative source of quantum measurements. In this Markovian limit, one can rely either on the Lindblad formalism [31], which is microscopically more accurate but is limited to very small system sizes, or introduce models with quantum circuits which display localization transitions but are very simplistic. In both cases, localization appears as a many-body Zeno effect. Here, the bath is non-perturbative and equivalent to annealed disorder. Hence, the localization observed here is a non-Markovian effect, more like the localization due to quenched impurities. It remains an open question to compare the differences of these two kinds of bath-induced localization.

ACKNOWLEDGMENTS

This paper is supported by Investissements d'Avenir LabEx PALM (No. ANR-10-LABX-0039-PALM; EquiDystant project, L. Foini) and is supported in part by the Swiss National Science Foundation under Division II. We thank T. Maimbourg for his involvement in the early stages of the project and for the careful reading of the manuscript. We also thank V. Schimmenti for helpful discussions. This work was granted access to the HPC resources of IDRIS under the allocation 2022-[AD011013581] and HPC resources of TGCC under the allocation 2022-[AD011013555] made by GENCI.

APPENDIX A: SYSTEM SIZE DEPENDENCE OF ORDER PARAMETER

In this section, we find an analytical expression for the quantity $\langle\cos[\phi(x,\tau)]\rangle$, which is equal to $\exp\{-\frac{1}{2}\langle[\phi(\vec{r})]^2\rangle\}$ for Gaussian theories.

For our variational ansatz, we need to calculate

$$\langle\cos[\phi(\vec{r})]\rangle = \exp(S_1) = \exp\left(-\frac{1}{2\beta L}\sum_{q,\omega_n}\frac{1}{\frac{u}{\pi K}q^2 + \frac{2\alpha}{\pi^2}|\omega_n| + 2a_1|\omega_n|^{3/2} + 2a_2\omega_n^2}\right).$$

To calculate the sum inside the exponential, we send the limit of integration over q from zero to infinity and the integral over ω from $1/\beta$ to $1/l_0$, where l_0 is the microscopic cutoff. By doing so, one can find the small ω behavior of the sum as below:

$$S_1 = \frac{1}{4}\sqrt{\frac{K}{\pi u}}\left[\frac{a_1\pi^3}{(2\alpha)^{3/2}l_0} - \frac{2\pi}{\sqrt{2\alpha l_0}}\right] + \sqrt{\frac{\pi K}{8u\alpha}}\frac{1}{\sqrt{\beta}} - \frac{a_1\pi^3}{4}\sqrt{\frac{K}{8u\alpha^3}}\frac{1}{\beta}. \tag{A1}$$

We put this back into the expression of $\langle\cos[\phi(\vec{r})]\rangle$, and from a large β (zero temperature limit) expansion, we obtain the finite-sized dependence of the order parameter:

$$\langle\cos[\phi(\vec{r})]\rangle_{\mathrm{var}} = c_1 + \frac{c_2}{\sqrt{\beta}} + \frac{c_3}{\beta},$$
$$c_1 = \exp\left\{\frac{1}{4}\sqrt{\frac{K}{\pi u}}\left[\frac{a_1\pi^3}{(2a)^{3/2}l_0} - \frac{2\pi}{\sqrt{2\alpha l_0}}\right]\right\},$$
$$c_2 = c_1\sqrt{\frac{\pi K}{8u\alpha}},$$
$$c_3 = c_1\left(\frac{\pi K}{16u\alpha} - \frac{a_1\pi^3}{4}\frac{K}{8u\alpha^3}\right). \tag{A2}$$

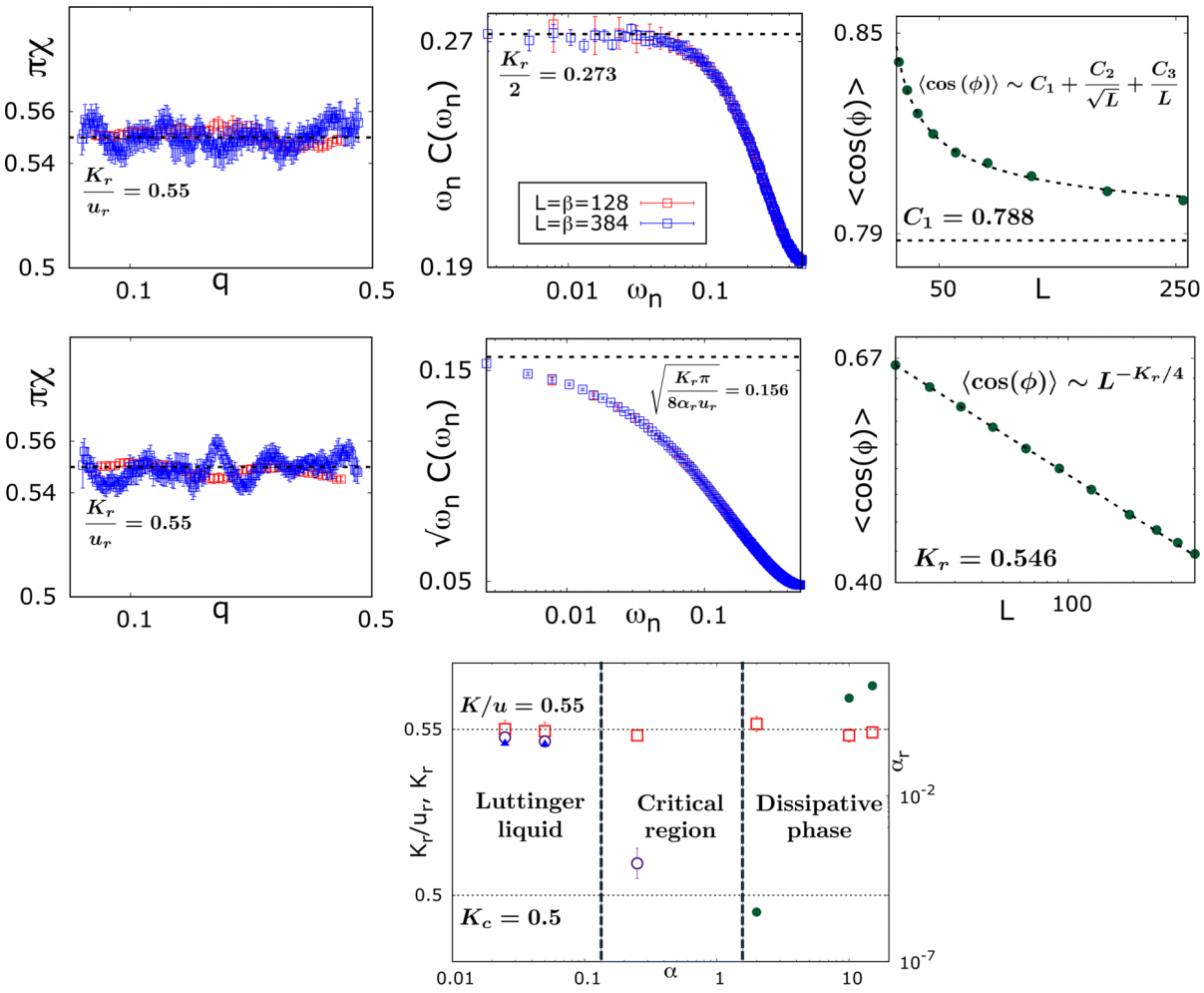

FIG. 4. Calculation of different quantities for $K = 0.55$ that characterizes Luttinger liquid (LL; $\alpha = 0.05$, top row) and dissipative phase ($\alpha = 10$, bottom row). Blue and red points correspond to $L = \beta = 384$ and 128, respectively. (left) Due to symmetry, $\pi\chi = K_r/u_r$ is equal to $K/u = 0.55$ for all values of α and all length scales. (middle) For $\alpha = 0.05$, $\omega_n C(\omega_n)$ saturates to $K_r/2 = 0.273$ as $\omega_n \to 0$; whereas for $\alpha = 10$, $\sqrt{\omega_n} C(\omega_n)$ saturates to $[K_r\pi/(8\alpha_r u_r)]^{1/2} = 0.156$. The other fitting constants are $a_1 = 16.61$ and $a_2 = 571.4$. (right) For $\alpha = 0.05$, $\langle\cos(\phi)\rangle$ decays as a power law, which allows us to extract $K_r = 0.546$, consistent with the fit of $\omega_n C(\omega_n)$. For $\alpha = 10$, it saturates to a constant, as predicted by the variational ansatz (the fit gives $c_1 = 0.788$, $c_2 = 0.215$, and $c_3 = 0.012$). (bottom row) Behavior of different renormalized parameters as a function of dissipative coupling α. K_r/u_r (red square points) remains constant and equal to $K/u = 0.55$ for all values of α. K_r, extracted from $\langle\cos(\phi)\rangle$ analysis (purple circular points) agrees with the one from the $C(\omega)$ analysis (blue triangular points). It approaches $K_c = 0.5$ as α reaches the critical point. The parameter α_r (green circular points) starts to be defined in the dissipative phase and increases rapidly with increase in α. This behavior of the parameter allows us to locate the different phases: For $\alpha < 0.25$, the system is in LL phase, whereas for $\alpha > 2$, the system is in dissipative phase. The phase transition takes place for $\alpha \in (0.25, 2)$. We believe $\alpha = 0.25$ to be in the critical region as K_r extracted from $\langle\cos(\phi)\rangle$ is very close to $K_c = 0.5$, α_r is very small, and $\omega_n C(\omega_n)$ saturates for a long range of ω_n but then starts decreasing.

APPENDIX B: TILT SYMMETRY OF THE ACTION

In this section, we explain why the parameter K/u, which identifies with the susceptibility χ, remains constant for all dissipative coupling α [32,33]. To compute the susceptibility, we introduce a finite magnetic field h in the z direction. Then the susceptibility can be written as $\chi = \frac{\partial^2}{\partial(h\beta)^2}(\ln Z[h])$, where Z is the partition function and β is the inverse temperature of the system. In the bosonized language, the term $-h\sum_j S_j^z$ in the Hamiltonian gives rise to the term $-\frac{h}{\pi}\int[\nabla\phi(x,\tau)]dxd\tau$ in the action. Hence, the partition function of the system can be written as

$$Z[h] = \int \mathcal{D}[\phi]\exp\left\{\left[-S_{\rm LL} - S_{\rm int} + \frac{h}{\pi}\int \nabla\phi(x,\tau)dxd\tau\right]\right\}. \tag{B1}$$

One can rewrite the terms $\frac{u}{2\pi K}(\nabla\phi)^2 - \frac{h}{\pi}\nabla\phi$ as $\frac{u}{2\pi K}(\nabla\phi - \frac{hK}{u})^2 - \frac{h^2K}{2\pi u}$. Introducing the tilt $\tilde{\phi} \to \phi - \frac{hKx}{u}$, the partition function can be rewritten:

$$Z[h] = \int \mathcal{D}[\tilde{\phi}]\exp\left\{\left(-S_{\rm LL}[\tilde{\phi}] - S_{\rm int}[\tilde{\phi}] + \frac{\beta^2h^2K}{2u\pi}\right)\right\}. \tag{B2}$$

The key point is that the interacting action $S_{\rm int}$ is invariant under the tilt transformation $S_{\rm int}(\tilde{\phi} + \frac{hkx}{u}) = S_{\rm int}(\tilde{\phi})$. From the previous equation, it can be easily seen that

$$\ln Z[h] = \frac{\beta^2 h^2 K}{2u\pi} + \ln Z[h=0]. \tag{B3}$$

From this expression, the susceptibility can be easily computed, which is finally given by

$$\chi = \frac{\partial^2}{\partial(\beta h)^2}\frac{\beta^2 h^2 K}{2u\pi} = \frac{K}{u\pi}. \tag{B4}$$

APPENDIX C: NUMERICAL DETAILS

In this section, we describe the numerical procedure for this paper. We denote the discretized two-dimensional field as ϕ_{ij}, where $i \in [1, L]$ and $j \in [1, \beta]$ with periodic boundary conditions in both directions. Our strategy is to start from a flat interface $\phi_{ij} = 0$ at $t = 0$ and then let it evolve according to the Langevin equation [34]:

$$\frac{d\phi_{ij}(t)}{dt} = -\frac{\delta S[\phi_{ij}(t)]}{\delta\phi_{ij}} + \eta_{ij}(t), \tag{C1}$$

where $\eta_{ij}(t)$ is a white noise, specified by the correlations $\langle\eta_{ij}(t)\rangle = 0$ and $\langle\eta_{ij}(t)\eta_{i'j'}(t')\rangle = 2\delta_{i,i'}\delta_{j,j'}\delta(t-t')$. Note that the time t that appears in Eq. (C1) should not be confused with the imaginary time τ. When $t \to \infty$, the surface $\phi_{i,j}(t)$ obtained by direct integration of Eq. (C1) is equilibrated with the action $S[\phi]$. Hence, the Langevin equation, which we numerically simulate, is given by

$$\begin{aligned}\frac{d\phi_{ij}(t)}{dt} &= \frac{\alpha}{\pi^2}\sum_{j'} D(|j-j'|)\sin[2(\phi_{ij'} - \phi_{ij})] \\ &+ \frac{1}{uK\pi}[\phi_{i,j+1} + \phi_{i,j-1} - 2\phi_{i,j}] \\ &+ \frac{u}{K\pi}[\phi_{i+1,j} + \phi_{i-1,j} - 2\phi_{i,j}] + \eta_{ij}(t).\end{aligned} \tag{C2}$$

To obtain a correct discretization of the long-range kernel $D(j-j')$, we use the same protocol as in Ref. [35]. For $\beta \to \infty$, we set

$$\begin{aligned}D(j-j') &= \int_0^{2\pi}\frac{d\omega}{2\pi}\exp[i\omega(j-j')]\{2[1-\cos(\omega)]\}^{1/2} \\ &= \frac{1}{(j-j')^2 - \frac{1}{4}}.\end{aligned}$$

At finite β, the periodic boundary conditions are implemented as

$$D(j-j') = \sum_{k=-\beta/2}^{\beta/2}\frac{1}{(|j-j'| + k\beta)^2 - \frac{1}{4}}. \tag{C3}$$

To conclude, we remark that, in the numerical integration, the term $\frac{\delta S[\phi_{ij}(t)]}{\delta(\phi)}$ is multiplied by Δt, whereas $\eta_{ij}(t)$ is multiplied by $\sqrt{\Delta t}$. Here, we use the stochastic second-order Runge-Kutta algorithm for white noise [34]. Using this is preferable, as this is much faster than the standard Euler's algorithm. We choose the value of the Langevin time step $\Delta t = 0.05$. To benchmark the equilibration time of the surface, we used the harmonic approximation $\sin[2(\phi_{ij'} - \phi_{ij})] \to 2(\phi_{ij'} - \phi_{ij})$ that can be analytically solved.

[1] P. W. Anderson, Absence of diffusion in certain random lattices, Phys. Rev. **109**, 1492 (1958).

[2] D. M. Basko, I. L. Aleiner, and B. L. Altshuler, Metal–insulator transition in a weakly interacting many-electron system with localized single-particle states, Ann. Phys. **321**, 1126 (2006).

[3] V. Ros, M. Müller, and A. Scardicchio, Integrals of motion in the many-body localized phase, Nucl. Phys. B **891**, 420 (2015).

[4] B. L. Altshuler, Y. Gefen, A. Kamenev, and L. S. Levitov, Quasiparticle Lifetime in a Finite System: A Nonperturbative Approach, Phys. Rev. Lett. **78**, 2803 (1997).

[5] R. Nandkishore and D. A. Huse, Many-body localization and thermalization in quantum statistical mechanics, Annu. Rev. Condens. Matter Phys. **6**, 15 (2015).

[6] F. Alet and N. Laflorencie, Many-body localization: An introduction and selected topics, C. R. Phys. **19**, 498 (2018).

[7] D. A. Abanin, E. Altman, I. Bloch, and M. Serbyn, Colloquium: Many-body localization, thermalization, and entanglement, Rev. Mod. Phys. **91**, 021001 (2019).

[8] B. Misra and E. C. G. Sudarshan, The Zeno's paradox in quantum theory, J. Math. Phys. **18**, 756 (1977).

[9] W. M. Itano, D. J. Heinzen, J. J. Bollinger, and D. J. Wineland, Quantum Zeno effect, Phys. Rev. A **41**, 2295 (1990).

[10] Y. Li, X. Chen, and M. P. A. Fisher, Quantum Zeno effect and the many-body entanglement transition, Phys. Rev. B **98**, 205136 (2018).

[11] A. Chan, R. M. Nandkishore, M. Pretko, and G. Smith, Unitary-projective entanglement dynamics, Phys. Rev. B **99**, 224307 (2019).

[12] B. Skinner, J. Ruhman, and A. Nahum, Measurement-Induced Phase Transitions in the Dynamics of Entanglement, Phys. Rev. X **9**, 031009 (2019).

[13] M. Szyniszewski, A. Romito, and H. Schomerus, Entanglement transition from variable-strength weak measurements, Phys. Rev. B **100**, 064204 (2019).

[14] X. Turkeshi, R. Fazio, and M. Dalmonte, Measurement-induced criticality in (2 + 1)-dimensional hybrid quantum circuits, Phys. Rev. B **102**, 014315 (2020).

[15] C.-M. Jian, Y.-Z. You, R. Vasseur, and A. W. W. Ludwig, Measurement-induced criticality in random quantum circuits, Phys. Rev. B **101**, 104302 (2020).

[16] A. Zabalo, M. J. Gullans, J. H. Wilson, S. Gopalakrishnan, D. A. Huse, and J. H. Pixley, Critical properties of the measurement-

induced transition in random quantum circuits, Phys. Rev. B **101**, 060301(R) (2020).
[17] Y. Bao, S. Choi, and E. Altman, Theory of the phase transition in random unitary circuits with measurements, Phys. Rev. B **101**, 104301 (2020).
[18] X. Cao, A. Tilloy, and A. D. Luca, Entanglement in a fermion chain under continuous monitoring, SciPost Phys. **7**, 024 (2019).
[19] L. Zhang, J. A. Reyes, S. Kourtis, C. Chamon, E. R. Mucciolo, and A. E. Ruckenstein, Nonuniversal entanglement level statistics in projection-driven quantum circuits, Phys. Rev. B **101**, 235104 (2020).
[20] A. J. Bray and M. A. Moore, Influence of Dissipation on Quantum Coherence, Phys. Rev. Lett. **49**, 1545 (1982).
[21] S. Chakravarty, Quantum Fluctuations in the Tunneling between Superconductors, Phys. Rev. Lett. **49**, 681 (1982).
[22] A. Schmid, Diffusion and Localization in a Dissipative Quantum System, Phys. Rev. Lett. **51**, 1506 (1983).
[23] A. J. Leggett, S. Chakravarty, A. T. Dorsey, M. P. A. Fisher, A. Garg, and W. Zwerger, Dynamics of the dissipative two-state system, Rev. Mod. Phys. **59**, 1 (1987).
[24] M. A. Cazalilla, F. Sols, and F. Guinea, Dissipation-Driven Quantum Phase Transitions in a Tomonaga-Luttinger Liquid Electrostatically Coupled to a Metallic Gate, Phys. Rev. Lett. **97**, 076401 (2006).
[25] Z. Cai, U. Schollwöck, and L. Pollet, Identifying a Bath-Induced Bose Liquid in Interacting Spin-Boson Models, Phys. Rev. Lett. **113**, 260403 (2014).
[26] T. Giamarchi, *Quantum Physics in One Dimension* (Oxford University Press, New York, 2004).
[27] A. M. Lobos, M. A. Cazalilla, and P. Chudzinski, Magnetic phases in the one-dimensional Kondo chain on a metallic surface, Phys. Rev. B **86**, 035455 (2012).
[28] T. Giamarchi and H. J. Schulz, Localization and interaction in one-dimensional quantum fluids, Europhys. Lett. **3**, 1287 (1987).
[29] E. V. H. Doggen, G. Lemarié, S. Capponi, and N. Laflorencie, Weak- versus strong-disorder superfluid—Bose glass transition in one dimension, Phys. Rev. B **96**, 180202(R) (2017).
[30] R. Santachiara, A. Rosso, and W. Krauth, Universal width distributions in non-Markovian gaussian processes, J. Stat. Mech. (2007) P02009.
[31] T. Maimbourg, D. M. Basko, M. Holzmann, and A. Rosso, Bath-Induced Zeno Localization in Driven Many-Body Quantum Systems, Phys. Rev. Lett. **126**, 120603 (2021).
[32] E. Agoritsas, V. Lecomte, and T. Giamarchi, Temperature-induced crossovers in the static roughness of a one-dimensional interface, Phys. Rev. B **82**, 184207 (2010).
[33] M. Mézard, On the glassy nature of random directed polymers in two dimensions, J. Phys. France **51**, 1831 (1990).
[34] R. L. Honeycutt, Stochastic Runge-Kutta algorithms. I. White noise, Phys. Rev. A **45**, 600 (1992).
[35] A. Zoia, A. Rosso, and M. Kardar, Fractional Laplacian in bounded domains, Phys. Rev. E **76**, 021116 (2007).

Localization induced by spatially uncorrelated subohmic baths in one dimension

Saptarshi Majumdar,[1] Laura Foini,[2] Thierry Giamarchi,[3] and Alberto Rosso[1]

[1] *Université Paris Saclay, CNRS,LPTMS, 91405, Orsay, France*
[2] *IPhT, CNRS, CEA, Université Paris Saclay, 91191 Gif-sur-Yvette, France*
[3] *Department of Quantum Matter Physics, University of Geneva, 24 Quai Ernest-Ansermet, CH-1211 Geneva, Switzerland*

(Dated: July 18, 2023)

We study an incommensurate XXZ spin chain coupled to a collection of local harmonic baths. At zero temperature, by varying the strength of the coupling to the bath the chain undergoes a quantum phase transition between a Luttinger liquid phase and a spin density wave (SDW). As opposed to the standard mechanism, the SDW emerges in the absence of the opening of a gap, but it is due to "fractional excitations" induced by the bath. We also show, by computing the DC conductivity, that the system is insulating in the presence of a subohmic bath. We interpret this phenomenon as localization induced by the bath à la Caldeira and Leggett.

I. INTRODUCTION

Open quantum systems, namely systems coupled with external degrees of freedom, are often studied in order to understand the phenomenon of decoherence and the emergence of classical laws from a quantum mechanical description. A common setup is to consider the Markovian dynamics of quantum systems subject to repeated measurements [1, 2]. One of the most intriguing results is the possibility to observe a phase transition in the behavior of the quantum trajectories. The transition is controlled by the measurement rate: For a low rate the entanglement grows linearly in time while at a high measurement rate, it saturates at a finite value [3–12]. Another important setup is to consider the effect of a thermal bath on the system. Following the pioneering works [13–16], we expect that a slow bath (i.e. subohmic and ohmic) can induce localization in simple systems, such as a particle or a spin. Note that this dynamical transition cannot be described by a Lindblad equation [17]. Indeed, in order to capture this localization phenomenon it is crucial to relax the Markovian assumption which is behind the Lindblad equation. Moreover from several variational studies of the ground state of the spin-boson model (namely, the Caldeira Leggett model for a single spin), a genuine thermodynamic transition has been shown to exist for strongly coupled subohmic bath [18, 19].

In this work, we investigate the possibility of such non-Markovian transition in many body systems. In particular, we focus on a one-dimensional (macroscopic) interacting and incommensurate spin chain coupled to *local* baths of harmonic oscillators (fig. 1). This problem was studied in [20] with a special focus on the ohmic case. Here we generalize the study to the superohmic and subohmic case, with particular emphasis on the nature of the dissipative phase both for thermodynamic and transport properties. In particular, we show that the dissipative phase is an incommensurate spin density wave of period π/q_F, where q_F is the Fermi momentum of the system. Unlike the Peierls scenario [21], this spin density wave emerges in the absence of the opening of a gap, but it is due to "fractional excitations" induced by the slow varying bath. The spin density wave order is not only particular to subohmic baths, but also survives in the presence of superohmic baths described by an exponent $s < 2$. However, for subohmic bath, i.e. $s < 1$, the environment can induce "localization" with a gapless insulating phase. The nature and the details of these "fractional" dissipative phases are derived by studying the bosonized action with a thorough variational approach and tested with respect to the exact action with numerical simulations for the subohmic case ($s = 0.5$).

The metal-insulator transition for subohmic baths is reminiscent of the (zero temperature) localization transition which occurs in interacting one-dimensional systems due to the presence of quenched disorder [22, 23]. Indeed, local baths can be thought of as spatially uncorrelated annealed disorder. In the dissipative phase, the degrees of freedom of the system and those of the bath optimize collectively to find a low energy configuration [24].

We also describe the finite size and finite temperature effects. At finite temperature, the order parameter vanishes but the spin density wave can be observed from correlation functions below a length scale which grows as β, where β is the inverse temperature of the system. For finite system size (and zero temperature) the order parameter vanishes for

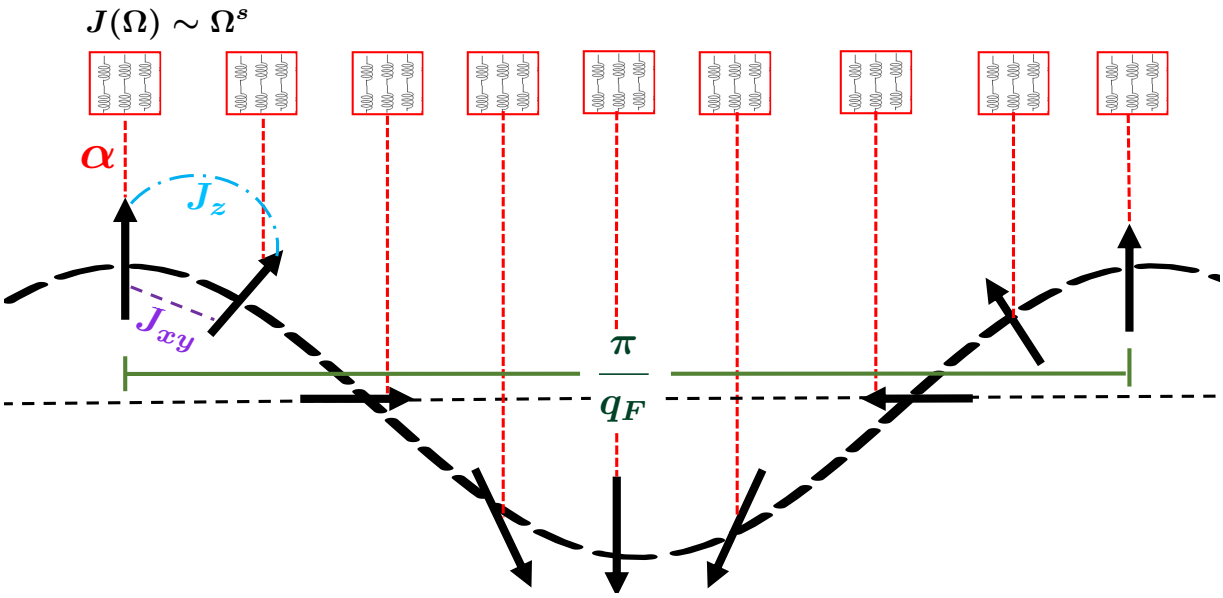

FIG. 1. Schematic diagram of a one-dimensional quantum XXZ spin chain coupled with local dissipative baths. J_{xy} denotes the hopping energy and J_z is the interaction between the two nearest neighbour spins. The baths are characterized by their spectral function $J(\Omega) \sim \alpha\Omega^s$. At zero temperature, the baths induce an SDW phase with periodicity π/q_F, where q_F is the Fermi-momentum related to the magnetization of the chain (see text).

$s > 1$ and one recovers the phase transition that occurs for the spin-boson model with for subohmic baths [19].

The manuscript is organized as follows: in Section II we introduce the model. The analytical variational solution of the model is described in Section III. Section IV consists of detailed discussions about the nature of the order parameter and the dissipative phase, followed by the comparison of the analytical solution obtained with the variational ansatz with exact numerical simulation; in Section V. In Section VI, we discuss the transport properties of the model, and in Section VII we conclude about the nature of the dissipative phase and the absence of linear response transport in the system.

II. MODEL

We investigate the zero-temperature low-energy phase diagram of an incommensurate XXZ spin chain in the presence of local subohmic baths. The Hamiltonian of the system is given by:

$$\begin{aligned} H &= H_{\rm S} + H_{\rm B} + H_{\rm SB} \\ H_{\rm S} &= \sum_{j=1}^{L} J_z \sigma_j^z \sigma_{j+1}^z + J_{xy}\left(\sigma_j^x \sigma_{j+1}^x + \sigma_j^y \sigma_{j+1}^y\right) + h\sigma_j^z \\ H_{\rm B} &= \sum_{jk} \frac{P_{jk}^2}{2m_k} + \frac{m_k \Omega_k^2}{2} X_{jk}^2 \\ H_{\rm SB} &= \sum_{j=1}^{N} \sigma_j^z \sum_k \lambda_k X_{jk} \end{aligned} \tag{1}$$

The dissipative baths are characterized by their spectral function $J(\Omega) \equiv \frac{\pi}{2}\sum_k (\lambda_k^2/m_k\Omega_k)\delta(\Omega - \Omega_k) = \pi\alpha\Omega^s$. In one dimension, XXZ spin chain is a general description of an interacting many-body system as it can be mapped onto spinless Fermionic chain and hard-core Bosonic chain via Jordan-Wigner [25] and Holstein-Primakoff transformation [26] respectively. Its phase diagram is well known; particularly, at zero temperature and in finite magnetization sector ($h \neq 0$), one can use bosonization to arrive at the so-called Luttinger Liq-

uid (LL) action [27]:

$$S_{\rm LL} = \frac{1}{2\pi K}\int dx d\tau \left[\frac{1}{u}(\partial_\tau \phi(x,\tau))^2 + u(\partial_x \phi(x,\tau))^2\right] \tag{2}$$

where $\phi(x,\tau)$ is a bosonic field defined in the two-dimensional space of position $x \in (0, L)$ and imaginary time $\tau \in (0, \beta)$, β being the inverse temperature of the system. u is the speed of sound, K is called Luttinger parameter and depends on the values of J_z and $J_{\rm xy}$. The contribution coming from the magnetic field, given by $-\frac{h}{\pi}\int \partial_x \phi$ in the bosonic language, can be absorbed into the action by using a tilt transformation $\phi \to \phi - hKx/u$. In this case, the Fermi momentum of the system $q_F = \pi(1-(M/N))/2a$ is incommensurate with the lattice spacing, hence we refer to the system as 'incommensurate spin chain'. Here N is the total number of spins, M is the total magnetization of the chain and a is the lattice spacing. This action is known to describe a metallic, perfectly conducting, and gapless phase.

To analyze the effect of the bath on the spin chain, we apply bosonization to map the σ_j^z operator onto the bosonic fields ϕ [27]:

$$\sigma^z(x) = \frac{1}{\pi}\left(-\nabla\phi + \frac{1}{a}\cos\left(2\phi(x) - 2q_F x\right)\right) \tag{3}$$

Then we integrate out the bath degrees of freedom to arrive at an effective field theory (more details can be found in Sec. III, [20]):

$$\begin{aligned} S_{\rm eff} &= S_{\rm LL} + S_{\rm diss} \qquad (4)\\ S_{\rm diss} &= -\frac{\alpha}{4\pi^2}\int dx d\tau d\tau' \frac{\cos\left(2\left(\phi(x,\tau) - \phi(x,\tau')\right)\right)}{|\tau-\tau'|^{1+s}} \end{aligned}$$

The local dissipative baths introduce a long-range cosine potential acting only along the τ direction, which can break symmetry and induce phase transition on the existing LL phase [28, 29]. A similar problem but with a single degree of freedom (particle) was shown to lead to phase transitions as a function of the exponent s [30, 31]. In the subsequent sections, we show that the ordered dissipative phase is described by an SDW of the form:

$$\langle \sigma^z(x)\rangle = \sigma_0 + \sigma_1 \cos(2q_F x) \tag{5}$$

Here σ_0 is the magnetization per spin $\sigma_0 = M/N$, while σ_1 is the amplitude of the SDW, which is the order parameter of the transition.

III. VARIATIONAL ANSATZ

The action from eq. (4) can't be exactly solved due to the presence of the cosine term. One can estimate the critical properties of the action using a perturbative RG method [32] (see also Appendix B). However, here we rely on the variational method [33] to describe the nature of the different phases: We find the best quadratic action $S_{\rm var} = \frac{1}{2\pi\beta L}\sum_{q,\omega_n} \phi^*(q,\omega_n) G_{\rm var}^{-1}(q,\omega_n)\phi(q,\omega_n)$ that describes the original action effectively at zero temperature. One can write the free energy of the original system as $F_{\rm eff} = T\log Z_{\rm eff} = F_0 - T\log\left[\langle \exp(S_{\rm eff} - S_{\rm var})\rangle_{S_{\rm var}}\right]$, where $F_0 = -T\ln Z_{\rm var}$, $Z_{\rm eff}$ is the exact partition function of the action that one wants to study and T is the temperature of the system. Now, we define a variational free energy $F_{\rm var} = -\frac{1}{\beta}\sum_{q,\omega_n}\log G(q,\omega_n) + \frac{1}{\beta}\langle S_{\rm eff} - S_{\rm var}\rangle_{S_{\rm var}}$. Due to the inequality $\langle\exp(-(S_{\rm eff} - S_{\rm var}))\rangle > \exp(-\langle(S_{\rm eff} - S_{\rm var})\rangle)$, it can be easily observed that $F_{\rm var} \geq F_{\rm eff}$. Hence, we minimize $F_{\rm var}$ with respect to the variational propagator by setting $\frac{\partial F_{\rm var}}{\partial G_{\rm var}} = 0$ to obtain a quadratic propagator that describes the system effectively. Applying this protocol to the action eq. (4), we find a self-consistent equation for $G_{\rm var}^{-1}$:

$$\begin{aligned} G_{\rm var}^{-1} = \frac{1}{\pi K}\left(uq^2 + \frac{\omega_n^2}{u}\right) + \frac{\alpha}{\pi^2}\int_{\tau_c}^{\infty} d\tau \frac{1-\cos\omega_n\tau}{\tau^{s+1}} \\ \times \exp\left(-\frac{4}{\pi^2}\int_0^\infty dq' d\omega_{n'}\; G_{\rm var}\left(1-\cos\omega_{n'}\tau\right)\right) \end{aligned} \tag{6}$$

Where τ_c is the time-scale after which the bath displays the power-law behavior. In the next two subsections, we describe the analytical solution of this self-consistent equation. In the third subsection, we provide numerical evidence that supports this solution.

A. Dissipative phase

We first observe that the dissipative phase is gapless. Namely, for $q = \omega_n = 0$, from eq. (6), we get $\Delta \equiv G_{\rm var}^{-1}(q=0,\omega_n=0) = 0$. Secondly, since $S_{\rm diss}$ is invariant under a tilt transformation $\phi \to \phi - \frac{h\phi x}{\pi}$, the susceptibility is not affected by the potential, namely $\chi = \lim_{q\to 0}\lim_{\omega_n\to 0}(q^2/\pi^2)G(q,\omega_n) = K/(u\pi)$ (See also Appendix B in [20]). Hence, to

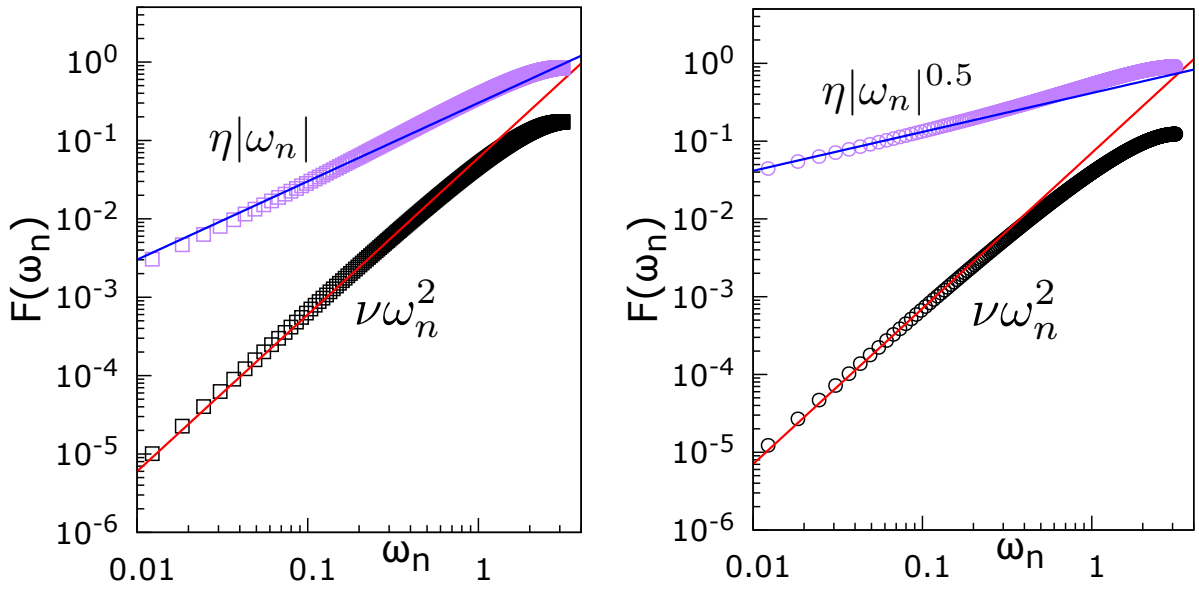

FIG. 2. $F(\omega_n)$ for ohmic ($s = 1$, *left*) and subohmic ($s = 0.5$, *right*) bath obtained by numerical solution of Eq. (12) (with $\beta = 1024$ and $\alpha = 5$). In the dissipative phase, $F(\omega_n)$ behaves as $0.301|\omega_n|$ (purple square points) for ohmic ($K = 0.15$) and $0.415\sqrt{|\omega_n|}$ for (purple circular points) subohmic bath ($K = 0.3$). In the LL phase, $F(\omega_n) = 0.06\omega_n^2$ for ohmic bath (black square points) and $F(\omega_n) = 0.054\omega_n^2$ for subohmic bath ($K = 1$) (black circular points).

solve this self-consistent equation, we assume that:

$$G_{\rm var}^{-1}(q,\omega_n) = \frac{1}{\pi K}\left(uq^2 + \frac{\omega_n^2}{u} + \frac{F(\omega_n)}{u}\right) \qquad (7)$$

where in the small ω_n limit, $F(\omega_n) = \eta(\alpha)\,|\omega_n|^{\psi_1} + a(\alpha)\,|\omega_n|^{\psi_2}$. We determine these parameters in the small ω_n limit.

Determination of ψ_1: Using this form of the propagator, it can be easily seen that at large τ limit, one has $\int_{-\infty}^{\infty} dq' d\omega_{n'} G_{\rm var}(q',\omega_{n'})\,(1-\cos\omega_{n'}\tau) \approx C(\alpha) - \left(\frac{\zeta_\tau(\alpha)}{\tau}\right)^{1-\frac{\psi_1}{2}}$, where $C(\alpha)$ and $\zeta_\tau(\alpha)$ are α-dependent constants. Using this, we obtain:

$$\eta(\alpha)\,|\omega_n|^{\psi_1} + a(\alpha)\,|\omega_n|^{\psi_2} \overset{\text{large }\tau}{\approx} \int d\tau \frac{(1-\cos\omega_n\tau)}{\tau^{s+1}}\left(1 + \left(\frac{\zeta_\tau(\alpha)}{\tau}\right)^{1-\frac{\psi_1}{2}}\right) \qquad (8)$$

From power counting of both sides, we find out that $\psi_1 = s$ and $\psi_2 = 1 + \frac{s}{2}$. Note that ψ_2 is sub-leading for $s > 0$.

Determination of η: The behavior of the coefficient of $|\omega_n|^s$ ($\eta(\alpha)$) is important to locate the transition point between the LL and the dissipative phase. It can be estimated from the variational method. Indeed, neglecting the subleading term, we get $G_{\rm var}^{-1}(q,\omega_n) = \frac{1}{\pi K}\left(uq^2 + \frac{\omega_n^2}{u} + \frac{\eta}{u}|\omega_n|^s\right)$. Using this form of the propagator, it can be easily seen that $\int_0^\infty dq \int_0^\Lambda d\omega_n\; G_{\rm var}(q,\omega_n) \approx \frac{2K}{2-s}\log\frac{4\Lambda^{2-s}}{\eta}$, where Λ is an ultraviolet cut-off. Plugging this result in eq. (6), we obtain:

$$\frac{\eta\omega_n^s}{uK} \overset{\text{small }\omega_n}{\approx} \alpha'\left(\frac{\eta}{\Lambda'^{2-s}}\right)^{\frac{2K}{2-s}}\omega_n^s \qquad (9)$$

Where α' depends on α, s and Λ, and $\Lambda' = 4^{\frac{1}{2-s}}\Lambda$. Comparing the coefficient of ω_n^s on both sides, we see that there is a critical point at $K_c = 1 - \frac{s}{2}$ where η goes to zero. For $K < K_c$, the solution reads:

$$\eta = \left[\alpha' uK\Lambda'^{-2K}\right]^{\frac{2-s}{2-s-2K}} \qquad (10)$$

B. LL phase

To calculate the (eventual) renormalization of the coefficient of ω_n^2 in the LL phase we consider that $F(\omega_n) = \nu\omega_n^2$. We assume that the correction coming from ν is small compared to

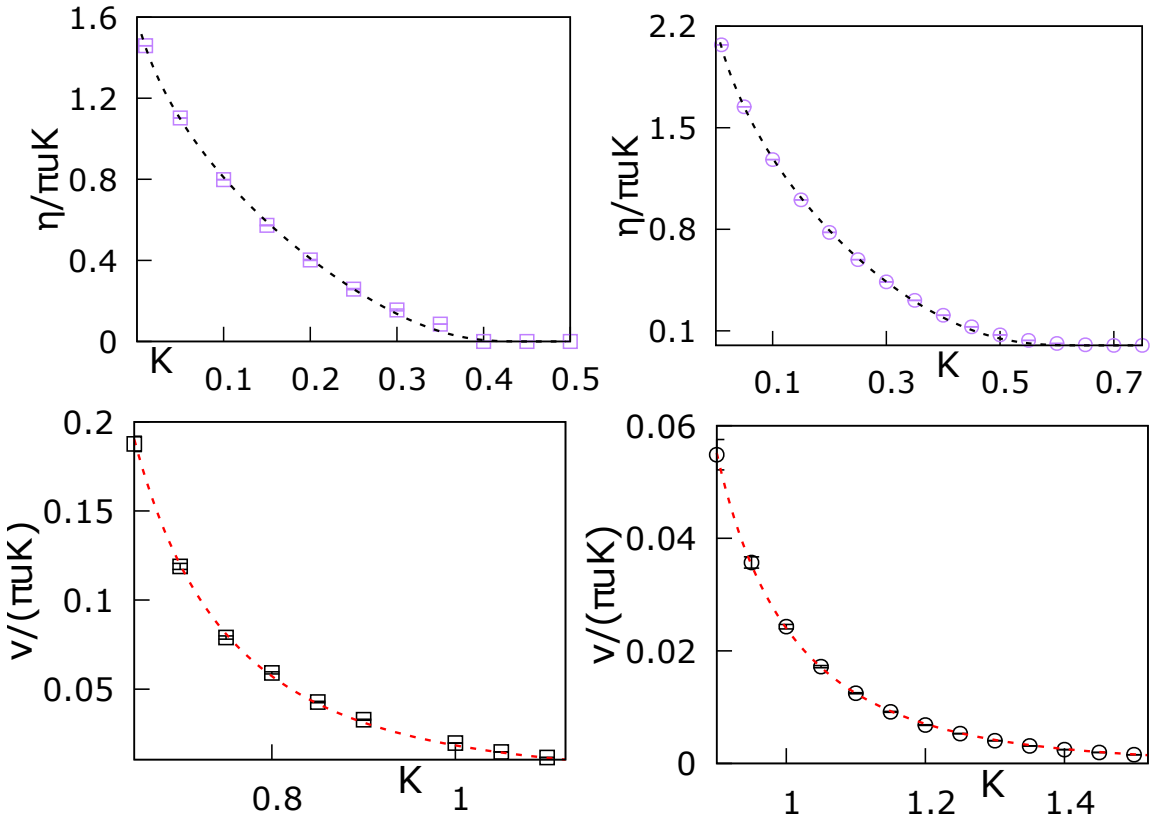

FIG. 3. The parameters η and ν obtained from the numerical solution of eq. (12) (with $\beta = 1024$ and $\alpha = 5$). For η (top row), we use α' and Λ from eq. (10) as fitting parameters. For the ohmic case (purple square), $\alpha' = 10.096, \Lambda = 1.963$, and for the subohmic case (purple circle), $\alpha' = 8.29, \Lambda = 3.29$. For the plot of ν (bottom row), the fitting parameters are τ_c and Λ from eq. (11). For the ohmic case (black square), $\tau_c = 1.68, \Lambda = 0.272$, and for the subohmic case (black circle), $\tau_c = 1.241, \Lambda = 0.415$.

K. Hence, to estimate ν, we replace G_{var} on the right side of the eq. (6) by the bare LL propagator $\pi K \left[uq^2 + \frac{\omega_n^2}{u}\right]^{-1}$. Hence, we find $\nu\omega_n^2 = \frac{\alpha}{\pi^2}\int_{\tau_c}^{\infty} d\tau \frac{1-\cos\omega_n\tau}{\tau^{1+s}} \exp\left(-2K\int_0^{\Lambda} d\omega_n' \frac{1-\cos\omega_n'\tau}{\omega_n'}\right)$. The integral over $\omega_{n'}$ yields $(\gamma_E + \ln\Lambda\tau)$, and after expanding $\cos\omega_n\tau$ for small ω_n, we find:

$$\nu = \frac{\tilde{\alpha}\exp(-2K\gamma)}{\tilde{\Lambda}^{2K}(2K+s-2)} \tag{11}$$

Where $\tilde{\alpha} = \frac{\alpha\tau_c^{2-s}}{2\pi^2}$ and $\tilde{\Lambda} = \Lambda\tau_c$. We see that this estimate for $K > 1 - s/2$, large Λ and small α represents a small correction to the action [34]. From the variational ansatz, we see that the Luttinger parameter K is normalized to $K_r = K/\sqrt{1+\nu}$. This renormalization results from the fact that the variational procedure captures the perturbative renormalization group (RG) flow of K up to the first order in α. In the Sine-Gordon model, the variational solution does not renormalize the parameters K, u and α [27]. Indeed, as we show in Appendix B, the perturbative RG flow of K is non-zero even in the first order, which is also captured by the variational method.

C. Numerical solution of the self-consistent equation

To support our claim, we also numerically solved the following self-consistent equation for $F(\omega_n)$ by

plugging eq. (7) in eq. (6):

$$F(\omega_n) = \frac{uK\alpha}{\pi}\sum_{\tau=1}^{\beta-1} D(\tau)(1-\cos\omega_n\tau) \times \exp\left(-\frac{2\pi K}{\beta}\sum_{n'=-\frac{\beta}{2}}^{\frac{\beta}{2}-1}\frac{1-\cos\omega_{n'}\tau}{\sqrt{\omega_{n'}^2+F(\omega_{n'})}}\right) \tag{12}$$

where $D(\tau)$ is the long-range kernel of eq. (6), realized on a discretized lattice with periodic boundary condition, namely $D(\tau) = \sum_{k=\beta/2}^{\beta/2-1}\mathcal{B}\left((\tau+k\beta)-\frac{s}{2}, s-1\right)$, where $\mathcal{B}()$ is the Beta-function (For more details, see App. C of [20]). In Fig. (2), we check the behavior of $F(\omega_n)$ for ohmic and subohmic baths in both LL and dissipative phases. Fig. (3) shows us the behavior of η and ν for dissipative phase and LL respectively for ohmic and subohmic baths. For fitting purposes, we use α' and Λ for η and τ_c and Λ for ν as fitting parameters because they depend on the boundary condition and discretization. The plots show us that indeed our analytical predictions of Eq. (10) and Eq. (11) are in fair agreement with the direct numerical solution of Eq. (12).

IV. ORDER PARAMETER AND DISSIPATIVE PHASE

In the dissipative phase, the spin chain develops a long-range order spin density wave. To better understand the properties of this phase we first study the order parameter of the transition, namely the amplitude of the SDW. Using Eq. (3), together with the symmetry $\phi \to -\phi$ to remove the terms $\langle\nabla\phi\rangle$ and $\langle\sin(2\phi)\rangle$, we see:

$$\langle\sigma^z(x)\rangle = \frac{1}{\pi a}\langle\cos(2\phi)\rangle\cos(2q_F x) \tag{13}$$

Comparing with eq. (5), we identify the amplitude of the SDW :

$$\sigma_1 = \frac{1}{\pi a}\langle\cos(2\phi(x,\tau))\rangle\ . \tag{14}$$

We note two important points:

- In contrast with the standard Peierls mechanism, the amplitude of the SDW is not associated with the formation of a gap. Indeed, the spin chain is gapless.
- For the incommensurate case the global shift $\phi \to \phi + c$ does not cost any energy, but in the dissipative phase, this symmetry will be broken by the presence of local field or impurity. It is then convenient to fix this constant by setting the center of mass of the interface to zero, namely $\phi(q=0,\omega_n=0)=0$.

.

In the thermodynamic limit $L\to\infty$ and zero temperature limit $\beta\to\infty$, the order parameter is zero, in the LL phase (no true long-range order) whereas it is constant in the dissipative phase. Indeed, we can estimate the value of the order parameter in the dissipative phase, using the variational ansatz $G_{\rm var}(q,\omega_n) = \pi K\left[uq^2+\eta\frac{|\omega_n|^s}{u}+\frac{\omega_n^2}{u}\right]^{-1}$:

$$\sigma_1 = \frac{1}{\pi a}\langle\cos(2\phi)\rangle = \frac{1}{\pi a}e^{-\frac{2}{\pi^2}\int_0^\Lambda {\rm d}\omega_n\int_0^\infty dq\ G_{\rm var}(q,\omega_n)} \tag{15}$$

It is instructive to consider the effect of finite temperature and finite size. One can easily find out that in the Fourier space, the order parameter is given by

$$\langle\cos 2\phi\rangle_{L,\beta} = \exp\left(-\frac{2}{\beta L}\sum_{\substack{q,\omega_n\\ q,\omega_n\neq 0}} G_{\rm var}(q,\omega_n)\right).$$

As shown in Appendix A, this sum can be decomposed into three contributions :

- The contribution of $\omega_n = 0, q\neq 0$ terms, which account for finite size effect.
- The contribution of $\omega_n\neq 0, q = 0$ terms, which account for finite temperature effect.
- The contribution of $\omega_n\neq 0, q\neq 0$ terms, which can be approximated by eq. (15) with subleading corrections.

Using the variational action (eq. (7)) with the LL ansatz $F(\omega_n)=\nu\omega_n^2$, one can find that (For details, see Appendix A):

$$\langle\cos 2\phi\rangle_{L,\beta}^{\rm LL} \sim e^{-\frac{\pi^2}{6}\left[\chi\frac{L}{\beta}+\rho_s\frac{\beta}{L}\right]-K_r\ln\min(\beta,L)} \tag{16}$$

Here χ is the susceptibility ($\pi\chi = K/u = K_r/u_r$) and $\rho_S = \lim_{q\to 0}\lim_{\omega_n\to 0}(\omega_n^2/\pi^2)G(q,\omega_n)$ is the spin stiffness ($\pi\rho_s = K_r u_r$).

Using the variational action with dissipative phase ansatz $F(\omega_n)=\eta|\omega_n|^s$, it behaves as:

$$\langle\cos 2\phi\rangle_{L,\beta}^{\rm diss} \sim \sigma_1 e^{-\chi\frac{\pi^2}{6}\frac{L}{\beta}+\frac{2uK}{\eta}\frac{b_0(s)}{(2\pi)^{s-1}}\frac{\beta^{\kappa(s)}}{L}+c_1\beta^{\frac{s}{2}-1}} \tag{17}$$

Three limits should be discussed :

- In the thermodynamic limit $L \to \infty$ and finite temperature, both order parameters vanish as $\sim \exp(-\pi^2 \chi L/6\beta)$.

- In the zero temperature limit $\beta \to \infty$ and for a finite length L, in the LL regime, the order parameter $\sigma^{\rm LL}_{1_{L,\infty}}$ vanishes exponentially as $\sim \exp(-\pi^2 \rho_s \beta/6L)$. In the dissipative regime, the order parameter $\sigma^{\rm diss}_{1_{L,\infty}}$ vanish as a stretched exponential $\sim \exp(-\beta^{s-1}/L)$ for superohmic bath, while it converges to a constant in the subohmic case. This ordered phase at finite L can be related to the transition observed for single particle models in the presence of a subohmic bath [30, 31].

- In the numerical simulation, we set $L = \beta$ and send $\beta \to \infty$. In this limit, we find:

$$\begin{aligned} \langle \cos 2\phi \rangle^{\rm LL}_{L=\beta=\infty} &\sim L^{-K_r} \qquad (18) \\ \langle \cos 2\phi \rangle^{\rm diss}_{L=\beta=\infty} &\sim \sigma_1 e^{-\frac{\pi^2 \chi}{6}} \left(1 + c_1 L^{\frac{s}{2}-1} + c_2 L^{s-2}\right) \end{aligned}$$

A. Two-point correlation function

To understand the nature of the order in the dissipative phase, it's important to introduce the two-point correlation functions:

$$\begin{aligned} \langle \sigma^z_{x,\tau} \sigma^z_{0,\tau} \rangle &\sim \langle e^{i2\phi(x,\tau)} e^{-i2\phi(0,\tau)} \rangle \cos(2q_F x) \\ \langle \sigma^z_{x,\tau} \sigma^z_{x,0} \rangle &\sim \langle e^{i2\phi(x,\tau)} e^{-i2\phi(x,0)} \rangle \qquad (19) \end{aligned}$$

Note that The spatial spin-spin correlator has an overall oscillating factor of $\cos(2q_F x)$, which doesn't affect the decay of the correlator at large x. Under the gaussian variational approximation, one can see that $\langle e^{i2\phi(x,\tau)} e^{-i2\phi(0,\tau)} \rangle = e^{-2\langle (\phi(x,\tau)-\phi(0,\tau))^2 \rangle} \equiv e^{-2B(x)}$ and similarly for $\langle e^{i2\phi(x,\tau)} e^{-i2\phi(x,0)} \rangle = e^{-2B(\tau)}$. From eq. (B7) and eq. (B11) of Appendix B, one can easily see that for large x at finite temperature and in the thermodynamic limit :

$$\begin{aligned} \langle \sigma^z_{x,\tau} \sigma^z_{0,\tau} \rangle_{\rm LL} &\sim \exp\left(-\frac{2\pi^2 \chi x}{\beta}\right) x^{-2K_r} \cos(2q_F x) \\ \langle \sigma^z_{x,\tau} \sigma^z_{0,\tau} \rangle_{\rm diss} &\sim \sigma_1^2 \exp\left(-\frac{2\pi^2 \chi x}{\beta}\right) \left(1 + a_2 x^{1-\frac{2}{s}}\right) \\ &\quad \times \cos(2q_F x) \qquad (20) \end{aligned}$$

and for large τ at zero temperature and for finite L:

$$\begin{aligned} \langle \sigma^z_{x,\tau} \sigma^z_{x,0} \rangle_{\rm LL} &\sim \exp\left(-\frac{2\pi^2 \rho_s \tau}{L}\right) (u_r \tau)^{-2K_r} \qquad (21) \\ \langle \sigma^z_{x,\tau} \sigma^z_{x,0} \rangle_{\rm diss} &\sim \sigma_1^2 \exp\left(-\frac{K u \tau^{f(s)}}{\eta L}\right) \left(1 + a_1 \tau^{\frac{s}{2}-1}\right) \end{aligned}$$

Where $f(s) = 0$ for subohmic bath and $f(s) = 1 - s$ for superohmic bath.

These results show that in the limit of finite temperature, above a lengthscale $\beta/2\pi^2\chi$, both the order in the dissipative phase as well as the quasi-order in the LL phase are exponentially suppressed. On the other hand at $T = 0$ there is long-range order:

$$\lim_{x\to\infty} \langle \sigma^z_{x,\tau} \sigma^z_{0,\tau} \rangle_{\rm diss} = \sigma_1^2 \cos(2q_F x) \qquad (22)$$

Connected spatial and imaginary time correlations decay in a power law fashion at $T = 0$, with an exponent which increases upon decreasing s. These results, along with the behavior of the order parameter, show that at zero temperature, the dissipative phase is indeed an SDW with a gapless spectrum and long-range order. This ordered phase exists due to the spontaneous breaking of the continuous symmetry $\phi \to \phi + c$ due to the presence of the long-range dissipative action $S_{\rm int}$.

V. NUMERICAL SIMULATIONS

We verify the validity of our variational ansatz, both qualitatively and quantitatively, via numerical simulation of the original action with the cosine potential, Eq. (4). We numerically solve the Langevin dynamics differential equation associated with the action, namely the stochastical differential equation $\frac{d\phi(t)}{dt} = -\frac{\partial S_{\rm eff}}{\partial \phi} + \Gamma(t)$, where $\Gamma(t)$ is Gaussian white noise with $\langle \Gamma(t) \rangle = 0$, $\langle \Gamma(t)\Gamma(t') \rangle = 2\delta(t - t')$. Note that Γ is the noise that thermalizes to $\exp(-S_{\rm eff})$ and is not related to the temperature of the dissipative bath, which is zero. Discretizing the action and applying periodic boundary conditions in both x and τ direction, we obtain the following differential equation that we simulate numerically:

$$\begin{aligned} \frac{d\phi_{ij}(t)}{dt} &= \frac{1}{K\pi u} \left(\phi_{i+1,j} + \phi_{i+1,j} - 2\phi_{i,j}\right) \\ &\quad + \frac{u}{K\pi} \left(\phi_{i,j+1} + \phi_{i,j-1} - 2\phi_{i,j}\right) + \Gamma_{ij}(t) \\ &\quad + \frac{\alpha}{\pi^2} \sum_{i'} D(|i - i'|) \sin\left[2\left(\phi_{i'j} - \phi_{ij}\right)\right] \end{aligned} \qquad (23)$$

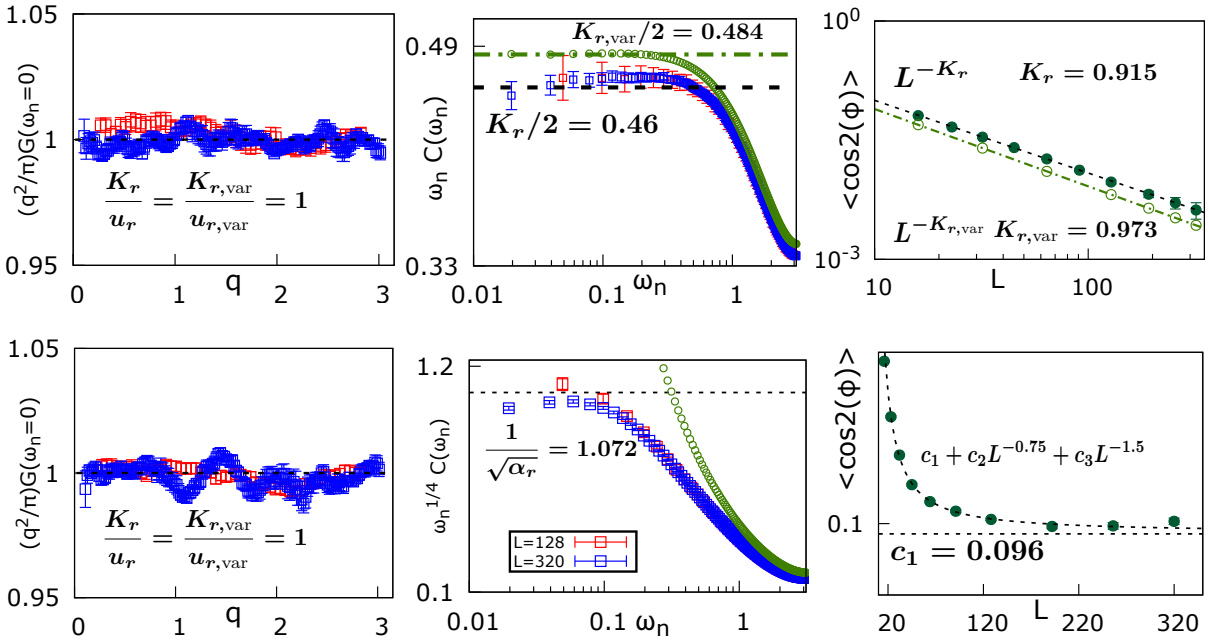

FIG. 4. Calculation of different quantities for $K = 1$ that characterizes LL ($\alpha = 2$, top row) and dissipative phase ($\alpha = 6$, bottom row). Red points correspond to $L = \beta = 128$ and blue points correspond to $L = \beta = 320$. Green points correspond to $\omega_n C(\omega_n)$ calculated from numerically solving the self-consistent variational eq. (6). (*left*) $\pi\chi$ remains unrenormalized for all values of α and q. (*middle*) For $\alpha = 2$, $\omega_n C(\omega_n)$ saturates to $K_r/2 = 0.46$ for small ω, whereas $\omega_n^{0.25} C(\omega_n)$ saturates to $1/\alpha_r = 1.072$ for $\alpha = 6$. The variational solution saturates to $K_{r,\mathrm{var}}/2 = 0.486$ for $\alpha = 2$ and fails to correctly predict the dissipative phase for $\alpha = 6$. (*right*) For $\alpha = 2$, $\langle \cos\phi \rangle$ decays as a power law with the exponent $K_r = 0.915$. However, it saturates to a constant c_1 algebraically for $\alpha = 6$. The fit for the order parameter in the dissipative phase gives $c_1 = 0.096, c_2 = 0.112$, and $c_3 = 3.37$. In the LL phase, $\langle \cos(2\phi) \rangle$ calculated with variational method decays with $K_{r,\mathrm{var}} = 0.973$.

Where $i \in (1, \beta)$ and $j \in (1, L)$ represents the discretized τ and x indices respectively. We solve this differential equation at long time and obtain equilibrated configurations $\phi_{\mathrm{eq}}(x, \tau)$. We then calculate various correlation functions on these configurations and match them against our analytical predictions. We compare the Langevin equation simulation with the variational method prediction, obtained from numerically solving Eq. (6). The values of the parameters chosen for both simulations are $K = 1, u = 1, s = 0.5$ and $dt = 0.05$, where dt is the Langevin time-step. We varied the value of α, and for each value of α, we simulate Eq. (23) for different sizes, scaling $L = \beta$. From the variational study, we expect that there exists a critical dissipative strength $\alpha_c(K)$ such that for $\alpha < \alpha_c$, the correlation functions will correspond to the LL propagator $G_{\mathrm{LL}}^{-1} = \frac{1}{\pi K}\left(uq^2 + \frac{\omega_n^2}{u}(1+\nu)\right)$, and for $\alpha > \alpha_c$, they will behave according to the dissipative phase propagator $G_{\mathrm{var}}^{-1} = \frac{1}{\pi K}\left(uq^2 + \frac{\eta|\omega_n|^s}{u} + \frac{a_1|\omega_n|^{1+\frac{s}{2}}}{u} + \frac{a_2\omega_n^2}{u}\right)$. In Fig. 4, we show the results for $\alpha = 2$ (top row), which we find to be in the LL phase, and $\alpha = 6$, which turns out to be in the dissipative phase. The first quantity we compute is $(q^2/\pi)G(q, \omega_n)$. Fig. 4, left, shows that this quantity, both with the Langevin method and the variational method, remains unrenormalized and equal to K/u for all values of q and both values of α. This is in agreement with our variational ansatz. Next, we compute $C(\omega_n) = \frac{1}{\pi L}\sum_q G(q, \omega_n)$. This quantity is useful for extracting and differentiating between the ω_n dependence of $G(q, \omega_n)$ in the two phases. Indeed, for small ω_n, $C(\omega_n)$ behaves as:

$$C(\omega_n \to 0) = \begin{cases} \frac{K_r}{2\omega_n}, & \text{LL} \\ \frac{1}{\sqrt{\alpha_r}\omega_n^s} & \text{dissipative} \end{cases} \tag{24}$$

where $K_r = \frac{K}{\sqrt{\nu+1}}$ and $\alpha_r = 4\eta/K^2$. We denote the renormalized value of K obtained from the Langevin simulation as K_r and the numerical variational solution as $K_{r,\mathrm{var}}$. Fig. 4, middle, shows that indeed for $\alpha = 2$, $\omega_n C(\omega_n)$ saturates to a constant, whereas for $\alpha = 6$, $\omega_n^{0.25} C(\omega_n)$ goes to a constant as $\omega_n \to 0$, indicating that $\alpha = 2$ is in LL phase and $\alpha = 6$ is in the dissipative phase. The variational solution also shows a renormalization of K, for example for $\alpha = 2$, we get $K_{r,\mathrm{var}} = 0.968$. This result is in fair agreement with the Langevin simulation, $K_r = 0.92$. However, at large α, the variational method fails and estimates the transition at $\alpha_c = 10$. From fig. 4, middle bottom, for $\alpha = 6$ the system is already in the dissipative phase. For our third and final check, we show the behavior of the order parameter (eq. (14)). To extrapolate to the zero temperature behavior, we compute $\langle \cos(2\,(\phi - \phi_{\mathrm{CoM}}))\rangle$. Fig. (4), left, shows that this quantity decays as a power law of the system size for $\alpha = 2$ (top) and saturates to a constant for $\alpha = 6$ (bottom). Therefore, we confirm the existence of a phase transition between LL and a new dissipative phase induced by the bath. This new phase has unaltered susceptibility, gapless spectrum, and vanishing spin stiffness ρ_s. In Fig. 5, we show the renormalized values of different parameters as a function of α, which tells us that for $K = 1$, $\alpha_c \in (3, 4)$.

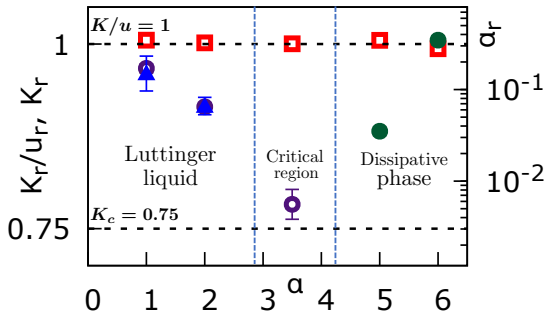

FIG. 5. Renormalized value of different parameters of the action for $K = 1, s = 0.5$. K_r/u_r (red square) remains constant and equal to 1 for all values of α. K_r decreases from $K = 1$ to $K_c = 0.75$ as α increases and approaches α_c. α_r becomes relevant in the dissipative phase and increases as a function of α. This behavior of the parameters helps us locate the critical region $\alpha_c \in (3, 4)$.

VI. CONDUCTIVITY

From Linear Response theory, the conductivity can be determined via the analytic continuation of the propagator [27]:

$$\sigma(\omega) = \frac{e^2}{\pi^2 \hbar} \left[\omega_n G(q = 0, \omega_n)\right]_{i\omega_n \to \omega + i\epsilon} \tag{25}$$

Where ϵ is a small positive number close to zero. Using our ansatz we find that the DC conductivity $\sigma_{\mathrm{DC}} \equiv \mathrm{Re}(\sigma(\omega \to 0)) = \lim_{\epsilon \to 0}(e^2/\pi^2\hbar)\epsilon^{1-s}$, which goes to zero for subohmic ($s < 1$) baths. This supports our claim that the system for a subohmic bath in the dissipative phase is insulating at zero temperature.

VII. CONCLUSIONS

In this work, exploiting the bosonization formalism, we have shown via analytical and numerical methods that an incommensurate XXZ spin chain coupled to local baths undergoes an LL-dissipative phase transition at $T = 0$. At transition, the chain undergoes a spontaneous symmetry breaking, with an order parameter $\langle \cos(2\phi)\rangle$, that identifies with the amplitude of a long-range ordered spin density wave. Remarkably, the spin wave is gapless and the order originates from the fractional nature of the excitations of the dissipative phase. Moreover, from the linear response, we observe a suppression of the DC conductivity that vanishes for subohmic baths. Hence, it is tempting to compare this dissipative transition with the localization transition observed for quenched disorder [22, 23, 35]. There, the localized phase is also gapless and the fluctuations along the imaginary time direction are suppressed. However, the order parameter $\langle \cos(2\phi)\rangle$ is zero (as there is no spontaneous breaking of a continuous symmetry) and the spatial spin-spin correlations decay to zero exponentially above a finite localization length. in the dissipative phase instead, the spin-spin correlations decay to a finite value with an s-dependent power law. For slower baths (small s), the decay becomes faster, and the exponent diverges in the limit $s \to 0$, signaling that (connected) correlations can decay exponentially.

In the future, we would like to study the properties of the model at finite temperatures by variational methods and numerical simulations. This would be very interesting in view of our interpretation of the bath as annealed disorder and this study could possibly shed some light on the ongoing discussion on the many-body localization transition.

Another direction that we we have taken is the study of the same model at half-filling. This was partially done in [36] and we plan to do it in full generality.

ACKNOWLEDGMENTS

Acknowledgments: This work was supported in part by the Swiss National Science Foundation under grant 200020-188687. This work was performed using HPC/AI resources from GENCI-IDRIS (Grant 2022-AD011013581) and GENCI-TGCC (Grant 2022-AD011013555). We thank Thibaud Maimbourg and Oscar Bouverot-Dupuis for their useful discussions.

Appendix A: System size dependence of Order Parameter

In this section, we compute $\langle \cos 2\phi \rangle_{L,\beta} = \exp\left(-\frac{2}{\beta L} \sum_{\substack{q,\omega_n \\ q=\omega_n \neq 0}} G_{\rm var}(q,\omega_n) \right)$. This sum can be decomposed into three terms:

$$S_1 = \frac{2}{\beta L}\left[\sum_{q\neq 0} G_{\rm var}(q,0) + \sum_{\omega_n \neq 0} G_{\rm var}(0,\omega_n) + \sum_{q\neq 0,\omega_n\neq 0} G_{\rm var}(q,\omega_n) \right] \tag{A1}$$

The $q \neq 0, \omega_n \neq 0$ contributions can be converted as $\frac{1}{\beta L} \sum_{q\neq 0,\omega_n\neq 0} \to \frac{1}{\pi^2} \int_{1/L} dq \int_{1/\beta} d\omega_n$. Using the eq. (7) with $F(\omega_n) = \nu \omega_n^2$, we see that:

$$\begin{aligned}
\frac{2}{\beta L}\sum_{q\neq 0} G(q,0) &= \frac{4\pi K}{u\beta L}\sum_{m=1}^{\infty} \frac{1}{\left(\frac{2\pi m}{L}\right)^2} \\
&= \frac{\pi K L}{6u\beta} \\
\frac{2}{\beta L}\sum_{\omega_n\neq 0} G(0,\omega_n) &= \frac{4\pi K u}{(1+\nu)\,\beta L}\sum_{n=1}^{\infty} \frac{1}{\left(\frac{2\pi n}{\beta}\right)^2} \\
&= \frac{\pi u K \beta}{6(1+\nu)L} \\
\frac{2}{\beta L}\sum_{q\neq 0,\omega_n\neq 0} G_{\rm var}(q,\omega_n) &= \frac{2K}{\pi}\int_{1/L}^{\Lambda_1}\int_{1/\beta}^{\Lambda_2} \frac{d\omega_n dq}{uq^2 + \frac{\omega_n^2}{u}(1+\nu)} \\
&\sim \frac{K}{\sqrt{1+\eta}} \ln \min(\beta, L)
\end{aligned}$$

Similarly, with $F(\omega_n) = \eta|\omega_n|^s$, we find that the contribution from the first term is the same. The contribution from the second term can be written as:

$$\frac{2}{\beta L}\sum_{\omega_n\neq 0} G(0,\omega_n) = \frac{2uK}{\eta}\frac{b_0(s)}{(2\pi)^{s-1}}\frac{\beta^{\kappa(s)}}{L} \tag{A2}$$

Where $\kappa(s) = 0$ and $b_0(s) \sim \frac{1}{1-s}$for a subohmic bath ($0 < s < 1$), $\kappa(s) = s-1$ and $b_0(s) \sim \zeta(s)$ for a superohmic bath ($1 < s < 2$). The ohmic case ($s = 1$) is special and $b_0(s)\beta^{\kappa(s)}$ should be replaced with $\ln\beta + \gamma_E$. The contribution from the third term is given by:

$$\begin{aligned}
\frac{2}{\beta L}\sum_{q\neq 0,\omega_n\neq 0} G(q,\omega_n) &= \frac{2K}{\pi}\int_{1/L}^{\infty}\int_{1/\beta}^{\Lambda} \frac{d\omega_n dq}{uq^2 + \frac{\omega_n^2}{u} + \frac{\eta\omega_n^s}{u}} \\
&\sim c_0 - c_1 \beta^{\frac{s}{2}-1}
\end{aligned} \tag{A3}$$

Where c_0 and c_1 are positive constants that depend on $K, u, \eta, s,$ and ultra-violet cut-off Λ. Putting these terms together, we find eq. (16) and (17).

Appendix B: Roughness of $\phi(x,\tau)$ in the dissipative phase

At zero temperature, in the Luttinger liquid phase, the field $\phi(x,\tau)$ grows logarithmically in both directions x and τ. Here we characterize the roughness of the field $\phi(x,\tau)$ in the dissipative phase. In particular, We compute the following correlation

functions:

$$B(\tau) \equiv \langle \big[\phi(x,0) - \phi(x,\tau)\big]^2 \rangle \quad \text{(B1)}$$

$$B(x) \equiv \langle \big[\phi(x,\tau) - \phi(0,\tau)\big]^2 \rangle \quad \text{(B2)}$$

In the dissipative phase, using eq. (7) with $F(\omega_n) = \nu|\omega_n|^s$, eq. (B1) can be written in the Fourier space as

$$B(\tau) = \frac{2}{\beta L} \sum_{q,\omega_n} (1 - \cos\omega_n\tau)\, G_{\rm var}(q,\omega_n) \quad \text{(B3)}$$

The $\omega_n = 0$ terms vanish due to the presence of the cosine term in the numerator. Hence, we write the contributions from the terms $q = 0, \omega_n \neq 0$ and $q \neq 0, \omega_n \neq 0$ separately:

$$\begin{aligned} B(\tau) &= \frac{2}{\beta L} \sum_{\omega_n \neq 0} (1 - \cos\omega_n\tau) G_{\rm var}(0,\omega_n) \quad \text{(B4)} \\ &+ \frac{2}{\beta L} \sum_{q\neq 0,\omega\neq 0} (1 - \cos\omega_n\tau) G_{\rm var}(q,\omega_n) \end{aligned}$$

The summation of the first term on the RHS of eq. (B4) gives:

$$\begin{aligned} &\frac{2}{\beta L} \sum_{\omega_n \neq 0} (1 - \cos\omega_n\tau) G_{\rm var}(0,\omega_n) \\ &= \frac{4\pi K u}{\beta L} \sum_{n=1}^{\infty} \frac{1 - \cos\omega_n\tau}{\omega_n^2 + \eta\omega_n^s} \quad \text{(B5)} \\ &\sim \frac{Ku}{\eta} \frac{\tau^{f(s)}}{L} \end{aligned}$$

Where $f(s) = 0$ for subohmic bath ($0 < s < 1$) and $f(s) = 1 - s$ for superohmic bath ($1 < s < 2$). For the ohmic case ($s = 1$), $\tau^{f(s)}$ should be replaced by $\ln\tau$. For the second term on the RHS of eq. (B4), we convert the sum $\frac{1}{\beta L} \sum_{q\neq 0,\omega_n\neq 0} \to \frac{1}{\pi^2} \int dq d\omega_n$ to find:

$$\begin{aligned} &\frac{2}{\beta L} \sum_{q\neq 0,\omega\neq 0} (1 - \cos\omega_n\tau) G_{\rm var}(0,\omega_n) \quad \text{(B6)} \\ &= \frac{2K}{\pi} \int_0^{\Lambda} d\omega_n \int_0^{\infty} dq \frac{(1 - \cos\omega_n\tau)}{uq^2 + \frac{\omega_n^2}{u} + \frac{\eta\omega_n^s}{u}} \end{aligned}$$

The integral over 1 in eq. (B7) gives us the same constant c_0 from eq. (A3). The integral over $\cos\omega_n\tau$ gives us the τ dependence of $B(\tau)$, and we see that for large τ :

$$B(\tau) \sim \frac{Ku}{\eta} \frac{\tau^{f(s)}}{L} + c_0 - a_1 \tau^{\frac{s}{2}-1} \quad \text{(B7)}$$

Where $a_1 = \frac{K}{\eta}\, \Gamma(1 - \frac{s}{2}) \sin\left(\frac{\pi s}{4}\right)$.

Similarly, eq. (B2) can be written in the Fourier space and calculated :

$$\begin{aligned} B(x) &= \frac{2}{\beta L} \sum_{q\neq 0} (1 - \cos qx)\, G_{\rm var}(q,0) \quad \text{(B8)} \\ &+ \frac{2}{\beta L} \sum_{q,\omega_n} (1 - \cos qx)\, G_{\rm var}(q,\omega_n) \end{aligned}$$

Like $B(\tau)$, we compute $B(x)$ termwise:

$$\begin{aligned} &\frac{2}{\beta L} \sum_{q\neq 0} (1 - \cos qx)\, G_{\rm var}(q,0) \quad \text{(B9)} \\ &= \frac{4\pi\chi}{\beta L} \sum_{n=1}^{\infty} \frac{1 - \cos qx}{q^2} \sim \frac{\pi^2\chi x}{\beta} \\ &\frac{2}{\beta L} \sum_{q,\omega_n} (1 - \cos qx)\, G_{\rm var}(q,\omega_n) \quad \text{(B10)} \\ &= \frac{2K}{\pi} \int_0^{\infty} d\omega_n \int_0^{\Lambda} dq \frac{(1 - \cos qx)}{uq^2 + \frac{\omega_n^2}{u} + \frac{\eta\omega_n^s}{u}} \\ &\sim c_0 - a_2 x^{1-\frac{2}{s}} \end{aligned}$$

where $a_2 = \frac{2Ku^{\frac{2}{s}-1}\eta^{-\frac{1}{s}}\Gamma\left(\frac{2}{s}-1\right)}{s}$. Putting all the terms together, we obtain that for large-x:

$$B(x) \approx \frac{\pi^2\chi x}{\beta} + c_0 - a_2 x^{1-\frac{2}{s}} \quad \text{(B11)}$$

In conclusion, in the thermodynamic limit where $L \to \infty$, the interface is flat in the τ direction. Along the x direction, it is rough at finite temperature and becomes flat at zero temperature. In this limit, both $B(x)$ and $B(\tau)$ algebraically saturate to the same constant but with different power laws, showing that there is long-range order in this phase.

Appendix C: RG calculation

In this section, we systematically derive the RG flow equations of the LL parameter K and the coupling strength α. To analyze the RG flow of the parameters, we calculate the following correlation function :

$$R(r_1 - r_2) = \langle e^{ia\phi(r_1)} e^{-ia\phi(r_2)} \rangle,\ r = (x, u\tau) \quad \text{(C1)}$$

We know that for the quadratic LL action, $R(r_1 - r_2) \sim \left(\frac{r_1-r_2}{b}\right)^{-a^2K/2}$, where b is some short-scale length cut-off. We perturbatively expand the correlation function with respect to S_{diss}. The perturbative series up to first order of α is given by $\langle e^{ia\phi(r_1)}e^{-ia\phi(r_2)}\rangle_{S_0} + \langle e^{ia\phi(r_1)}e^{-ia\phi(r_2)}\rangle_{S_0}\langle S_{int}\rangle_{S_0} - \langle e^{ia\phi(r_1)}e^{-ia\phi(r_2)}S_{int}\rangle_{S_0}$. The 0th order term can be easily computed and is given by $\exp(\frac{-a^2K}{2}F(r_1 - r_2)), F(r) = \frac{1}{2}\log\left[\frac{x^2+(u|\tau|+b)^2}{b^2}\right]$. After computing the first-order contribution, we obtain:

$$R(r_1 - r_2) = e^{\frac{-a^2K}{2}F(r_1-r_2)}[1 + \frac{\alpha}{2\pi bu^2}\int d^2r'd^2r''e^{-2KF(x'-x',\tau'-\tau'')}B\sum_{\epsilon=+-}\left[e^{aK\epsilon(F(r_1-r')-F(r_1-r'')-F(r_2-r')+F(r_2-r''))} - 1\right]] \quad \text{(C2)}$$

where $B = \delta(x'-x'')D(\tau'-\tau'')$. After transforming the equation into CoM $R = \frac{r'+r''}{2}$ and relative coordinates $r = r' - r''$ and taylor expanding F for small r, we expand the exponential for small value of r:

$$R(r_1 - r_2) = e^{\frac{-a^2K}{2}F(r_1-r_2)}[1 + \frac{\alpha a^2K^2}{2\pi bu^2}\int d^2rd^2Re^{-2KF(r)}B \times(r.\nabla_R[F(r_1 - R) - F(r_2 - R)])^2 \quad \text{(C3)}$$

The term inside the square produces terms like $r_ir_j(\nabla_{R_i}[F(r_1 - R) - F(r_2 - R)]))(\nabla_{R_j}[F(r_1 - R) - F(r_2 - R)]))$, where i, j denotes the two possible coordinates $x, y = u\tau$. For the integral over d^2r and by symmetry $x \to -x, y \to -y$, only the diagonal $i = j$ terms survive. The action is anisotropic whose effect can be included with an additional term in F of the form $d\cos(2\theta)$, where θ is the angle between vector $(x, u\tau)$ and x axis and d is the measure of anisotropy. After expanding the gradient terms and integrating by parts over R, we obtain two terms $I_\pm = \int d^2R[F(r_1-R)-F(r_2-R)](\partial_X^2 \pm \partial_Y^2)[F(r_1 - R)-F(r_2-R)]$. The I_+ term renormalizes K and α, whereas the other term renormalizes the anisotropy which we are not interested in. Hence,

$$R(r_1 - r_2) = e^{\frac{-a^2K}{2}F(r_1-r_2)} \times [1 - \frac{\alpha a^2K^2}{4\pi bu^2}\int d^2rd^2Re^{-2KF(r)}r^2B[F(r_1 - R) - F(r_2 - R)](\nabla_X^2 + \nabla_Y^2)[F(r_1 - R) - F(r_2 - R)] \quad \text{(C4)}$$

As F is a logarithmic function, we know that $(\nabla_X^2 + \nabla_Y^2)F(R) = 2\pi\delta(R)$. After re-exponentiating the term inside the bracket, we obtain :

$$K_{\text{eff}} = K - \frac{2\alpha K^2}{bu^2}\int_{r>b} d^2rr^2\exp(-2KF(r))B \quad \text{(C5)}$$

To understand the scaling of K and α, we express d^2r and r^2 in terms of $x, u\tau$ and compute the integral over $\delta(x)$. Noticing that $D(\tau)$ cancels out τ^2, we find:

$$K_{\text{eff}} = K - 2\alpha K^2\int_b^\infty \frac{dy}{b}(\frac{y}{b})^{-2K},\ y = u\tau \quad \text{(C6)}$$

Sending b to $b' = b + db$, we find :

$$K_{\text{eff}} = K - 2\alpha K^2\frac{db}{b} - 2\alpha K^2\int_{b'}^\infty \frac{dy}{b}(\frac{y}{b})^{-2K} \implies K(b') = K(b) - 2\alpha(b)K^2(b)\frac{db}{b} \quad \text{(C7)}$$

Similarly,

$$\alpha(b') = \alpha(b)\left(\frac{b'}{b}\right)^{1-2K} \quad \text{(C8)}$$

If we parametrize $b = b_0e^l$, we obtain the following flow equations:

$$\frac{dK}{dl} = -2\alpha K^2 \qquad \frac{d\alpha}{dl} = (2 - s - 2K)\alpha \quad \text{(C9)}$$

These equations indicate the existence of a critical point $K_c = 1 - \frac{s}{2}$, as in [32], but the precise value of the numerical coefficient in the first equation of (C9) differs of a factor of 2.

[1] W. M. Itano, D. J. Heinzen, J. J. Bollinger, and D. J. Wineland, Phys. Rev. A **41**, 2295 (1990).
[2] B. Misra and E. C. G. Sudarshan, Journal of Mathematical Physics **18**, 756 (1977), https://doi.org/10.1063/1.523304.
[3] Y. Li, X. Chen, and M. P. A. Fisher, Phys. Rev. B **98**, 205136 (2018).
[4] A. Chan, R. M. Nandkishore, M. Pretko, and G. Smith, Phys. Rev. B **99**, 224307 (2019).
[5] B. Skinner, J. Ruhman, and A. Nahum, Phys. Rev. X **9**, 031009 (2019).
[6] M. Szyniszewski, A. Romito, and H. Schomerus, Phys. Rev. B **100**, 064204 (2019).
[7] X. Turkeshi, R. Fazio, and M. Dalmonte, Phys. Rev. B **102**, 014315 (2020).
[8] C.-M. Jian, Y.-Z. You, R. Vasseur, and A. W. W. Ludwig, Phys. Rev. B **101**, 104302 (2020).
[9] A. Zabalo, M. J. Gullans, J. H. Wilson, S. Gopalakrishnan, D. A. Huse, and J. H. Pixley, Phys. Rev. B **101**, 060301 (2020).
[10] Y. Bao, S. Choi, and E. Altman, Phys. Rev. B **101**, 104301 (2020).
[11] X. Cao, A. Tilloy, and A. D. Luca, SciPost Phys. **7**, 24 (2019).
[12] L. Zhang, J. A. Reyes, S. Kourtis, C. Chamon, E. R. Mucciolo, and A. E. Ruckenstein, Phys. Rev. B **101**, 235104 (2020).
[13] S. Chakravarty, Phys. Rev. Lett. **49**, 681 (1982).
[14] A. J. Leggett, S. Chakravarty, A. T. Dorsey, M. P. A. Fisher, A. Garg, and W. Zwerger, Rev. Mod. Phys. **59**, 1 (1987).
[15] A. J. Bray and M. A. Moore, Phys. Rev. Lett. **49**, 1545 (1982).
[16] A. Schmid, Phys. Rev. Lett. **51**, 1506 (1983).
[17] T. Maimbourg, D. M. Basko, M. Holzmann, and A. Rosso, Phys. Rev. Lett. **126**, 120603 (2021).
[18] A. W. Chin, J. Prior, S. F. Huelga, and M. B. Plenio, Phys. Rev. Lett. **107**, 160601 (2011).
[19] K. L. Hur, Quantum phase transitions in spin-boson systems: Dissipation and light phenomena (2009), arXiv:0909.4822 [cond-mat.other].
[20] S. Majumdar, L. Foini, T. Giamarchi, and A. Rosso, Phys. Rev. B **107**, 165113 (2023).
[21] G. Grüner, Rev. Mod. Phys. **60**, 1129 (1988).
[22] T. Giamarchi and H. J. Schulz, Europhysics Letters (EPL) **3**, 1287 (1987).
[23] T. Giamarchi and H. J. Schulz, Phys. Rev. B **37**, 325 (1988).
[24] L. Foini and J. Kurchan, SciPost Phys. **12**, 080 (2022).
[25] P. Jordan and E. Wigner, Zeitschrift für Physik **47**, 631 (1928).
[26] T. Holstein and H. Primakoff, Phys. Rev. **58**, 1098 (1940).
[27] T. Giamarchi, Quantum Physics in One Dimension, International Series of Monographs on Physics (Clarendon Press, 2004).
[28] G. Giachetti, A. Trombettoni, S. Ruffo, and N. Defenu, Phys. Rev. B **106**, 014106 (2022).
[29] A. M. Lobos, A. Iucci, M. Müller, and T. Giamarchi, Phys. Rev. B **80**, 214515 (2009).
[30] B. Horovitz, T. Giamarchi, and P. Le Doussal, Phys. Rev. Lett. **111**, 115302 (2013).
[31] B. Horovitz, T. Giamarchi, and P. Le Doussal, Phys. Rev. Lett. **121**, 166803 (2018).
[32] M. A. Cazalilla, F. Sols, and F. Guinea, Phys. Rev. Lett. **97**, 076401 (2006).
[33] R. Feynman, Statistical Mechanics: A Set Of Lectures, Advanced Books Classics (Avalon Publishing, 1998).
[34] For more details, see O. Bouverot-Dupuis, S. Majumdar, A. Rosso and, L. Foini, in preparation.
[35] E. V. H. Doggen, G. Lemarié, S. Capponi, and N. Laflorencie, Phys. Rev. B **96**, 180202 (2017).
[36] E. Malatsetxebarria, Z. Cai, U. Schollwöck, and M. A. Cazalilla, Phys. Rev. A **88**, 063630 (2013).

Résumé en Français

La découverte de la localisation dans les systèmes quantiques et classiques demeure majeure à ce jour. Le phénomène a été introduit par P.W. Anderson dans son article fondateur de 1958 [1], dans lequel il était démontré que la fonction d'onde d'un seul degré de liberté quantique (tel qu'une particule ou un spin) cessait de diffuser spatialement dans un réseau en présence d'impuretés (modélisées par un potentiel local et aléatoire). Dans ce cas, la fonction d'onde du degré de liberté ψ décroît exponentiellement sur une longueur charactéristique finie comme $\sim e^{-x/\xi}$, où ξ est la 'longueur de localisation' qui quantifie l'extension spatiale de la localisation du système. Ce travail a été approfondi dans la fameuse lettre du 'Gang of Four' [2], qui démontre, via un argument d'échelle, l'impossibilité d'avoir une transition de localisation à température finie dans les conditions suivantes : un système sans interaction, ayant un 'bord de mobilité' ('mobility edge') et en dimension spatiale $d \geq 3$. Cela a d'abord donné l'impression que les transitions de phase de localisation étaient absentes des systèmes quantiques unidimensionnels; cependant, dans le célèbre modèle Aubry-André-Harper [3–5], il a été montré qu'un bord de mobilité peut exister dans les systèmes quantiques unidimensionnels en présence d'un potentiel quasi-périodique, c'est-à-dire un potentiel ayant une période incommensurable avec celle du réseau. En outre, l'existence d'une transition de phase localisée-délocalisée à température zéro a été prouvée dans les systèmes désordonnés de dimensions inférieures et en présence d'interaction. Des exemples importants de ces phénomènes ont été trouvés en une dimension dans la transition de verre de Bose-superfluide en présence d'interactions dans des systèmes bosoniques, d'abord de manière analytique [6, 7] puis numérique [8]. Dans les systèmes fermioniques, il a été démontré que des chaînes fermioniques couplées, avec et sans spin, présentent une transition entre des phases localisée et supraconductrice [9], en particulier lorsque l'interaction est de nature attractive.

L'un des nombreux aspects intéressants de ce phénomène est que le système devient isolant car le transport est rendu impossible par l'absence de diffusion dans la phase localisée. Jusqu'à

présent, la localisation a été observée dans différents systèmes présentant un désordre statique (gelé). Mais peut-elle être induite à température nulle dans un système 1D couplé à des bains dissipatifs? Intuitivement, on peut comprendre que l'environnement puisse être assimilé à une source de phonons (ou à de simples oscillateurs harmoniques). Si ces phonons sont couplés au système de telle sorte que chaque degré de liberté du système possède son propre réservoir de phonons indépendant des autres, ils agissent alors comme un potentiel local, dynamique et aléatoire (désordre recuit) pour le système. En particulier, si les phonons sont dynamiquement lents, ils peuvent, dans une limite de couplage fort, inhiber les propriétés de transport du système, induisant une transition de phase. C'est ce scénario que nous abordons dans cette thèse.

Notre travail est également motivé par le point de vue des systèmes quantiques ouverts. Le formalisme que nous adoptons dans cette thèse tient compte de l'environnement d'une manière non markovienne et non perturbative. Celui-ci a été introduit pour la première fois par A.O. Caldeira et A.J. Leggett dans leur travail sur le mouvement brownien quantique [23], où ils ont montré que l'équation de Langevin correspondant à la version quantique du mouvement brownien $m\frac{d^2x}{dt^2} + \alpha\frac{dx}{dt} + V'(x) = F(t)$ (où m est la masse de la particule, α est une constante d'amortissement, V est un potentiel générique et F est la force aléatoire avec la corrélation $\langle F(t)F(t')\rangle = \frac{1}{2\pi}\int e^{-i\omega(t-t')}\alpha\hbar\omega\coth\left(\frac{\hbar\omega}{2KT}\right)$) peut être transposée à un système en contact avec un réservoir via le formalisme de l'intégrale de chemin de Feynman-Vernon [24]. Plus précisément, le système dissipatif est composé d'une particule dans un potentiel V(x) couplée à un bain d'oscillateurs harmoniques simples, donné par le Hamiltonien :

$$\begin{aligned} H_{\text{sys}} &= \frac{p^2}{2m} + V(x) \\ H_{\text{bain}} &= \frac{1}{2}\sum_k \left[\frac{P_k^2}{M_k} + M_k\Omega_k^2 R_k^2\right] \\ H_{\text{SB}} &= x\sum_k C_k R_k \end{aligned}$$

où R_k, Ω_k et P_k sont respectivement le déplacement, la fréquence propre et l'impulsion du k-ème oscillateur dans le réservoir. C_k représente l'énergie de couplage de la particule au k-ème oscillateur. Caldeira et Leggett ont montré que ces deux systèmes, la particule brownienne et le système dissipatif, sont équivalents lorsque la densité spectrale de basse énergie des oscillateurs harmoniques, définie par $J(\omega) = \frac{\pi}{2}\sum_k \frac{C_k^2}{m_k\Omega_k}\delta(\omega - \Omega_k)$, est linéairement proportionnelle à la fréquence comme $\alpha\omega$. Dans ce cas, l'effet du bain est équivalent à celui d'une résistance dans un circuit électrique. C'est pourquoi ce type d'environnement a été qualifié de 'bain ohmique'.

Ce travail a suscité de nombreux développements intéressants [25–27], dont une étude des systèmes dissipatifs à deux états [28]. Ce modèle est actuellement connu sous le nom de modèle 'Spin-Boson', où le système à deux états considéré est une unique particule quantique de spin-1/2 dans un champ magnétique constant le long des directions z et x: $H_{\rm sys} = \frac{1}{2}\left(\epsilon\sigma^z - \hbar\Delta_o\sigma^z\right)$. La dissipation pour ce modèle est la même que pour le mouvement brownien quantique (décrit par $H_{\rm bain}$), et le couplage entre le bain et le système est donné par $H_{\rm SB} = \frac{1}{2}\sigma^z \sum_k C_k R_k$, c'est-à-dire que la coordonnée de la particule brownienne est remplacée par la composante z du spin. Dans certaines limites, ce système peut être mis en correspondance avec un système où une particule se trouve dans un potentiel à double puits. En l'absence de dissipation et dans la limite $\hbar\Delta_0/\epsilon \gg 1$, on sait que le spin oscille constamment entre l'état de spin haut et l'état de spin bas (ce qui revient à dire que la particule saute entre le puits gauche et le puits droit du potentiel). Plus précisément, si $P(t)$ représente la différence entre la probabilité de trouver le spin (particule) dans l'état de spin haut (puits de gauche) et dans l'état de spin bas (puits de droite), alors $P(t) = \cos\Delta_0 t$, en supposant que $P(0) = 1$. Cependant, ce comportement change radicalement lorsque le système est couplé à un bain dissipatif ayant une fonction spectrale de la forme plus générale $J(\omega) \sim \alpha\omega^s$. La dynamique du bain peut être contrôlée dans ce contexte par l'exposant s ; une valeur plus petite de s dénote un bain avec une dynamique plus lente. Ce type d'environnement contraste avec l'image de la mesure aléatoire expliquée précédemment, où la dissipation est instantanée et correspond à $J(\omega) = const.$ En référence à [23], le cas correspondant à $s = 1$ est appelé un 'bain ohmique', $1 < s < 2$ est appelé 'le bain superohmique' et $0 < s < 1$ est appelé un 'bain subohmique'. L'un des résultats intéressants du modèle spin-boson est qu'à une température nulle, pour un bain subohmique, le spin conserve la mémoire de son état initial au lieu d'osciller entre les deux états (en d'autres termes, la particule reste localisée dans le puits où elle se trouvait initialement). Cela peut être interprété comme une signature de localisation induite par la dissipation dans un système quantique à zéro dimension. Cela va à l'encontre du consencus général de l'époque, car il avait été démontré précédemment que des phonons acoustiques délocalisés pouvaient induire une conductivité non nulle dans un système localisé par un mécanisme connu sous le nom de 'Variable Range Hopping' [29–31].

Notre travail a été d'étendre ce travail aux systèmes unidimensionnels en interaction. Une autre série de questions que nous voulions aborder était la suivante: ces bains dissipatifs peuvent-ils induire une transition de phase à température nulle ? Si oui, est-il possible d'avoir une bonne description effective de la phase à basse énergie ? Enfin, quelles sont les propriétés thermodynamiques et dynamiques de cette nouvelle phase dissipative ? Nous répondons ici à ces questions

et montrons que les résultats corroborent le scénario de localisation décrit précédemment.

Panorama de la thèse

Nous présentons ici une vue d'ensemble du travail, qui servira de guide pour orienter les lecteurs à travers les chapitres de cette thèse. Dans le chapitre 1, nous décrivons en détail l'état actuel de l'art dans le domaine des 'systèmes quantiques ouverts', qui traite de la caractérisation du comportement des modèles et matériaux quantiques en présence d'un environnement externe. Cet environnement peut se présenter sous la forme de mesures, ou sous la forme de phonons externes se couplant avec le système, et nous discuterons de ces approches en détail, tout en rendant notre formulation de l'environnement plus compacte d'un point de vue mathématique.

Le chapitre 2 présente le modèle quantique que nous étudions, à savoir une chaîne de spin XXZ 1D couplée à des bains dissipatifs locaux. Ces bains agissent sur le système comme un désordre recuit ou dynamique. Nous introduisons une technique importante appelée 'bosonisation' et l'appliquons à la chaîne de spin pour obtenir une théorie des champs classique à deux dimensions. Dans ce scénario, l'effet des bains locaux est capturé par un potentiel en cosinus à longue portée agissant seulement le long de la direction du temps imaginaire, et nous soutenons qu'il est capable d'induire une transition de phase sur le liquide de Luttinger déjà existant en brisant spontanément la symétrie à température zéro. Nous montrons également que deux limites de ce modèle doivent être clairement différenciées : l'action issue de la théorie des champs effective pour la chaîne de spin doit être étudiée séparément selon que l'on considère une magnétisation nulle ou une magnétisation finie.

Pour décrire la transition de phase et la nouvelle phase dissipative, nous utilisons des techniques analytiques et numériques que nous décrivons en détail au chapitre 3. En particulier, nous utilisons le groupe de renormalisation (GR) perturbatif et une méthode d'approximation variationnelle. A titre d'exemple, nous montrons l'application de ces méthodes au célèbre modèle de sine-Gordon, qui peut être vu comme une limite non-dissipative du système que nous étudions. Dans la dernière section, nous abordons la théorie de la dynamique de Langevin, qui est à la base de nos simulations numériques. Nous montrons que cette méthode peut être utilisée comme une technique de Monte-Carlo pour notre système et qu'elle peut nous aider à échantilloner l'espace des configurations de l'action.

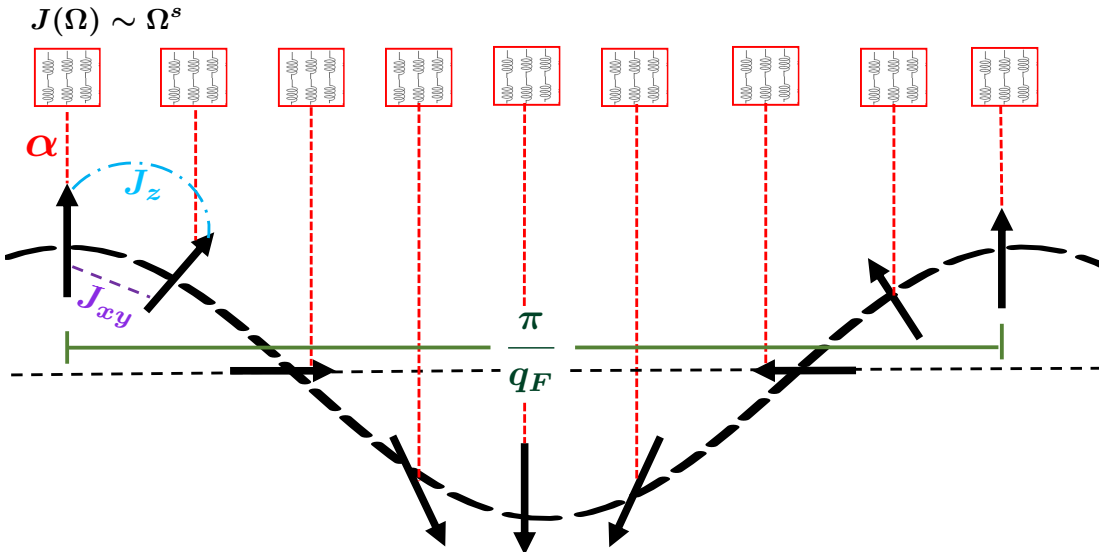

Figure 6.4: Schéma de la phase dissipative. Les flèches noires désignent les spins et les boîtes rouges les bains dissipatifs de Caldeira-Leggett. La phase dissipative est un SDW sans gap avec un ordre à longue portée avec une périodicité π/q_F.

Nous nous concentrons sur l'étude du système à magnétisation finie dans les deux chapitres suivants (chapitres 4 et 5). En utilisant le GR perturbatif, nous localisons un point critique de type Berezinski-Kosterlitz-Thouless. Cela nous indique que dans l'espace de phase du couplage dissipatif et du paramètre de Luttinger, soit le système reste dans la phase liquide de Luttinger originale avec des paramètres renormalisés, soit il part dans une nouvelle phase dissipative où le potentiel en cosinus devient pertinent. Dans la phase liquide de Luttinger, la procédure de renormalisation indique que la valeur du paramètre de Luttinger est réduite. Des effets similaires ont été étudiés dans [10], où il a été montré que le paramètre de Luttinger K d'un liquide de Luttinger est réduit à K' lorsque le système est couplé à un environnement dissipatif externe avec une résistance finie R comme $1/K' = 1/K + (e^2R)/h$. D'autre part, pour comprendre la phase dissipative, nous utilisons une analyse variationnelle de l'action, et trouvons que les excitations de basse énergie de cette phase peuvent être décrites par une action gaussienne sans gap et avec un terme fractionnaire en les fréquences de Matsubara. Pour caractériser la phase dissipative, nous analysons ses propriétés thermodynamiques et dynamiques telles que la susceptibilité, la corrélation spin-spin, la conductivité, la rigidité de la charge, etc. Nous définissons un paramètre d'ordre pour la transition de phase, que nous relions à l'amplitude d'une densité de spin via la bosonisation. Comme cette quantité reste finie à température zéro et dans la limite thermodynamique dans la phase dissipative, nous soutenons que cette phase

est une onde de densité de spin sans gap (fig. (6.4)) avec une susceptibilité inaltérée et une densité superfluide nulle. Dans le cas d'un bain subohmique, la conductivité DC de la phase dissipative s'annulle, signalant une transition de phase conducteur-isolant. En outre, nous simulons l'action avec le potentiel en cosinus pour générer des configurations équilibrées par cette action. Nous étayons nos prédictions analytiques en calculant les fonctions de corrélation susmentionnées à partir de ces configurations générées numériquement. Ces travaux ont donné lieu à une publication [11] et à une préimpression [12].

Le 6ème chapitre se concentre sur une autre limite de ce modèle, où l'on considère la chaîne de spin XXZ à une magnétisation nulle. Ce travail est actuellement en cours, mais nous sommes en mesure de prédire que dans ce scénario, la physique à température zéro du système s'avère être très différente de la situtation à magnétisation finie décrite précédemment. En particulier, l'onde de densité de spin sans gap est remplacée par une phase gappée, que nous pensons être antiferromagnétique (isolant de Mott). Nous fournissons des preuves numériques préliminaires pour appuyer ce résultat. Tous les résultats importants de la thèse ont été mis en évidence par des encadrés.

Appendix A

Details of Bosonization

In Chapter 2, we limit our discussion to the application of bosonization to our model. In this appendix, we discuss certain details of bosonization that can be referred to understand different technical aspects of the technique.

A.1 Commutation of density fluctuation operators

Previously, we have defined $\rho_r^\dagger(q) = \sum\limits_k c_{r,k+q}^\dagger c_{r,q}$ and $\rho_r(q) = \rho_r^\dagger(-q), r = \pm$ to be the density fluctuation creation and destruction operators, respectively. Here we show the calculation of the commutation relationship of $\left[\rho_r^\dagger(q), \rho_r(-q)\right] = \left[\rho_r^\dagger(q), \rho_r^\dagger(-q')\right]$, which will highlight the bosonic nature of these operators and the importance of normal ordering. Using $[AB, C] = A\{B, C\} - \{A, C\}B$ and usual fermionic commutation relationships, we find that:

$$\begin{aligned}
\left[\rho_r^\dagger(q), \rho_r^\dagger(-q')\right] &= \sum_{k_1,k_2} \left[c_{r,k_1+q}^\dagger c_{r,k_1}, c_{r,k_2-q'}^\dagger c_{r,k_2}\right] \\
&= \sum_{k_1,k_2} \left(c_{r,k_1+q}^\dagger \left\{c_{r,k_1}, c_{r,k_2-q'}^\dagger\right\} c_{r,k_2} - c_{r,k_2-q'}^\dagger \left\{c_{r,k_1+q}^\dagger, c_{r,k_2}\right\} c_{r,k_1}\right) \\
&= \sum_{k_1,k_2} \left(c_{r,k_1+q}^\dagger c_{r,k_2} \delta_{k_1,k_2-q'} - c_{r,k_2-q'}^\dagger c_{r,k_1} \delta_{k_1+q,k_2}\right) \\
&= \sum_{k_2} \left(c_{r,k_2+q-q'}^\dagger c_{r,k_2} - c_{r,k_2-q'}^\dagger c_{r,k_2-q}\right) \qquad \text{(A.1)}
\end{aligned}$$

At first glance, it seems that one can redefine the variable $k_2 - q' \to k_2'$ in the first term and that cancels out the second term exactly. However, that is not feasible here as there is an

infinite number of states due to the linear nature of the dispersion of the Tomonaga-Luttinger hamiltonian (eq. (2.18)). Hence, we need to use normal ordering to get the correct commutation relationship. Doing that, the normal-ordered operators cancel each other and the commutator is given by:

$$\begin{aligned}\left[\rho_r^\dagger(q),\rho_r^\dagger(-q')\right] &= \sum_{k_2}\left(\langle 0|\, c^\dagger_{r,k_2+q-q'}c_{r,k_2}\,|0\rangle - \langle 0|\, c^\dagger_{r,k_2-q'}c_{r,k_2-q}\,|0\rangle\right)\\ &= \delta_{q,q'}\left(\langle 0|\, c^\dagger_{r,k_2}c_{r,k_2}\,|0\rangle - \langle 0|\, c^\dagger_{r,k_2-q}c_{r,k_2-q}\,|0\rangle\right)\\ &= -\delta_{q,q'}\frac{rLq}{2\pi}\end{aligned} \tag{A.2}$$

We see that the commutation relationship $\left[\rho^\dagger(q),\rho(q')\right] = \delta_{q,-q'}$ is bosonic upto some normalization constant. This tells us the validity of the $\rho(q)$ operators as a basis for the construction of bosonic operators.

A.2 Exact form of the bosonic operators

This section will act as a set of dictionaries for mapping out exact relationships between different relevant operators. In the basis of $\rho_r(q)$, the bosonic operators are given by:

$$\begin{aligned}b_q^\dagger &= \left(\frac{2\pi}{L|p|}\right)^{\frac{1}{2}}\sum_r Y(rq)\rho_r^\dagger(q)\\ b_q &= \left(\frac{2\pi}{L|p|}\right)^{\frac{1}{2}}\sum_r Y(rq)\rho_r(q)\end{aligned} \tag{A.3}$$

Where Y is the step function. One can also map the bosonic fields ϕ and θ to the density fluctuation operators in the following way:

$$\begin{aligned}\phi(x) &= -\frac{\pi}{L}\left[\left(N_+ + N_-\right)x + i\sum_{q\neq 0}\frac{e^{-\frac{a|q|}{2}-iqx}}{q}\left(\rho_+^\dagger(q)+\rho_-^\dagger(q)\right)\right]\\ \theta(x) &= \frac{\pi}{L}\left[\left(N_+ - N_-\right)x + i\sum_{q\neq 0}\frac{e^{-\frac{a|q|}{2}-iqx}}{q}\left(\rho_+^\dagger(q)-\rho_-^\dagger(q)\right)\right]\end{aligned} \tag{A.4}$$

Where $N_\pm$ are the number of particles on the corresponding bands and a is a UV cut-off for the momentum, usually taken as the lattice spacing. In the thermodynamic continuum limit

$L \to \infty, a \to 0$, it is easy to see that:

$$\begin{aligned} \nabla\phi(x) &= -\pi\left[\rho_+(x) + \rho_-(x)\right] = -\pi\left[\psi_+^\dagger(x)\psi_+(x) + \psi_-^\dagger(x)\psi_-(x)\right] && \text{(A.5)} \\ \nabla\theta(x) &= \pi\left[\rho_+(x) - \rho_-(x)\right] = \pi\left[\psi_+^\dagger(x)\psi_+(x) - \psi_-^\dagger(x)\psi_-(x)\right] && \text{(A.6)} \end{aligned}$$

Where $\psi_\pm^\dagger(x)$ are single-particle creation operators. We finally check one more commutation relationship in the thermodynamic limit:

$$\begin{aligned} [\phi(x_1), \nabla\theta(x_2)] &= i\int_0^\infty dq \cos\left(q\left(x_2 - x_1\right)\right) e^{-a|q|} \\ &= i\pi\delta(x_2 - x_1) && \text{(A.7)} \end{aligned}$$

This confirms that $\Pi(x) = \frac{1}{\pi}\nabla\theta(x)$ is the canonically conjugate momemntum to $\phi(x)$.

Appendix B

Details of Path Integral and Correlation functions

B.1 Gaussian integral over complex variable

In this section, we will show how to compute a Gaussian integral of the form

$$Z = \int \mathcal{D}\phi\,(x,\tau)\, e^{-\frac{1}{2\pi K}\int d\tau dx\left[u(\nabla\phi(x,\tau))^2+\frac{1}{u}(\partial_\tau\phi(x,\tau))^2\right]} \tag{B.1}$$

To solve this integral, first, we apply the following fourier transform on the field $\phi(x,\tau) = \frac{1}{\beta L}\sum_{q,\omega_n}\phi(q,\omega_n)e^{i(qx-\omega_n\tau)}$. Using this and changing the path integral measure, the Gaussian integral transforms into

$$\begin{aligned} Z &= \left[\prod_{q,\omega_n}\mathcal{N}\int\mathcal{D}\phi\,(q,\omega_n)\,\mathcal{D}\phi^*\,(q,\omega_n)\right] e^{-\frac{1}{2\pi K\beta L}\sum\limits_{q,\omega_n} G^{-1}(q,\omega_n)|\phi(q,\omega_n)|^2} \\ &= \prod_{q,\omega_n}\left[\mathcal{N}\int\mathcal{D}\phi\,(q,\omega_n)\,\mathcal{D}\phi^*\,(q,\omega_n)\, e^{-\frac{1}{2\pi K\beta L}G^{-1}(q,\omega_n)|\phi(q,\omega_n)|^2}\right] \end{aligned} \tag{B.2}$$

Where $\phi^*(q,\omega_n) = \phi(-q,-\omega_n)$ as the field is real, $\mathcal{N}$ is a normalization constant coming from the change of the path integral measure, which can be chosen accordingly, and $G^{-1}(q,\omega_n) = (uq^2+\omega_n^2/u)$ is the propagator of the LL. In the last step of eq. (B.2), we convert the sum inside the exponential into a product, which turns the path integral into the product of independent Gaussian integrals. Each of these Gaussian integral produces a factor of $\pi\sqrt{2K\beta LG(q,\omega_n)}$, and

hence the complete integral is given by:

$$Z = \prod_{q,\omega_n} \mathcal{N}\pi\sqrt{2K\beta LG(q,\omega_n)} \tag{B.3}$$

B.2 Behaviour of roughness function in the LL phase

The spatial and temporal roughness functions, $B(x)$ and $B(\tau)$, are respectively defined as:

$$B(x) = \langle[\phi(x,\tau) - \phi(0,\tau)]^2\rangle \tag{B.4}$$

$$B(\tau) = \langle[\phi(x,\tau) - \phi(x,0)]^2\rangle \tag{B.5}$$

Before we proceed with the calculation, I will note down an important formula below, which will be used repeatedly throughout the thesis for calculating different correlation functions. This formula is for calculating a two-point correlation function in the fourier space for a gaussian action:

$$\begin{aligned}\langle\phi^*(q_1,\omega_{n_1})\phi(q_2,\omega_{n_2})\rangle &= \frac{\int \mathcal{D}\phi[q]\phi^*(q_1,\omega_{n_1})\phi(q_2,\omega_{n_2})e^{-\frac{1}{2}\sum\limits_{q,\omega_n}\phi^*(q,\omega_n)A(q,\omega_n)\phi(q,\omega_n)}}{\int \mathcal{D}\phi[q]e^{-\frac{1}{2}\sum\limits_{q,\omega_n}\phi^*(q,\omega_n)A(q,\omega_n)\phi(q,\omega_n)}} \\ &= A^{-1}(q_1,\omega_{n_1})\delta_{q_1,q_2}\delta_{\omega_{n_1},\omega_{n_2}}\end{aligned} \tag{B.6}$$

With this formula, we are ready to compute the correlation functions of eq. (B.4) and eq. (B.5). I will show a step-by-step derivation of $B(x)$ here, $B(\tau)$ can be obtained similarly. First, we do a fourier transform of the field $\phi(x,\tau) = \frac{1}{\beta L}\sum\limits_{q,\omega_n} e^{i(qx-\omega_n\tau)}\phi(q,\omega_n)$. Plugging this back, we obtain:

$$\begin{aligned}B(x) &= \frac{1}{(\beta L)^2}\left\langle\left[\sum_{q_1,\omega_{n_1}} e^{i\left(q_1x-\omega_{n_1}\tau\right)}\phi(q_1,\omega_{n_1}) - \sum_{q_2,\omega_{n_2}} e^{-i\omega_{n_2}\tau}\phi(q_2,\omega_{n_2})\right]^2\right\rangle \\ &= \frac{1}{(\beta L)^2}\sum_{\substack{q_1,\omega_{n_1}\\ q_2,\omega_{n_2}}}\langle\phi(q_1,\omega_{n_1})\phi(q_2,\omega_{n_2})\rangle\left(e^{i\left(q_1x-\omega_{n_1}\tau\right)} - e^{-i\omega_{n_1}\tau}\right)\left(e^{i\left(q_2x-\omega_{n_2}\tau\right)} - e^{-i\omega_{n_2}\tau}\right)\end{aligned}$$

A quadratic action can be generally written as $S = \frac{1}{2\beta L}\sum_{q,\omega_n} \phi^*(q,\omega_n)G^{-1}(q,\omega_n)\phi(q,\omega_n)$. Using eq. (B.6), we obtain:

$$\begin{aligned} B(x) &= \frac{1}{\beta L}\sum_{\substack{q_1,\omega_{n_1}\\ q_2,\omega_{n_2}}} \left(e^{i\left(q_1 x-\omega_{n_1}\tau\right)} - e^{-i\omega_{n_1}\tau}\right)\left(e^{i\left(q_2 x-\omega_{n_2}\tau\right)} - e^{-i\omega_{n_2}\tau}\right)\delta_{q_1,-q_2}\delta_{\omega_{n_1},-\omega_{n_2}}G(q_1,\omega_{n_1}) \\ &= \frac{2}{\beta L}\sum_{q,\omega_n}\left(1-\cos\left(qx\right)\right)G(q,\omega_n) \end{aligned} \tag{B.7}$$

Similarly, it can be shown that the temporal roughness function in Fourier space can be written as:

$$B(\tau) = \frac{2}{\beta L}\sum_{q,\omega_n}\left(1-\cos\left(\omega_n\tau\right)\right)G(q,\omega_n) \tag{B.8}$$

Together for a general form of the roughness function $B(x,\tau) = \langle[\phi(x,\tau)-\phi(0,\tau)]^2\rangle$, it can be shown that $B(x,\tau) = \frac{2}{\beta}\sum_{\omega_n}\int_{-\infty}^{\infty}\frac{dq}{2\pi}\left(1-\cos\left(qx+\omega_n\tau\right)\right)G(q,\omega_n)$, where we have already taken the thermodynamic limit $\frac{1}{L}\sum_q = \int_{-\infty}^{\infty}\frac{dq}{2\pi}$. In the LL phase, $G_{\rm LL} = \pi u K\left[(uq)^2+\omega_n^2\right]^{-1}$. To compute $B(x,\tau)$ in this phase, we introduce a large momentum cut-off Λ by multiplying a term $e^{-\Lambda|q|}$. Thus, the roughness function $B(x,\tau)$ can be equated to $KF_1(x,\tau)$, where $F_1(x,\tau)$ is given by:

$$\begin{aligned} F_1(r) &= \frac{u}{\beta}\sum_{n=-\infty}^{\infty}\int_{\infty}^{\infty}dq\frac{\left[(1-\cos(qx+\omega_n\tau)\right]}{\omega_n^2+u^2qk^2}\left(e^{-\Lambda|q|}\right) \\ &= \frac{2u}{\beta}\sum_{n=-\infty}^{\infty}\int_{0}^{\infty}dq\frac{\left[(1-\cos(qx-i(i\omega_n)\tau)\right]}{\omega_n^2+u^2q^2}\left(e^{-\Lambda q}\right) \end{aligned} \tag{B.9}$$

Where ω_n are the Bosonic matsubara frequencies $\frac{2\pi n}{\beta}$. We can compute the sum over ω_n using the matsubara sum technique [88]. Let's define $z = i\omega_n$. Now,

$$\begin{aligned} \cos(qx-i\omega_n\tau) &= \cos(qx)\cosh(z\tau) + i\sin(qx)\sinh(z\tau) \\ &= \cos(qx)\frac{e^{z\tau}+e^{-z\tau}}{2} + i\sin(qx)\frac{e^{z\tau}-e^{-z\tau}}{2} \\ &= \frac{e^{z\tau}}{2}e^{iqx} + \frac{e^{-z\tau}}{2}e^{-iqx} \end{aligned} \tag{B.10}$$

$$\implies F_1(r) = \frac{2u}{\beta}\sum_{n=-\infty}^{\infty}\int_{0}^{\infty}dq\frac{1-\frac{e^{iqx}}{2}e^{i\omega_n\tau}-\frac{e^{-iqx}}{2}e^{-i\omega_n\tau}}{\omega_n^2+u^2q^2}\left(e^{-\Lambda q}\right) \tag{B.11}$$

Let's take $\beta > \tau > 0$. In the second term of the numerator, set $\omega_n \to -\omega_n$. These won't affect the sum because we are summing over both positive and negative matsubara frequencies. Then

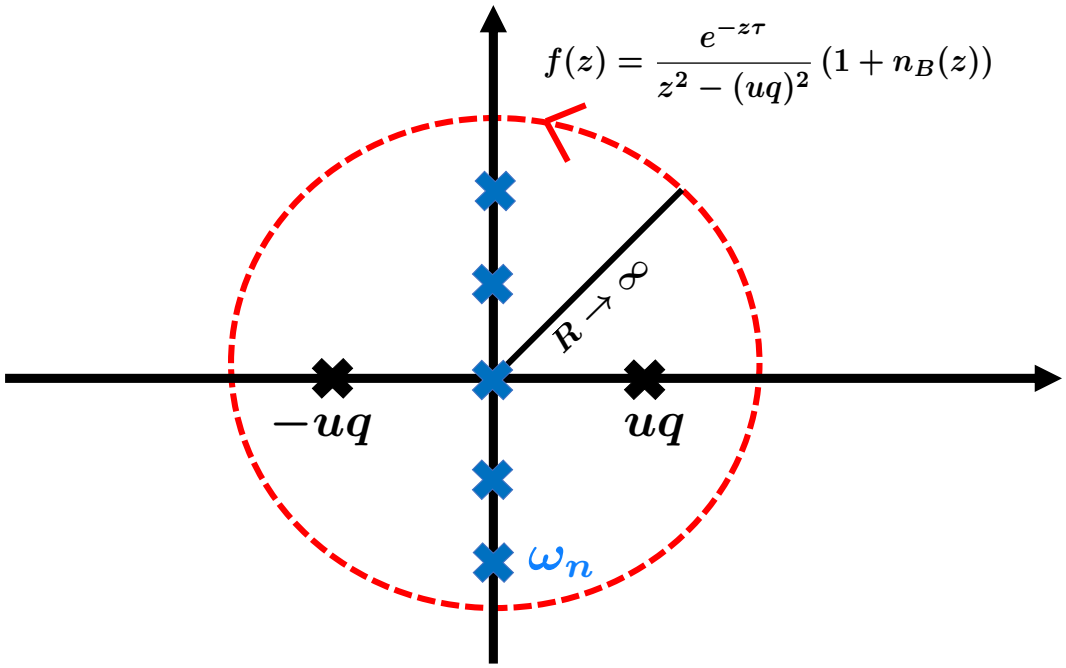

Figure B.1: Diagrammatic representation of the matsubara sum technique. The function $f(z)$ has two poles on the real axis uq and $-uq$; and the poles on the imaginary axis correspond to the matsubara frequencies ω_n. As the radius of the circle $R \to \infty$, the integral over the circle goes to 0, which lets us convert the sum over ω_n to a sum over q.

summing the second and third terms, we get:

$$F_1(x,\tau) = \frac{2u}{\beta}\sum_{n=-\infty}^{\infty}\int dq \frac{1-\cos(qx)e^{-i\omega_n\tau}}{\omega_n^2+u^2q^2}\left(e^{-\Lambda q}\right) \tag{B.12}$$

One can now make the observation that ω_n are the poles of the bose-einstein function $n_B(z) = 1/(e^{\beta z}-1)$; also $n_B(-z) = -(1+n_B(z))$. Thus, the sum over the Matsubara frequencies is given by:

$$\frac{1}{\beta}\sum_{n=-\infty}^{\infty}\frac{1}{\omega_n^2+u^2q^2} = \frac{n_B(uq)}{2uq} - \frac{n_B(-uq)}{2uq} = \frac{n_B(uq)}{uq} + \frac{1}{2uq} \tag{B.13}$$

$$\frac{1}{\beta}\sum_{n=-\infty}^{\infty}\frac{e^{-i\omega_n\tau}}{\omega_n^2+u^2q^2} = \frac{e^{-uq\tau}}{2uq} + \frac{1}{uq}\cosh(uq\tau)n_B(uq) \tag{B.14}$$

In these equations, to calculate (B.14) (let's call the sum S), We take a look at the function $\frac{e^{-z\tau}}{z^2-(uq)^2}(1+n_B(z))$. This function converges everywhere on the whole complex plane at this limit, so we calculate the integral $I = \lim_{R\to\infty}\oint \frac{dz}{2\pi i}\frac{e^{-z\tau}}{z^2-(uq)^2}(1+n_B(z))$. At this particular limit,

this integral is 0 by Jordan's lemma [111]. On the other hand, using the residue method [112], we get (fig. (B.1)) :

$$\begin{aligned} I &= -S + \frac{e^{-uq\tau}}{2uq}(1+n_B(uq)) - \frac{e^{uq\tau}}{2uq}(1+n_B(-uq)) \\ \Longrightarrow S &= n_B(uq)\frac{\cosh(uq\tau)}{uq} + \frac{e^{-uq\tau}}{2uq} \end{aligned} \tag{B.15}$$

Putting it back in (B.12), we get :

$$F_1(r) = \int_0^\infty dq \left(\frac{2n_B(uq)}{q}\left[1-\cos(qx)\cosh(uq\tau)\right] + \frac{1}{q}\left[1-\cos(qx)e^{-uq\tau}\right]\right) \tag{B.16}$$

In the zero temperature limit $\beta \to \infty$, $n_B(z) = 0$. Thus $F_1(x,\tau)$ reduces to $\int_0^\infty dq \frac{1}{q}\left[1-\cos(qx)e^{-uq\tau}\right]$. Now this integral can be calculated exactly, and thus the roughness function is given by:

$$B(x,\tau) = \frac{K}{2}\ln\left(\frac{x^2+(u|\tau|+a)^2}{a^2}\right) \tag{B.17}$$

B.3 Correlation of exponential functions

In this section, we will show how to compute a correlation function of the generalized form:

$$I = \left\langle e^{\,i\sum\limits_{x,\tau} A(x,\tau)\phi(x,\tau)} \right\rangle$$

By applying the fourier transformation $A(x,\tau) = \frac{1}{\beta L}\sum_{q,\omega_n} A(q,\omega_n)e^{i(qx-\omega_n\tau)}$, we find:

$$\begin{aligned} \sum_{x,\tau} A(x,\tau)\phi(x,\tau) &= \frac{1}{(\beta L)^2}\sum_{x,\tau}\sum_{\substack{q_1,\omega_{n_1}\\ q_2,\omega_{n_2}}} A(q_1,\omega_{n_1})\phi(q_2,\omega_{n_2})e^{i\left((q_1+q_2)x-(\omega_{n_1}+\omega_{n_2})\tau\right)} \\ &= \frac{1}{\beta L}\sum_{q,\omega_n} A(q,\omega_n)\phi(-q,-\omega_n) \end{aligned} \tag{B.18}$$

Assuming that we are calculating the correlation function with respect to a gaussian action of the form $S[\phi] = \frac{1}{2\beta L}\sum\limits_{q,\omega_n} \phi^*(q,\omega_n)G^{-1}(q,\omega_n)\phi(q,\omega_n)$. One can then re-write the correlation function as:

$$\begin{aligned} I &= \frac{1}{Z}\int \mathcal{D}\phi e^{-\frac{1}{2\beta L}\sum\limits_{q,\omega_n}\left(\phi^*(q,\omega_n)G^{-1}(q,\omega_n)\phi(q,\omega_n) - 2iA(q,\omega_n)\phi(-q,-\omega_n)\right)} \\ &= \frac{1}{Z}\int \mathcal{D}\phi e^{-\frac{1}{2\beta L}\sum\limits_{q,\omega_n}\left(\phi^*(q,\omega_n)G^{-1}(q,\omega_n)\phi(q,\omega_n) - iA(q,\omega_n)\phi(-q,-\omega_n) - iA(-q,-\omega_n)\phi(q,\omega_n)\right)} \end{aligned} \tag{B.19}$$

By performing the gaussian integral over ϕ, we find:

$$I = e^{-\frac{1}{2\beta L}\sum\limits_{q,\omega_n} A(-q,-\omega_n)G(q,\omega_n)A(q,\omega_n)} \tag{B.20}$$

Now let us calculate a different quantity $\left\langle \left(\sum\limits_{\vec{x}} A(\vec{x})\phi(\vec{x}) \right)^2 \right\rangle$, where we will use the shortened notation $\vec{x} = (x, \tau)$ and $\vec{q} = (q, \omega_n)$ for better presentation. This quantity can be fourier transformed to the following:

$$\begin{aligned}
\left\langle \left(\sum_{\vec{x}} A(\vec{x})\phi(\vec{x}) \right)^2 \right\rangle &= \sum_{\vec{x_1}\vec{x_2}} A(\vec{x_1})A(\vec{x_2})\langle \phi(\vec{x_1})\phi(\vec{x_2})\rangle \\
&= \frac{1}{(\beta L)^4} \sum_{\vec{x_1}\vec{x_2}} \sum_{\substack{\vec{q_1}\vec{q_2} \\ \vec{q_3}\vec{q_4}}} A(\vec{q_1})A(\vec{q_2}) \left\langle \phi(\vec{q_3})\phi(\vec{q_4}) \right\rangle e^{i((\vec{q_1}+\vec{q_3}).\vec{x_1}+(\vec{q_2}+\vec{q_4}).\vec{x_2})} \\
&= \frac{1}{(\beta L)^3} \sum_{\vec{x_1}\vec{x_2}} \sum_{\substack{\vec{q_1}\vec{q_2} \\ \vec{q_3}}} A(\vec{q_1})A(\vec{q_2})G(\vec{q_3}) e^{i((\vec{q_1}+\vec{q_3}).\vec{x_1}+(\vec{q_2}-\vec{q_3}).\vec{x_2})} \\
&= \frac{1}{\beta L} \sum_{\vec{q}} A(\vec{q})G(\vec{q})A(-\vec{q})
\end{aligned} \tag{B.21}$$

This is the same as the argument of the exponential in eq. (B.20). Hence comparing, we find the following equation, which is known from the computation of the Debye-Waller factor [113, 114]:

$$\left\langle e^{i\sum\limits_{x,\tau} A(x,\tau)\phi(x,\tau)} \right\rangle = e^{-\frac{1}{2}\left\langle \left(\sum\limits_{x,\tau} A(x,\tau)\phi(x,\tau) \right)^2 \right\rangle} \tag{B.22}$$

Appendix C

Numerical methods

In Section 3.3, we have discussed the physical concepts behind the numerical analysis of the dissipative systems. Namely, we write the associated Langevin equation for the dynamics of the field, which is a differential equation. In this appendix, we elaborate on the more technical details of the numerical procedure.

We start by discretizing the field $\phi(x,\tau)$, now described by the two indices $\phi_{ij}(t)$, where $i \in (1,\beta)$ and $j \in (1,L)$ represents the τ and x indices respectively of the original field theory. t represents the Langevin time, i.e., the time of the simulation, and should not be confused with the imaginary time τ. We take a flat surface as our initial condition, i.e., $\phi_{ij}(0) = 0 \; \forall \; (i,j)$. We also implement periodic boundary conditions in both x and τ direction, i.e. $\phi(i+\beta,j) = \phi(i,j)$ and $\phi(i,j+L) = \phi(i,j)$. In the discretized language, the Langevin differential equation is given by:

$$\begin{aligned}
\frac{d\phi_{ij}(t)}{dt} &= -\frac{\delta S_{\text{tot}}[\phi_{ij}]}{\delta\phi_{ij}} + \eta_{ij}(t) \\
&= \frac{1}{\pi K}\left[u\left(\phi_{i,j+1}(t) + \phi_{i,j-1}(t) - 2\phi_{i,j}(t)\right) + \frac{1}{u}\left(\phi_{i+1,j}(t) + \phi_{i-1,j}(t) - 2\phi_{i,j}(t)\right)\right] \\
&+ \frac{\alpha}{\pi^2}\sum_{i'} D\left(|i-i'|\right)\sin\left(2\left(\phi_{ij}(t) - \phi_{i'j}(t)\right)\right) + \eta_{ij}(t)
\end{aligned} \tag{C.1}$$

Where η_{ij} is a white gaussian noise with mean $\langle\eta_{ij}(t)\rangle = 0$ and variance $\langle\eta_{ij}(t)\eta_{i'j'}(t')\rangle = 2\delta_{i,i'}\delta_{j,j'}\delta_{t,t'}$ (note that the Langevin time t is discretized as well). $D\left(|i-i'|\right)$ is the discretized, periodic long-range kernel $1/|\tau-\tau'|^{1+s}$ and we discuss its implementation in the numerics in the next paragraph. From the principle of the Langevin equation, we expect the ϕ_{ij}, obtained by integrating eq. (C.1), to be equilibrated under S_{tot} (eq. (2.1)).

To discretize the long-range kernel correctly, we make an observation that it is equivalent to $|\omega_n|^s$ in the fourier space. The discretization of this term is obvious and it can be one by substituting $|\omega_n| = \sqrt{2\,(1-\cos\omega_n)}$. Now one can use the results from [115] to obtain for $\beta \to \infty$:

$$\begin{aligned} D(|i-i'|) &= \int_0^{2\pi} d\omega_n e^{i\omega_n(i-i')} \left[2\,(1-\cos\omega_n)\right]^{\frac{s}{2}} \\ &= \mathcal{B}\left(|i-i'| - \frac{s}{2}, s+1\right) \end{aligned} \tag{C.2}$$

Where $\mathcal{B}$ denotes the Beta function. Eq. (C.2) is discrete, but not β-periodic yet. To make $D(|i-i'|)$ symmetric with respect to $\beta/2$ and periodic, one can make the substitution $f(|i-i'|) \to \sum_{k=-\frac{\beta}{2}}^{\frac{\beta}{2}} f(|i-i'|+k\beta)$. This essentially sums the distance between two points on a circular lattice from different directions. Note that a trivial implementation of the periodic boundary condition can also be $|i-i'| \to \min\left(|i-i'|, \beta - |i-i'|\right)$. However, this makes the kernel very sharp by leaving a cusp at $|i-i'| = \beta/2$. On the other hand, our implementation smoothens $D(|i-i'|)$ at the point of symmetry and we have benchmarked it to be more efficient and precise for these simulations. Thus, the final form of the long-range kernel that we use in the numerical solution is given by:

$$D(|i-i'|) = \sum_{k=-\frac{\beta}{2}}^{\frac{\beta}{2}} \mathcal{B}\left(|i-i'| + k\beta - \frac{s}{2}, s+1\right) \tag{C.3}$$

To integrate eq. (C.1), we use the Runge-Kutta (RK) algorithm [116,117] which is an improved version of the Euler algorithm. This method calculates multiple slopes between n and $n+1$-th time step as opposed to the single slope calculation in Euler method, thus rendering this method faster and more accurate for integrating differential equations numerically. The second-order Runge-Kutta algorithm customized for gaussian white noise is well described in [118]. The reader is encouraged to look in the publication to understand the derivation of the algorithm, here we just write the formulation that we use in our numerical procedure:

$$\begin{aligned} \phi_{i,j}(t+dt) &= \phi(t) + \frac{dt}{2}\left[K_1 + K_2\right] + \sqrt{2\mathrm{dt}}\eta_{ij}(t) \\ K_1 &= F\left(\phi(t)\right) \\ K_2 &= F\left(\phi(t) + K_1 dt + \sqrt{2\mathrm{dt}}\eta_{ij}(t)\right) \end{aligned} \tag{C.4}$$

Where dt denotes the value of the increment in Langevin time and $F(\phi) = -\frac{\delta S_{\text{tot}}[\phi_{ij}]}{\delta \phi_{ij}}$ has already been described in eq. (C.1). For our simulations, we keep $dt = 0.05$. Note that in eq. (C.4), the noise is incremented with $\sqrt{dt}$, which we have already seen in Section 3.3. To benchmark the equation, we use the harmonic approximation $\sin[2(\phi_{ij} - \phi_{i'j})] \to 2(\phi_{ij} - \phi_{i'j})$. With this transformation, the problem becomes exactly solvable, thus making it possible to compare numerical results against analytical formulations.

Appendix D

Supplementary Results

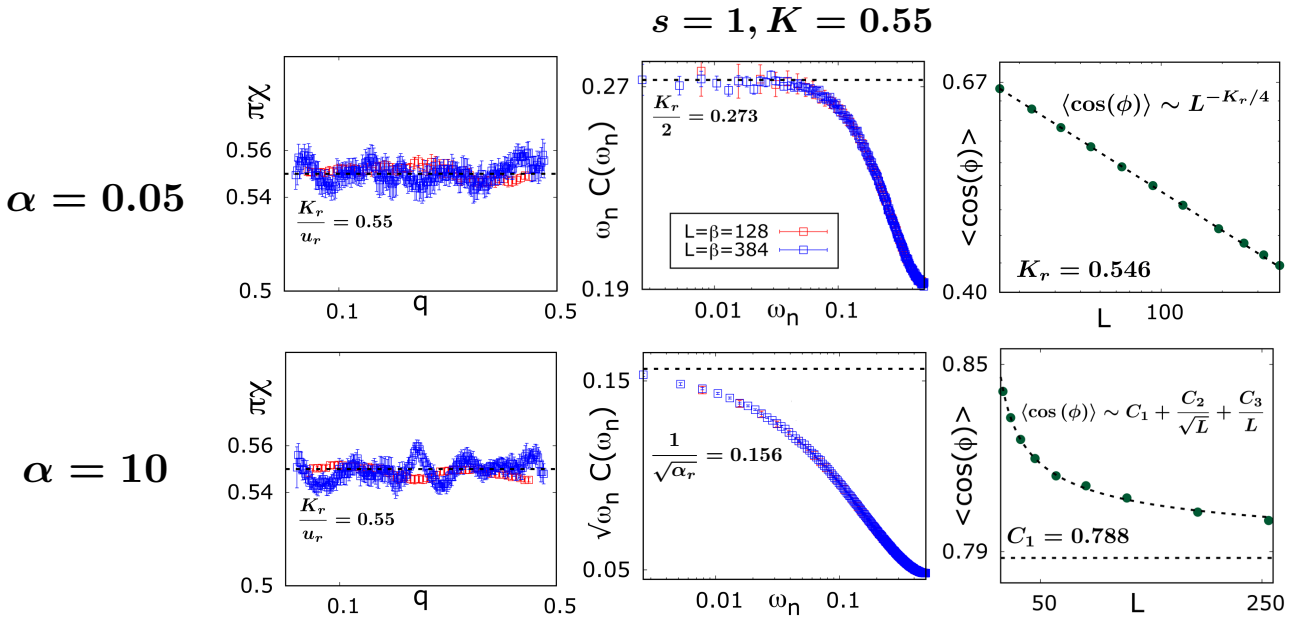

Figure D.1: Additional numerical results for the incommensurate Ohmic case with $K = 0.55$, $\alpha = 0.05$ (*top*) and $\alpha = 0.05$ (*bottom*). The system sizes correspond to $L = 128$ (*red*) and $L = 384$, and averages were done over 10000 to 12000 configurations. *left*: $\pi\chi = K_r/u_r$ is invariant for both values of α which shows the existence of statistical tilt symmetry in the system. *middle*: For small-ω_n, $\omega_n C(\omega_n)$ and $\sqrt{\omega_n} C(\omega_n)$ saturates to a constant $K_r/2 = 0.273$ and $1/\sqrt{\alpha_r} = 0.156$ for $\alpha = 0.05$ and $\alpha = 10$, respectively. *right*: For $\alpha = 0.05$, $\langle\cos\phi\rangle$ goes to zero as $L^{-K_r/4}$ with $K_r = 0.546$ and saturates to a constant $c_1 = 0.788$ as $c_1 + c_2/\sqrt{L} + c_3/L$ with $c_2 = 0.215$ and $c_3 = 0.012$.

In this appendix, we show additional numerical results that we obtained during our analysis of the incommensurate system in the presence of dissipative ohmic baths [11]. It's going to be a short section with similar numerical analysis as Section 5.3 for $s = 1, K = 0.55$, and $u = 1$.

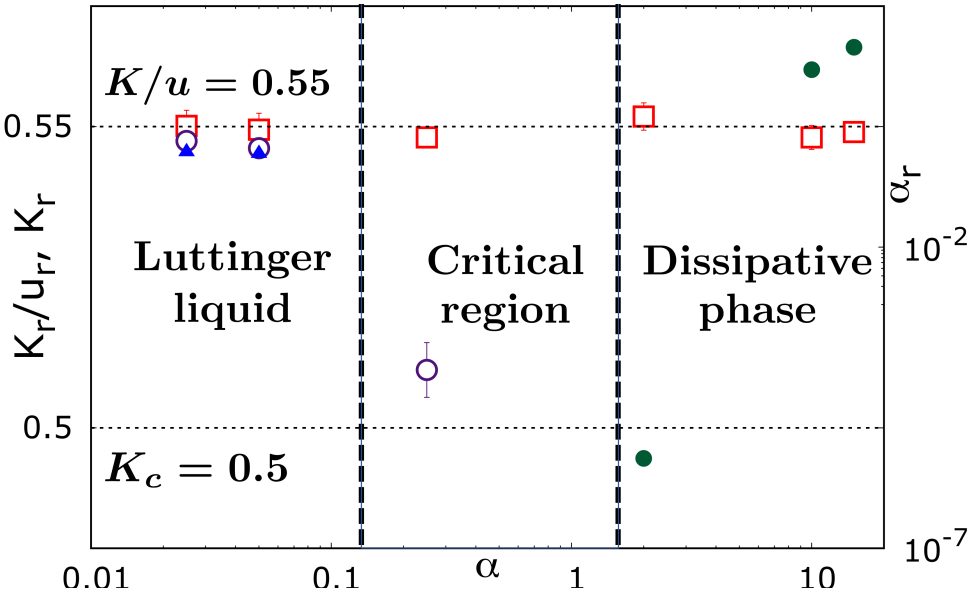

Figure D.2: Phase diagram of the incommensurate Ohmic case with $K = 0.55$. The ratio K_r/u_r (*red squares*) remains constant for all values of α. As α increases, K_r, both obtained from $\langle \cos 2\phi \rangle$ (*purple circles*) and $C(\omega_n)$ (*blue triangle*) decreases and approaches $K_c = 1/2$. In the dissipative phase, α_r increases (*green solid circles*) rapidly as α increases. We identify the critical regime for both cases to be $\alpha_C \in (0.25, 2)$.

Here we present the correlation functions for two values of α, i,e., $\alpha = 0.05$ and $\alpha = 10$. We scale $L = \beta$ for all the sizes.

Due to the incommensurate action having statistical tilt symmetry, the susceptibility $\chi = K_r/(u_r\pi)$ of the system remains invariant and independent from the value of α (fig. (D.1), *left*). However, fig. (D.1), *middle* tells us that for $\alpha = 0.05$, $\omega_n C(\omega_n)$ saturates to a constant $K_r/2 = 0.273$, whereas $\sqrt{\omega_n} C(\omega_n)$ goes to a constant for $\alpha = 10$. Thus, we understand that for $K = 0.55$, $\alpha = 0.05$ is in the LL phase and $\alpha = 10$ is in the dissipative phase. This is further supported by the order parameter $\langle \cos(\phi - \phi_{\mathrm{CoM}}) \rangle$, which decreases as a power law $L^{-K_r/4}$ with $K_r = 0.546$ for $\alpha = 0.05$ and saturates to a constant $c_1 = 0.788$ while decaying algebraically for $\alpha = 10$ (fig. (D.1), *right*). We find the corresponding phase diagram in fig. (D.2), where we see that as α is increased, K_r/u_r remains constant, but K_r decreases and flows towards $K_c = 0.5$. In the dissipative phase, α_r increases rapidly. From this behavior, we identify $\alpha_c \in (0.25, 2)$.

Bibliography

[1] P. W. Anderson, "Absence of diffusion in certain random lattices," *Phys. Rev.*, vol. 109, pp. 1492–1505, Mar 1958.

[2] E. Abrahams, P. W. Anderson, D. C. Licciardello, and T. V. Ramakrishnan, "Scaling theory of localization: Absence of quantum diffusion in two dimensions," *Phys. Rev. Lett.*, vol. 42, pp. 673–676, Mar 1979.

[3] S. Aubry and G. André, "Analyticity breaking and anderson localization in incommensurate lattices," 1980.

[4] P. G. Harper, "Single band motion of conduction electrons in a uniform magnetic field," *Proceedings of the Physical Society. Section A*, vol. 68, no. 10, p. 874, 1955.

[5] S. Ganeshan, J. H. Pixley, and S. Das Sarma, "Nearest neighbor tight binding models with an exact mobility edge in one dimension," *Phys. Rev. Lett.*, vol. 114, p. 146601, Apr 2015.

[6] T. Giamarchi and H. J. Schulz, "Localization and interaction in one-dimensional quantum fluids," *Europhysics Letters*, vol. 3, p. 1287, jun 1987.

[7] T. Giamarchi and H. J. Schulz, "Anderson localization and interactions in one-dimensional metals," *Phys. Rev. B*, vol. 37, pp. 325–340, Jan 1988.

[8] E. V. H. Doggen, G. Lemarié, S. Capponi, and N. Laflorencie, "Weak- versus strong-disorder superfluid—bose glass transition in one dimension," *Phys. Rev. B*, vol. 96, p. 180202, Nov 2017.

[9] E. Orignac and T. Giamarchi, "Effects of disorder on two strongly correlated coupled chains," *Phys. Rev. B*, vol. 56, pp. 7167–7188, Sep 1997.

[10] I. Safi and H. Saleur, "One-channel conductor in an ohmic environment: Mapping to a tomonaga-luttinger liquid and full counting statistics," *Phys. Rev. Lett.*, vol. 93, p. 126602, Sep 2004.

[11] S. Majumdar, L. Foini, T. Giamarchi, and A. Rosso, "Bath-induced phase transition in a luttinger liquid," *Phys. Rev. B*, vol. 107, p. 165113, Apr 2023.

[12] S. Majumdar, L. Foini, T. Giamarchi, and A. Rosso, "Localization induced by spatially uncorrelated subohmic baths in one dimension," 2023.

[13] B. Misra and E. C. G. Sudarshan, "The Zeno's paradox in quantum theory," *Journal of Mathematical Physics*, vol. 18, pp. 756–763, 08 2008.

[14] W. M. Itano, D. J. Heinzen, J. J. Bollinger, and D. J. Wineland, "Quantum zeno effect," *Phys. Rev. A*, vol. 41, pp. 2295–2300, Mar 1990.

[15] D. A. Huse, R. Nandkishore, F. Pietracaprina, V. Ros, and A. Scardicchio, "Localized systems coupled to small baths: From anderson to zeno," *Phys. Rev. B*, vol. 92, p. 014203, Jul 2015.

[16] A. Chan, R. M. Nandkishore, M. Pretko, and G. Smith, "Unitary-projective entanglement dynamics," *Phys. Rev. B*, vol. 99, p. 224307, Jun 2019.

[17] Y. Li, X. Chen, and M. P. A. Fisher, "Quantum zeno effect and the many-body entanglement transition," *Phys. Rev. B*, vol. 98, p. 205136, Nov 2018.

[18] X. Turkeshi, R. Fazio, and M. Dalmonte, "Measurement-induced criticality in $(2 + 1)$-dimensional hybrid quantum circuits," *Phys. Rev. B*, vol. 102, p. 014315, Jul 2020.

[19] B. Xing, X. Turkeshi, M. Schiró, R. Fazio, and D. Poletti, "Interactions and integrability in weakly monitored hamiltonian systems," 2023.

[20] H. Breuer and F. Petruccione, *The Theory of Open Quantum Systems*. Oxford University Press, 2002.

[21] X. Cao, A. Tilloy, and A. D. Luca, "Entanglement in a fermion chain under continuous monitoring," *SciPost Phys.*, vol. 7, p. 024, 2019.

[22] T. Maimbourg, D. M. Basko, M. Holzmann, and A. Rosso, "Bath-induced zeno localization in driven many-body quantum systems," *Phys. Rev. Lett.*, vol. 126, p. 120603, Mar 2021.

[23] A. Caldeira and A. Leggett, "Path integral approach to quantum brownian motion," *Physica A: Statistical Mechanics and its Applications*, vol. 121, no. 3, pp. 587–616, 1983.

[24] R. Feynman and F. Vernon, "The theory of a general quantum system interacting with a linear dissipative system," *Annals of Physics*, vol. 24, pp. 118–173, 1963.

[25] A. J. Bray and M. A. Moore, "Influence of dissipation on quantum coherence," *Phys. Rev. Lett.*, vol. 49, pp. 1545–1549, Nov 1982.

[26] S. Chakravarty, "Quantum fluctuations in the tunneling between superconductors," *Phys. Rev. Lett.*, vol. 49, pp. 681–684, Aug 1982.

[27] A. Schmid, "Diffusion and localization in a dissipative quantum system," *Phys. Rev. Lett.*, vol. 51, pp. 1506–1509, Oct 1983.

[28] A. J. Leggett, S. Chakravarty, A. T. Dorsey, M. P. A. Fisher, A. Garg, and W. Zwerger, "Dynamics of the dissipative two-state system," *Rev. Mod. Phys.*, vol. 59, pp. 1–85, Jan 1987.

[29] N. Mott, *Metal-insulator transitions*. CRC Press, 2004.

[30] A. L. Efros and B. I. Shklovskii, "Coulomb gap and low temperature conductivity of disordered systems," *Journal of Physics C: Solid State Physics*, vol. 8, p. L49, feb 1975.

[31] T. Nattermann, T. Giamarchi, and P. Le Doussal, "Variable-range hopping and quantum creep in one dimension," *Phys. Rev. Lett.*, vol. 91, p. 056603, Jul 2003.

[32] P. Jordan and E. Wigner, "Über das paulische äquivalenzverbot," *Zeitschrift für Physik*, vol. 47, pp. 631–651, 1928.

[33] L. Landau and E. Lifshitz, *Statistical Physics: Volume 5*. No. vol. 5, Elsevier Science, 2013.

[34] L. D. Landau, "The Theory of a Fermi Liquid," *Zh. Eksp. Teor. Fiz.*, vol. 30, no. 6, p. 1058, 1956.

[35] L. D. Landau, "Oscillations in a Fermi Liquid," *J. Exptl. Theoret.Phys.*, vol. 5, no. 1, p. 59, 1957.

[36] P. Coleman, *Landau Fermi-liquid theory*, p. 127–175. Cambridge University Press, 2015.

[37] T. Giamarchi, *Quantum physics in one dimension*. Internat. Ser. Mono. Phys., Oxford: Clarendon Press, 2004.

[38] A. Gogolin, A. Nersesyan, and A. Tsvelik, *Bosonization and Strongly Correlated Systems*. Cambridge University Press, 2004.

[39] H. Schulz, "Proceedings of les houches summer school lxi," 1995.

[40] S.-i. Tomonaga, "Remarks on Bloch's Method of Sound Waves applied to Many-Fermion Problems," *Progress of Theoretical Physics*, vol. 5, pp. 544–569, 07 1950.

[41] J. M. Luttinger, "An Exactly Soluble Model of a Many-Fermion System," *Journal of Mathematical Physics*, vol. 4, pp. 1154–1162, 12 2004.

[42] T. Matsubara, "A New approach to quantum statistical mechanics," *Prog. Theor. Phys.*, vol. 14, pp. 351–378, 1955.

[43] A. Altland and B. D. Simons, *Feynman path integral*, p. 95–155. Cambridge University Press, 2 ed., 2010.

[44] P. Coleman, *Finite-temperature many-body physics*, p. 234–291. Cambridge University Press, 2015.

[45] F. D. M. Haldane, "'luttinger liquid theory' of one-dimensional quantum fluids. i. properties of the luttinger model and their extension to the general 1d interacting spinless fermi gas," *Journal of Physics C: Solid State Physics*, vol. 14, p. 2585, jul 1981.

[46] E. L. Pollock and D. M. Ceperley, "Path-integral computation of superfluid densities," *Phys. Rev. B*, vol. 36, pp. 8343–8352, Dec 1987.

[47] F. D. M. Haldane, "General relation of correlation exponents and spectral properties of one-dimensional fermi systems: Application to the anisotropic $s = \frac{1}{2}$ heisenberg chain," *Phys. Rev. Lett.*, vol. 45, pp. 1358–1362, Oct 1980.

[48] T. Giamarchi and P. Le Doussal, "Elastic theory of flux lattices in the presence of weak disorder," *Phys. Rev. B*, vol. 52, pp. 1242–1270, Jul 1995.

[49] F. D. M. Haldane, "Effective harmonic-fluid approach to low-energy properties of one-dimensional quantum fluids," *Phys. Rev. Lett.*, vol. 47, pp. 1840–1843, Dec 1981.

[50] G. Giachetti, N. Defenu, S. Ruffo, and A. Trombettoni, "Berezinskii-kosterlitz-thouless phase transitions with long-range couplings," *Phys. Rev. Lett.*, vol. 127, p. 156801, Oct 2021.

[51] E. Bour, *Théorie de la déformation des surfaces*. 1862.

[52] V. E. Korepin, N. M. Bogoliubov, and A. G. Izergin, *Quantum Inverse Scattering Method and Correlation Functions*. Cambridge Monographs on Mathematical Physics, Cambridge: Cambridge University Press, 1993.

[53] S. Takada and S. Misawa, "The Quantum Sine-Gordon Model and the Fermi-Bose Relation," *Progress of Theoretical Physics*, vol. 66, pp. 101–117, 07 1981.

[54] P. Chaikin and T. Lubensky, *Principles of Condensed Matter Physics*. Cambridge University Press, 2000.

[55] J. José, "Sine-gordon theory and the classical two-dimensional $x - y$ model," *Phys. Rev. D*, vol. 14, pp. 2826–2829, Nov 1976.

[56] W. E. Thirring, "A soluble relativistic field theory," *Annals of Physics*, vol. 3, no. 1, pp. 91–112, 1958.

[57] S. Coleman, "Quantum sine-gordon equation as the massive thirring model," *Phys. Rev. D*, vol. 11, pp. 2088–2097, Apr 1975.

[58] T. Ohta, "Phase Transition in 2-D Sine-Gordon System," *Progress of Theoretical Physics*, vol. 60, pp. 968–974, 10 1978.

[59] V. L. Berezinskiĭ, "Destruction of Long-range Order in One-dimensional and Two-dimensional Systems having a Continuous Symmetry Group I. Classical Systems," *Soviet Journal of Experimental and Theoretical Physics*, vol. 32, p. 493, Jan. 1971.

[60] V. L. Berezinskiĭ, "Destruction of Long-range Order in One-dimensional and Two-dimensional Systems Possessing a Continuous Symmetry Group. II. Quantum Systems," *Soviet Journal of Experimental and Theoretical Physics*, vol. 34, p. 610, Jan. 1972.

[61] J. M. Kosterlitz and D. J. Thouless, "Ordering, metastability and phase transitions in two-dimensional systems," *Journal of Physics C: Solid State Physics*, vol. 6, p. 1181, apr 1973.

[62] J. M. Kosterlitz, "The critical properties of the two-dimensional xy model," *Journal of Physics C: Solid State Physics*, vol. 7, p. 1046, mar 1974.

[63] N. F. Mott and R. Peierls, "Discussion of the paper by de boer and verwey," *Proceedings of the Physical Society*, vol. 49, p. 72, aug 1937.

[64] N. F. Mott, "The basis of the electron theory of metals, with special reference to the transition metals," *Proceedings of the Physical Society. Section A*, vol. 62, p. 416, jul 1949.

[65] H. A. Bethe, "Zur theorie der metalle," *Zeitschrift für Physik*, vol. 71, pp. 205–226, 1931.

[66] R. J. Baxter, *Exactly solved models in statistical mechanics*. Elsevier, 2016.

[67] T. Barthel, "Precise evaluation of thermal response functions by optimized density matrix renormalization group schemes," *New Journal of Physics*, vol. 15, p. 073010, jul 2013.

[68] I. E. Dzyaloshinskiĭ and A. Larkin, "Correlation functions for a one-dimensional fermi system with long-range interaction (tomonaga model) - jetp 38, 202 (1974)," 1996.

[69] L. P. Kadanoff, "Scaling laws for ising models near T_c," *Physics Physique Fizika*, vol. 2, pp. 263–272, Jun 1966.

[70] K. G. Wilson, "The renormalization group: Critical phenomena and the kondo problem," *Rev. Mod. Phys.*, vol. 47, pp. 773–840, Oct 1975.

[71] J. V. José, L. P. Kadanoff, S. Kirkpatrick, and D. R. Nelson, "Renormalization, vortices, and symmetry-breaking perturbations in the two-dimensional planar model," *Phys. Rev. B*, vol. 16, pp. 1217–1241, Aug 1977.

[72] D. S. Fisher, "Random transverse field ising spin chains," *Phys. Rev. Lett.*, vol. 69, pp. 534–537, Jul 1992.

[73] G. Refael and E. Altman, "Strong disorder renormalization group primer and the superfluid–insulator transition," *Comptes Rendus Physique*, vol. 14, no. 8, pp. 725–739, 2013. Disordered systems / Systèmes désordonnés.

[74] J. Berges, N. Tetradis, and C. Wetterich, "Non-perturbative renormalization flow in quantum field theory and statistical physics," *Physics Reports*, vol. 363, no. 4, pp. 223–386, 2002. Renormalization group theory in the new millennium. IV.

[75] R. Feynman, *Statistical Mechanics: A Set Of Lectures*, p. 86. Advanced Books Classics, Avalon Publishing, 1998.

[76] D. Griffiths, *Introduction to Quantum Mechanics*. Cambridge University Press, 2017.

[77] T. Sommerfeld, "Lorentz trial function for the hydrogen atom: A simple, elegant exercise," *Journal of Chemical Education*, vol. 88, no. 11, pp. 1521–1524, 2011.

[78] Y. Suzumura, "Collective Modes and Response Functions for the BGD Model," *Progress of Theoretical Physics*, vol. 61, pp. 1–10, 01 1979.

[79] D. S. Lemons and A. Gythiel, "Paul Langevin's 1908 paper "On the Theory of Brownian Motion" ["Sur la théorie du mouvement brownien," C. R. Acad. Sci. (Paris) 146, 530–533 (1908)]," *American Journal of Physics*, vol. 65, pp. 1079–1081, 11 1997.

[80] J. B. Johnson, "Thermal agitation of electricity in conductors," *Phys. Rev.*, vol. 32, pp. 97–109, Jul 1928.

[81] M. Namiki, *Stochastic Quantization*. No. v. 9 in Lecture Notes in Artificial Intelligence, Springer Berlin Heidelberg, 1992.

[82] A. Einstein, *Investigations on the Theory of the Brownian Movement*. Dover Books on Physics Series, Dover Publications, 1956.

[83] G. Pavliotis, *Stochastic Processes and Applications: Diffusion Processes, the Fokker-Planck and Langevin Equations*. Texts in Applied Mathematics, Springer New York, 2014.

[84] A. D. Fokker, "Die mittlere energie rotierender elektrischer dipole im strahlungsfeld," *Annalen der Physik*, vol. 348, no. 5, pp. 810–820, 1914.

[85] M. Planck, "Über einen satz der statistischen dynamik und seine erweiterung in der quantentheorie," *Sitzungsberichte der Preussischen Akademie der Wissenschaften zu Berlin*, vol. Jan-Dec 1917, pp. 324–341, 1917. https://www.biodiversitylibrary.org/bibliography/42231.

[86] S. Serfaty, "Microscopic description of log and coulomb gases," 2017.

[87] M. A. Cazalilla, F. Sols, and F. Guinea, "Dissipation-driven quantum phase transitions in a tomonaga-luttinger liquid electrostatically coupled to a metallic gate," *Phys. Rev. Lett.*, vol. 97, p. 076401, Aug 2006.

[88] G. D. Mahan, *Nonzero Temperatures*, pp. 109–185. Boston, MA: Springer US, 2000.

[89] E. Agoritsas, V. Lecomte, and T. Giamarchi, "Temperature-induced crossovers in the static roughness of a one-dimensional interface," *Phys. Rev. B*, vol. 82, p. 184207, Nov 2010.

[90] Mézard, Marc, "On the glassy nature of random directed polymers in two dimensions," *J. Phys. France*, vol. 51, no. 17, pp. 1831–1846, 1990.

[91] S. Brown and G. Grüner, "Charge and Spin Density Waves," *Scientific American*, vol. 270, pp. 50–56, Apr. 1994.

[92] G. Grüner, "The dynamics of charge-density waves," *Rev. Mod. Phys.*, vol. 60, pp. 1129–1181, Oct 1988.

[93] B. Horovitz, T. Giamarchi, and P. Le Doussal, "Phase transitions for a collective coordinate coupled to luttinger liquids," *Phys. Rev. Lett.*, vol. 111, p. 115302, Sep 2013.

[94] B. Horovitz, T. Giamarchi, and P. Le Doussal, "Transconducting transition for a dynamic boundary coupled to several luttinger liquids," *Phys. Rev. Lett.*, vol. 121, p. 166803, Oct 2018.

[95] P. Drude, "Zur elektronentheorie der metalle," *Annalen der Physik*, vol. 306, no. 3, pp. 566–613, 1900.

[96] P. Drude, "Zur elektronentheorie der metalle; ii. teil. galvanomagnetische und thermomagnetische effecte," *Annalen der Physik*, vol. 308, no. 11, pp. 369–402, 1900.

[97] W. Kohn, "Theory of the insulating state," *Phys. Rev.*, vol. 133, pp. A171–A181, Jan 1964.

[98] B. S. Shastry and B. Sutherland, "Twisted boundary conditions and effective mass in heisenberg-ising and hubbard rings," *Phys. Rev. Lett.*, vol. 65, pp. 243–246, Jul 1990.

[99] D. J. Scalapino, S. R. White, and S. C. Zhang, "Superfluid density and the drude weight of the hubbard model," *Phys. Rev. Lett.*, vol. 68, pp. 2830–2833, May 1992.

[100] W. Meissner and R. Ochsenfeld, "Ein neuer effekt bei eintritt der supraleitfähigkeit," *Naturwissenschaften*, vol. 21, pp. 787–788, 1933.

[101] Z. Cai, U. Schollwöck, and L. Pollet, "Identifying a bath-induced bose liquid in interacting spin-boson models," *Phys. Rev. Lett.*, vol. 113, p. 260403, Dec 2014.

[102] E. Malatsetxebarria, Z. Cai, U. Schollwöck, and M. A. Cazalilla, "Dissipative effects on the superfluid-to-insulator transition in mixed-dimensional optical lattices," *Phys. Rev. A*, vol. 88, p. 063630, Dec 2013.

[103] R. Citro, E. Orignac, and T. Giamarchi, "Adiabatic-antiadiabatic crossover in a spin-peierls chain," *Phys. Rev. B*, vol. 72, p. 024434, Jul 2005.

[104] R. Rajaraman, *Solitons and Instantons: An Introduction to Solitons and Instantons in Quantum Field Theory*. North-Holland personal library, North-Holland Publishing Company, 1982.

[105] A. Scott, F. Chu, and D. McLaughlin, "The soliton: A new concept in applied science," *Proceedings of the IEEE*, vol. 61, no. 10, pp. 1443–1483, 1973.

[106] I. Safi and H. J. Schulz, "Interacting electrons with spin in a one-dimensional dirty wire connected to leads," *Phys. Rev. B*, vol. 59, pp. 3040–3059, Jan 1999.

[107] I. Safi and H. J. Schulz, "Interacting electrons with spin in a one-dimensional dirty wire connected to leads," 1996.

[108] G. Schehr and H. Rieger, "Strong-disorder fixed point in the dissipative random transverse-field ising model," *Phys. Rev. Lett.*, vol. 96, p. 227201, Jun 2006.

[109] G. Schehr and H. Rieger, "Finite temperature behavior of strongly disordered quantum magnets coupled to a dissipative bath*," *Journal of Statistical Mechanics: Theory and Experiment*, vol. 2008, p. P04012, apr 2008.

[110] G. Chiriacò, M. Tsitsishvili, D. Poletti, R. Fazio, and M. Dalmonte, "Diagrammatic method for many-body non-markovian dynamics: memory effects and entanglement transitions," 2023.

[111] J. W. Brown and R. V. Churchill, *Complex Variables and Applications*. Boston, MA: McGraw-Hill Higher Education, eighth ed., 2009.

[112] D. Mitrinović and J. Kečkić, *The Cauchy Method of Residues: Theory and Applications. Vol. 2*. Cauchy method of residues: theory and applications, D. Reidel, 1993.

[113] P. Debye, "Interferenz von röntgenstrahlen und wärmebewegung," Jan. 1913.

[114] I. Waller, "Zur frage der einwirkung der wärmebewegung auf die interferenz von röntgenstrahlen," *Zeitschrift für Physik*, vol. 17, pp. 398–408, 1923.

[115] A. Zoia, A. Rosso, and M. Kardar, "Fractional laplacian in bounded domains," *Phys. Rev. E*, vol. 76, p. 021116, Aug 2007.

[116] C. Runge, "Ueber die numerische auflösung von differentialgleichungen," *Mathematische Annalen*, vol. 46, pp. 167–178, 1895.

[117] W. Kutta, *Beitrag zur näherungsweisen Integration totaler Differentialgleichungen*. Teubner, 1901.

[118] R. L. Honeycutt, "Stochastic runge-kutta algorithms. i. white noise," *Phys. Rev. A*, vol. 45, pp. 600–603, Jan 1992.